

Synthesis of Molecular Rulers to Study Distance and Orientation  
Dependent Förster Resonance Energy Transfer (FRET)

By

Dhananjaya Sahoo

A thesis submitted in partial fulfillment  
of the requirements for the degree of  
Doctor der Naturwissenschaften (Dr. rer. Nat.)  
in Chemistry

---

Department of Chemistry,  
Bielefeld University, Bielefeld, Germany

October 2009

---

Approved, Thesis Committee:

Prof. Dr. Adelheid Godt

Prof. Dr. Markus Sauer

20<sup>th</sup> October 2009



---

## Declaration of Authorship

I, Dhananjaya Sahoo, declare that this thesis entitled, “Synthesis of Molecular Rulers to Study Distance and Orientation Dependent Förster Resonance Energy Transfer (FRET)” and the work presented in it is my own. I confirm that:

- This work was done wholly or mainly while in candidature for a doctoral degree in chemistry at Bielefeld University.
- Where I have consulted the published work of others, this is always clearly attributed.
- Where I have quoted from the work of others, the source is always given. With the exception of such quotations, this thesis is entirely my own work.
- I have acknowledged all main sources of help.
- Where the thesis is based on work done by myself jointly with others, I have made clear exactly what was done by others and what I have contributed by myself.

Date:

Signature:

To my family and friends

“The dream is not what you see in sleep, dream is the thing, which does not let you sleep” --Dr. A. P. J. Abdul Kalam

## Acknowledgements

First of all, I would like to thank my supervisor Prof. Dr. Adelheid Godt for giving me opportunity to work in her group. I am grateful to her for her guidance, advice, fruitful discussions, encouragement, and support throughout my research as well as in my private life at Bielefeld University. I express my deepest gratitude for her time and efforts.

I wish to acknowledge the former and present group members of Prof. Dr. Adelheid Godt for friendly atmosphere. In particular, Mr. Christian Schmidt for making me familiar with the pressure tube reaction. I also thank to Ms. Miriam Schulte for her technical help in the laboratory and synthesizing amino-substituted perylenemonoimide compounds.

I would like to thank Prof. Dr. Markus Sauer, for his outstanding cooperation, scientific discussion, and helpful suggestions and also for giving me the opportunity to work in his laboratory for the photophysical studies of my compounds.

I am thankful to Dr. Ralf Brune for making me familiar with UV-vis and emission spectroscopy, life-time measurements, HPLC, and origin software. I am also thankful to him for his valuable discussions and suggestions.

My special thanks to Dr. Navid Ramezani and Ms. Daniela Maag for their kind help as translator during my early days and to Mr. Muhammad Sajid for his moral support.

I would like to thank Dr. Apurba Lal Koner, Mr. Mrutunjaya Parida, Mr. Sukanta Patra and Dr. Subrata Jana for their encouragement and moral support.

I am very grateful to my family for their love and their blessings.

Finally, I would like to thank to Bielefeld University and DFG for financial support.

---

## Contents

1	Introducion	1-12
1.1	Introduction	1
1.2	Principles of Förster resonance energy transfer	2
1.3	Applications and alternatives	10
2	Synthesis of perylenemonoimide derivatives and their photophysical studies	13-32
2.1	Introduction	13
2.2	Synthesis	13
2.2.1	Perylenemonoimide	14
2.2.2	Aryl-oxy substituted perylenemonoimide	17
2.2.3	Amino-substituted perylenemonoimide	20
2.3	Photophysical studies	23
3	Synthesis of oligo( <i>para</i> -phenyleneethynylene)s as spacer	33-42
3.1	Introduction	33
3.2	Synthesis of oligoPPEs using hydroxymethyl (HOM) and TIPS as orthogonal protecting groups	33



---

3.3 Synthesis of oligoPPEs using hydroxyethyl (HOE) and TIPS as orthogonal protecting groups	38
4 Molecular rulers and their photophysical studies	43-73
4.1 Introduction	43
4.2 Molecular ruler for inter-fluorophore distance measurements	43
4.2.1 Synthesis of PMI(OAr) <sub>3</sub> -(PPE) <sub>2</sub> -PMI(Py) Dyad <b>14</b> <sub>2</sub>	45
4.2.2 Photophysical studies	46
4.3 An improved molecular ruler for inter-fluorophore distance measurements	54
4.3.1 Linear PMI(OAr) <sub>3</sub> -(PPE) <sub>n</sub> -PMI(Py) dyads	54
4.3.2 Kinked PMI(OAr) <sub>3</sub> -(PPE) <sub>n</sub> -PMI(Py) dyads	58
4.3.3 Photophysical studies	63
5 Alkynyl-substituted perylenemonoimide	74-78
5.1 Introduction	74
5.2 Strategy	75
5.3 Synthesis	76
5.4 Photophysical studies	77

---

6 Summary	79-80
7 Experimental	81-137
7.1 General methods	81
7.2 General procedures	83
7.3 Synthesis of perylenemonoimide derivatives	85
7.4 Synthesis of oligoPPEs	93
7.5 Synthesis of PMI(Py) labeled oligoPPEs	103
7.6 Synthesis of PMI(OAr) <sub>3</sub> labeled oligoPPEs <b>15<sub>n</sub></b>	108
7.7 Synthesis of free acetylene <b>16<sub>n</sub></b>	113
7.8 Synthesis of PMI labeled oligoPPEs <b>17<sub>n</sub></b>	116
7.9 Synthesis of free acetylene <b>18<sub>n</sub></b>	119
7.10 Synthesis of linear PMI-(PPE) <sub>2</sub> -PMI(OAr) <sub>3</sub> dyads <b>19<sub>n</sub></b>	122
7.11 Synthesis of <b>21</b>	126
7.12 Synthesis of PMI labeled oligoPPE <b>22<sub>5</sub></b>	126
7.13 Synthesis of free acetylene <b>23<sub>5</sub></b>	127
7.14 Synthesis of kinked PMI-(PPE) <sub>2</sub> -PMI(OAr) <sub>3</sub> dyads <b>24<sub>n</sub></b>	128
7.15 Synthesis of <b>25</b>	132
7.16 Synthesis of bromo compound <b>26</b>	134

---

7.17 Synthesis of tribrominated perylenemonoimide <b>27</b>	135
7.18 Synthesis of alkynyl-substituted perylenemonoimide <b>28</b>	136
8 References	138-143
9 Appendix I	144-146

---

## List of Tables

Table 2.1	Absorption and emission spectral data of amino-substituted PMI ( <b>6c-6e</b> and <b>6g</b> ) in various solvents with different polarity	24
Table 2.2	Percentage of the intensity of the short-wavelength emission band w.r.t. the long-wavelength emission band of the dyes <b>6c-6e</b> and <b>6g</b> in various solvents with increasing polarity from toluene to AcCN	26
Table 2.3	Lifetime decays of amino-substituted PMI ( <b>6c-d</b> , and <b>6g</b> ) in toluene and acetonitrile	30
Table 4.1	The photophysical data of PMI <b>3b</b> , PMI(OAr) <sub>3</sub> <b>25a</b> , and PMI(Py) <b>13<sub>0</sub></b>	48
Table 4.2	The lifetime decays of PMI <b>3b</b> , PMI(OAr) <sub>3</sub> <b>25a</b> , linear dyads <b>19<sub>n</sub></b> (n = 2, 5, 7, and 9), and kinked dyads <b>24<sub>n</sub></b> (n = 5, 7, and 9) in toluene	69
Table 4.3	The FRET efficiencies <i>E</i> of PMI-(PPE) <sub>n</sub> -PMI(OAr) <sub>3</sub> dyads <b>19<sub>n</sub></b> and <b>24<sub>n</sub></b> with respect to the decrease in emission intensity of donor ( <i>F<sub>D</sub></i> ), increase in emission intensity of acceptor ( <i>F<sub>A</sub></i> ) and decrease in the lifetimes of donor ( <i>τ<sub>D</sub></i> ) in toluene	70

---

## List of Figures

Figure 1.1	Jablonski diagram showing FRET	3
Figure 1.2	Spectral characteristics and changes of donor fluorescein and acceptor tetramethylrhodamine undergoing energy transfer	5
Figure 1.3	The figure on left shows visualization of the angles used to define the relative orientations of the donor (D) and acceptor (A) transition moments and the separation vector $R$ and on right <sup>41</sup> illustrates the value of $\kappa^2$ depending on the different orientations of D and A	6
Figure 1.4	Distance $R$ between the donor and acceptor versus efficiency $E$ of energy transfer	9
Figure 2.1	$^1\text{H}$ - $^1\text{H}$ COSY of the mixture of compound PMI(OAr) <sub>3</sub> <b>4a</b> (A) and PMI(OAr) <sub>2</sub> <b>4b</b> (B); solvent: CHCl <sub>3</sub> , 500 MHz	19
Figure 2.2	$^1\text{H}$ - $^1\text{H}$ COSY of the mixture of constitutional isomers of PMI(OAr) <sub>2</sub> <b>4b</b> (I and II); solvent: CHCl <sub>3</sub> , 500 MHz	19
Figure 2.3	Absorption and emission spectra for PMI(Me) <sub>2</sub> <b>6g</b> , PMI(Pip) <b>6c</b> , PMI(EtHex) <b>6d</b> , and PMI(Py) <b>6e</b> in various solvents with different polarity	23
Figure 2.4	Excitation spectra for PMI(EtHex) <b>6d</b> and PMI(Py) <b>6e</b> in CHCl <sub>3</sub> and THF at different emission	28
Figure 2.5	Lifetime decays of the PMI(Me) <sub>2</sub> <b>6g</b> , PMI(PiP) <b>6c</b> , PMI(EtHex) <b>6d</b> , PMI(Py) <b>6e</b> and the prompt	29
Figure 3.1	Structural representation of carbomatalation product <b>8d<sub>n</sub></b>	35

- Figure 4.1 Structural representation of PMI **3b**, PMI(OAr)<sub>3</sub> **25a** and PMI(Py) **13<sub>0</sub>** on left. Absorption spectra (top right) and emission spectra (bottom right) for PMI **3b**, PMI(OAr)<sub>3</sub> **25a** and PMI(Py) **13<sub>0</sub>** in toluene 46
- Figure 4.2 Emission spectra (left) for PMI **3b**, PMI(OAr)<sub>3</sub> **25a** and PMI(Py) **13<sub>0</sub>** in toluene 47
- Figure 4.3 Absorption spectra (left) and emission spectra (right) for donor **25a**, acceptor **13<sub>0</sub>** and PMI(OAr)<sub>3</sub>-(PPE)<sub>2</sub>-PMI(Py) dyad **14<sub>2</sub>** in toluene 48
- Figure 4.4 Absorption spectra (left) and Emission spectra (right) for PMI(Py) **6<sub>e</sub>**, PMI(Py) **6<sub>e</sub>** + TFA, PMI(Py) **6<sub>e</sub>** + TFA + TEA in toluene 50
- Figure 4.5 Absorption spectra (left) and emission spectra (right) for PMI **3b** and PMI(Py) **6<sub>e</sub>** + TFA in toluene 51
- Figure 4.6 Absorption (left) and emission spectra (right) for **25a**, **13<sub>0</sub>**, and PMI(OAr)<sub>3</sub>-(PPE)<sub>2</sub>-PMI(Py) dyad **14<sub>2</sub>** after protonation with TFA in toluene 52
- Figure 4.7 Structural representation of the direction of energy transfer for PMI(OAr)<sub>3</sub>-(PPE)<sub>2</sub>-PMI(Py) dyad **14<sub>2</sub>** before and after protonation 52
- Figure 4.8 Figures representing the structure of PMI **3b**, PMI(OAr)<sub>3</sub> **25a**, linear dyads **19<sub>n</sub>** (n = 2, 5, 7, and 9), and kinked dyads **24<sub>n</sub>** (n = 5, 7, and 9) 64
- Figure 4.9 Emission spectrum of the donor PMI **3b** and absorption spectrum of the acceptor PMI(OAr)<sub>3</sub> **25a** in toluene and the area cover by gray color is their overlap 65
- Figure 4.10 Emission spectra of PMI **3b**, the PMI(OAr)<sub>3</sub> **25a**, the sum of the emission of PMI and PMI(OAr)<sub>3</sub>, and linear PMI-(PPE)<sub>n</sub>-PMI(OAr)<sub>3</sub> dyads **19<sub>n</sub>** with n

---

	= 2, 5, 7, and 9 and kinked PMI-(PPE) <sub>n</sub> -PMI(OAr) <sub>3</sub> dyads <b>24<sub>n</sub></b> with n = 5, 7, and 9	65
Figure 4.11	Excited-state lifetime decays of prompt, PMI <b>3b</b> , PMI(OAr) <sub>3</sub> <b>25a</b> , linear PMI-(PPE) <sub>n</sub> -PMI(OAr) <sub>3</sub> dyads <b>19<sub>n</sub></b> and the kinked PMI-(PPE) <sub>n</sub> -PMI(OAr) <sub>3</sub> dyads <b>24<sub>n</sub></b>	67
Figure 4.12	FRET efficiency <i>E</i> versus calculated inter-fluorophore distances <i>R</i>	71
Figure 5.1	Absorption (left) and emission (right) spectra of <b>3b</b> , <b>25a</b> , and <b>28</b>	77
Figure 5.2	The normalized emission spectra of <b>25a</b> and <b>28</b>	78

---

## List of Schemes

Scheme 2.1	Synthesis of bromoaniline	14
Scheme 2.2	Synthesis of perylenemonoimide	15
Scheme 2.3	Synthesis of aryloxy-substituted perylenemonoimide	18
Scheme 2.4	Synthesis of amino-substituted perylenemonoimide starting from PMI(Br) <sub>3</sub> <b>4</b>	21
Scheme 2.5	Synthesis of amino-substituted perylenemonoimide starting from PMI(Br) <b>4c</b>	21
Scheme 3.1	Synthesis of dimer <b>8a<sub>2</sub></b>	34
Scheme 3.2	Synthesis of iodotrimer <b>7a<sub>3</sub></b> , pentamer <b>8a<sub>5</sub></b> , and heptamer <b>8a<sub>7</sub></b>	37
Scheme 3.3	Synthesis of iodomonomer <b>7b<sub>1</sub></b> and iododimer <b>7b<sub>2</sub></b>	39
Scheme 3.4	Synthesis of oligomers <b>8b<sub>n</sub></b> , and non-polar acetylenes <b>9b<sub>n</sub></b> (n = 6, 7, 9)	40
Scheme 3.5	Schematic representation of aldehyde <b>11a<sub>5</sub></b> and ketone <b>11b<sub>9</sub></b>	41
Scheme 4.1	Structural representation of PMI(OAr) <sub>3</sub> -(PPE) <sub>n</sub> -PMI(Py) dyad <b>14<sub>n</sub></b> and their corresponding building blocks.	44
Scheme 4.2	Synthesis of PMI(OAr) <sub>3</sub> -(PPE) <sub>n</sub> -PMI(Py) Dyads <b>14<sub>n</sub></b>	45
Scheme 4.3	Structural representation of linear PMI-(PPE) <sub>n</sub> -PMI(OAr) <sub>3</sub> dyads and their corresponding building blocks	55
Scheme 4.4	Synthesis of linear PMI-(PPE) <sub>n</sub> -PMI(OAr) <sub>3</sub> dyads <b>19<sub>n</sub></b>	56



---

Scheme 4.5	Structural representation of kinked PMI-(PPE) <sub>n</sub> -PMI(OAr) <sub>3</sub> dyads	58
Scheme 4.6	Synthesis of kinked PMI-(PPE) <sub>5</sub> -PMI(OAr) <sub>3</sub> dyad <b>24<sub>5</sub></b>	59
Scheme 4.7	Retro synthesis of kinked PMI-(PPE) <sub>n</sub> -PMI(OAr) <sub>3</sub> dyads <b>24<sub>n</sub></b> with n = 7, 9	61
Scheme 4.8	Synthesis of kinked PMI-(PPE) <sub>n</sub> -PMI(OAr) <sub>3</sub> dyads <b>24<sub>n</sub></b> (n = 7, 9)	63
Scheme 5.1	Retro synthesis of alkynyl-substituted perylenemonoimide	75
Scheme 5.2	Synthesis of alkynyl-substituted perylenemonoimide	76

---

## GLOSSARY

### Acronyms

A	Acceptor
AcCN	Acetonitrile
CT	Charge transfer state
D	Donor
FRET	Förster Resonance Energy Transfer/Fluorescence Resonance Energy Transfer
HOM	Hydroxymethyl
HOE	Hydroxyethyl
HPLC	High performance liquid chromatography
IRF	Instrumental response function
LS	Local excited state
MeOH	Methanol
oligoPPEs	oligo( <i>para</i> -phenyleneethynylene)s
PMI	Perylenemonoimide
PMI(OAr) <sub>3</sub>	Tri(aryloxy)-substituted perylenemonoimide
PMI(Me) <sub>2</sub>	dimethylamino-substituted perylenemonoimide
PMI(Pip)	Piperinyl-substituted perylenemonoimide
PMI(Ethex)	2-Ethylhexylamino-substituted perylenemonoimide
PMI(Py)	Pyrrolidinyl-substituted perylenemonoimide
S <sub>0</sub>	Ground electronic state
S <sub>1</sub>	First excited singlet state

---

$S_2$	Second excited singlet state
TFA	Trifluoro acetic acid
THF	Tetrahydrofuran
TIPS	Triisopropylsilyl
TICT	Twisted intramolecular charge-transfer state
W.R.T.	With respect to

### Mathematical Terms

$E$	Efficiency of energy transfer
$R_0$	Förster distance in resonance energy transfer
$R$	Inter-fluorophore distance between donor and acceptor/reference
$\kappa_{nr}$	Nonradiative decay rate constant
$\kappa_T$	Transfer rate in resonance energy transfer
$F$	Fluorescence or steady-state intensity
$J(\lambda)$	Spectral overlap between donor emission and acceptor absorbance
$\varepsilon$	Extinction coefficient
$\Phi$	Fluorescence quantum yield
$\kappa^2$	Orientation factor in resonance energy transfer
$\lambda_{ex}$	Excitation wavelength
$\lambda_{em}$	Emission wavelength
$\eta$	Refractive index
$OD$	optical density
$\alpha_i$	Preexponential function in a multiexponential decay

---

$\chi_R^2$	Goodness-of-fit parameter, reduced chi-squared
$\tau$	Fluorescence decay time or fluorescence lifetime
$\tau_D$	Donor fluorescence lifetime
$\tau_{DA}$	Donor lifetime in presence of acceptor
$\mu_e$	dipole moment in excited state
$\mu_g$	dipole moment in ground state

# Chapter 1

## Introduction

### 1.1 Introduction

Förster resonance energy transfer/Fluorescence resonance energy transfer (FRET) is a non-radiative process, in which a donor fluorophore in its electronic excited state transfers the excitation energy to the nearby acceptor chromophore. A correlation between the efficiency ( $E$ ) of resonance energy transfer and the distance ( $R$ ) between donor and acceptor was established by the German physicist Theodor Förster in 1947.<sup>1</sup> The FRET efficiency  $E$  is proportional to the inverse sixth power of the distance  $R$  between the donor and the acceptor, which is represented by

$$E = [1 + (R/R_0)^6]^{-1} \quad (1.1)$$

where,  $R_0$  is known as Förster radius that equals to the inter-fluorophore distance  $R$  at  $E = 50\%$ .

In 1967 Stryer and Haugland reported FRET experiments using naphthyl and dansyl as the donor and acceptor, respectively and poly-L-prolines as the backbone for the FRET system.<sup>2</sup> The authors found that the  $R^6$  distance dependence predicted by Förster was nicely reproduced by the experimental results.<sup>2</sup> This study has been subsequently considered as the proof of Förster theory and familiarly known as “spectroscopic ruler” for distance measurements, especially in the field of biosciences.<sup>3-</sup>

Single-molecule spectroscopic technique has led to the rebirth of FRET.<sup>10-20</sup> Eaton *et al.*<sup>19</sup> have used the single-molecule spectroscopic technique to determine the FRET efficiency taking Alex Fluor 488 maleimide and Alex Fluor 594 succinimidyl ester as the donor and the acceptor, respectively and poly-L-prolines as backbone, thereby testing once more the usefulness of FRET as a “spectroscopic ruler”. FRET at the single-molecule level had also been applied for measuring the end-to-end distance of molecules.<sup>19-23.</sup>

## 1.2 Principles of Förster resonance energy transfer

The FRET process involves the following steps.

- i) Upon irradiation, the donor fluorophore gets excited from ground state to the excited state. Several excited states are available to the donor, however internal conversion and vibrational relaxation to the lowest excited state is very rapid (within picosecond).<sup>3,4</sup>
- ii) If a suitable acceptor is in close proximity to the donor, the non-radiative energy transfer takes place between the donor and the acceptor. This energy transfer involves a resonance between the singlet-singlet electronic transitions of the donor and acceptor, generated by the coupling of the emission transition dipole of the donor and the absorption transition dipole of the acceptor (Figure 1.1).<sup>3,4</sup>

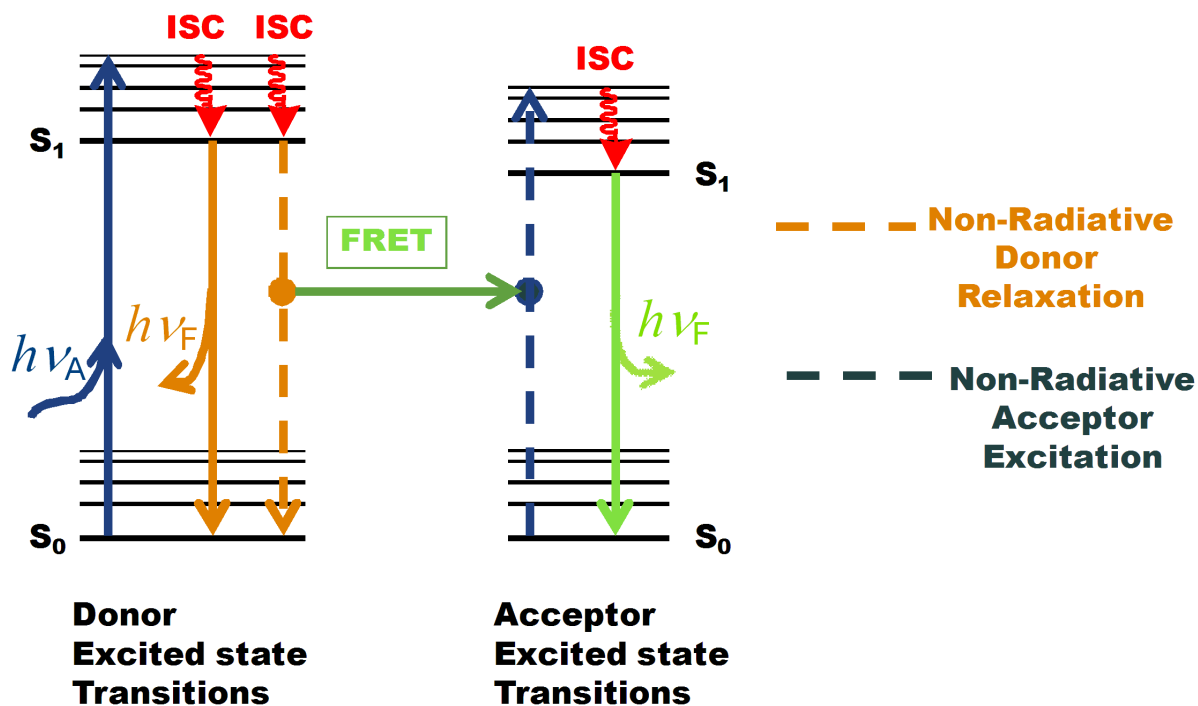


**Figure 1.1** Jablonski energy level diagram showing FRET. The figure was adopted from <http://www.olympusmicro.com/primer/techniques/fluorescence/fret/fretintro.html>

The Jablonski diagram in figure 1.1 shows the coupled transitions between the donor emission and the acceptor absorbance involve in the process of fluorescence resonance energy transfer. Absorption and emission transitions are represented by linear vertical arrows (blue and orange or/and green respectively), while vibrational relaxation is indicated by wavy red arrows. The coupled transitions are drawn with dashed lines. In the presence of a suitable acceptor, the donor fluorophore can transfer excited state energy directly to the acceptor without emitting a photon (illustrated by a blue arrow in figure 1.1). As a result of that, the electron of the acceptor gets excited like the donor and consequently, returns to the ground state by emitting photon. The resulting sensitized emission has identical emission characteristics of the acceptor (See figure 1.2).

The extent of resonance energy transfer or FRET efficiency depends on the following factors:

- i) The fluorescent quantum yield of the donor.<sup>3,4</sup>
- ii) The overlap of the emission spectrum of the donor and the absorption spectrum of the acceptor.<sup>3,4,39</sup>
- iii) The relative orientation of the transition dipole moment of the donor and that of the acceptor.<sup>3,4,40</sup>
- iv) The distance between the donor and the acceptor.<sup>2,3,4</sup>

According to the Förster theory, the rate constant  $K_T$  for resonance energy transfer from a donor to an acceptor is given by

$$K_T = (1/\tau_D) (R_0/R)^6 \quad (1.2)$$

where,  $\tau_D$  is the excited-state lifetime of the donor in the absence of acceptor,  $R$  is the inter-fluorophore distance, and  $R_0$  is the Förster radius.

Förster radius  $R_0$  is the distance at which one half of the energy is transferred from the donor to the acceptor.  $R_0$  is expressed by

$$R_0 = \{8.79 \times 10^{-5} [\kappa^2 \eta^4 \phi_D J(\lambda)]\}^{-1/6} \text{ (in \AA)} \quad (1.3)$$

where,  $\phi_D$  = the fluorescence quantum yield of the donor only,  $\eta$  = refractive index of the environment,  $J(\lambda)$  = the spectral overlap integral of the donor and acceptor, and  $\kappa^2 =$



the orientation factor, which depends on the relative orientation of the transition dipole moments of the donor and the acceptor.

The spectral overlap integral  $J(\lambda)$  can be calculated according to eq. 1.4.

$$J(\lambda) = \frac{\int F_D(\lambda)\epsilon_A(\lambda)\lambda^4 d\lambda}{\int F_D(\lambda)d\lambda} \quad (\text{in } \text{M}^{-1}\text{cm}^{-1}\text{nm}^4) \quad (1.4)$$

where,  $F_D$  is the fluorescence intensity of the donor and  $\epsilon_A$  is the extinction coefficient of the acceptor with  $\lambda$  as integral parameter.

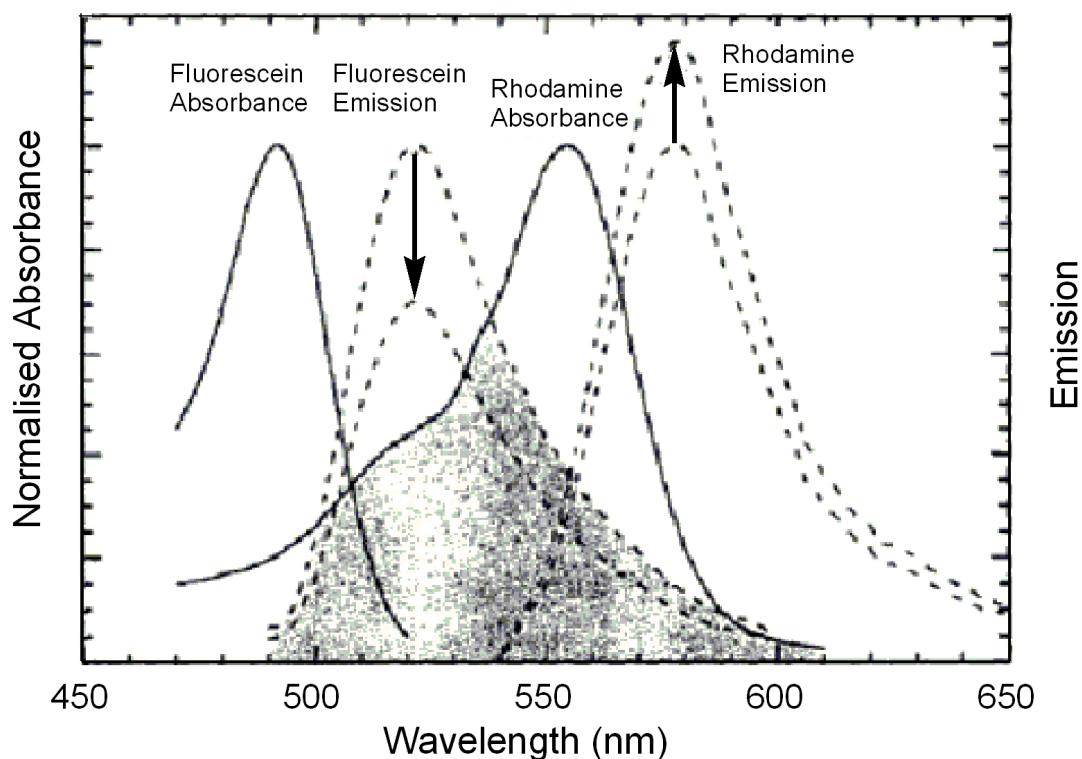


**Figure 1.2** The figure shows spectral characteristics of fluorescein (donor) and tetramethylrhodamine (acceptor) undergoing energy transfer. As energy transfer takes place, the emission intensity of the donor decreases and emission intensity of the acceptor increases. The gray area represents the spectral overlap region of the donor emission and the acceptor absorption, which is responsible for energy transfer. The figure is taken from the *Ref.* 8.

The figure 1.2 shows the absorption and emission spectra of the donor fluorescein and the acceptor tetramethylrhodamine for their potential application as a FRET pair.<sup>8</sup> Absorption spectra for both of the fluorophores are illustrated as solid lines, while the emission spectra are presented as dashed lines. The region of overlap between the donor emission and acceptor absorption spectra is represented by grey area. Whenever the spectral overlap of the fluorophores is high, a phenomenon known as spectral bleed-through or crossover occurs. In this phenomenon, the emission from the excited acceptor arises from the excitation of the donor, which transfers energy to the acceptor in a non-radiative fashion through dipole-dipole interaction and the direct excitation of the acceptor. The result is a high background signal that must be subtracted from the weak acceptor fluorescence emission.

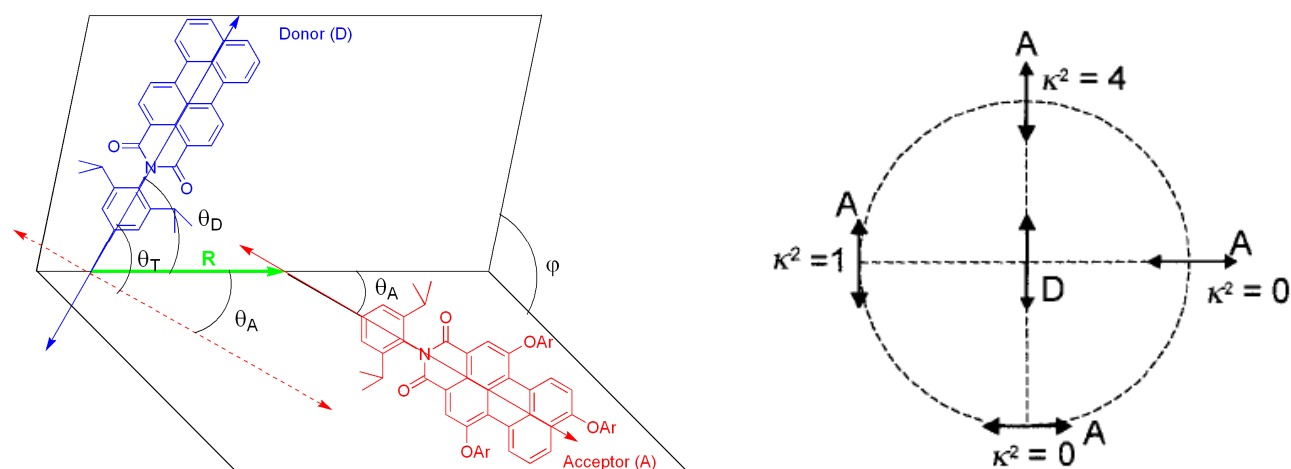


**Figure 1.3** The figure on left shows visualization of the angles used to define the relative orientations of the donor (D) and acceptor (A) transition dipole moments and separated with distance vector  $R$  and on the right shows the value of  $k^2$  depending on the different orientation of D and A. The Figure on right hand side is taken from *Ref. 4*.

The orientation factor  $\kappa^2$  or the relative orientations of the donor emission dipole and the acceptor absorption dipole is given by the eqs. 1.5 and 1.6.<sup>3,8</sup>

$$\kappa^2 = (\cos \theta_T - 3\cos \theta_D \cos \theta_A)^2 \quad (1.5)$$

$$\kappa^2 = (\sin \theta_D \sin \theta_A \cos \varphi - 2\cos \theta_D \cos \theta_A)^2 \quad (1.6)$$

where,  $\theta_T$  is the angle between the emission transition dipole of the donor and the absorption transition dipole of the acceptor,  $\theta_D$  and  $\theta_A$  are the angles between these dipoles and the vector joining the donor and the acceptor, and  $\varphi$  is the angle between the planes containing the two transition dipoles (Figure 1.3, left).

The value of  $\kappa^2$  is 0 when the orientation of transition dipole moments of the donor and that of the acceptor are orthogonal to each other (See the right and bottom of the circle in figure 1.3, right). On the other hand the value of  $\kappa^2$  is 1 and 4 when the orientation of the transition dipole moments of the donor and acceptor are parallel and collinear, respectively (See the left and top of the circle in figure 1.3, right).

For FRET, the donor must be fluorescent however the acceptor chromophore is not necessarily to be fluorescent. The extent of resonance energy transfer can be determined from decreased fluorescence intensity of the donor in the presence of an acceptor or from the increased fluorescence intensity of the acceptor in the presence of the donor, in case that the acceptor is a fluorophore (Figure 1.2). Additionally, decrease in lifetime of the donor in the presence of the acceptor also gives information about the extent of resonance energy transfer.<sup>3,4,7,8</sup>

The efficiency of resonance energy transfer ( $E$ ) can be calculated by the following three different ways.

I. Decrease in donor fluorescence intensity

$$E = 1 - F_{DA}/F_D \quad (1.7)$$

where,  $F_D$  is the fluorescence intensity of the donor only and  $F_{DA}$  is the fluorescence intensity of donor in the presence of the acceptor.

II. Increase in fluorescence intensity of the acceptor

$$E = (\mathcal{E}_D/\mathcal{E}_A)[(F_{AD}/F_A)-1] \quad (1.8)$$

where,  $F_A$  is the fluorescence intensity of the acceptor only,  $F_{AD}$  is the fluorescence intensity of the acceptor in the presence of the donor (sum of the fluorescence arising from the energy transfer and from the direct excitation of the acceptor),  $\mathcal{E}_A$  and  $\mathcal{E}_D$  are the molar extinction coefficients of the acceptor and the donor respectively, at the wavelength of donor excitation.

III. Decrease in excited state lifetime decay of the donor

$$E = 1 - (\tau_{DA}/\tau_D) \quad (1.9)$$

where,  $\tau_D$  is the excited state lifetime of the donor only and  $\tau_{DA}$  is the excited state lifetime of the donor in the presence of the acceptor.

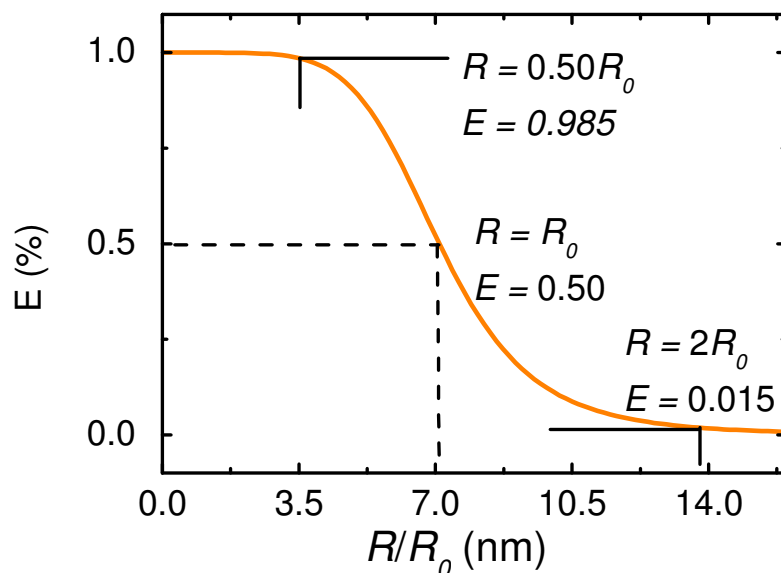


**Figure 1.4** Distance  $R$  between the donor and the acceptor versus efficiency  $E$  of energy transfer. The figure is adopted from *Ref. 3*.

The distance between the donor and the acceptor plays a key role for FRET efficiency. This is due to the dependence of the FRET efficiency  $E$  on the inverse sixth power of the distance  $R$  between the donor and the acceptor (Eq. 1.1). When the distance  $R$  between the donor and acceptor is equal to the Förster radius  $R_0$  of the system, the FRET efficiency  $E$  is equal to 50% (Figure 1.4). When the distance  $R$  decreases from  $R_0$  to  $0.5R_0$  the FRET efficiency  $E$  approaches one. On the other hand by increasing the distance  $R$  from  $R_0$  to  $2R_0$  the FRET efficiency  $E$  approaches zero. The distance  $R$  between the donor and the acceptor of a system can be measured within a range of  $0.5R_0$  to  $2R_0$ . Beyond this range, the slope of the curve is too shallow to give reliable information on the distance  $R$  between the two fluorophores.

### 1.3 Applications and alternatives

Measurement of distance between the donor and the acceptor of macromolecules or biomolecules is just one of the several applications of FRET. The other applications of FRET are to measure the conformational changes,<sup>24</sup> dynamic processes,<sup>25</sup> rates of diffusion and distances of closest approach,<sup>7</sup> and chemosensors for metal cations like Ag(I) and Hg(II).<sup>26-28</sup> Hartwig and co-workers used FRET as a tool for reaction discovery and screening of catalyst for Heck coupling,<sup>29</sup> arylation of ethyl cyanoacetate,<sup>30</sup> and arylation of amines.<sup>31</sup> For all of these cases dansyl was used as the donor and attached to one of the reactants whereas, azo-dye was used as the acceptor and attached to the other reactants which carrying a halide group. The catalyst was screened from the yield of the reaction. The yields of the reactions were determined by plotting the mole fraction of the products (FRET pair) versus emission intensity of the product, donor attached to the reactant, and acceptor attached with the reactant containing the halide group.<sup>29-31</sup>

Generation of new fluorophores with spectral characteristics that combine the best of both the donor and the acceptor fluorophore is also one of the applications of FRET.<sup>32,33</sup> In this case the donor and the acceptor attaches covalently to each other in a close proximity. In the simplest case, where the absorption and emission of the individual fluorophore do not change whereas, the absorption characteristic of the new fluorophore is the sum of the two individual fluorophores.<sup>33</sup> Simultaneously, the emission of the new fluorophore is dominated by the acceptor emission with large stokes shifts and remarkably high quantum yield.<sup>33</sup>

The alternative techniques which give structural information are X-ray crystallography, nuclear magnetic resonance (NMR), and electron paramagnetic

---

resonance (EPR). X-ray crystallography and NMR both produce potentially complete structural information but require large quantities of material. X-ray crystallography and NMR are limited to *in vitro* measurements and can analyze only relatively small molecules, restrictions which do not apply to FRET.<sup>8</sup> Additionally, in case of X-ray crystallography, one could face the problem of crystallization and isomorphous replacement.<sup>7,34</sup>

Interestingly, one can get structural information by using EPR technique on the spin labeled molecule of interest. This technique measures the dipole-dipole interaction between two spin labels in the nanometer range.<sup>35-37</sup> Godt *et al.*<sup>38</sup> reported the end to end distance distribution of oligo(*para*-phenyleneethynylene)s (oligoPPEs) by using EPR technique. Because EPR and FRET can measure end to end distances in the range of 1-10 nm, we are interested to compare these two methods. For that reason “molecular rulers” were developed for FRET study, taking oligoPPEs as the backbone for a fair comparison.

During my PhD work, I have synthesized the perylenemonoimide dye derivatives and studied their photophysical properties (chapter 2 and 5). Perylenemonoimide dye derivatives with suitable photophysical properties were chosen as the donor and the acceptor of the molecular ruler. A series of shape persistent oligoPPEs with appropriate lengths were synthesized by following divergent and convergent approaches (chapter 3). Afterward these oligoPPEs were used as spacers for the construction of the molecular ruler (chapter 4). A series of linear dyads/donor-acceptor labeled oligoPPEs were synthesized as molecular ruler and the photophysical studies (Chapter 4) were performed to calculate end-to-end distance of oligoPPEs for comparison with EPR data.

A second series of kinked dyads/donor-acceptor oligoPPEs were synthesized keeping a fixed angle of  $120^\circ$  between the long axis of the fluorophores and the photophysical properties were studied to investigate the dependence of FRET efficiency on the relative orientation of fluorophores (Chapter 4).



## Chapter 2

# Perylenemonoimide derivatives and their photophysical studies

### 2.1 Introduction

Perylenemonoimide (PMI) dyes have found wide spread applications ranging from industrial pigments<sup>41,42</sup> to components of molecular photonic devices.<sup>43</sup> PMI dyes have drawn attention due to their unique properties such as high fluorescence quantum yield (nearly unity),<sup>44-46</sup> high thermal, chemical, and photochemical stability.<sup>47</sup> PMI dyes have been implemented as a suitable candidate for energy transfer.<sup>48-51</sup> The synthetic chemistry of PMI dyes has developed rapidly over the past few years, Langhal's group has introduced a method to convert the commercially available perylene-dianhydride into PMI, which provides the starting point for the substituted PMI dyes.<sup>47</sup> Müllen's group and Lindsey's group have developed methods for the halogenation and subsequent substitution of the halogenated PMI dyes.<sup>52-56</sup>

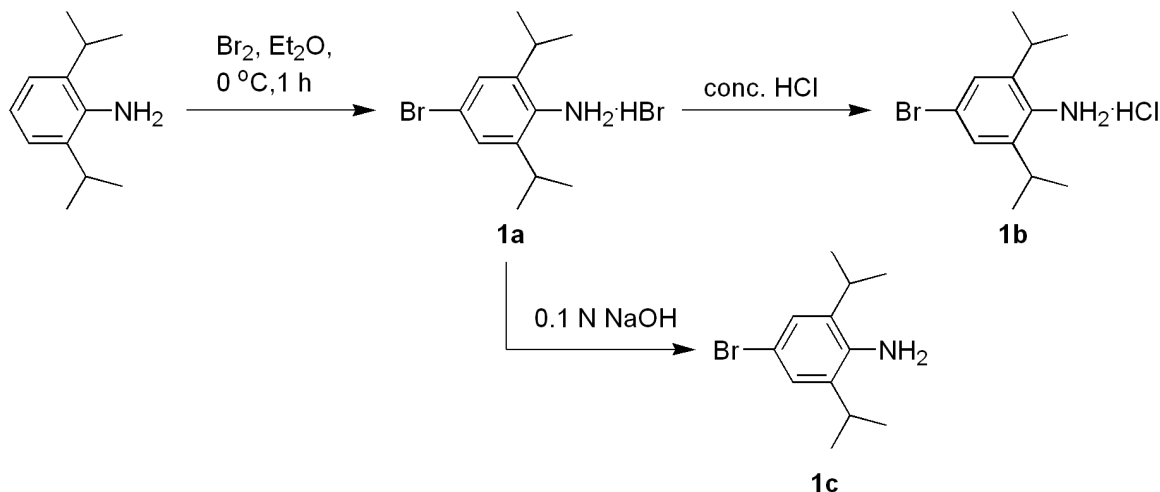
### 2.2 Synthesis

A primary challenge in working with peryleneimide dyes is to overcome their poor solubility. A widespread approach with PMI has been to incorporate 2,6-di-*tert*-butyl<sup>47,49,56,57</sup> or 2,6-diisopropyl<sup>52,57</sup> phenyl group at the *N*-atom of the imide moiety. Additional solubility has been achieved by introducing aryl-oxy substituents at the bay region of the PMI.<sup>52,54,57,58</sup> We chose to incorporate 2,6-diisopropyl phenyl group at the *N*-atom of the imide group of the PMI. The objective was not only to improve the

solubility, but also to break the conjugation between the imide group and the phenylene unit of the PMI.

## 2.2.1 Perylenemonoimide

**Scheme 2.1** Synthesis of bromo aniline.



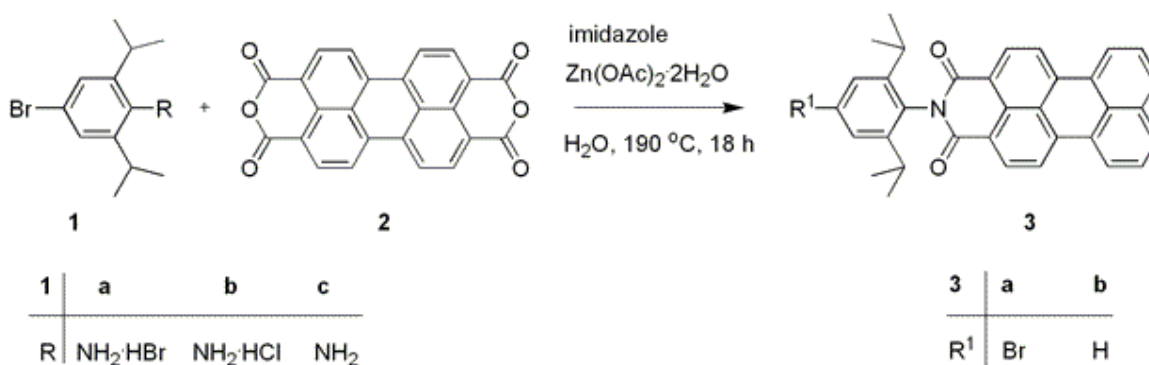
Treatment of the commercially available 2,6-diisopropylaniline with bromine in diethyl ether afforded the 4-bromo-2,6-diisopropylaniline hydrobromide (**1a**) in 71% yield. Treatment of the hydrobromide **1a** with concentrated  $\text{HCl}$  afforded hydrochloride **1b**. Similarly, treatment of the hydrobromide **1a** with  $0.1\text{ N NaOH}$  solution afforded the free amine **1c** (Scheme 2.1).

Following the procedure described by Lindsey *et al.*<sup>56</sup> commercially available perylene-dianhydride **2** and hydrobromide **1a** were filled under argon into a thick walled pressure tube along with  $\text{Zn}(\text{OAc})_2$ , imidazole, and distilled water. The tube was sealed with a Teflon screw cap and heated at  $190\text{ }^\circ\text{C}$  for 18 h to afford **3a** in 30% yield. Debrominated perylenemonoimide **3b** was isolated as a side product (Scheme 2.2). The yield of the reaction was low in comparison to the reported yield of 46%.<sup>56</sup> The only difference between the reported procedure and ours was that in the former case free

aniline **1c** was used, whereas we used the hydrobromide **1a**. Therefore, we also performed the reaction taking the free aniline **1c** and the hydrochloride **1b**. Surprisingly, for both of these reactions the yields were only 26%, which was even lower than our previous finding. For all of these three variations debrominated product **3b** was observed.

Lindsey *et al.*<sup>57</sup> used 2,5-di-*tert*-butylaniline and performed the reaction in an autoclave at 190 °C for 20 h and isolated an analogue of **3b** in 49% yield. We used 2,6-diisopropylaniline and followed the same reaction conditions as for the hydrobromide **1a**. **3b** was isolated in 47-48% yield which was nearly the same as that of the **3b** analogue reported by Lindsey.<sup>57</sup> Even though we used a different aniline than the reported one, it is fair to compare the results by considering the fact that the isopropyl group at 2 and 6 position of aniline will not change the nucleophilicity of the aniline dramatically in comparison to the *tert*-butyl group at 2 and 5 position. This result suggests that the low yield of **3a** may be partly due to the formation of side product **3b**. Secondly, the nucleophilicity of *para*-bromoaniline is somehow less than that of the aniline itself, which may be responsible for the low conversion of **3a**.

**Scheme 2.2** Synthesis of perylenemonoimide.



For the compounds **1b** and **1c** the yields of the reactions dropped from 26% to 20%, when the reactions were scaled up from 2.0 mmol to about 3.5 mmol. For these reactions the same thick walled tubes (35 mL, 17.8 cm x 25.4 mm) were used and as a consequence only a part of the reaction mixture was immersed in the oil bath, whereas for small scale reaction the reaction mixture was completely immersed. Therefore, the material above the oil layer gets insufficient heating in comparison to the counterpart inside the oil bath. We also found that the stirring was not sufficient enough to have a homogenous mixture. As a result of this, the material above the oil bath did not get sufficient heating to give the product, which may also be responsible for the lower yield.

At this point, we decided to run several parallel reactions on small scale and combine them for work up. The hydrobromide **1a** was used for the scale up purpose because the yield of the reaction is higher than the reactions in which hydrochloride **1b** and free aniline **1c** were used. The other reason was the easier access of **1a**. The scale-up was done in eight batches, out of which four batches consisted of three different thick walled pressure tubes whereas the other four batches consisted of two different thick walled tubes each. Each thick walled pressure tube (35 mL, 17.8 cm x 25.4 mm) was filled with 1.48 mmol of hydrobromide **1a** and dianhydride **2** along with the required amount of  $\text{Zn}(\text{OAc})_2$ , imidazole, and  $\text{H}_2\text{O}$ .

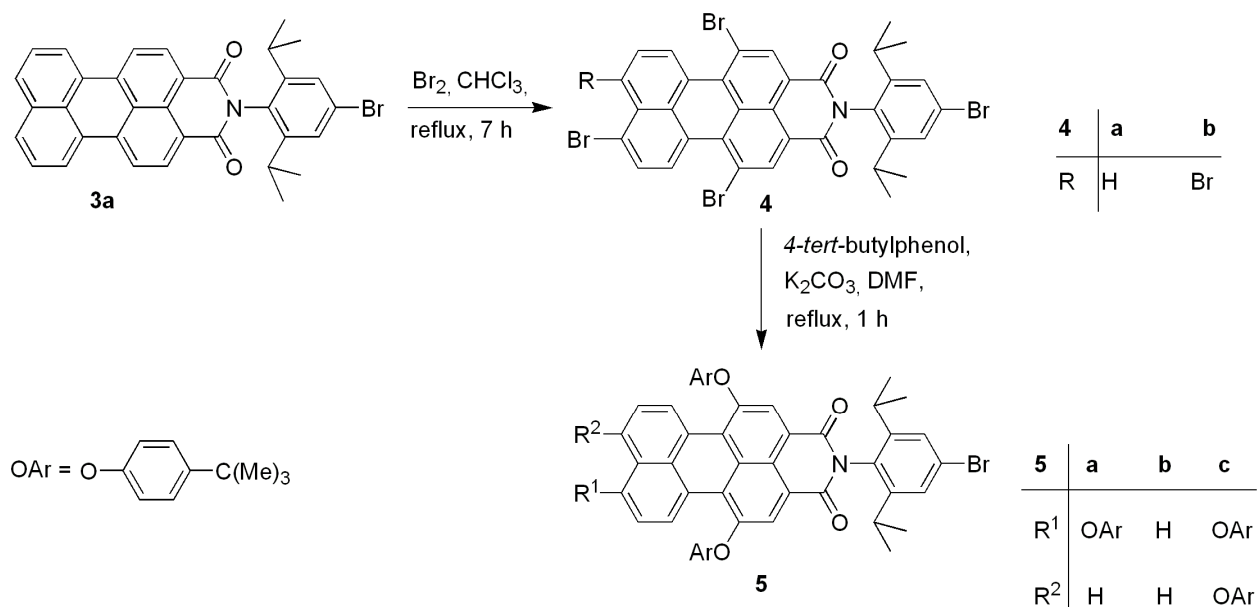
We had noticed that for reaction at small scales, a substantial amount of insoluble material remains on the top of the silica column after chromatography. These materials may be the unreacted anhydride or decomposed material. It would have taken much effort to isolate **3a** from the crude products collected from eight batches. In order to reduce the workload, after aqueous work up the crude materials from eight batches

were combined in a flask (2.5 L in capacity) and suspended in  $\text{CHCl}_3$  (1.5 L) for 48 h. The suspension was filtered and the solvent was evaporated to afford 4.81 g of red solid. The yield of **3a** was estimated to be 26% from the  $^1\text{H}$  NMR spectroscopy taking the consideration of PMI **3b** and perylene. In order to make sure that there was no more **3a** in the solid that had been filtered off from the suspension, this solid was resuspended in  $\text{CHCl}_3$  and stirred for 48 h. After filtering the suspension and evaporating the solvents from the filtration only a few mg of material was found, which shows that substantially all of **3a** had been extracted during the first filtration itself. 3.45 g (22%) of **3a** was isolated by column chromatography. The remaining 4% material stuck on the silica during chromatography.

We found that the temperature plays a crucial role for the conversion. It was found that 190 °C is the optimal temperature as described by Langhals.<sup>47</sup> When the reaction was carried out at 180 °C, it failed to give the desired product emphasizing small changes in temperature. Also the amount of water plays a crucial role in the preparation of **3a**: doubling the amount of water resulted in complete failure of the reaction.

### 2.2.2 Aryloxy-substituted perylenemonoimide

PMIs are known to undergo bromination selectively at the 1-, 6-, and 9-positions.<sup>54-58</sup> Treatment of PMI **3a** with excess bromine in refluxing chloroform afforded the brominated PMI derivative **4** in 45-52% yields (Scheme 2.3). The  $^1\text{H}$  NMR spectrum shows the presence of 2-11% tetrabrominated product  $\text{PMI}(\text{Br})_4$  **4b**. The compounds  $\text{PMI}(\text{Br})_3$  **4a** and  $\text{PMI}(\text{Br})_4$  **4b** have the same  $R_f$  values so we decided to carry out the further reaction taking the mixture.

**Scheme 2.3** Synthesis of aryloxy-substituted perylenemonoimide.

The mixture of PMI(Br)<sub>3</sub> **4a** and PMI(Br)<sub>4</sub> **4b** was taken along with 4-*tert*-butylphenol and potassium carbonate in DMF and refluxed for 1 h to obtain **5** in 49-66% yield (Scheme 2.3).<sup>56</sup> About 3-10% of PMI(OAr)<sub>2</sub> **5b** was estimated from the signals of <sup>1</sup>H NMR spectroscopy. The structural identity of PMI(OAr)<sub>2</sub> **5b** was confirmed by <sup>1</sup>H-<sup>1</sup>H COSY (Figure 2.1). Besides **5a** and **5b** tetraphenoxy substituted PMI **5c** was isolated with traces of unknown impurity. From another reaction, a constitutional isomer of PMI(OAr)<sub>2</sub> **5b** was isolated, which was confirmed by the <sup>1</sup>H-<sup>1</sup>H COSY (Figure 2.2).

Compounds PMI(OAr)<sub>3</sub> **5a** and PMI(OAr)<sub>2</sub> **5b** were not separable by standard chromatography, however separation was successful on analytical scale by HPLC using (60:40) THF and H<sub>2</sub>O as the mobile phase on bifunctional reverse phase column (octadecyl and phenyl, 4.6 x 250 mm, 5 μm). The mixture of compounds **5a** and **5b** were used as such for the next step.

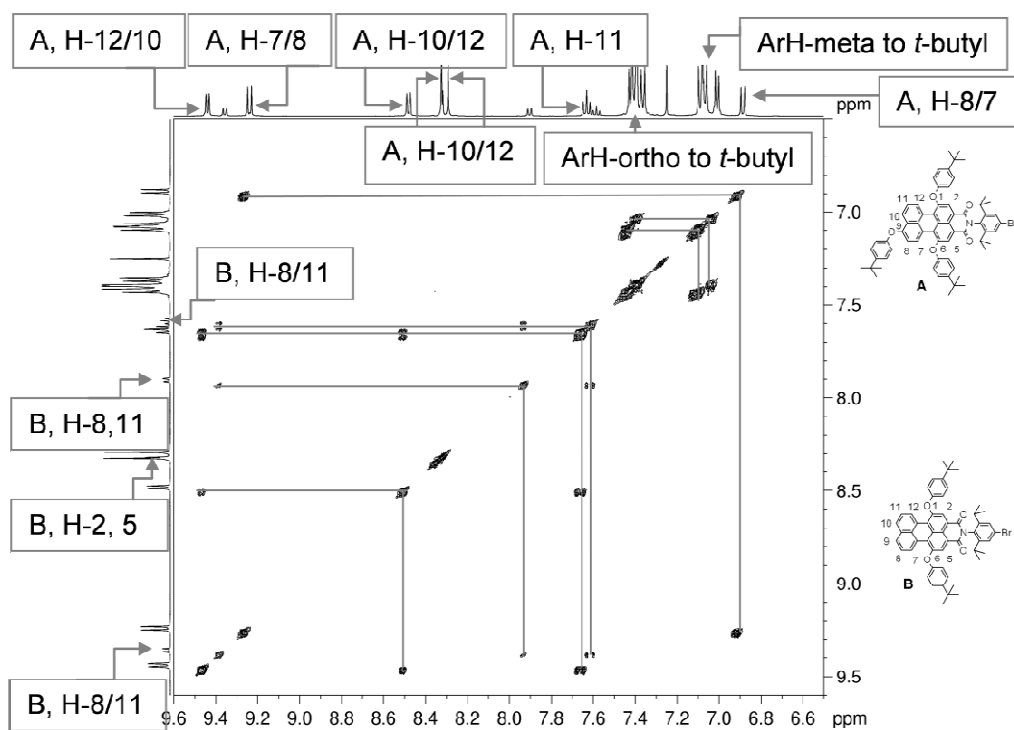


**Figure 2.1**  $^1\text{H}$ - $^1\text{H}$  COSY of the mixture of compounds PMI(OAr)<sub>3</sub> **4a** (A) and PMI(OAr)<sub>2</sub> **4b** (B); solvent: CHCl<sub>3</sub>, 500 MHz.

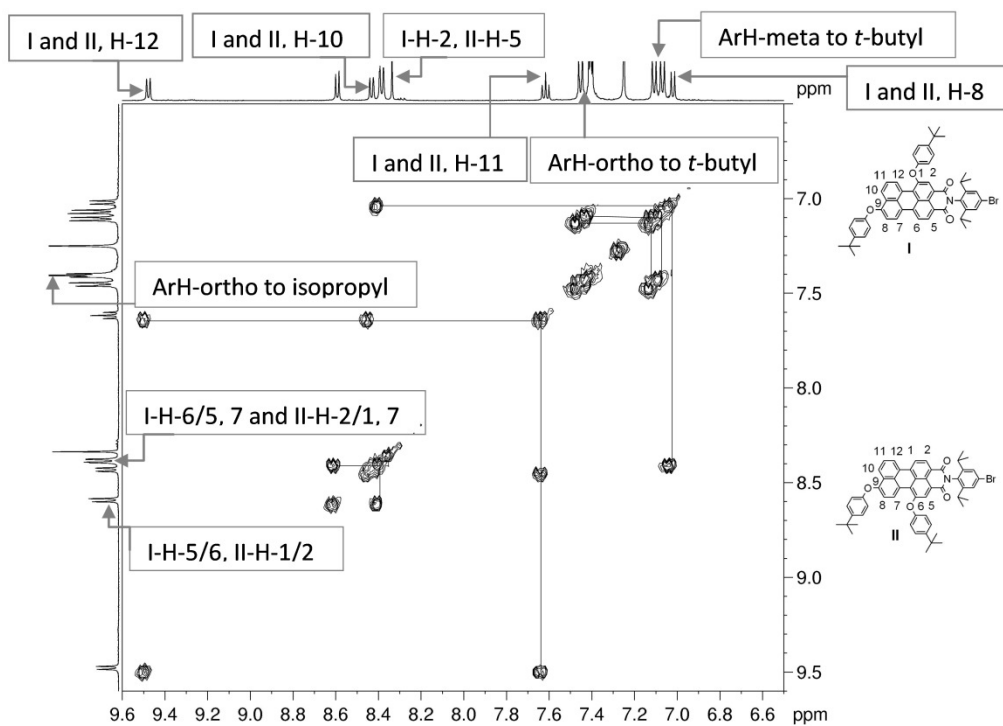


**Figure 2.2**  $^1\text{H}$ - $^1\text{H}$  COSY of the mixture of constitutional isomers of PMI(OAr)<sub>2</sub> **4b** (I and II); solvent: CHCl<sub>3</sub>, 500 MHz.

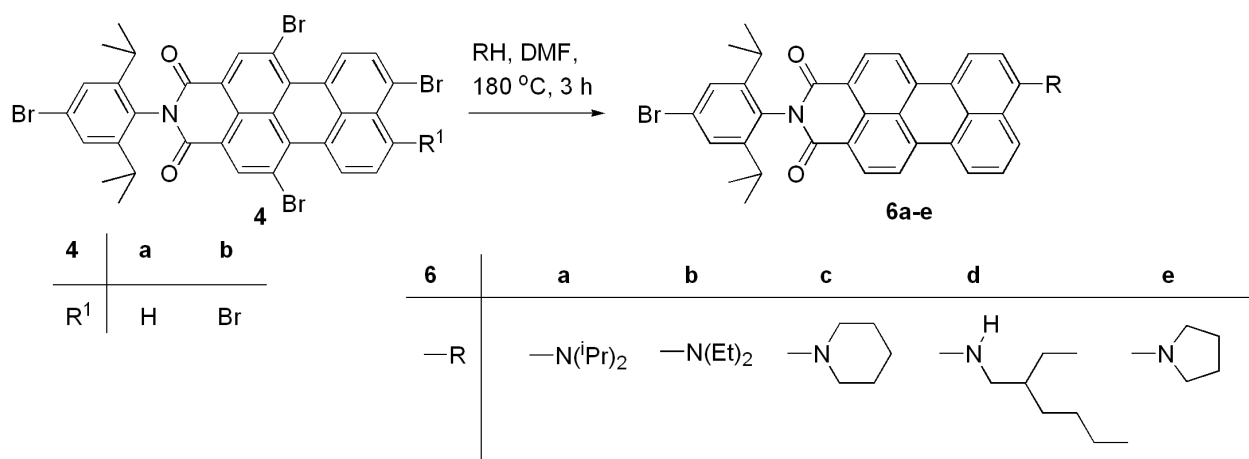
It was observed that when the reaction was carried out at a bath temperature of 185 °C, the formation of the PMI(OAr)<sub>2</sub> **5b** was high (up to 23%), whereas at a bath temperature of 170 °C, the formation of the PMI(OAr)<sub>2</sub> **5b** was low (up to 3%).

### 2.2.3 Amino-substituted perylenemonoimide

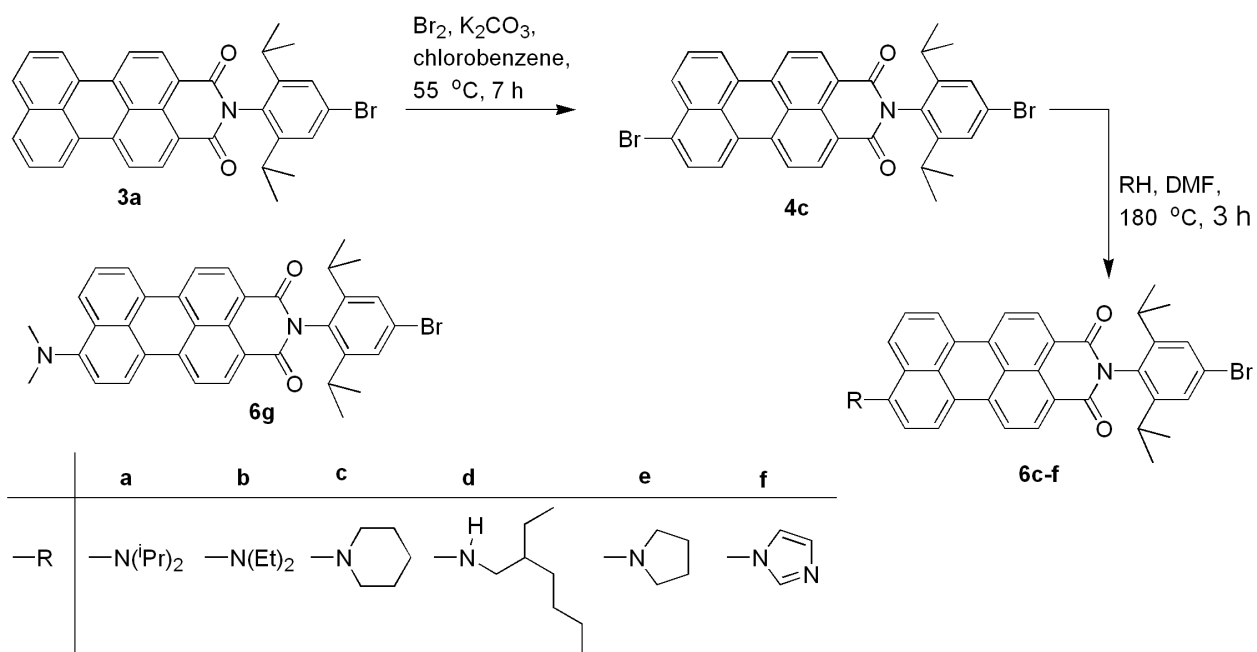
To the best of our knowledge, only three synthetic routes have been reported for amino-substituted PMI derivatives until now: Fieler *et al.*<sup>47</sup> used a conventional synthetic route to prepare a primary amino-substituted PMI by the nitration of PMI with nitrogen dioxide and reduction of the product with iron powder and HCl. Becker *et al.*<sup>60</sup> have developed a method to introduce diphenylmethylenimino group at the 9-position of PMI by using palladium catalyzed *N*-aryl-coupling reaction. The amino compound was isolated by hydrolysis of the *N*-aryl coupling product by using catalytic amount of HCl in wet THF. Wasielewski's group have introduced pyrrolidine at the 9-position of PMI with additional substituents at 1- and 6- position by nucleophilic substitution of bromine.<sup>58,59</sup> Later, Hudhomme's group prepared the 9-pyrrolidino PMI by following the same procedure described by Wasielewski.<sup>60</sup> We followed the procedure reported by the Wasielewski's group to synthesize the triamino substituted PMI starting from the PMI(Br)<sub>3</sub> **4a**. Instead of getting the triamino substituted PMI, we isolated monoamino substituted PMI as the major product.

We synthesized a series of amino-substituted perylenemonoimide starting from a 1:20 mixture of PMI(Br)<sub>4</sub> **4b** and PMI(Br)<sub>3</sub> **4a** (Scheme 2.4). The compound **4** was refluxed with excess of the amines (*i*Pr)<sub>2</sub>NH, Et<sub>2</sub>NH, piperidine, 2-ethylhexyl amine, and pyrrolidine in DMF for 3 h to obtain required products **6**. However, for (*i*Pr)<sub>2</sub>NH and Et<sub>2</sub>NH the reactions failed to give the product even after refluxing for 24 h.



**Scheme 2.4** Synthesis of amino-substituted starting from PMI(Br)<sub>3</sub> **4**.

In case of the other amines, mono substitution product **6c-e** were obtained within a reaction time of 3 h. A 1:20 mixture of PMI(Br)<sub>4</sub> **4b** and PMI(Br)<sub>3</sub> **4a** was refluxed with excess pyrrolidine in DMF for 3 h to afford the PMI(Py) **6e** as a blue solid in 80% yield. However, later the amino-substituted compounds **6c-f** were prepared from starting the monobromo PMI **4c** (Scheme 2.5).

**Scheme 2.5** Synthesis of amino-substituted PMI starting from PMI(Br) **4c**.

The monobromo PMI **4c** was synthesized starting from the PMI **3a** following the procedure described by Lindsey.<sup>56</sup> A solution of PMI **3a** in chlorobenzene was treated with excess bromine and heated at 55 °C for 7 h to obtain the monobromo PMI **4c** in quantitative yield (Scheme 2.5).<sup>56</sup> The crude material was used as such for the next reactions. The PMI(Br) **4c** was refluxed with excess amines (*i*Pr)<sub>2</sub>NH, (Et)<sub>2</sub>NH, piperidine, 2-ethylehexylamine, pyrrolidine and imidazole in DMF (Scheme 2.5). The reactions for amines like piperidine, 2-ethylhexyl amine, and pyrrolidine completed within 3 h and the yield was 70-77%. For (Et)<sub>2</sub>NH and (*i*Pr)<sub>2</sub>NH, the reaction mixture was refluxed for 24 h. There was no product or very little of the desired product for the former, whereas in case of later dimethylamino-substituted PMI PMI(Me)<sub>2</sub> **6g** was isolated as major product instead of the desired product. Similarly, the reaction was slow for imidazole and it took around 24 h for completion. A very small amount of PMI(Me)<sub>2</sub> **6g** was isolated as a side product along with the desired product **6f**.

## 2.3 Photophysical studies

The absorption and emission spectra of the amino-substituted PMI (**6c-6e** and **6g**) were recorded in various solvents of different polarity (toluene, THF,  $\text{CHCl}_3$ , and AcCN) and the spectral data have been collected in table 2.1 and the corresponding spectra are shown in figure 2.3.

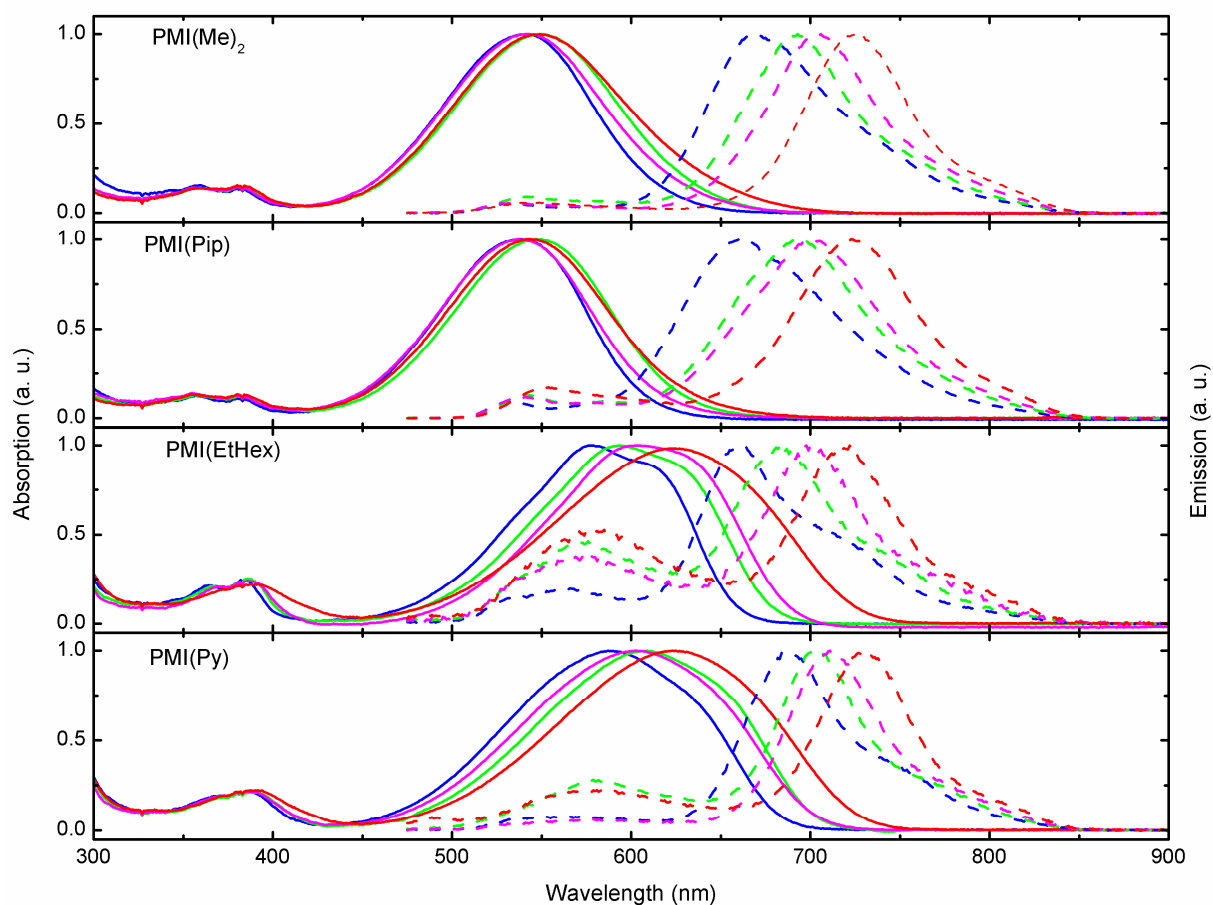


**Figure 2.3** Absorption (solid) and emission spectra (dashed) for PMI( $\text{Me}$ )<sub>2</sub> **6g**, PMI(Pip) **6c**, PMI(EtHex) **6d**, and PMI(Py) **6e** in various solvents with different polarity (toluene (blue), THF (magenta),  $\text{CHCl}_3$  (green), and AcCN (red)). The absorption and emission spectra are normalized at their respective peak maximum. The excitation wavelength was at 465 nm with 5 nm slit widths.

**Table 2.1** Absorption and emission spectral data of amino-substituted PMI (**6c-6e** and **6g**) in various solvents with increasing polarity from left to right.<sup>a,b</sup>

Samples	Absorption Max. ( $\lambda_{\max}$ , nm)				$\epsilon^c$	Emission Max. ( $\lambda_{\max}$ , nm)				Stokes shift ( $\text{cm}^{-1}$ ) AcCN <sup>d</sup>
	Toluene	THF	CHCl <sub>3</sub>	AcCN <sup>d</sup>		Toluene	Toluene	THF	CHCl <sub>3</sub>	
<b>6g</b>	542	542	550	549	32600	669	706	693	726	53476
<b>6c</b>	539	537	547	544	32867	660	701	691	723	55866
<b>6d</b>	578	604	593	614	30138	660	698	685	722	84746
<b>6e</b>	587	603	609	625	27714	687	711	705	732	93458

<sup>a</sup>Emission spectra were measured after exciting the solution at 465 nm. <sup>b</sup>Concentrations of the dyes **6g** and **6c** were set at 2.98  $\mu\text{M}$  and 2.97  $\mu\text{M}$  respectively, and for the dyes **6d** and **6e** were set at 2.93  $\mu\text{M}$  in toluene, CHCl<sub>3</sub>, and THF. <sup>c</sup>Molar extinction coefficient ( $\text{mol}^{-1}\text{cm}^{-1}\text{L}$ ) measured in toluene at the respective absorption maxima. <sup>d</sup>Dilute solutions with OD  $\approx$  0.098 at absorption maximum (typically corresponded to a concentration in micromolar range) were used for the measurements.

In principle, absorption of light excites the fluorophores from ground state  $S_0$  to the first singlet excited state  $S_1$ . If the fluorophores further excited to the second singlet excited state  $S_2$ , it rapidly decays to the  $S_1$  state in  $10^{-12}$  s due to internal conversion.<sup>3,4</sup> Emission from fluorophores generally occurs at higher wavelength than those at which absorption occurs. This loss of energy is due to the various processes i.e. internal conversion and vibrational relaxation that occur immediately after light absorption. Solvent effects shift the emission to still lower energy due to stabilization of the excited state by polar solvents; as a consequence the emission occurs in higher wavelength. The fluorophore has a larger dipole moment ( $\mu_e$ ) in excited state than the ground state

( $\mu_g$ ). After excitation the solvent dipoles undergo reorientation or relaxation around the excited dipole moment  $\mu_e$  of the dye, which stabilize the energy further and lower the energy of the excited states and the solvent relaxation occurs within 10-100 ps.<sup>3,4</sup> As the solvent polarity increases, this effect becomes larger and resulting emission occurs at higher wavelength. Usually absorption spectra are less sensitive to solvent effects, because absorption of light occurs in about  $10^{-15}$  s, which is too short for the motion of solvents or fluorophores.<sup>3,4</sup>

The result in table 2.1 shows a 5-8 nm bathochromic shift of the absorption maxima for dyes **6g** and **6c**, whereas for the dyes **6d** and **6e** a bathochromic shift of 5-38 nm by changing solvent from toluene to acetonitrile. This big bathochromic shift observed in case of the later dyes is not explainable by the normal solvent effects. This could be due to some specific solvent effects like hydrogen bonding, preferential solvation, acid-base chemistry, or charge-transfers interactions.<sup>3,4,62,63</sup> Specific solvent effects occur both in ground state or excited state. If it occurs in ground state, then one should expect changes in absorption spectrum,<sup>3</sup> which we observed for the dyes **6d** and **6e**. For these dyes the specific solvent effects could be explained by the charge-transfer interactions.

The dashed lines in figure 2.3 consist of two emission bands, a short-wavelength band and a long-wavelength for all of the dyes **6c-6e** and **6g**. The short-wavelength emission band for the dyes **6g** and **6c** appears in 530-550 nm range, where as for the dyes **6d** and **6e**, it appears in the range of 570-585 nm. The percentage of intensity of the short-wavelength emission bands w.r.t. the long-wavelength emission bands are presented in table 2.2. This result suggests that the intensity of short-wavelength band

increases with increase in polarity except **6g**. Additionally; it shows that the intensities in the short-wavelength region of the dyes are higher for CHCl<sub>3</sub> and AcCN. The dyes **6d** and **6e** have higher intensity in comparison to the other two dyes in the short-wavelength region. The data on table 2.2 shows a good correlation between the solvent polarities with the intensity of short-wavelength band.

**Table 2.2** Percentage of the intensity of the short-wavelength emission bands w.r.t. the long-wavelength emission bands of the dyes **6c-6e** and **6g** in various solvents with increasing solvent polarity from toluene to AcCN.

Solvents	PMI(Me) <sub>2</sub> <b>6g</b>	PMI(Pip) <b>6c</b>	PMI(EtHex) <b>6d</b>	PMI(Py) <b>6e</b>
Toluene	6%	9%	20%	8%
THF	6%	12%	39%	6%
CHCl <sub>3</sub>	9%	13%	46%	28%
AcCN	6%	17%	53%	23%

According to the twisted intramolecular charge-transfer state (TICT) hypothesis, if a fluorophore contains both an electron donating and an electron-accepting group, for instance, the dyes **6c-6e** and **6g** contain the amino groups as the electron-donating group and the imides groups as the electron-accepting groups, after excitation at specific wavelength a short-wavelength emission band could be due to the coplanar state known as locally excited (LS) state and the long-wavelength emission band appears due to the twisted conformation, which causes full charge-separation/charge transfer (CT) between the amino group and the imide group of the perylene-core.<sup>3,4,62-66</sup> The charge-separation between the amino and imide group of the perylene-core in twisted state is further enhanced in comparison to the LS by increasing the solvent

polarity, as a result stabilization of excited states occurs by the reorientation of the solvent dipoles giving emission in longer wavelength region.

The effect of the solvent polarity on emission maximum is more significant than that on the absorption maximum. A change of solvent from toluene to acetonitrile leads to a red shift of the absorption maximum of the dyes **6g** and **6c** by 7 nm and 5 nm respectively, whereas, the magnitude of the spectral shifts in emission are 8 and 12 times. This bathochromic shift in emission spectra could be well explained by the increase of solvent polarity and also specific solvent effects like TICT. These results also suggest that the excited state of the system is more polar than the ground state and also the dipole moment of excited state is higher than the ground state.

The excitation spectra of the dyes (the same solutions used for emission measurement) were recorded keeping the emission wavelength at 600 nm and 800 nm in various solvents with different polarity and a few representative spectra are shown in figure 2.4. A short-wavelength band is found in the excitation spectra upon emission at 600 nm which corresponds to the short-wavelength emission. This result suggests the presence of twisted state in the ground state.

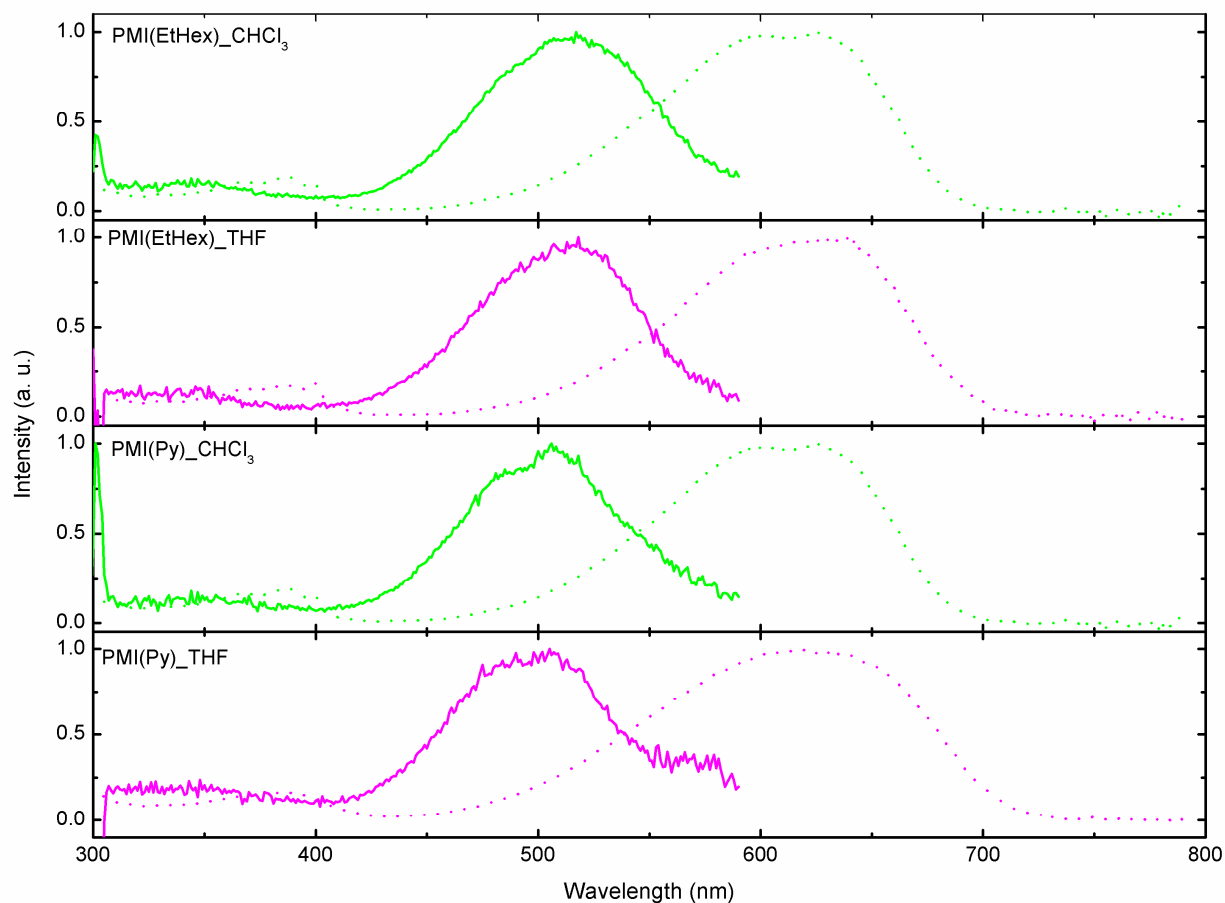


**Figure 2.4** Excitation spectra for PMI(EtHex) **6d** and PMI(Py) **6e** in CHCl<sub>3</sub> (green) and THF (magenta) at different emissions. The emissions were at 600 nm (solid line) and 800 nm (dotted line).

The lifetime decays of the dyes **6c-6e** and **6g** have been studied in toluene and AcCN and the data have been presented in table 2.3. The dyes in toluene were excited at 495 nm and lifetime decays were measured at 670 nm. Similarly, the dyes in AcCN were excited at 495 nm and the lifetime decays were measured at different emissions (570 nm, 670 nm, and 720 nm).

The data on table 2.3 shows relatively longer lifetime decays ( $\tau_1$ ) with major components for all of the dyes in AcCN (excitation at 495 nm and collected emission at



720 nm). The shorter lifetime decays ( $\tau_2$ ) are almost negligible (2-5%). This result suggests that the longer lifetime decays ( $\tau_1$ ) are due to the long-wavelength emission of the dyes. Similarly, the data on table 2.3 shows predominantly longer lifetime decays ( $\tau_1$ ) with major components (around 100%) for the dyes **6c** and **6g** in AcCN (excitation at 495 nm and collected emission at 670 nm).

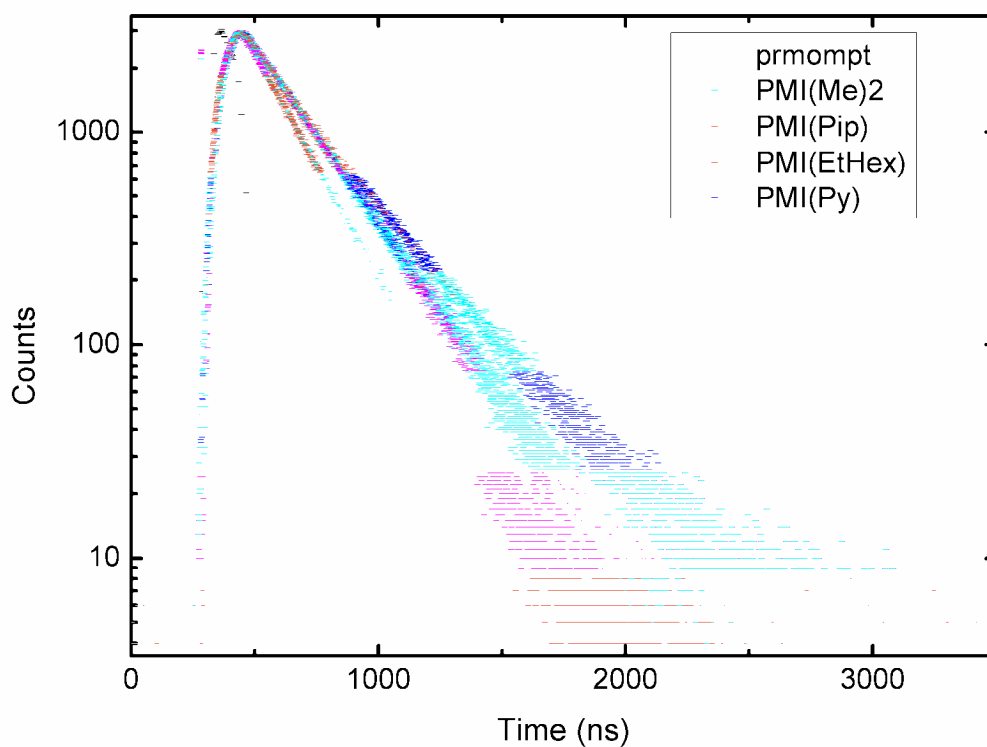


**Figure 2.5** Lifetime decays of the PMI(Me)<sub>2</sub> **6g** (blue), PMI(PiP) **6c** (magenta), PMI(EtHex) **6d** (cyan), PMI(Py) **6e** (orange) and the prompt (black). The prompt is the instrument response function (IRF), which is the response of instrument to a zero lifetime sample. This curve is typically collected using a dilute scattering solution such as colloidal silica (Ludox) and no emission filter. The excitation wavelength was 495 nm and emission was 670 nm.

**Table 2.3** Lifetime decays of amino-substituted PMI (**6c-d**, and **6g**) in toluene<sup>a</sup> and acetonitrile.<sup>b</sup>

Sam- ples	Toluene <sup>c</sup> ( $\lambda_{\text{ex}} = 495 \text{ nm}$ )				Acetonitrile <sup>c</sup> ( $\lambda_{\text{ex}} = 495 \text{ nm}$ )											
	$\lambda_{\text{em}} = 670 \text{ nm}$				$\lambda_{\text{em}} = 570 \text{ nm}$				$\lambda_{\text{em}} = 670 \text{ nm}$				$\lambda_{\text{em}} = 720 \text{ nm}$			
	$\tau(\text{ns})$		$\alpha$		$\tau(\text{ns})$		$\alpha$		$\tau(\text{ns})$		$\alpha$		$\tau(\text{ns})$		$\alpha$	
	$\tau_1$	$\tau_2$	$\alpha_1$	$\alpha_2$	$\tau_1$	$\tau_2$	$\alpha_1$	$\alpha_2$	$\tau_1$	$\tau_2$	$\alpha_1$	$\alpha_2$	$\tau_1$	$\tau_2$	$\alpha_1$	$\alpha_2$
<b>6g</b>	3.72	0.13	97	3	4.61	1.77	69	31	3.53	0.12	99	1	3.52	0.13	98	2
<b>6c</b>	3.24	0.12	98	2	5.17	0.12	100	0	3.46	0.13	97	3	3.44	0.12	97	3
<b>6d</b>	2.50	0.12	95	5	4.85	1.15	96	4	3.64	1.83	65	35	2.51	0.12	95	5
<b>6e</b>	4.41	2.54	60	40	4.69	0.12	100	0	4.71	2.78	81	19	3.62	0.13	97	3

<sup>a</sup>The solutions were excited at 495 nm and the lifetime decays were measured at 670 nm. <sup>b</sup>The solutions were excited at 495 nm and the lifetime decays were measured at different emissions (570 nm, 670 nm, and 720 nm). <sup>c</sup>The lifetime decays for the dyes were fitted by a biexponential function. The lifetime decay fitting were done by Dr. Ralf Brune.

Again these lifetime decay values are similar to the previously obtained values at the emission of 720 nm. These results suggest that the lifetime decays for dyes **6c** and **6g** are due to the longer emission band and it is in good agreement with the result obtained from emission spectra. Whereas for the dyes **6d** and **6e** the data shows two lifetime decays, which suggest that the two lifetime decays arise due to the presence of the longer wavelength band and shorter wavelength band components of the dyes. The relatively longer lifetime decays are due to the short-wavelength band and the shorter lifetime decays are due to the long wavelength band of the dyes. The result shows predominantly longer lifetime decay with major component (around 100%) for the dyes **6c-6e** in AcCN at the emission of 570 nm. This suggests that these lifetime decays arise exclusively due to the short-wavelength band. Whereas, for the dye **6g** there are two lifetime decays one with longer lifetime decay and the other with shorter. These results suggest that the longer lifetime decay for the dye **6g** is due to the short-wavelength band components and the shorter lifetime decay is due to long-wavelength band. These results are in good agreement with our emission data and also explain the dual fluorescence.

It is fair to compare the obtained lifetime decays of the dyes in toluene and acetonitrile at the excitation wavelength of 495 nm and monitoring the emission at 670 nm (Table 2.3). These results show that the major components with relative longer lifetime decay for all dyes except for the dye **6g** increases with polarity of the solvent. These results also support the fact that the percentage of the short-wavelength band increases with increasing polarity of the solvents.

The photophysical properties of the bench mark perylenemonoimide dyes **3b** and **25a** were reported on literature.<sup>54</sup> The synthesis of dye **25a** was discussed in chapter 4. Considering the photophysical properties the dye **25a** was chosen as one of the fluorophores for FRET study.

The photophysical studies of the fluorophores **6c-6e** and **6g** show that the PMI(Py) **6e** has higher absorption and emission maxima in comparison to the other fluorophores. Therefore, PMI(Py) was chosen as the second fluorophore for the construction of molecular ruler (Chapter 4, sec 4.2).

## Chapter 3

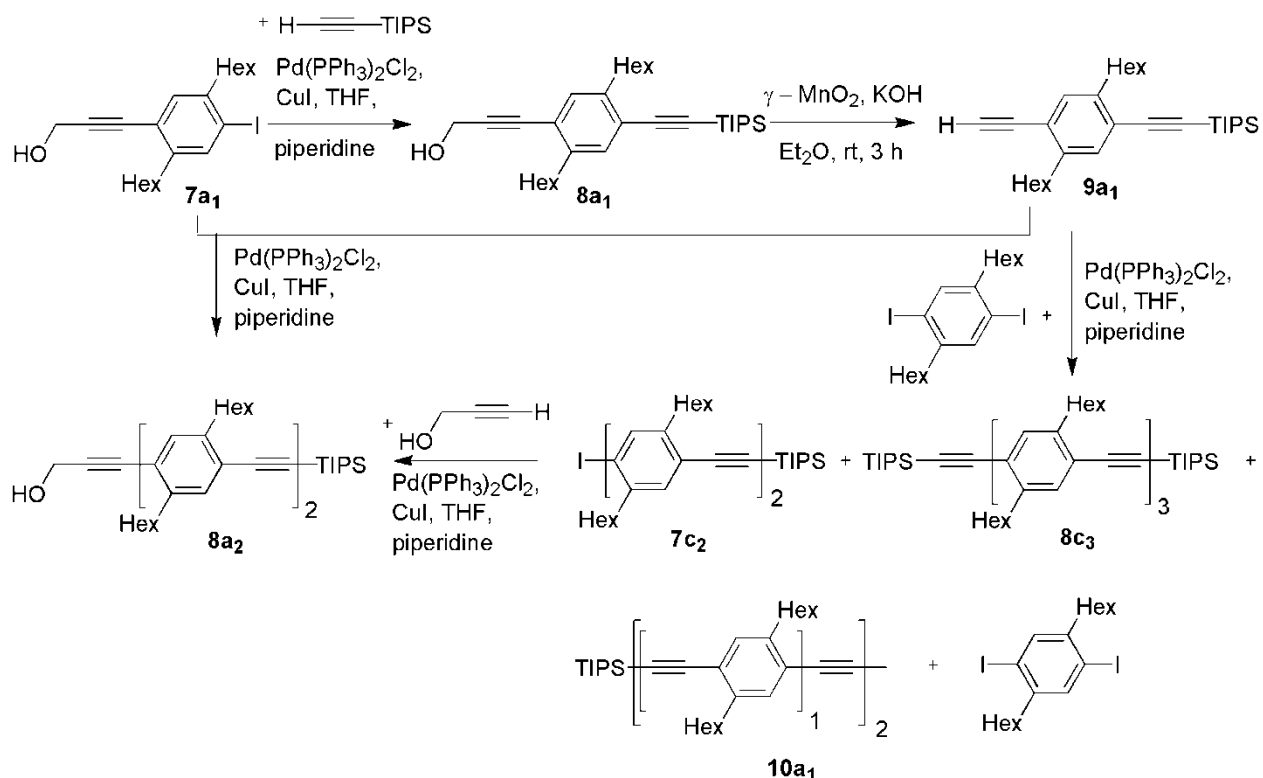
# Synthesis of oligo(*para*-phenyleneethynylene)s as spacer

### 3.1 Introduction

Monodisperse and shape persistent oligomers, e.g. oligo(*para*-phenyleneethynylene)s (oligoPPEs) are attractive building blocks for molecular and supramolecular architectures.<sup>67,68</sup> Recently Godt *et al.*<sup>38</sup> used the oligoPPEs as the backbone for the spin labeled oligomers for measuring the spin-to-spin distance distribution and extracted the end-to-end distance distribution of the oligoPPEs by EPR measurement. Similarly one can obtain such type of information on fluorescent labeled molecules by FRET.<sup>3-8</sup> We were interested for comparing these two very different methods. For a fair comparison of these two methods, a series of oligoPPEs of different lengths were chosen as the backbone and attached to suitable fluorophores. In this section, I will discuss the details about the synthesis of oligoPPEs.

### 3.2 Synthesis of monodisperse oligoPPEs using hydroxymethyl (HOM) and TIPS as orthogonal protecting groups

A series of oligoPPEs of different lengths were synthesized following the divergent and convergent approach described by Kukula *et al.*<sup>69</sup> Previously synthesized compounds 1,4-dihexyl-2,5-diiodobenzene and iodo monomer **7a**<sub>1</sub>, which contain an iodo group at one end and the hydroxymethyl (HOM) at the other end were used as the starting material for the synthesis of the oligoPPEs.

**Scheme 3.1** Synthesis of dimer **8a<sub>2</sub>**.

The initial idea was to synthesize iodo dimer **7c<sub>2</sub>** with two repeating phenyleneethynylene units for the shortest fluorophore labeled oligoPPEs. Therefore, the iodo monomer **7a<sub>1</sub>** was coupled with TIPS acetylene to afford **8a<sub>1</sub>** (Scheme 3.1). The reaction was carried out at 50 °C for overnight and afterwards monitored by thin layer chromatography (TLC). The TLC analysis showed incomplete reaction, therefore 0.5 equiv. of TIPS acetylene and equal amounts of catalysts were added and the reaction was continued for another 8 h to obtain **8a<sub>1</sub>**. A byproduct **8d<sub>1</sub>** (Figure 3.1) was formed in 35 mol% (estimated from the  $^1\text{H-NMR}$  spectrum of the crude product). However, later the monomer **8a<sub>1</sub>** was successfully synthesized by the coupling of the iodo monomer **7a<sub>1</sub>** with TIPS acetylene at room temperature for 18 h along with 5 mol% (estimated from the  $^1\text{H-NMR}$  spectrum of the crude products) of the carbometalation product **8d<sub>1</sub>**

(Figure 3.1). The monomer **8a<sub>1</sub>** contains two orthogonal acetylene protecting units HOM and TIPS at both ends of the compound.

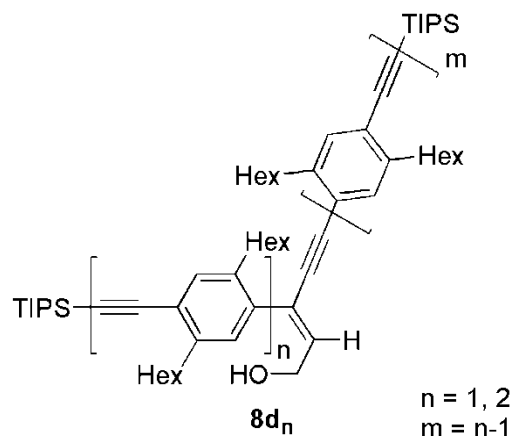


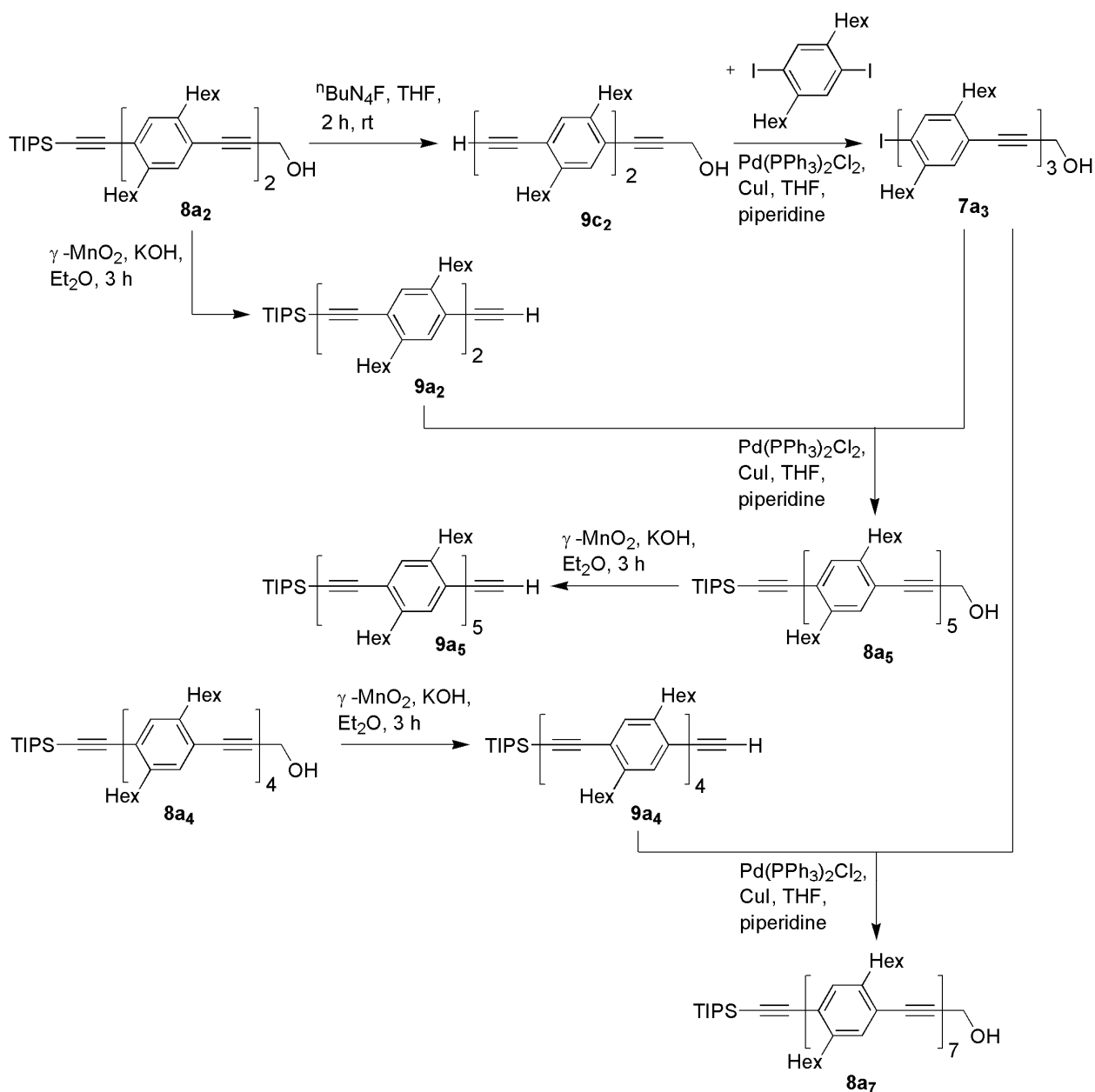
**Figure 3.1** Structural representation of carbomatalation product **8d<sub>n</sub>**.

The monomer **8a<sub>1</sub>** was treated with  $\gamma$ -MnO<sub>2</sub>/KOH in Et<sub>2</sub>O to afford non-polar acetylene **9a<sub>1</sub>** as described by Kukula *et al.*<sup>69</sup> and the yields were around 72-82%. The non-polar acetylene **9a<sub>1</sub>** was coupled with 1.5 equiv. of 1,4-dihexyl-2,5-diiodobenzene to afford the iodo dimer **7c<sub>2</sub>**. In this reaction, the desired product **7c<sub>2</sub>** was formed along with other side products e.g. the disubstituted product **8c<sub>3</sub>**, the acetylene dimerization product **10a<sub>1</sub>** and the unreacted 1,4-dihexyl-2,5-diiodobenzene. Unfortunately, the  $R_f$  values of the compounds **7c<sub>2</sub>**, **8c<sub>3</sub>**, **10a<sub>1</sub>**, and 1,4-dihexyl-2,5-diiodobenzene are very close to each other with a  $R_f$  value of 0.15 in 1:1 Et<sub>2</sub>O and *n*-pentane. Therefore, isolation of the desired product **7c<sub>2</sub>** was not successful by flash chromatography. At this point, I decided to run further reaction by treating the crude material with excess 2-propynol to obtain dimer **8a<sub>2</sub>** instead of isolating the iododimer **7c<sub>2</sub>** by chromatographic separation.

The crude material containing the mixture of compounds **7c<sub>2</sub>**, **8c<sub>3</sub>**, **10a<sub>1</sub>**, and 1,4-dihexyl-2,5-diiodobenzene was treated with excess 2-propynol, so that the iodo dimer **7c<sub>2</sub>** gave the desired product **8a<sub>2</sub>**, which has one HOM group and comparatively more polar than compounds **8c<sub>3</sub>**, and **10a<sub>1</sub>**. Simultaneously, the unreacted 1,4-dihexyl-2,5-diiodobenzene coupled with two equivalents of 2-propynol to afford highly polar disubstituted compound with two HOM groups. The TLC analysis showed three spots with  $R_f$  values 0.15, 0.43, and 0.74. The desired product **8a<sub>2</sub>** ( $R_f = 0.43$ ) was isolated by flash chromatography. However, later the dimer **8a<sub>2</sub>** was synthesized by the coupling of the iodo monomer **7a<sub>1</sub>** with the non-polar acetylene **9a<sub>1</sub>** in 80-87% yields. Traces amount of separable carbometalation product **8d<sub>2</sub>** was formed as a byproduct (Figure 3.1).

The next target was to synthesize the higher homologs of **8a<sub>n</sub>**. Therefore, the dimer **8a<sub>2</sub>** was treated with the  $\gamma$ -MnO<sub>2</sub>/KOH in Et<sub>2</sub>O to afford non-polar acetylene **9a<sub>2</sub>** in 72-80% yields (Scheme 3.2).<sup>69,70</sup> On the other hand, the dimer **8a<sub>2</sub>** was treated with <sup>n</sup>Bu<sub>4</sub>NF in THF to afford polar acetylene **9c<sub>2</sub>** quantitatively. The polar acetylene **9c<sub>2</sub>** was coupled with 1.5 equiv. of 1,4-dihexyl-2,5-diiodobenzene to afford iodo trimer **7a<sub>3</sub>** in 53-58% yields. The iodo trimer **7a<sub>3</sub>** was coupled with the non-polar acetylene **9a<sub>2</sub>** to afford pentamer **8a<sub>5</sub>** in 72-73% yields and subsequently the HOM group was removed to isolate the non-polar acetylene **9a<sub>5</sub>** in 67-72% yields (Scheme 3. 2).



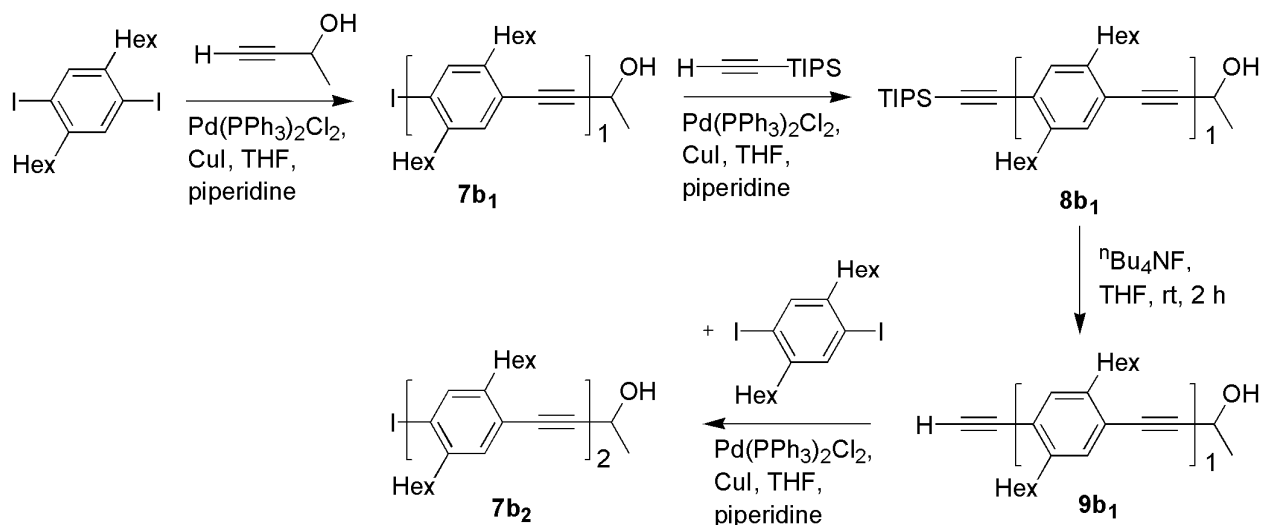
**Scheme 3.2** Synthesis of iodo trimer **7a<sub>3</sub>**, pentamer **8a<sub>5</sub>**, and heptamer **8a<sub>7</sub>**.

The previously synthesized tetramer **8a<sub>4</sub>** was treated with the  $\gamma\text{MnO}_2/\text{KOH}$  in  $\text{Et}_2\text{O}$  to afford non-polar acetylene **9a<sub>4</sub>** in 94% yield, which was subsequently coupled with the iodo trimer **7a<sub>3</sub>** to afford heptamer **8a<sub>7</sub>** in 92% yield (Scheme 3.2).

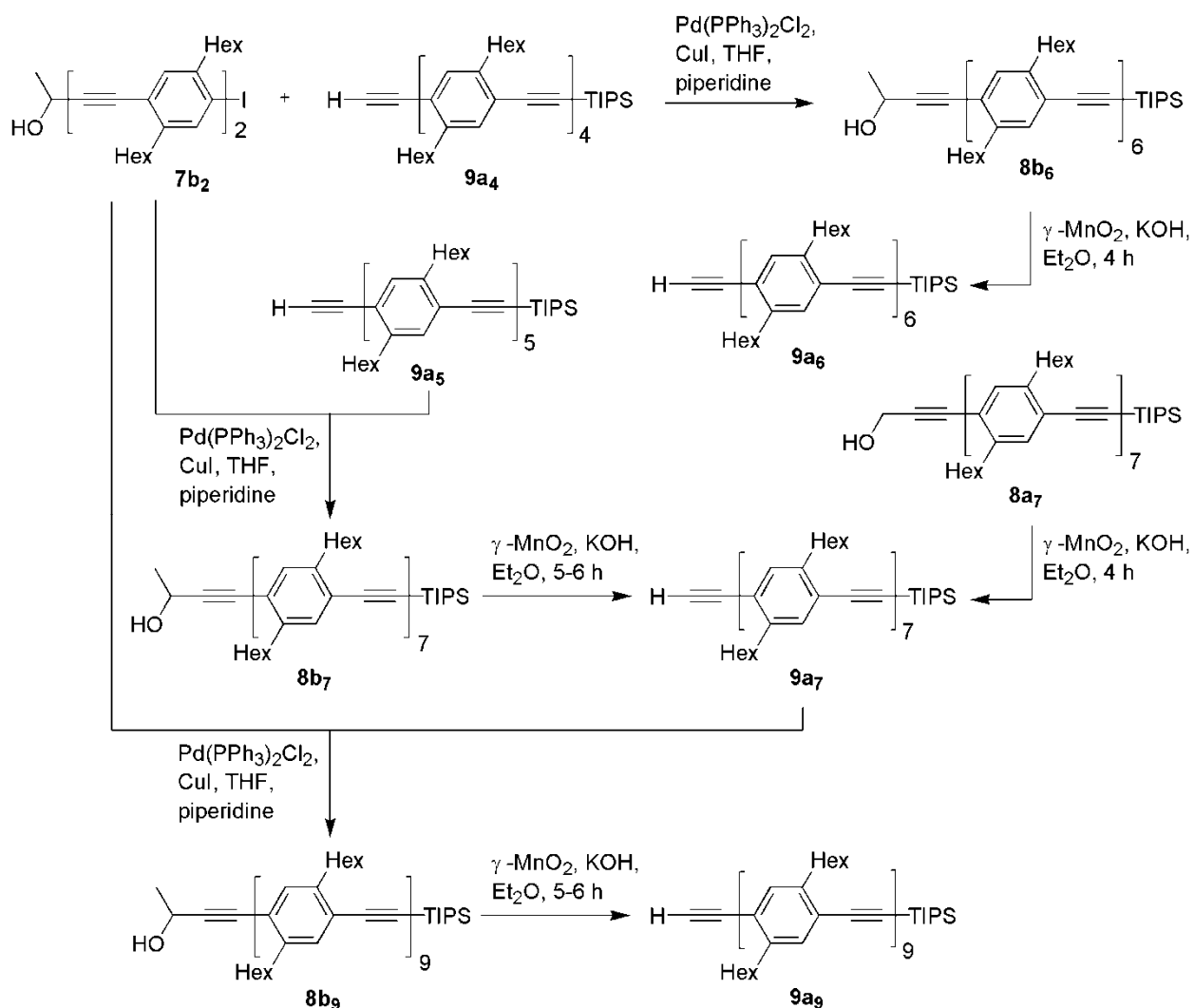
### 3.3 Synthesis of monodisperse oligoPPEs using hydroxyethyl (HOE) and TIPS as orthogonal protecting groups

Kukula *et al.*<sup>69</sup> have reported the carbometalation product as a side product in the synthesis of the monomer **8a<sub>1</sub>** whereas, I have also found the carbometalation product in the synthesis of both the monomer **8a<sub>1</sub>**, and the dimer **8a<sub>2</sub>**. Ms. Schulte has demonstrated that the formation of carbometalation product can be suppressed by using 3-butyn-2-ol instead of the 2-propynol. She has also demonstrated that the 4-aryl-3-butyn-2-ol can be deprotected to give the arylethyne with  $\gamma$ -MnO<sub>2</sub>/KOH in Et<sub>2</sub>O at room temperature. Therefore, we were interested to investigate whether the same methodology can be applied for the higher homologs of **8a<sub>n</sub>**. The iodo dimer **7b<sub>2</sub>**, which was used for the synthesis of hexamer **8b<sub>6</sub>**, heptamer **8b<sub>7</sub>**, and nonamer **8b<sub>9</sub>** was synthesized by Ms. Schulte. Later, I have also synthesized the iodo dimer **7b<sub>2</sub>** (Scheme 3.3).

The 3-butyn-2-ol was coupled with 1.5 equiv. of 1,4-dihexyl-2,5-diiodobenzene to afford iodo monomer **7b<sub>1</sub>** in 62% yield, which subsequently coupled with the TIPS acetylene at room temperature to afford monomer **8b<sub>1</sub>** in 75% yield. Unfortunately, the carbometalation product was found in 2 mol% (estimated from the <sup>1</sup>H-NMR spectra of the crude product) as a byproduct. The monomer **8b<sub>1</sub>** was treated with <sup>n</sup>Bu<sub>4</sub>NF in THF at room temperature to afford the polar acetylene **9b<sub>1</sub>** in quantitative amount. The polar acetylene **9b<sub>1</sub>** was coupled with 1.5 equiv. of 1,4-dihexyl-2,5-diiodobenzene to afford iodo dimer **7b<sub>2</sub>** in 52% yield (Scheme 3.3).

**Scheme 3.3** Synthesis of iodo monomer **7b<sub>1</sub>** and iodo dimer **7b<sub>2</sub>**.

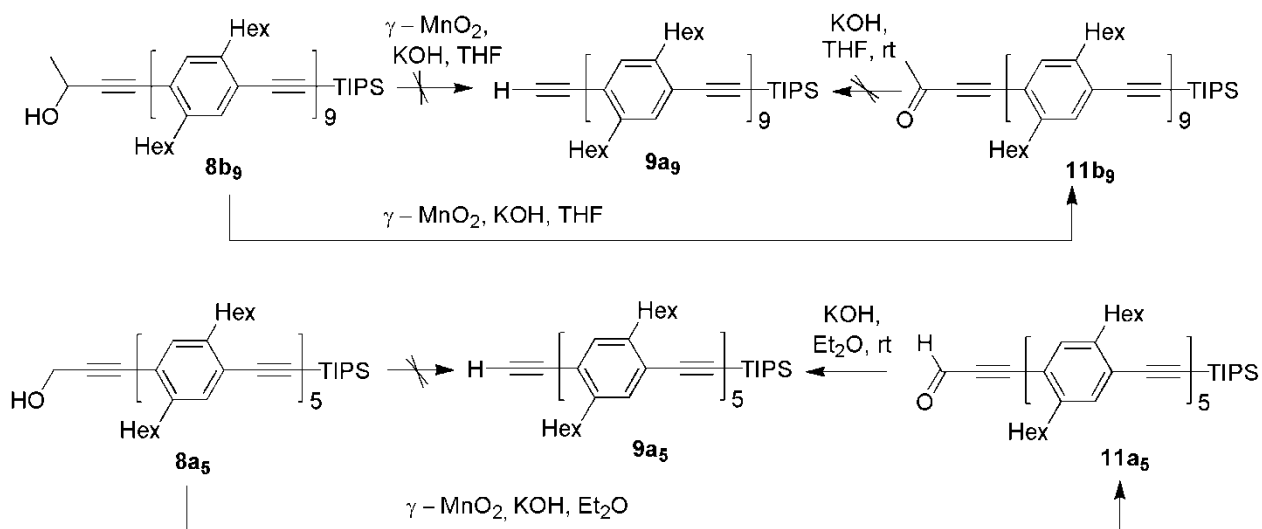
The iodo dimer **7b<sub>2</sub>** was coupled with non-polar acetylene **9a<sub>4</sub>** and **9a<sub>5</sub>** to afford hexamer **8b<sub>6</sub>** and heptamer **8b<sub>7</sub>** respectively, in 79-97% yields, which contain two orthogonal protecting groups TIPS and hydroxyethyl (HOE). As expected, the HOE group of the hexamer **8b<sub>6</sub>** and the heptamer **8b<sub>7</sub>** was removed by the  $\gamma\text{MnO}_2/\text{KOH}$  in  $\text{Et}_2\text{O}$  at room temperature to afford the respective non-polar acetylenes **9a<sub>6</sub>** and **9a<sub>7</sub>**. Treatment of the heptamer **8a<sub>7</sub>** with  $\gamma\text{MnO}_2/\text{KOH}$  in  $\text{Et}_2\text{O}$  at room temperature also afforded non-polar acetylene **9a<sub>7</sub>**. The nonamer **8b<sub>9</sub>** was synthesized by coupling the iodo dimer **7b<sub>2</sub>** and the non-polar acetylene **9a<sub>7</sub>** and the yield was 71-94%. The nonamer **8b<sub>9</sub>** was not sufficiently soluble in  $\text{Et}_2\text{O}$ , so THF was used as solvent for the removal of HOE group. The nonamer **8b<sub>9</sub>** was treated with the  $\gamma\text{MnO}_2/\text{KOH}$  in THF to afford **9a<sub>9</sub>** in 70-79% yields (Scheme 3.4).

**Scheme 3.4** Synthesis of oligomers **8b<sub>n</sub>**, and non-polar acetylenes **9b<sub>n</sub>** (n = 6, 7, 9).

When the nonamer **8b<sub>9</sub>** was treated with  $\gamma\text{-MnO}_2/\text{KOH}$  from a previously synthesized batch (more than six months old), the nonamer **8b<sub>9</sub>** was oxidized to give the ketone **11b<sub>9</sub>** rather than the free acetylene **9a<sub>9</sub>** (Scheme 3.5). For our curiosity, to check the reactivity of the  $\gamma\text{-MnO}_2$ , we treated the pentamer **8a<sub>5</sub>** with  $\gamma\text{-MnO}_2/\text{KOH}$  from the same batch which was used in the former case. The pentamer **8a<sub>5</sub>** was oxidized to

give aldehyde **11a<sub>5</sub>** in preference to the free acetylene **9a<sub>5</sub>**. This clearly shows that, freshly prepared  $\gamma$ MnO<sub>2</sub> is required for the removal of HOM and HOE groups.

**Scheme 3.5** Schematic representation of aldehyde **11a<sub>5</sub>** and ketone **11b<sub>9</sub>**.



The intermediate aldehyde **11a<sub>5</sub>** was treated with excess powdered KOH to afford the free acetylene **9a<sub>5</sub>** (Scheme 3.5). Similarly, the intermediate **11a<sub>9</sub>** was treated with excess KOH and the reaction was monitored for 24 h, but there was no change in the reaction. These observations show that the  $\gamma$ MnO<sub>2</sub> might have some influence for the conversion of ketone to free acetylene.

In summary, I have synthesized the oligoPPEs **8a<sub>n</sub>** with  $n = 2, 5$  and oligoPPEs **8b<sub>n</sub>** with  $n = 6, 7,$  and  $9$ . The former molecules contain HOM and TIPS as the orthogonal protecting groups and the HOM group was removed by treatment of  $\gamma$ MnO<sub>2</sub>/KOH in Et<sub>2</sub>O. In the later series all of molecules contain HOE and TIPS as the orthogonal protecting groups. Interestingly, the HOE group was successfully removed by treatment with the  $\gamma$ MnO<sub>2</sub>/KOH. Freshly prepared  $\gamma$ MnO<sub>2</sub> is required for the removal of

HOM/HOE group. The oligoPPEs **9a<sub>n</sub>** with  $n = 2, 5, 7,$  and  $9$ , which contain a TIPS group at one end and the ethynylene group at the other end were used as spacer for the construction of the molecular ruler, which will be discussed in next chapter.

## Chapter 4

# Molecular rulers and their photophysical studies

### 4.1 Introduction

FRET is used as a “spectroscopic ruler”, particularly in the field of biosciences.<sup>3-8</sup> Two fluorophores are required for this technique and out of the two, one acts as donor and the other one as acceptor, which is not necessarily fluorescent. The energy transfer process takes place through a non-radiative long-range dipole-dipole interaction, only when the two fluorophores are in a close proximity of 1-10 nm.

One can also determine the end-to-end distances by EPR on spin labeled molecules.<sup>35-38</sup> The aim of the present work is to compare these two different methods FRET and EPR. For that reason, a molecular ruler was constructed taking oligoPPEs as the spacer.

Perylenemonoimide dye was chosen as fluorescent probe due to the following outstanding properties: i) high fluorescence quantum yield, ii) high thermal and photochemical stability, iii) absorbs and emits at higher wavelength than oligoPPEs.<sup>56,69,71,72</sup>

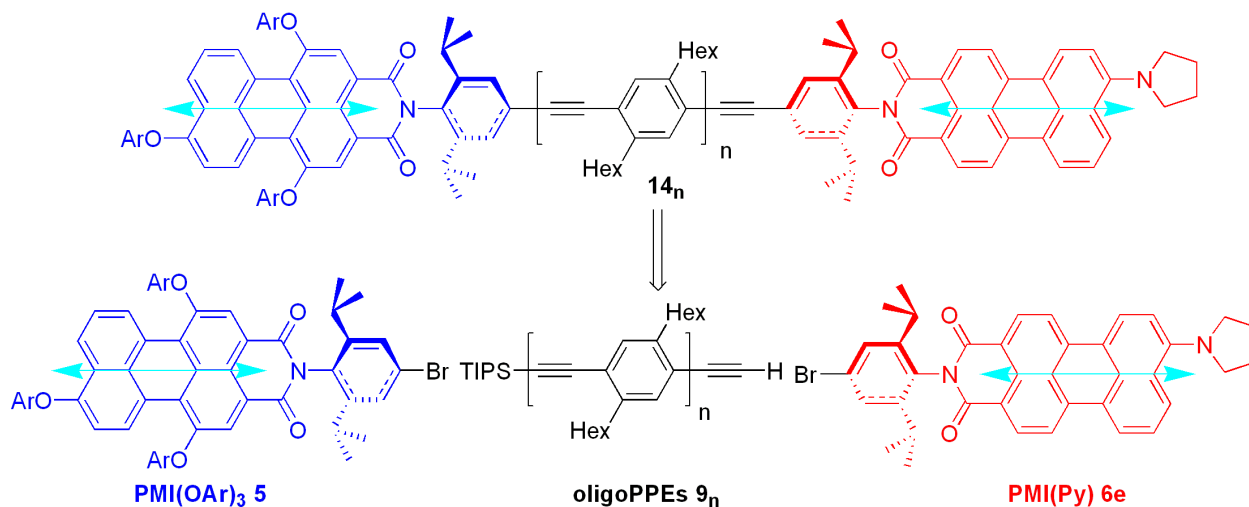
### 4.2 Molecular ruler for the inter-fluorophore distance measurements

PMI(OAr)<sub>3</sub> was chosen as fluorescent probe due to the above mentioned outstanding properties. The photophysical properties of different amino-substituted compounds as discussed in chapter 2, show that the PMI(Py) **6e** has higher absorption and emission maxima in comparison to the other amino-substituted PMI. Secondly, it

absorbs and emits at higher wavelength than the  $\text{PMI(OAr)}_3$  (see figure 4.1) and also the absorption of the former overlaps with the emission of the latter. Therefore we chose  $\text{PMI(Py)}$  **6e** as the second fluorophore for the construction of the molecular ruler for FRET study.

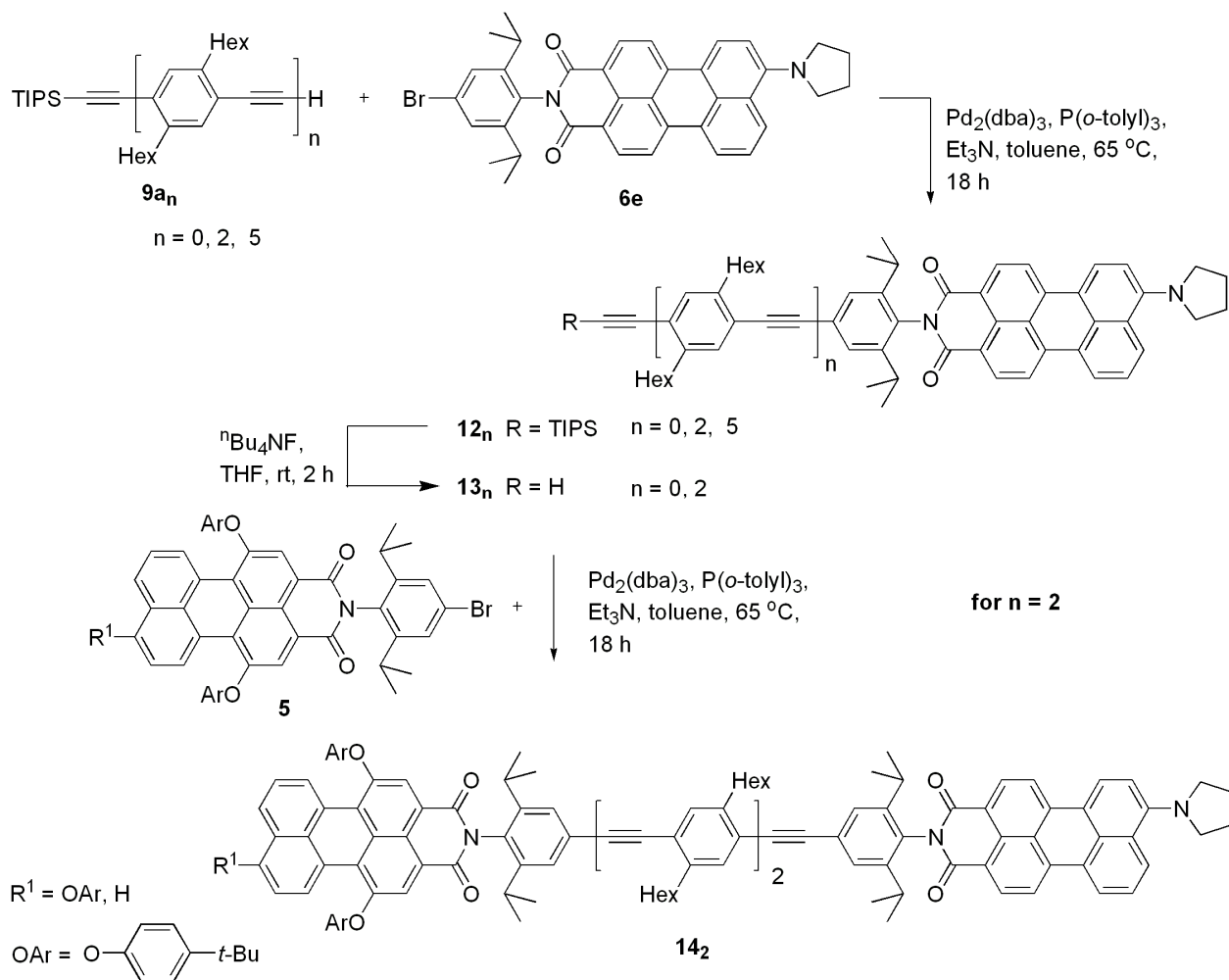
The objective was to build linear  $\text{PMI(OAr)}_3\text{-(PPE)}_n\text{-PMI(Py)}$  dyads **14<sub>n</sub>**. The synthesis can be achieved by two approaches (Scheme 4.1). In the first approach, Pd-catalyzed coupling of  $\text{PMI(Py)}$  **6e** with the oligoPPEs **9a<sub>n</sub>** bearing TIPS protected ethynyl unit at the other end produces  $\text{PMI(Py)}$  labeled oligoPPEs. Removal of the TIPS group would provide the free acetylene, which subsequently couples with the mixture of  $\text{PMI(OAr)}_3$  **5a** and  $\text{PMI(OAr)}_2$  **5b** to achieve the desired dyads **14<sub>n</sub>**.

**Scheme 4.1** Structural representation of  $\text{PMI(OAr)}_3\text{-(PPE)}_n\text{-PMI(Py)}$  dyad **14<sub>n</sub>** and their corresponding building blocks.



In the second approach, Pd-catalyzed coupling of the mixture of  $\text{PMI(OAr)}_3$  **5a** and  $\text{PMI(OAr)}_2$  **5b** with the oligoPPEs **9a<sub>n</sub>** followed by removal of TIPS group would give the free acetylene. The resulting free acetylene couples with  $\text{PMI(Py)}$  **6e** to achieve the required product **14<sub>n</sub>**.



4.2.1 Synthesis of PMI(OAr)<sub>3</sub>-(PPE)<sub>2</sub>-PMI(Py) dyad **14**<sub>2</sub>**Scheme 4.2** Synthesis of PMI(OAr)<sub>3</sub>-(PPE)<sub>n</sub>-PMI(Py) dyad **14**<sub>2</sub>.

Following the first approach, the PMI(Py) **6e** was attached to the oligoPPEs **9a<sub>n</sub>** by Pd-catalyzed alkynyl-aryl coupling to afford **12<sub>n</sub>** with  $n = 0, 2$ , and 5 as a blue solid in 60-80% yields (Scheme 4.2).<sup>57,70</sup> The PMI(Py) labeled oligoPPEs **12<sub>n</sub>** with  $n = 0, 2$  were treated with  $n\text{Bu}_4\text{NF}$  in THF to afford the free acetylene **13<sub>n</sub>** in 85% yield. The free acetylene **13<sub>2</sub>** was coupled with the mixture of PMI(OAr)<sub>3</sub> **5a** and PMI(OAr)<sub>2</sub> **5b** to afford dyad **14<sub>2</sub>** in 75% yield (Scheme 4.2).

## 4.2.2 Photophysical studies

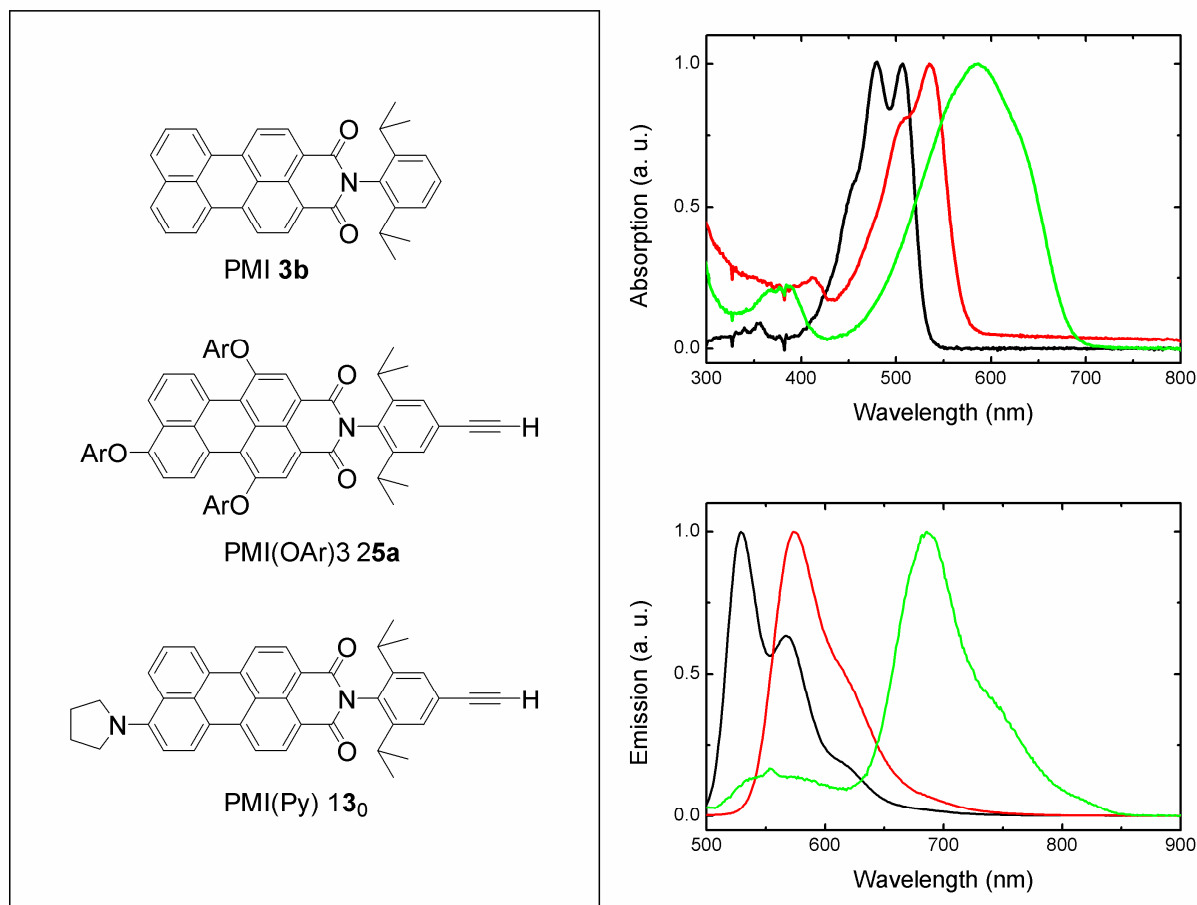


**Figure 4.1** The figure on left shows structural representation of dyes for PMI **3b**, PMI(OAr)<sub>3</sub> **25a**, and PMI(Py) **13<sub>0</sub>**. Absorption spectra (top right) and emission spectra (bottom right) for PMI **3b** (black), PMI(OAr)<sub>3</sub> **25a** (red) and PMI(Py) **13<sub>0</sub>** (green) in toluene. The emission spectra were normalized with the maximum and excitation wavelength is 475 nm.

The photophysical studies were conducted for the dye **13<sub>0</sub>** in toluene and compared with the benchmark perylene dyes PMI **3b** and PMI(OAr)<sub>3</sub> **25a**. The absorption and emission spectra for the dyes PMI **3b**, PMI(OAr)<sub>3</sub> **25a**, and PMI(Py) **13<sub>0</sub>** were recorded in toluene (Figure 4.1). Dilute solutions with OD  $\approx$  0.05 at absorption maxima (typically corresponded to a concentration in micromolar range) were used for the measurements.

The absorption spectrum shows that the absorption maximum of PMI(Py) **13<sub>0</sub>** was red shifted by 80 nm and 52 nm in comparison to the absorption maximum of PMI **3b** and PMI(OAr)<sub>3</sub> **25a** respectively. Similarly, the emission maximum of the PMI(Py) **13<sub>0</sub>** was red shifted by 157 nm and 112 nm in comparison to the emission maximum of PMI **3b** and PMI(OAr)<sub>3</sub> **25a** respectively (Table 4.1).

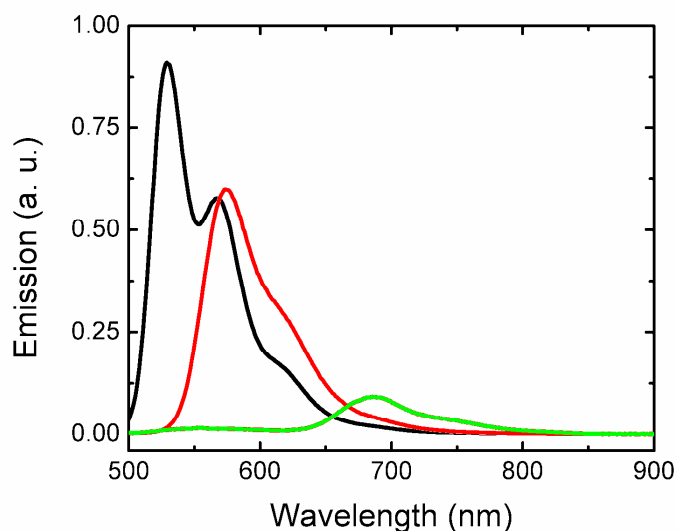


**Figure 4.2.** Emission spectra for PMI **3b** (black), PMI(OAr)<sub>3</sub> **25a** (red) and PMI(Py) **13<sub>0</sub>** (green) in toluene. The emission spectra were normalized with the OD, at their respective excitation wavelength. Excitation wavelength: 475 nm.

The fluorescence quantum yield of PMI(Py) **13<sub>0</sub>** was measured by using Eq. 4.1. PMI **3b** and PMI(OAr)<sub>3</sub> **25a** were used as the references<sup>73</sup> (Figure 4.2, Table 4.1).

$$\phi = \phi_R (I/I_R)(OD_R/OD)(\eta^2/\eta_R^2) \quad (4.1)$$

where,  $\phi$  is the quantum yield,  $I$  is the integrated intensity,  $OD$  is the optical density, and  $\eta$  is the refractive index of the solvent used.

The subscript *R* refers to the reference fluorophore of known quantum yield.

**Table 4.1:** The photophysical data of PMI **3b**, PMI(OAr)<sub>3</sub> **25a**, and PMI(Py) **13<sub>0</sub>**.

Samples	$\lambda_{abs}$ (nm)	$\lambda_{em}$ (nm)	$\phi_f$
<b>3b</b>	479, 506	529, 569	0.91 <sup>73</sup>
<b>25a</b>	511, 536	577, 623	0.86 <sup>73</sup>
<b>13<sub>0</sub></b>	586	687	0.15

The absorption and emission spectra of the donor **25a**, acceptor **13<sub>0</sub>**, and the dyad **14<sub>2</sub>** were shown in figure 4.3. The absorption spectrum of dyad **14<sub>2</sub>** shows a short wavelength peak at 350 nm, which is due to the oligoPPE and the second peak at 540 nm due to the sum of the absorbance of the donor **25a** and the acceptor **13<sub>0</sub>**.

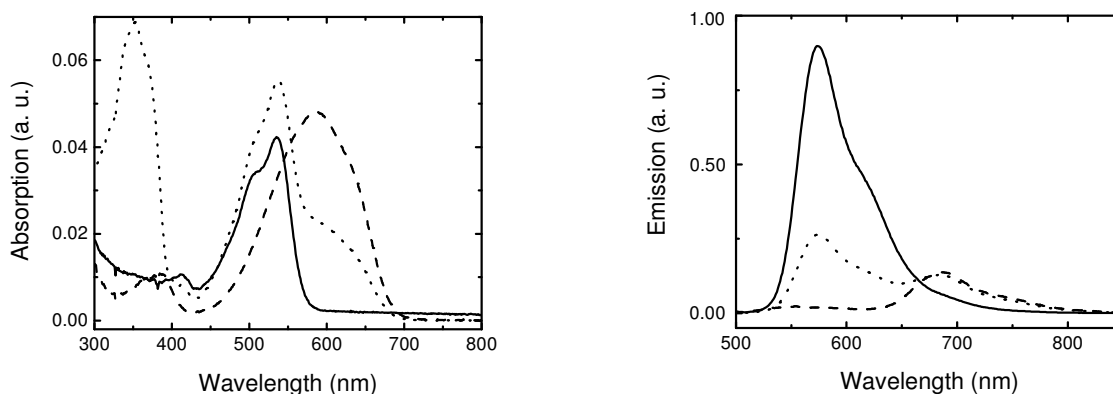


**Figure 4.3** Absorption spectra (left) and emission spectra (right) for donor **25a** (solid line), acceptor **13<sub>0</sub>** (dashed line) and PMI(OAr)<sub>3</sub>-(PPE)<sub>2</sub>-PMI(Py) dyad **14<sub>2</sub>** (dotted line) in toluene. The emission spectra were normalized with the OD, at their respective excitation wavelength. Excitation wavelength: 475 nm.

The emission spectrum of the dyad **14<sub>2</sub>** (Figure 4.3) shows a longer wavelength peak, corresponding to the emission of the acceptor **13<sub>0</sub>**, whereas the shorter wavelength peak corresponds to the emission of the donor **25a**. Considering the emission intensity of the donor only and the emission intensity of dyad **14<sub>2</sub>** in the relevant region, it is clear that the energy transfer takes place from the PMI(OAr)<sub>3</sub> to PMI(Py). This result proves that PMI(OAr)<sub>3</sub>-(PPE)<sub>2</sub>-PMI(Py) dyad **14<sub>2</sub>** can be used as a molecular ruler for FRET study, where PMI(OAr)<sub>3</sub> acts as the donor and PMI(Py) as the acceptor.

The absorption and emission spectra for the dye **6e** are broad, structureless, and also red-shifted as compared to those of PMI and PMI(OAr)<sub>3</sub> (Figure 4.1). Stracke *et al.*<sup>74</sup> reported similar amino substituted peryleneimide derivatives. The unstructured absorption spectrum of the reported amino compound resembles that of the PMI(Py). This unstructured spectrum is due to the charge transfer transition resulting from donation of electron density from the lone-pair on the nitrogen atom of amino group into perylene core.<sup>74,75</sup> The extended  $\pi$ -conjugation/donation of electron density is possible only when the overlap of orbital containing the amino lone-pair with the  $\pi$ -system of the perylene core is maximized and this is achieved when the amino group adopts an  $sp^2$  hybridisation. Zoon *et al.*<sup>76</sup> reported for pyrrolidine substituted PMI that the amino group adopts an intermediate hybridization between  $sp^2$  and  $sp^3$ . Therefore the above mentioned hypothesis is applicable for the unstructured absorbance of PMI(Py) and this hypothesis was supported by the protonation and deprotonation of the pyrrolidine nitrogen (Figure 4.4).

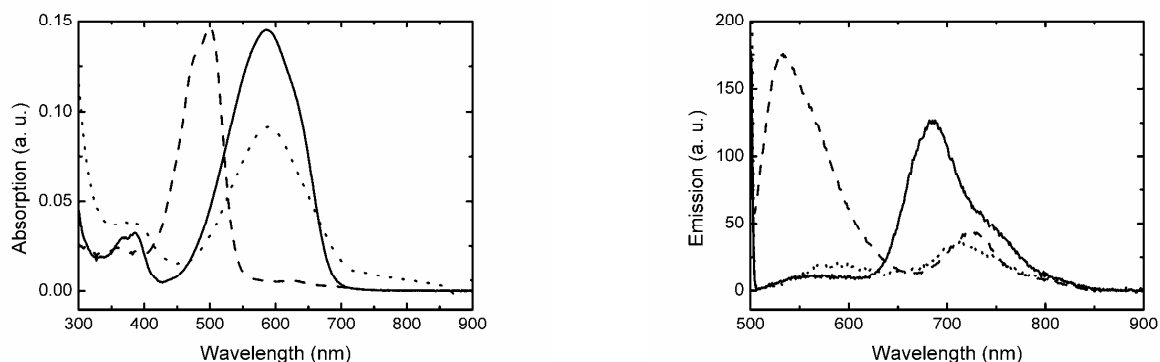


**Figure 4.4** Absorption spectra (left) and emission spectra (right) for PMI(Py) **6e** (solid line), PMI(Py) **6e** + TFA (dashed line), PMI(Py) **6e** + TFA + TEA (dotted line) in toluene. The emission spectra were normalized with the OD, at their respective excitation wavelengths. Excitation wavelength: 500 nm.

The absorption and emission spectra for PMI(Py) were measured in toluene. The same sample was protonated by the addition of a drop of trifluoroacetic acid (TFA), so that the lone-pair electron present on pyrrolidine nitrogen will no longer be available for conjugation and the absorption and the emission spectra were measured (Figure 4.4). As expected, there was a blue shift in the absorption and emission maxima of the protonated PMI(Py) **6e** (dashed line, Figure 4.4). Drop of Et<sub>3</sub>N was added to the above protonated PMI(Py) **6e** solution to obtain the free PMI(Py) and the absorption and emission spectra were recorded. Interestingly, a bathochromic shift was observed for the absorption and emission spectrum and these spectra appear in the same wavelength region as that of the parent PMI(Py) (dotted line, Figure 4.4). Additionally, it was observed that, the absorbance and emission of protonated PMI(Py) **6e** appear in the same region as that of PMI **3b** (Figure 4.5). This result suggests that when the lone-pair electron of pyrrolidine nitrogen is no longer available, the system behaves as the PMI **3b**. Similarly, the absorption and emission of the dye PMI(OAr)<sub>3</sub> **25a** was measured after protonation. There was no shift in the peak except the peak gets broader.

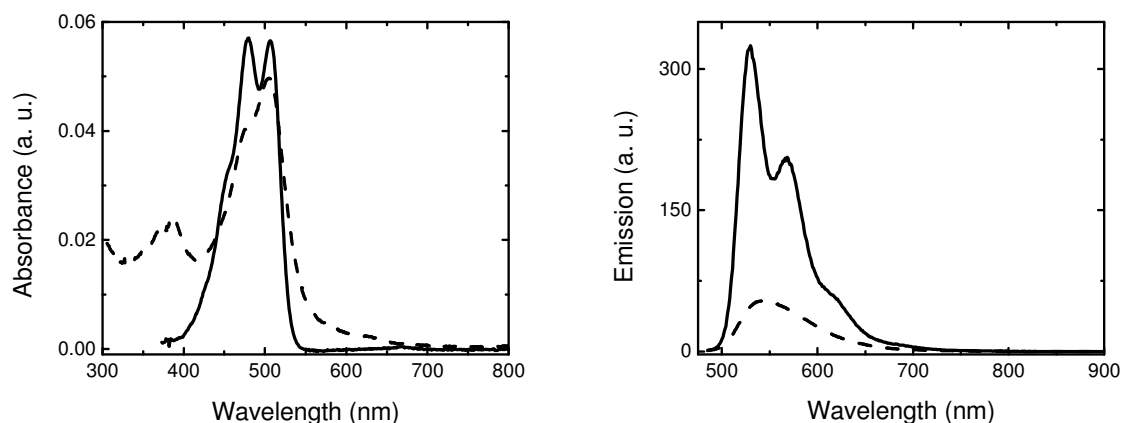


**Figure 4.5** Absorption spectra (left) and emission spectra (right) for PMI (solid line) and PMI(Py) **6<sub>e</sub>** + TFA (dashed line) in toluene. The emission spectra were normalized with the OD, at their respective excitation wavelength. Excitation wavelength: 475 nm.

These interesting results motivated us to investigate the photophysical properties of the protonated dyad **14<sub>2</sub>**. The absorbance and emission of the donor **25a**, the acceptor **13<sub>0</sub>**, and the dyad **14<sub>2</sub>** were measured in toluene and then the same solutions were protonated by addition of a drop of TFA.

The absorption and emission of the above protonated solution were measured (Figure 4.6). The absorption spectrum for the protonated dyad **14<sub>2</sub>** shows two peaks, one at the shorter wavelength (350 nm) due to the oligoPPE. The second peak at longer wavelength (540 nm) is the sum of the absorbance of the protonated donor **25a** and acceptor **13<sub>0</sub>**. The shoulder of the dyad **14<sub>2</sub>** around 700 nm disappears after protonation.

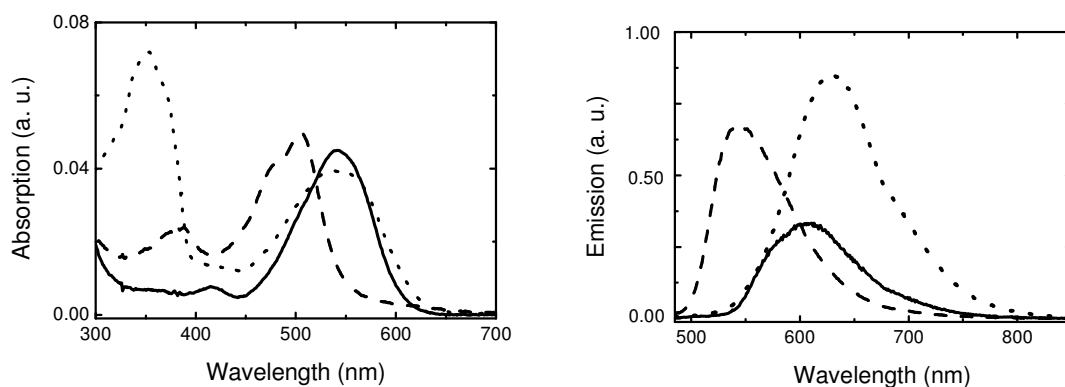


**Figure 4.6.** Absorption (left) and emission spectra (right) for **25a** (solid line), **13<sub>0</sub>** (dashed line), and PMI(OAr)<sub>3</sub>-(PPE)<sub>2</sub>-PMI(Py) dyad **14<sub>2</sub>** (dotted line) after protonation with TFA in toluene. The emission spectra were normalized with the OD, at their respective excitation wavelength. Excitation wavelength: 475 nm.

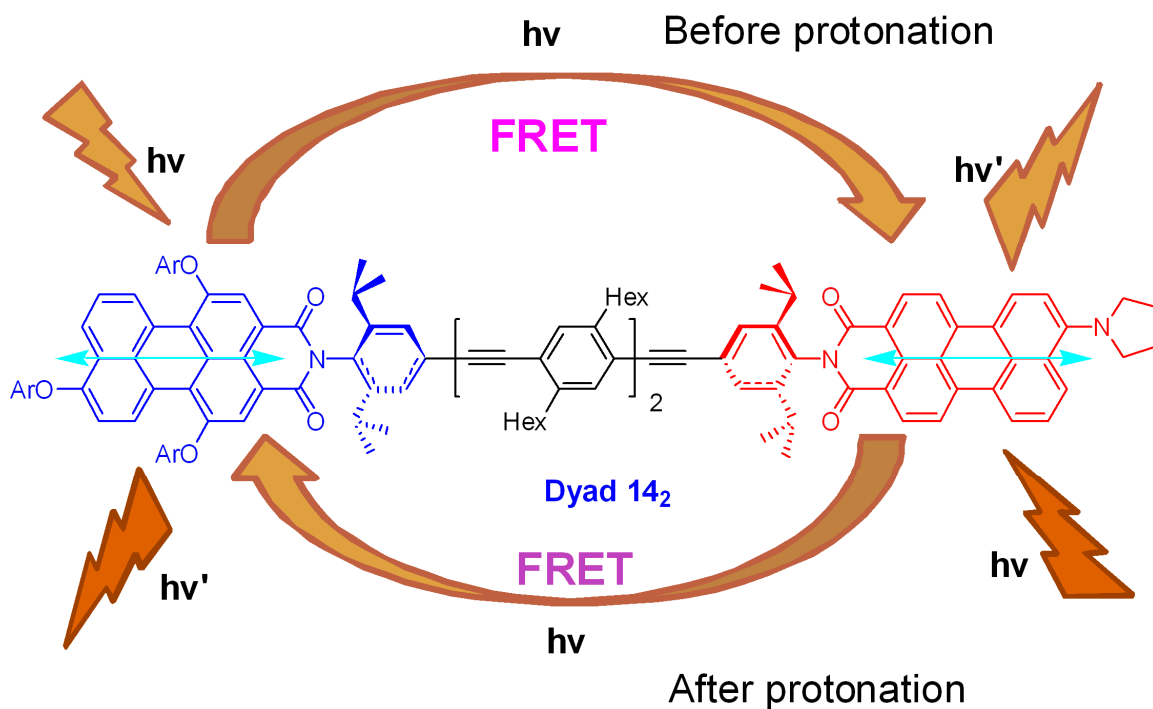


**Figure 4.7** Structural representation of the direction of energy transfer for PMI(OAr)<sub>3</sub>-(PPE)<sub>2</sub>-PMI(Py) dyad **14<sub>2</sub>** before and after protonation.



The emission spectrum of the protonated dyad **14<sub>2</sub>** (Figure 4.6) obtained by excitation at 475 nm shows just one major peak which corresponds to emission of the PMI(OAr)<sub>3</sub> after protonation. The emission intensity of the protonated dyad **14<sub>2</sub>** at the shorter wavelength (540 nm) had almost disappeared. Considering the emission intensity of protonated **13<sub>0</sub>** and the protonated dyad **14<sub>2</sub>** in the relevant region, It is clear that the energy transfer is highly efficient and takes place from protonated PMI(Py) to PMI(OAr)<sub>3</sub> (Figure 4.6). That means the direction of energy transfer for the dyad **14<sub>2</sub>** gets reversed upon protonation.

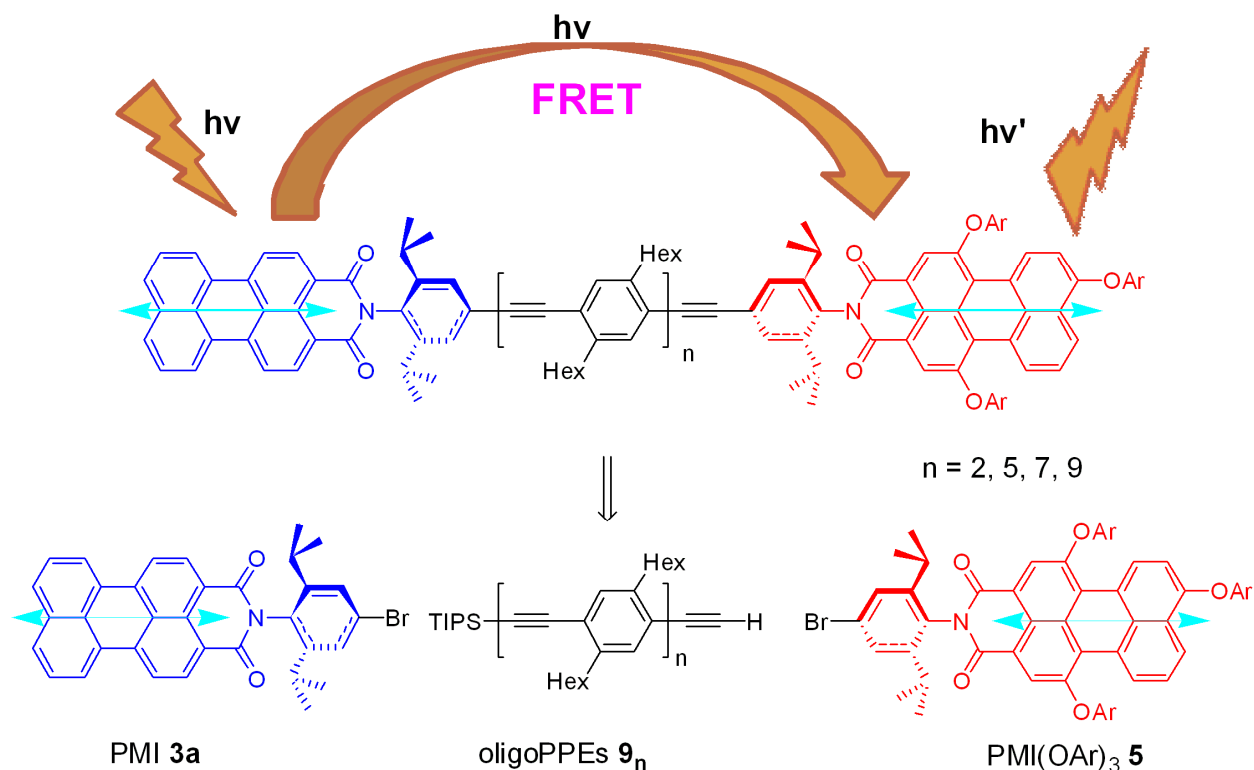
### 4.3 An improved molecular ruler for the inter-fluorophore distance measurements

In the previous section, I discussed about the PMI(OAr)<sub>3</sub>-(PPE)<sub>2</sub>-PMI(Py) dyad **14<sub>2</sub>**, where the energy transfer takes place from PMI(OAr)<sub>3</sub> to PMI(Py). The same system in acidic environment undergoes energy transfer from the protonated PMI(Py) to the PMI(OAr)<sub>3</sub>. Interestingly, the UV-vis and emission spectrum of the protonated PMI(Py) are identical to that of the PMI (Figure 4.4). This gave me the idea that PMI can be used as donor along with PMI(OAr)<sub>3</sub> for FRET study. Additionally, by using PMI as donor, the number of synthetic steps involved for the synthesis of PMI-(PPE)<sub>n</sub>-PMI(OAr)<sub>3</sub> dyads could be reduced by 2-3 steps in comparison to the protonated dyad **14<sub>2</sub>**. Therefore, the PMI(Py) of PMI(OAr)<sub>3</sub>-(PPE)<sub>2</sub>-PMI(Py) dyad **14<sub>2</sub>** was replaced by PMI, to achieve PMI-(PPE)<sub>n</sub>-PMI(OAr)<sub>3</sub> dyads (Scheme 4. 3).

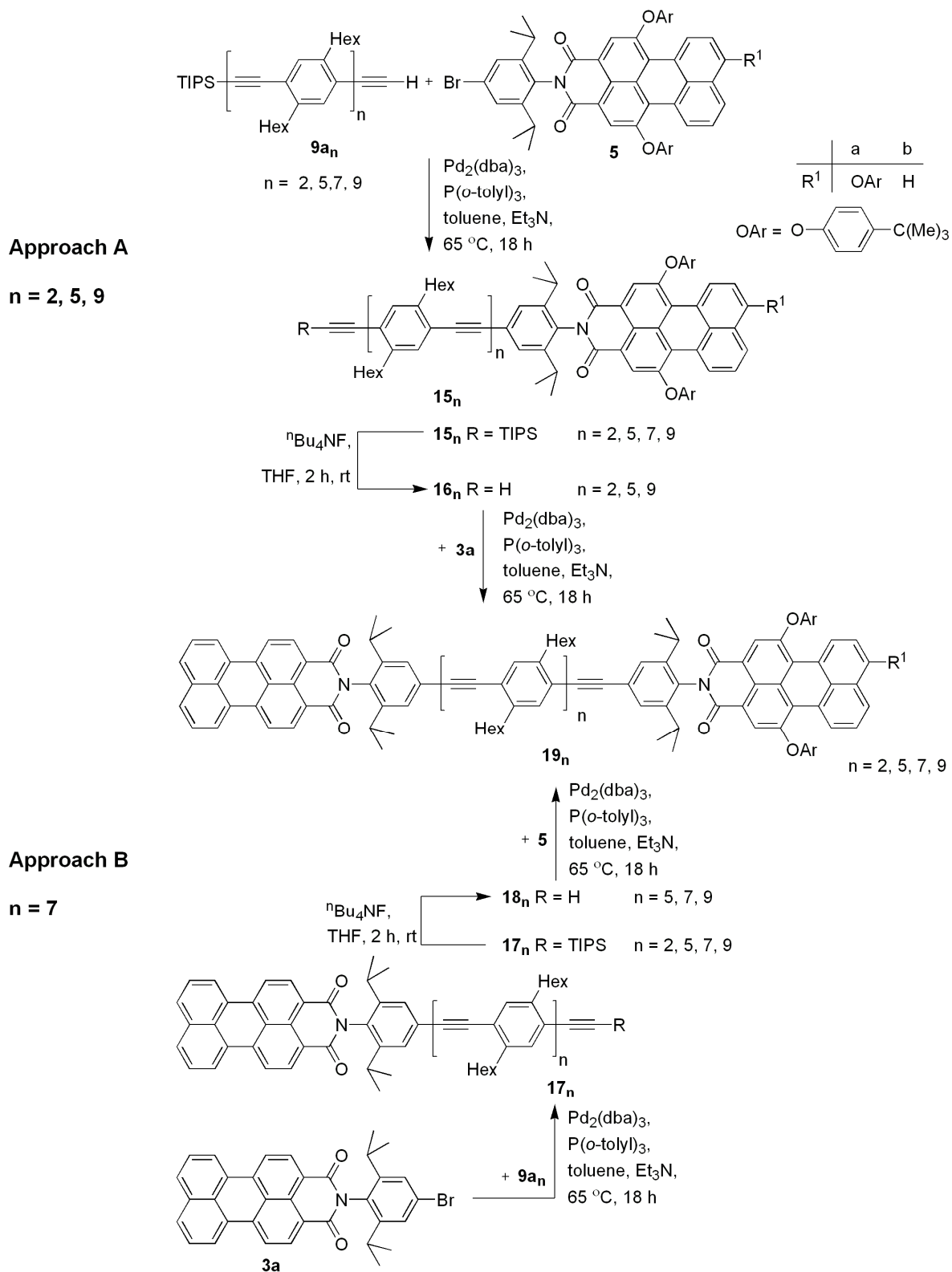
#### 4.3.1 Linear PMI-(PPE)<sub>n</sub>-PMI(OAr)<sub>3</sub> dyads

The target dyads PMI-(PPE)<sub>n</sub>-PMI(OAr)<sub>3</sub> can be synthesized in two different approaches and either of the two approaches follows Pd-catalyzed coupling reactions. In approach A, a mixture of PMI(OAr)<sub>3</sub> **5a** and PMI(OAr)<sub>2</sub> **5b** couples with oligoPPEs **9a<sub>n</sub>** to afford fluorescent labeled oligoPPEs **15<sub>n</sub>**. Treatment of the fluorescent labeled oligoPPEs **15<sub>n</sub>** with <sup>n</sup>Bu<sub>4</sub>NF affords free acetylene **16<sub>n</sub>**, which subsequently couples with the PMI **3a** to get the required dyads **19<sub>n</sub>**. In approach B, firstly the PMI **3a** couples with the oligoPPEs **9a<sub>n</sub>** to afford the precursor **17<sub>n</sub>**. Treatment of **17<sub>n</sub>** with <sup>n</sup>Bu<sub>4</sub>NF affords free acetylene **18<sub>n</sub>**, which subsequently couples with the mixture of PMI(OAr)<sub>3</sub> **5a** and PMI(OAr)<sub>2</sub> **5b** to afford the desired linear dyads **19<sub>n</sub>**.

**Scheme 4.3** Structural representation of linear PMI-(PPE)<sub>n</sub>-PMI(OAr)<sub>3</sub> dyads and their corresponding building blocks.



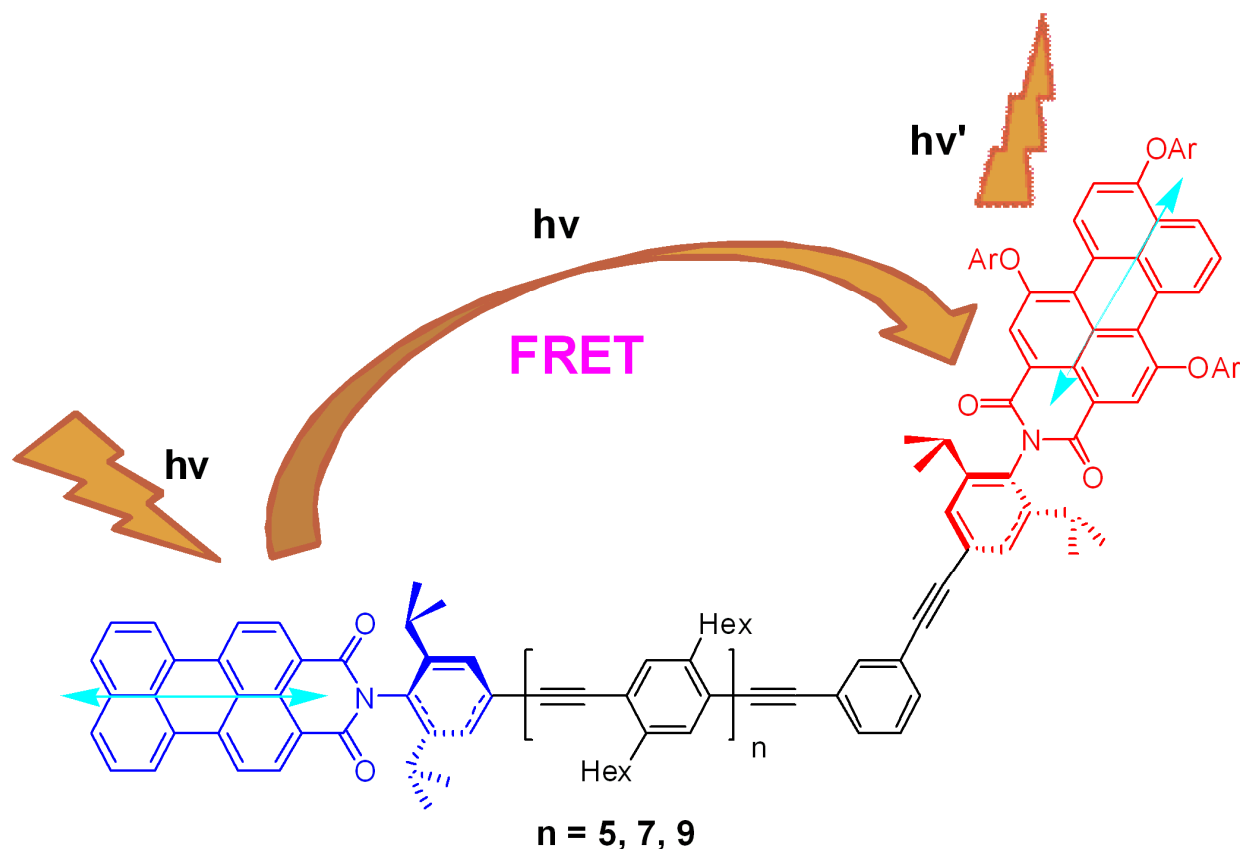
We found that PMI(OAr)<sub>3</sub> has better solubility than PMI as described in the literature.<sup>54-58</sup> I was not expecting that there will be a dramatic change in the solubility of PMI after attaching the oligoPPEs. Therefore, the oligoPPEs were attached to the more soluble PMI(OAr)<sub>3</sub> expecting that the resulting PMI(OAr)<sub>3</sub> labeled oligoPPEs would have better solubility than the PMI labeled oligoPPEs. Following approach A, the dyads **19**<sub>2</sub>, **19**<sub>5</sub>, and **19**<sub>9</sub> were synthesized. However, later it was found that when the PMI **3a** was coupled to the oligoPPEs, the solubility of resulting compounds **17**<sub>n</sub> were dramatically improved in comparison to that of the PMI **3a**. These results showed that one can achieve the desired dyads PMI-(PPE)<sub>n</sub>-PMI(OAr)<sub>3</sub> **19**<sub>n</sub> by following either of the two approaches. The dyad **19**<sub>7</sub> was successfully synthesized by following the approach B.

Scheme 4.4 Synthesis of linear PMI-(PPE)<sub>n</sub>-PMI(OAr)<sub>3</sub> dyads.

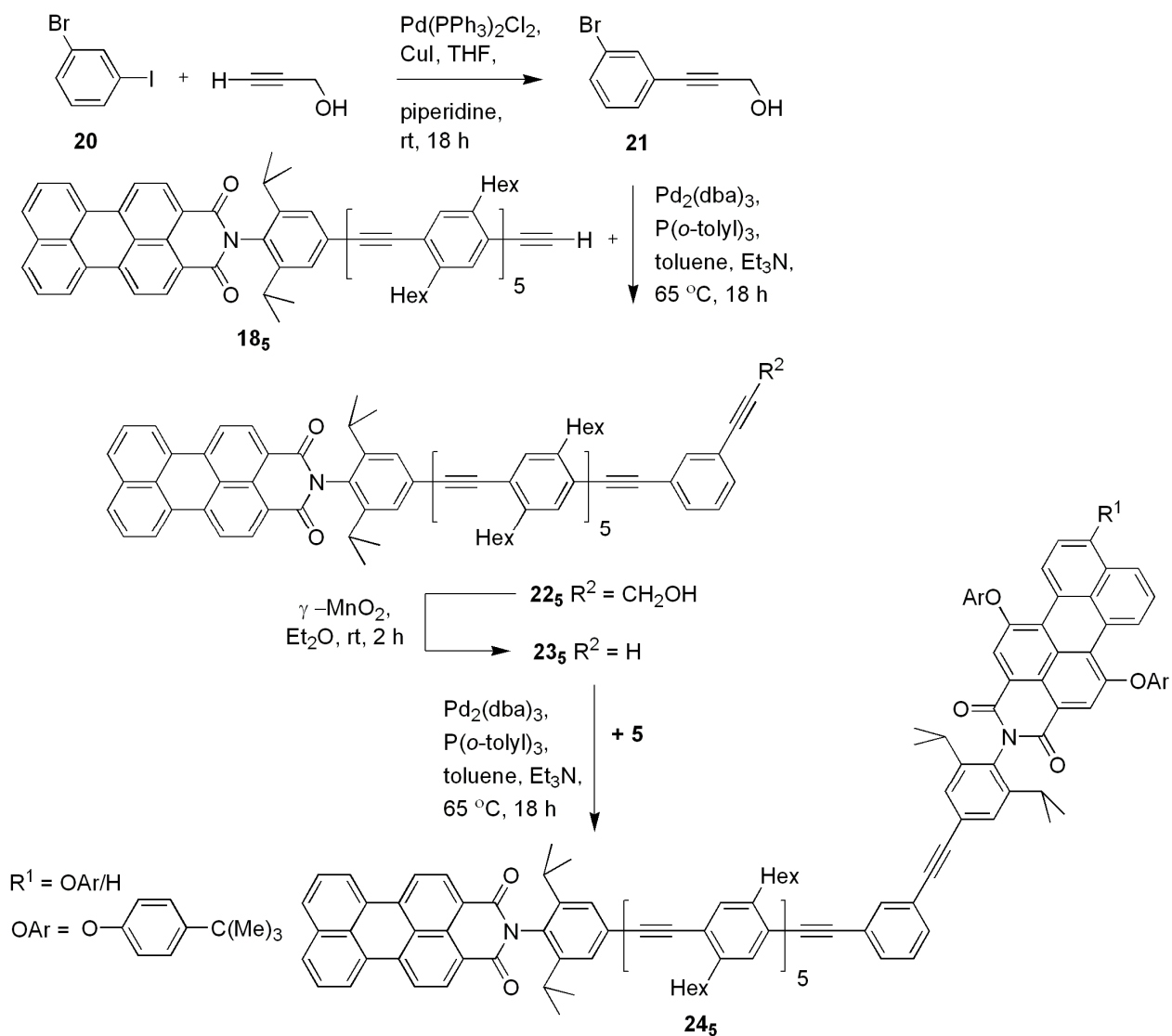
The oligoPPEs **9a<sub>n</sub>** were coupled with a mixture of PMI(OAr)<sub>3</sub> **5a** and PMI(OAr)<sub>2</sub> **5b** to afford **15<sub>n</sub>** in 70-80% yield (Scheme 4.4).<sup>56</sup> The PMI(OAr)<sub>3</sub> labeled oligoPPEs **15<sub>n</sub>** were treated with <sup>n</sup>Bu<sub>4</sub>NF to afford the free acetylenes **16<sub>n</sub>** in 90-95% yield.<sup>56,69</sup> For the synthesis of **15<sub>2</sub>**, a 93:7 mixture of compounds **5a** and **5b** was used, whereas in other cases (**15<sub>5</sub>**, **15<sub>7</sub>**, and **15<sub>9</sub>**) a 97:3 mixture of compounds **5a** and **5b** was used.

The PMI **3a** was coupled with the free acetylenes **16<sub>n</sub>** (n = 2, 5, and 9) to afford the required linear dyads **19<sub>n</sub>** in 67-80% yields (Scheme 4.4). Unfortunately, the yield of **19<sub>5</sub>** was only 51% due to the necessary repeated chromatography for purification. The compound **19<sub>5</sub>** has very good solubility in common organic solvents (Et<sub>2</sub>O, CH<sub>2</sub>Cl<sub>2</sub>, CHCl<sub>3</sub>, and THF). At this point the main aim was to take advantage of the good solubility and avoid the solvent CHCl<sub>3</sub> for chromatography. Therefore, a 1:1 mixture of Et<sub>2</sub>O and *n*-pentane was used for chromatography. Unfortunately, I was not able to isolate pure product after chromatography for several times. Finally, the compound **19<sub>5</sub>** was purified with chromatography using the usual 1:1 mixture of CHCl<sub>3</sub> and *n*-hexane.

Following the second approach, the PMI **3a** was coupled with the oligoPPEs **9a<sub>n</sub>** to afford **17<sub>n</sub>** in 70-80% yields. The PMI labeled oligoPPEs **17<sub>n</sub>** (n = 5, 7, and 9) were treated with <sup>n</sup>Bu<sub>4</sub>NF to afford the free acetylenes **18<sub>n</sub>** in 90-95% yield (Scheme 4.4). The alkyne **18<sub>7</sub>** was coupled with a 97:3 mixture of PMI(OAr)<sub>3</sub> **5a** and PMI(OAr)<sub>2</sub> **5b** to afford **19<sub>7</sub>** in 65% yield (Scheme 4.4).

4.3.2 Kinked PMI-(PPE)<sub>n</sub>-PMI(OAr)<sub>3</sub> dyads**Scheme 4.5** Structural representation of kinked PMI-(PPE)<sub>n</sub>-PMI(OAr)<sub>3</sub> dyads **24<sub>n</sub>**.

According to Förster theory, the efficiency of energy transfer is dependent on the inverse sixth power of the inter-fluorophore distance and also on the Förster radius of the fluorophore pair (Chapter 1.1, eq. 1.1). The Förster radius depends on the relative orientation of the transition dipoles of the two fluorophores. As a consequence the rate of energy transfer depends on the fluorophore alignment. In order to investigate this fact, kinked PMI-(PPE)<sub>n</sub>-PMI(OAr)<sub>3</sub> dyads were designed with a fixed angle of 120° between the long axis of PMI and PMI(OAr)<sub>3</sub> (Scheme 4.5).

**Scheme 4.6** Synthesis of kinked PMI-(PPE)<sub>5</sub>-PMI(OAr)<sub>3</sub> dyad **24<sub>5</sub>**.

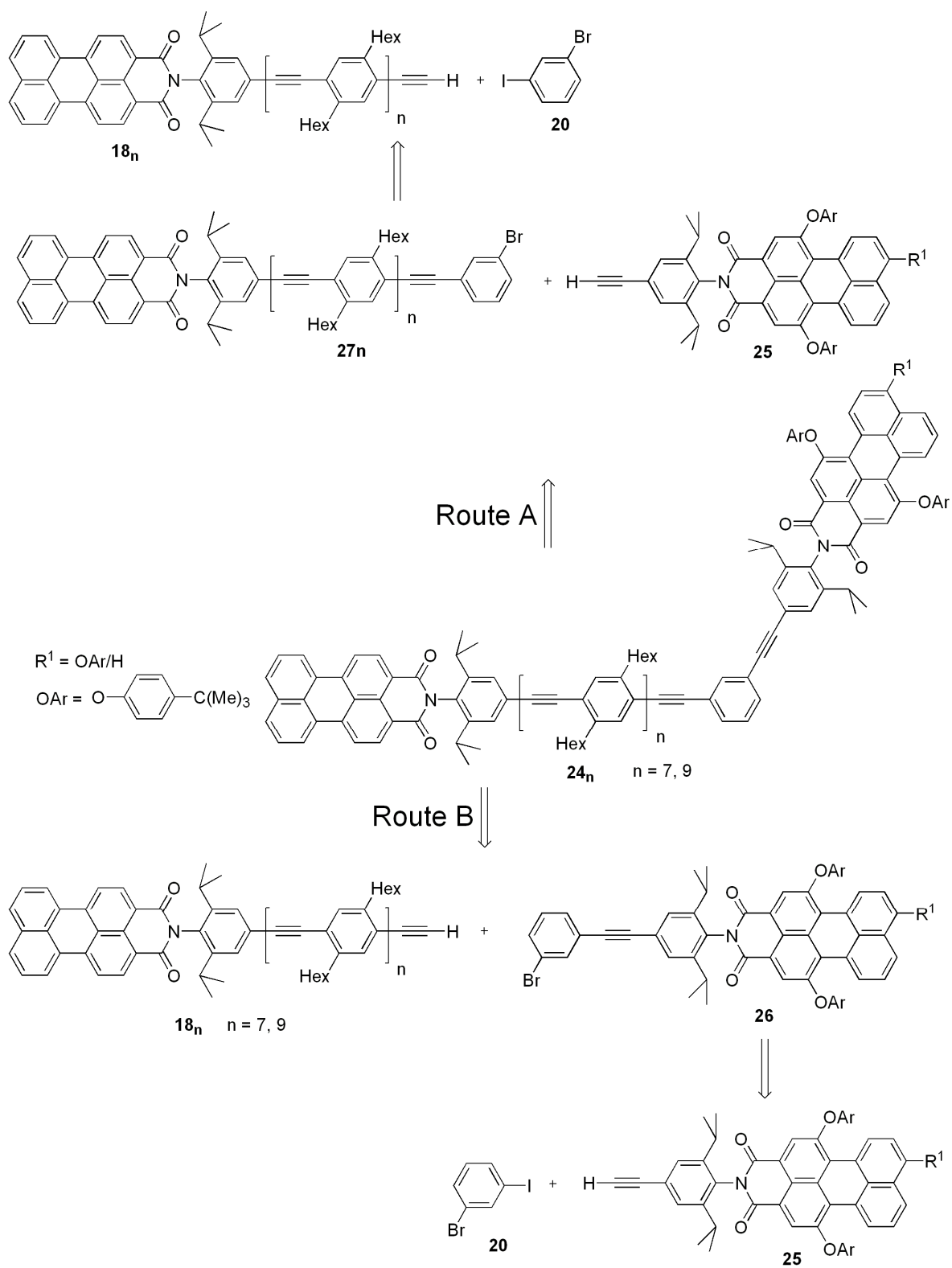
The initial idea was to incorporate the kink moiety into the PMI labeled oligoPPEs **18<sub>n</sub>** and then couple with the PMI(OAr)<sub>3</sub> to achieve the kinked dyads **24<sub>n</sub>**. The free acetylene **18<sub>5</sub>** was coupled with bromo compound **21** using Pd-mediated coupling reaction to afford the compound **22<sub>5</sub>** in 34% yields.<sup>56</sup> The bromo compound **21** was synthesized in 89% yield by Pd/Cu catalyzed coupling of 1-bromo-3-iodobenzene (**20**) with 2-propynol (Scheme 4.6).<sup>72</sup>

From our previous experience with the synthesis of oligoPPEs, it was noticed that the TMS acetylene coupled product and starting iodo compounds have nearly same  $R_f$  values as a result of that one could face difficulties in chromatographic separation. Therefore, polar protecting group 2-propanol was chosen instead of TMS acetylene for the synthesis of bromo compound **21**. As expected, a big difference in the  $R_f$  values of **20** and **21** was found.

The hydroxymethyl protected compound **22<sub>5</sub>** was treated with  $\gamma$ -MnO<sub>2</sub> and powdered KOH in CH<sub>2</sub>Cl<sub>2</sub> to afford free acetylene **23<sub>5</sub>** in 67% yield.<sup>69,70</sup> Treatment of the unprotected acetylene **23<sub>5</sub>** with a 97:3 mixture of PMI(OAr)<sub>3</sub> **5a** and PMI(OAr)<sub>2</sub> **5b** by the usual Pd-mediated coupling reaction afforded **24<sub>5</sub>** in 70% yield (Scheme 4.7).<sup>56</sup> The compound **22<sub>5</sub>** has poor solubility in comparison to linear molecule **17<sub>5</sub>** which has a TIPS end group. Additionally, the free acetylene **23<sub>5</sub>** has better solubility in comparison to **22<sub>5</sub>**. These facts support that the poor solubility of **22<sub>5</sub>** is due to the hydroxymethyl group.

As we encountered low solubility of **22<sub>5</sub>** and also low yield, a different synthetic approach was followed for the synthesis of kinked dyads **24<sub>n</sub>** with  $n = 7, 9$ . There are two possible alternate routes (Scheme 4.7) to the earlier synthetic route followed for **24<sub>5</sub>** (Scheme 4.6). In route A, the kink moiety **20** will be attached individually with each of the free acetylene **18<sub>n</sub>** and subsequently couple with the free acetylene **25** to afford the desired dyads **24<sub>n</sub>**.

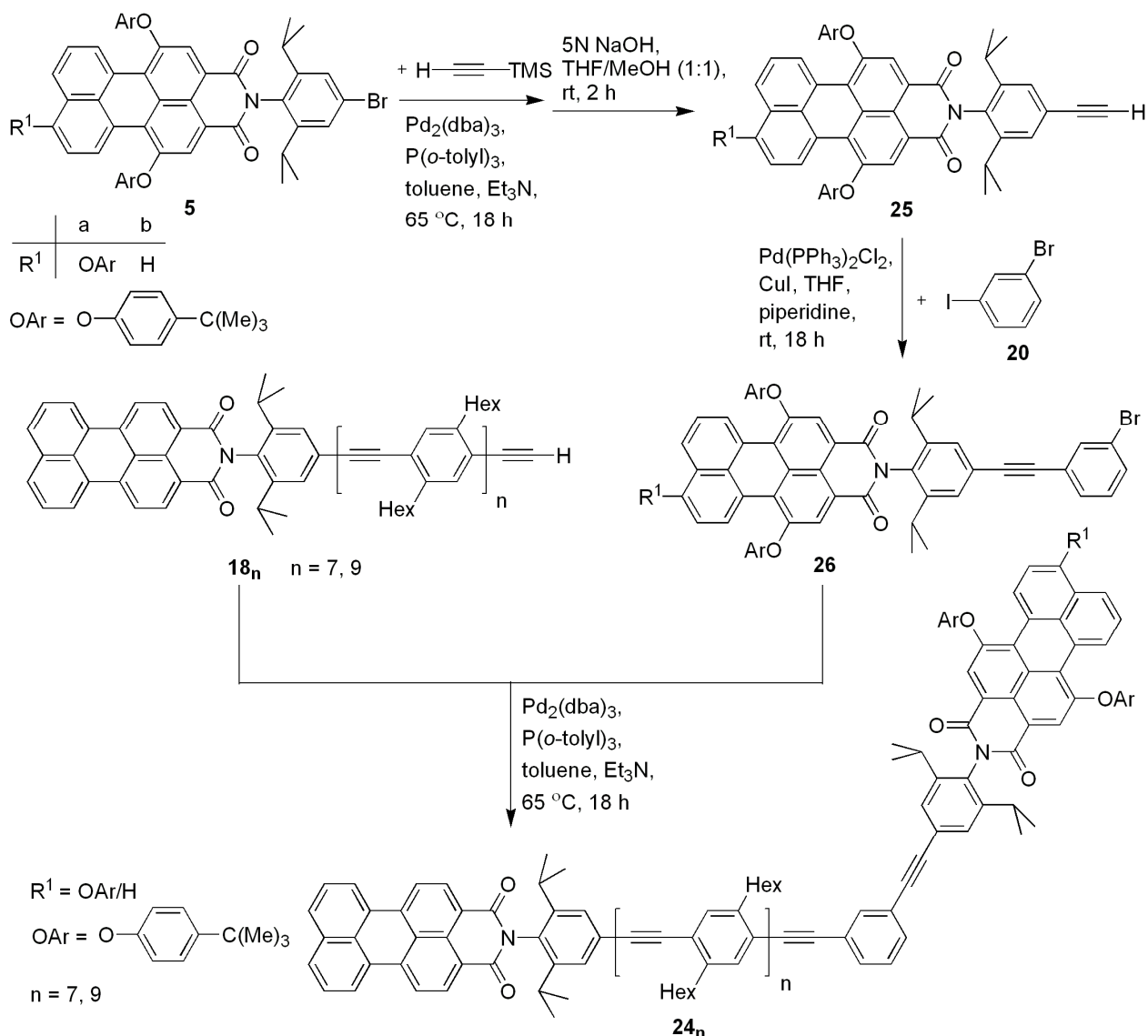


**Scheme 4.7** Retro synthesis of kinked PMI-(PPE)<sub>n</sub>-PMI(OAr)<sub>3</sub> dyads **24<sub>n</sub>** (n = 7, 9).

By following route B, the kink moiety **20** will couple with the free acetylene **25** to afford bromo compound **26** which subsequently couples with **18<sub>n</sub>** to afford the desired dyads **24<sub>n</sub>** (Scheme 4.7).

By following either of the two routes one needs to go through two step synthesis. The key difference between the two routes lies in the first step of the synthesis. By following route A, one will couple the kink moiety **20** with the limited amount of precious material **18<sub>n</sub>** to achieve bromo compound **27<sub>n</sub>** in the first step and run the reaction for “n” number of time. Whereas by following route B, one would couple the kink moiety **20** with the acetylene **25** to afford bromo compound **26** in the first step and run the reaction only once. Then in the second step for either of the two routes, one would run the same number of reactions to achieve the desired product **24<sub>n</sub>**. Therefore, there are two advantages for following route B over route A. Firstly, as a whole the number of reactions in first step will be reduced. Secondly, the loss of precious material **18<sub>n</sub>** will be less.

Therefore route B was followed and the kink moiety **20** was attached with the free acetylene **25**. The unprotected acetylene **25** was synthesized by coupling of a 97:3 mixture of PMI(OAr)<sub>3</sub> **5a** and PMI(OAr)<sub>2</sub> **5b** with TMS acetylene to obtain the TMS protected PMI(OAr)<sub>3</sub>, which was subsequently treated with 5N NaOH in a 1:1 mixture of THF and MeOH. The kink moiety **20** was coupled with the unprotected acetylene **25** to achieve the bromo compound **26** in 73% yield (Scheme 4.8).<sup>72</sup> The bromo compound **26** was coupled with the free acetylenes **18<sub>7</sub>** and **18<sub>9</sub>** to afford **24<sub>7</sub>** and **24<sub>9</sub>** in 60% and 63% yields, respectively (Scheme 4.8).

**Scheme 4.8** Synthesis of kinked PMI-(PPE)<sub>n</sub>-PMI(OAr)<sub>3</sub> dyads **24<sub>n</sub>** (n = 7, 9).

### 4.3.3 Photophysical studies

The donor PMI **3b**, the acceptor PMI(OAr)<sub>3</sub> **25a**, the linear PMI-(PPE)<sub>n</sub>-PMI(OAr)<sub>3</sub> dyads **19<sub>n</sub>**, and kinked PMI-(PPE)<sub>n</sub>-PMI(OAr)<sub>3</sub> **24<sub>n</sub>** are shown in Figure 4.8. The distance *R* between the two fluorophores for the linear dyads **19<sub>n</sub>** and kinked dyads **24<sub>n</sub>** were calculated taking the standard bond lengths and are summarized in table 4.2.<sup>77,79</sup>

The distance  $R$  for the linear and kinked dyads ( $n = 5, 7,$  and  $9$ ) are nearly same (Figure 4.8 and table 4.2).

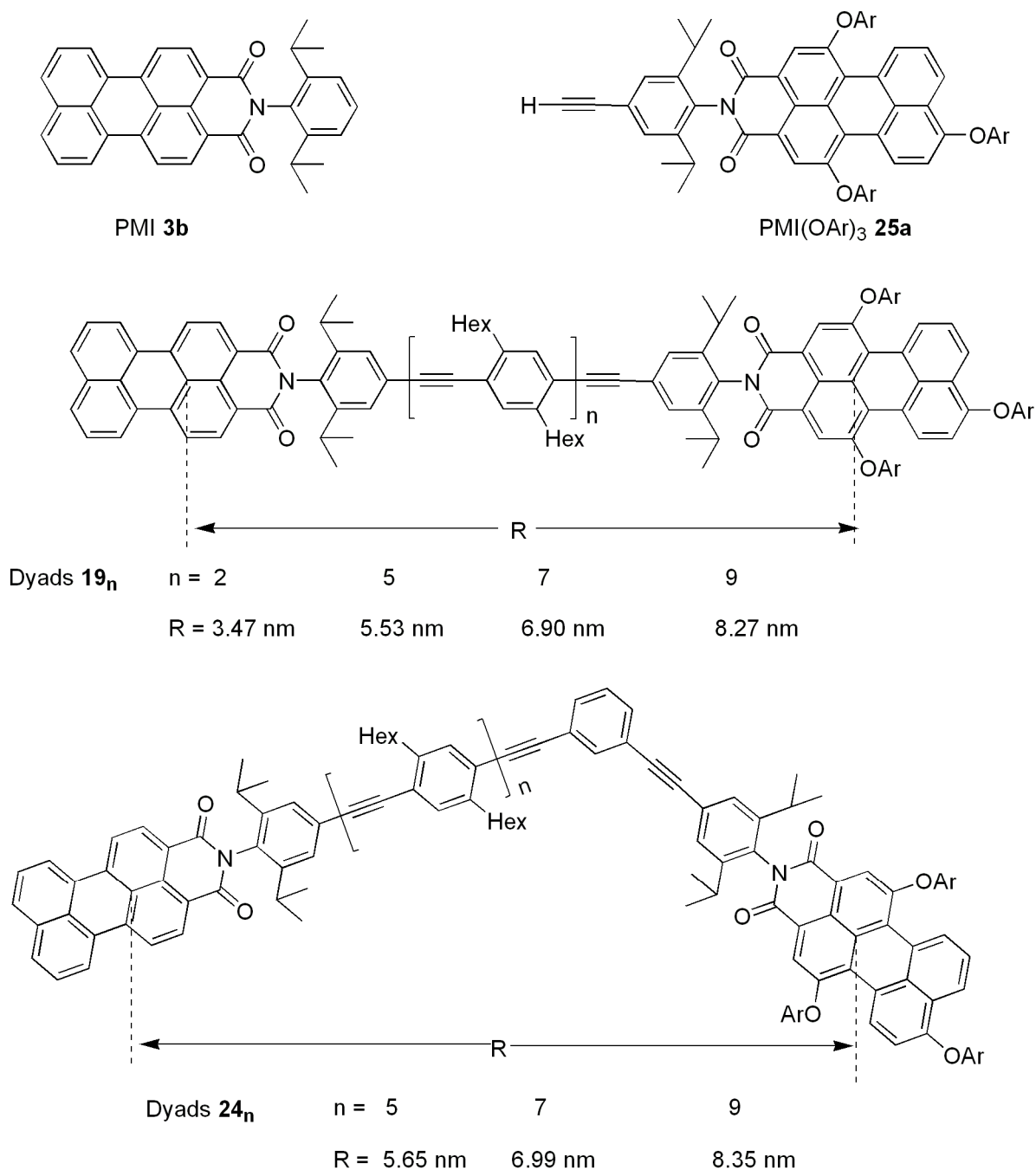


**Figure 4.8** Figures representing the structure of PMI **3b**, PMI(OAr)<sub>3</sub> **25a**, linear dyads **19<sub>n</sub>** ( $n = 2, 5, 7,$  and  $9$ ), and kinked dyads **24<sub>n</sub>** ( $n = 5, 7,$  and  $9$ ).  $R$  is the calculated distance between the centers of the two fluorophores.

The UV-vis absorption and emission spectra of PMI **3b**, PMI(OAr)<sub>3</sub> **25a**, and the linear dyads **19<sub>n</sub>** were measured in toluene. The Förster radius  $R_0$  for the above mentioned fluorophores was calculated from the spectral overlap integral of the emission spectrum of the PMI and the absorption spectrum of the PMI(OAr)<sub>3</sub> by using Eq. 1.3 and found to be 7.1 nm (Figure 4.9).

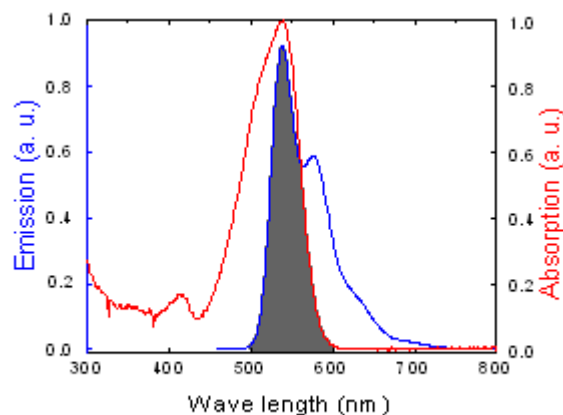


**Figure 4.9** Emission spectrum (blue) of the donor PMI **3b** and absorption spectrum (red) of the acceptor PMI(OAr)<sub>3</sub>**25a** in toluene and the area cover by gray color is their overlap.

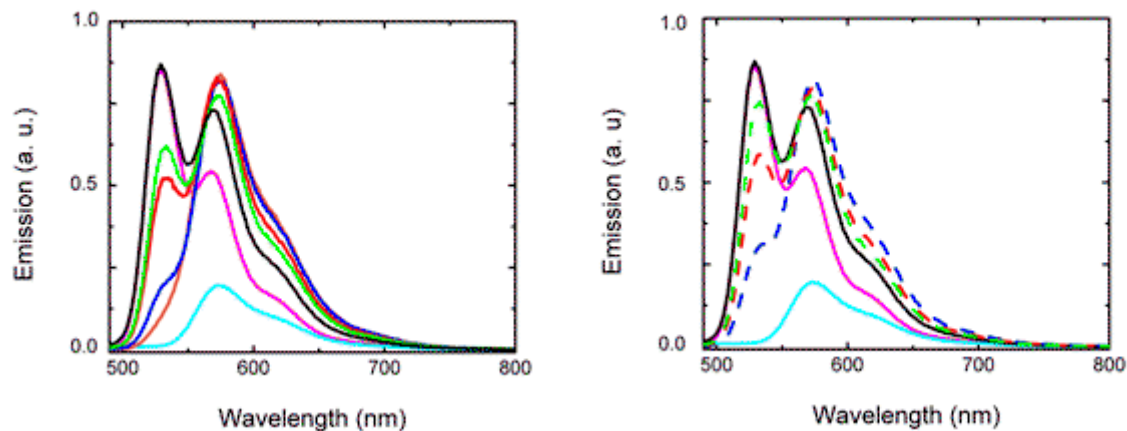


**Figure 4.10** Emission spectra of PMI **3b** (magenta), the PMI(OAr)<sub>3</sub> **25a** (cyan), the sum of the emission of PMI and PMI(OAr)<sub>3</sub> (black), and linear PMI-(PPE)<sub>n</sub>-PMI(OAr)<sub>3</sub> dyads **19<sub>n</sub>** ( $n = 2$  (orange), 5 (blue), 7 (red), and 9 (green)) on left. The emission spectra of PMI **3b** (magenta), the PMI(OAr)<sub>3</sub> **25a** (cyan), the

sum of the emission of PMI and PMI(OAr)<sub>3</sub> (black), and kinked PMI-(PPE)<sub>n</sub>-PMI(OAr)<sub>3</sub> dyads **24<sub>n</sub>** (n = 5 (blue-dashed), 7 (red-dashed), and 9 (green-dashed)) are shown on the right. Excitation wavelength was 450 nm and the emission spectra were normalized with the concentration.

The black curve in Figure 4.10 is the sum of the emission of the donor PMI and the acceptor PMI(OAr)<sub>3</sub> with equal concentrations. This type of curve appears when there is no interaction between the two fluorophores. The left side spectra show the emission of PMI **3b**, PMI(OAr)<sub>3</sub> **25a**, and linear PMI-(PPE)<sub>n</sub>-PMI(OAr)<sub>3</sub> dyads **19<sub>n</sub>** (n = 2, 5, 7, and 9). The orange curve represents the emission of the PMI-(PPE)<sub>2</sub>-PMI(OAr)<sub>3</sub>, and the emission intensity at the PMI emission region (510-540 nm) almost vanished. This decrease in emission intensity of the PMI-(PPE)<sub>2</sub>-PMI(OAr)<sub>3</sub> dyad **19<sub>2</sub>** at the PMI emission region clearly suggests that there is energy transfer from PMI to PMI(OAr)<sub>3</sub>. When one goes from n = 2-9, the emission intensity at the donor's emission region increases. That means, the emission intensity of donor in presence of acceptor increases as the distance between the donor and the acceptor increases, which suggests that the energy transfer depends on the inter-fluorophore distance *R*.

The spectra on the right side of Figure 4.10 show the emission of PMI **3b**, PMI(OAr)<sub>3</sub> **25a**, and kinked PMI-(PPE)<sub>n</sub>-PMI(OAr)<sub>3</sub> dyads **24<sub>n</sub>** (n = 5, 7, and 9), where the angle between the long axes of the fluorophores is 120°. The kinked PMI-(PPE)<sub>5</sub>-PMI(OAr)<sub>3</sub> dyad **24<sub>5</sub>** has smaller emission intensity at the donor emission region in comparison to the donor PMI **3b**. This reduced emission intensity in the donor emission region suggests that there is energy transfer in the dyad **24<sub>5</sub>**. As the inter-fluorophore distances increases with n = 5-9, the emission intensity at the donor region increases. This clearly shows that the efficiency of energy transfer decreases as the inter-fluorophore distance increases. By comparing the emission spectra of the linear dyads

$19_n$  and kinked dyads  $24_n$  ( $n = 5, 7,$  and  $9$ ), we found that the emission intensities of the kinked dyads  $24_n$  in the donor emission region are higher than the corresponding linear dyads. This suggests that the FRET efficiencies for kinked dyads are lower in comparison to their linear counterparts. This proves that the FRET efficiency depends on the alignment of the fluorophores.

The FRET efficiencies for the linear and kinked molecules were calculated from the decrease in emission intensity of donor and also from the increase in acceptor emission intensity by using Eq.1.7 and Eq. 1.8 and the results are summarized in table 4.3.

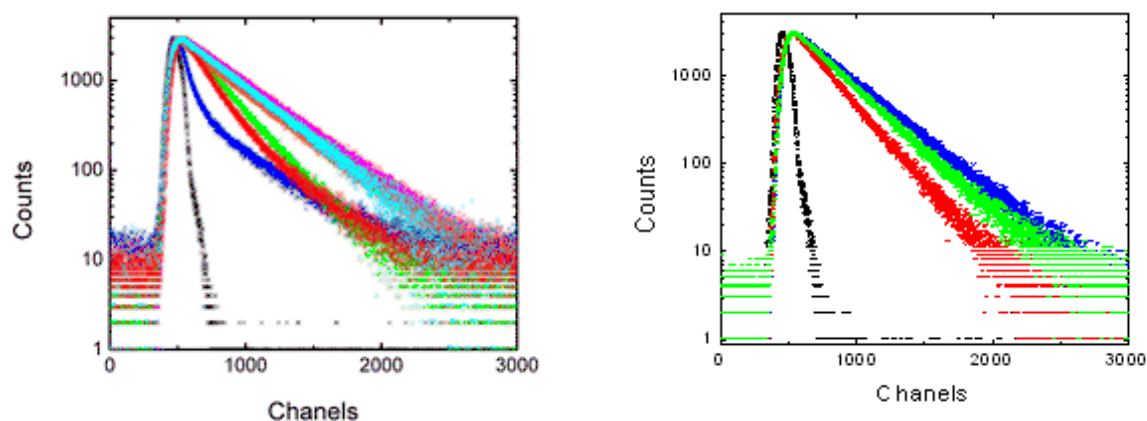


**Figure 4.11** Excited-state lifetime decays of the PMI **3b** (magenta), PMI(OAr)<sub>3</sub> **25a** (cyan), linear PMI-(PPE)<sub>n</sub>-PMI(OAr)<sub>3</sub> dyads  $19_n$  ( $n = 2$  (orange),  $5$  (blue),  $7$  (red), and  $9$  (green)) and the prompt (black) (left). The prompt is the IRF. The figure on the right side shows the excited-state lifetime decays of the kinked PMI-(PPE)<sub>n</sub>-PMI(OAr)<sub>3</sub> dyads  $25_n$  ( $n = 5$  (blue),  $7$  (red), and  $9$  (green)), and the prompt (black). The excited-state lifetime decays were measured by exciting the donor at  $450$  nm and the emission was detected at  $525$  nm in toluene.

The time-resolved lifetime decays of PMI **3b**, PMI(OAr)<sub>3</sub> **25a**, and the linear dyads **19<sub>n</sub>** are determined by time-correlated single photon counting in toluene by exciting at 450 nm and fluorescence decays were collected at 525 nm (Figure 4.11 left). The lifetime decays for the donor PMI **3b** and the acceptor PMI(OAr)<sub>3</sub> **25a** were fitted by a biexponential function and the lifetime decays were found to be 4.84 and 4.52 respectively (Table 4.2), which suggests that these dyes have single exponential decay.

The dyes **3b** and **25a** are integral part of the dyads **19<sub>n</sub>** with  $n = 2, 5, 7,$  and  $9$ . When one would measure the lifetime decay of dyads **19<sub>n</sub>**, one would expect to obtain two lifetime decays corresponding to the respective donor **3a** and the acceptor **25** since both the dyes have emission at 450 nm. If there will be energy transfer process between the donor and the acceptor, one would expect that the life time of donor in presence of acceptor should be less than the lifetime decay of the donor only. Keeping these facts in mind the lifetime decays for the linear dyads **19<sub>n</sub>** with  $n = 2, 5, 7,$  and  $9$  were fitted by a biexponential function keeping the lifetime of the acceptor (4.52 nm) fixed and the results are summarized in table 4.2 (entry 3-6). This result shows that the shorter lifetime decays due to the donor in presence of acceptor  $\tau_{DA}$  for the dyads **19<sub>n</sub>** are smaller than the lifetime  $\tau_D$  of the donor only. This decrease in lifetime of the donor in presence of acceptor supports once again that the energy transfer takes place from PMI to PMI(OAr)<sub>3</sub>. The FRET efficiencies were calculated from the decrease in lifetime of the donor by using Eq.1.9 and the results are summarized in table 4.3.



**Table 4.2** The lifetime decays of PMI, PMI(OAr)<sub>3</sub>, linear dyads **19<sub>n</sub>** (n = 2, 5, 7, and 9), and kinked dyads **24<sub>n</sub>** (n = 5, 7, and 9) in toluene. The excited-state lifetime decays were measured by exciting the donor at 450 nm and the emission was detected at 525 nm in toluene.

Entries	Compounds	Linear dyads <b>19<sub>n</sub></b>				Kinked dyads <b>24<sub>n</sub></b>					
		$\tau^a$		$\alpha^b$		$\tau^a$			$\alpha^b$		
		$\tau_1$	$\tau_2$	$\alpha_1$	$\alpha_2$	$\tau_1$	$\tau_2$	$\tau_3$	$\alpha_1$	$\alpha_2$	$\alpha_3$
1	PMI <b>3b</b>	4.84	-	100	-	-	-	-	-	-	-
2	PMI(OAr) <sub>3</sub> <b>25a</b>	4.52	-	100	-	-	-	-	-	-	-
3	n = 2	0.53	4.52	7	93	-	-	-	-	-	-
4	n = 5	0.67	4.52	60	40	0.11	1.36	4.33	-7.86	89.34	18.52
5	n = 7	1.81	4.52	69	31	0.12	2.84	4.38	-2.97	98.01	4.97
6	n = 9	3.01	4.52	96	4	0.12	3.56	4.34	-3.38	92.66	10.72

<sup>a</sup>  $\tau_1$ ,  $\tau_2$  and  $\tau_3$  are the lifetime components obtained from the biexponential and triexponential fitting, by keeping the lifetime of the acceptor fixed.

<sup>b</sup> The amplitude of the lifetime component.

The lifetime decay fitting and calculation for FRET efficiency for the linear dyads **19<sub>n</sub>** and kinked dyads **24<sub>n</sub>** were conducted by Dr. Brune.<sup>79</sup>

Similarly, the lifetime decays of kinked PMI-(PPE)<sub>n</sub>-PMI(OAr)<sub>3</sub> dyads **24<sub>n</sub>** were determined by time-correlated single photon counting in toluene by exciting at 450 nm and lifetime decays were collected at 525 nm (Figure 4.11 left). The decays were fitted by a triexponential function and the results are summarized in table 4.2. As expected, the lifetimes of the donor in presence of acceptor  $\tau_{DA}$  for the dyads **24<sub>n</sub>** are smaller than the lifetime  $\tau_D$  of the donor only. Comparing the lifetime decay  $\tau_{DA}$  for the linear dyads **19<sub>n</sub>** and kinked dyads **24<sub>n</sub>**, the lifetime  $\tau_{DA}$  of kinked dyads are higher than the linear ones, which suggests that the efficiencies of energy transfer for kinked dyads are less than the linear dyads. This result supports the fact that FRET efficiency depends on the alignment of fluorophores. The FRET efficiencies were calculated from the decrease in lifetime of the donor using Eq.1.9 and the results are summarized in table 4.3.

**Table 4.3** The FRET efficiencies  $E$  of PMI-(PPE)<sub>n</sub>-PMI(OAr)<sub>3</sub> dyads **19<sub>n</sub>** and **24<sub>n</sub>** with respect to the decrease in emission intensity of donor ( $F_D$ ), increase in emission intensity of acceptor ( $F_A$ ) and decrease in the lifetime decays of donor ( $\tau_D$ ) in toluene.  $R$  is the calculated distance between the fluorophores.

Compounds	Linear PMI-(PPE) <sub>n</sub> -PMI(OAr) <sub>3</sub> dyads <b>19<sub>n</sub></b>				Kinked PMI-(PPE) <sub>n</sub> -PMI(OAr) <sub>3</sub> dyads <b>24<sub>n</sub></b>			
	$R$ (nm)	$E_D$	$E_A$	$E_\tau$	$R$ (nm)	$E_D$	$E_A$	$E_\tau$
n = 2	3.47	1.031	0.964	0.956	-	-	-	-
n = 5	5.53	0.827	0.782	0.821	5.65	0.674	0.658	0.674
n = 7	6.90	0.552	0.542	0.536	6.99	0.319	0.316	0.319
n = 9	8.27	0.272	0.292	0.290	8.35	0.117	0.135	0.142

The FRET efficiencies  $E$  calculated by the decrease in emission intensity of donor, increase in emission intensity of acceptor, and decrease in lifetime decay are plotted against the distance  $R$  (calculated distance between the centers of the donor and the acceptor; see Figure 4.8 and table 4.3) (Figure 4.12).

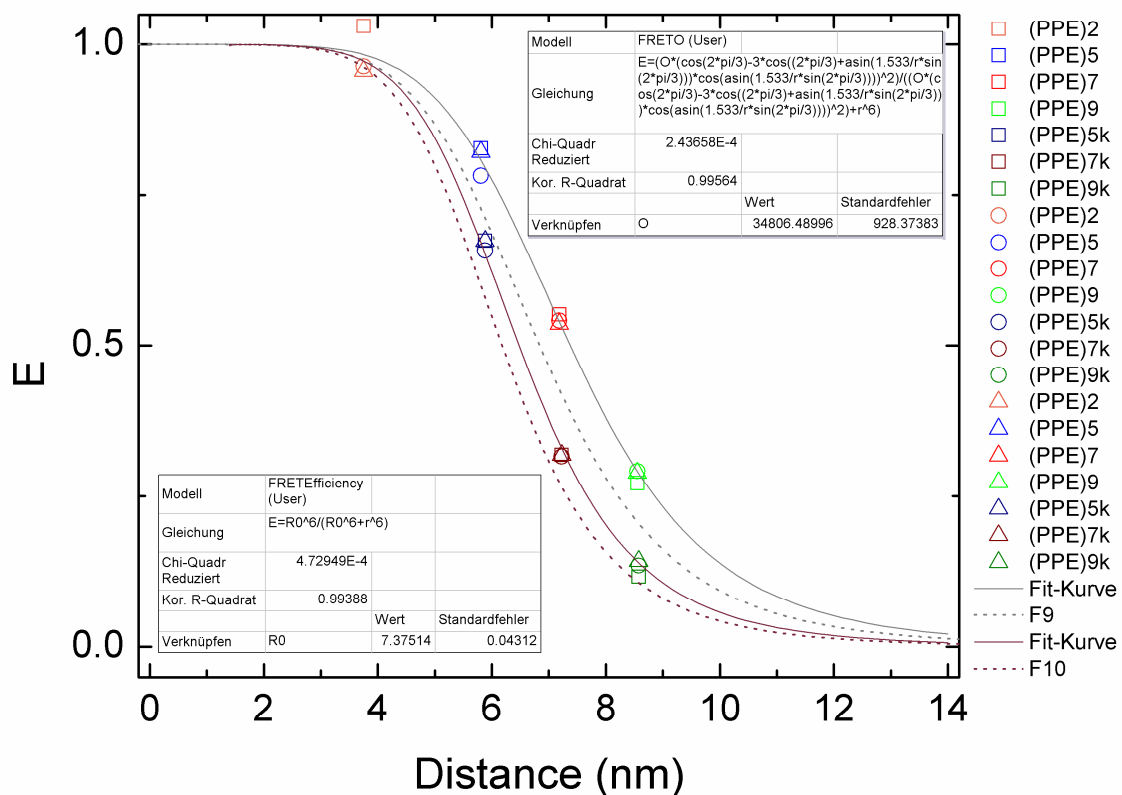


**Figure 4.12** FRET efficiency  $E$  versus calculated inter-fluorophore distances  $R$ .

The gray-dashed curve and wine-dashed curve are the typical FRET curves due to the fitting of the FRET efficiency  $E$  versus  $R_0$  for linear dyads and kinked dyads respectively. The solid gray curve and solid wine curve were generated by plotting the FRET efficiencies  $E$  versus the calculated inter-fluorophore distance  $R$  for linear molecules and the kinked molecules, respectively [(PMI-(PPE) $_n$ -PMI(OAr) $_3$ ], where  $n = 2$

(orange), 5 (blue), 7 (red), and 9 (green)]. The FRET efficiencies due to decrease in fluorescent intensity of donor, increase in fluorescence intensity of acceptor, and decrease in lifetime decay of donor in presence of acceptor are represented by circle, square and triangle respectively.

The solid gray and wine curves in Figure 4.12 show the correlation between the FRET efficiencies  $E$  and the calculated inter-fluorophore distances  $R$  for the linear and kinked dyads. These results are in good agreement with Förster theory and it also proves that the FRET efficiency  $E$  depends on the inverse sixth power of the inter-fluorophore distance  $R$ . Additionally, the FRET efficiencies for the kinked dyads **24<sub>n</sub>** are smaller than that of the straight dyads **19<sub>n</sub>**. This finding also supports the fact that the FRET efficiency depends on the direction of the transition dipole moment of fluorophores.

In summary, I have successfully synthesized the PMI(OAr)<sub>3</sub>-(PPE)<sub>2</sub>-PMI(Py) dyad **14<sub>2</sub>** and studied the photophysical properties, which show the energy transfer takes place from PMI(OAr)<sub>3</sub> to PMI(Py). The photophysical studies for the dyad **14<sub>2</sub>** show that the direction of the energy transfer changed upon protonation. Additionally, PMI(Py) was found to be a suitable candidate for proton sensor.

I have also successfully synthesized a series of PMI/PMI(OAr)<sub>3</sub> labeled oligoPPEs, where the angle between the long axes of PMI and PMI(OAr)<sub>3</sub> is 0°. The steady-state and time-resolved measurements show the energy transfer process takes place from the PMI to the PMI(OAr)<sub>3</sub>. The FRET efficiency decreases as the distance between the centers of the donor and acceptor increases, which is in good agreement

with the Förster theory. A second series of PMI/PMI(OAr)<sub>3</sub> labeled oligoPPEs was synthesized, where the angle between the long axes of PMI and PMI(OAr)<sub>3</sub> is 120°. The steady-state and time-resolved measurements show that the FRET efficiencies for these kinked molecules are comparatively smaller than those of their linear counterparts, which is in good agreement with the Förster theory, that the FRET efficiency depends on the relative orientation of the fluorophores. These studies show that the PMI/PMI(OAr)<sub>3</sub> labeled oligoPPEs are an efficient system and can be used as molecular ruler for FRET study.

## Chapter 5

# Alkynyl-substituted perylenemonoimide

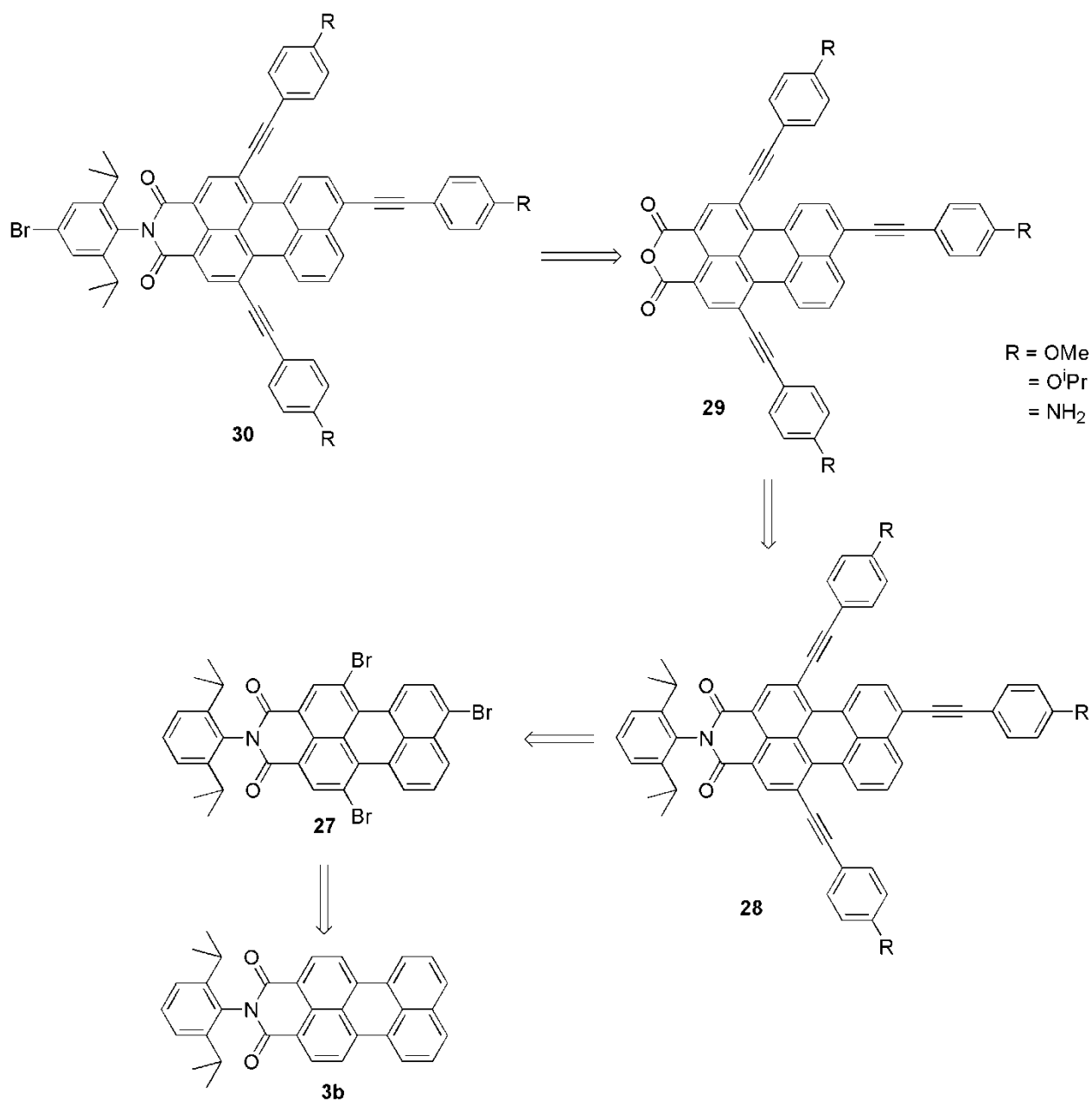
(Ongoing Project)

### 5.1 Introduction

Perylenemonoimide dye and its derivatives are attractive due their high quantum yield, photophysical stability, and thermal stability.<sup>41-44</sup> In chapter 4, I have shown that PMI(OAr)<sub>3</sub> and PMI(Py) can be used as an acceptor fluorophore for energy transfer. The PMI(Py) is also used as donor for electron transfer process.<sup>58</sup> PMI dye derivatives having absorbance and emission at higher wavelength and high fluorescence quantum yield are still in high demand, due to their potential applications for FRET study and also electron transfer process.

By introducing substituents on the bay region of PMI not only the solubility changes, but also the spectral properties change. The presence of three *p*-(*tert*)-butylphenoxy substituents at the bay region of the PMI show a red shift of approximately 30 nm and 45 nm in the absorption and emission maximum, respectively.<sup>73</sup> Similarly, *N*-pyrrolidinyl substituents at the 9-position of PMI results in a bathochromic shift of the absorption and emission maximum by 80 nm and 156 nm respectively, and the fluorescence quantum yield drops to 0.15 (See Chapter 2.3, Table 2.1). These spectral changes are due to the fact of extended  $\pi$ -conjugation of the substituents with the perylene core.<sup>60</sup> Keeping this fact in mind, a PMI derivative was designed, where the substituents are *para*-alkoxyphenyleneethynylene units (Scheme 4. 1). Recently, Edvinsson *et al.*<sup>78</sup> reported similar PMI-derivatives for the purpose of solar cells.

## 5.2 Strategy

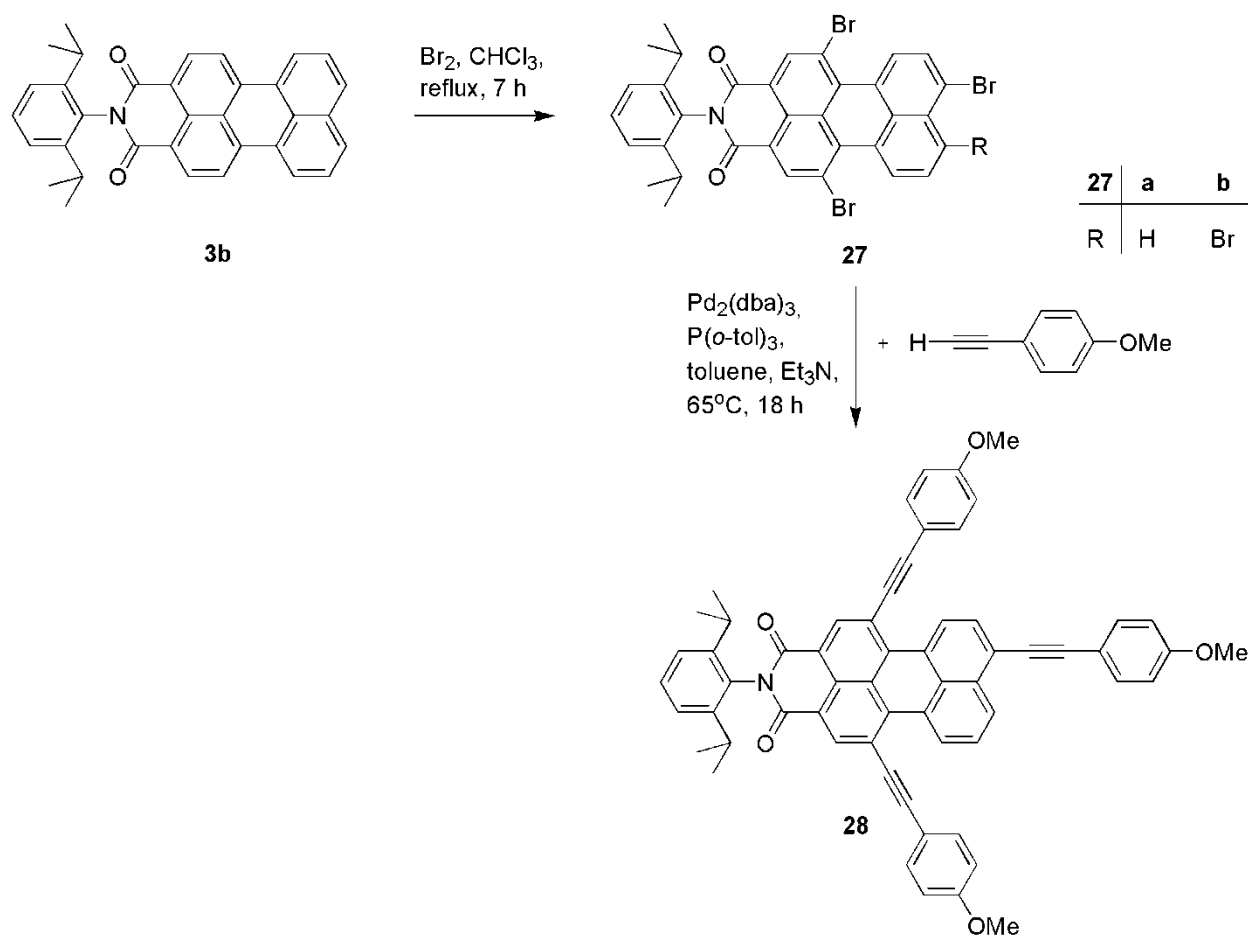
**Scheme 5.1** Retro synthesis of alkynyl-substituted perylenemonoimide.

The alkynyl-substituted PMI **30** carrying a bromo phenylene unit at the imide position will be an ideal fluorophore for attaching with a suitable fluorophore for FRET (Scheme 5.1). For synthesis of the compound **30**, the ideal starting point will be the PMI **3b**. Bromination of the PMI **3b** will produce tribrominated PMI **27**, which subsequently

couples with the ethyne to produce the alkynyl-substituted PMI **28**. The compound **28** can be hydrolyzed under basic condition to achieve the anhydride **29**, which will subsequently treated with 4-bromo-2,6-diisopropylaniline to produce the desired product **30**.

### 5.3 Synthesis

**Scheme 5.2** Synthesis of alkynyl-substituted perylenemonoimide.



A solution of PMI **3b** in chloroform was refluxed with excess bromine to afford brominated PMI derivatives **27** in 45-52 % yield (Scheme 5.2).<sup>56,57</sup> The compound **27** was characterized by <sup>1</sup>H NMR which confirms that it contains a mixture of tribrominated



PMI **27a** and 6-7 mol% of tetrabrominated PMI **27b**. The compounds **27a** and **27b** have same  $R_f$  on TLC, so we decided to carry out the further reaction taking the mixture.

The mixture of tribrominated PMI **27a** with 6-7 mol% of tetrabrominated PMI **27b** was coupled with the 3-(4-methoxyphenyl)ethyne by Pd-catalyzed coupling to afford the alkynyl-substituted perylenemonoimide **28** as a pink solid in 34% yield (Scheme 5.2). The compound **28** is only soluble in  $\text{CHCl}_3$ .

## 5.4 Photophysical studies

The absorption and emission spectra of compound **28** was measured in toluene and the fluorescence quantum yield was determined taking the benchmark perylene dyes **3b** and **25a** (Figure 4.8) as the reference.

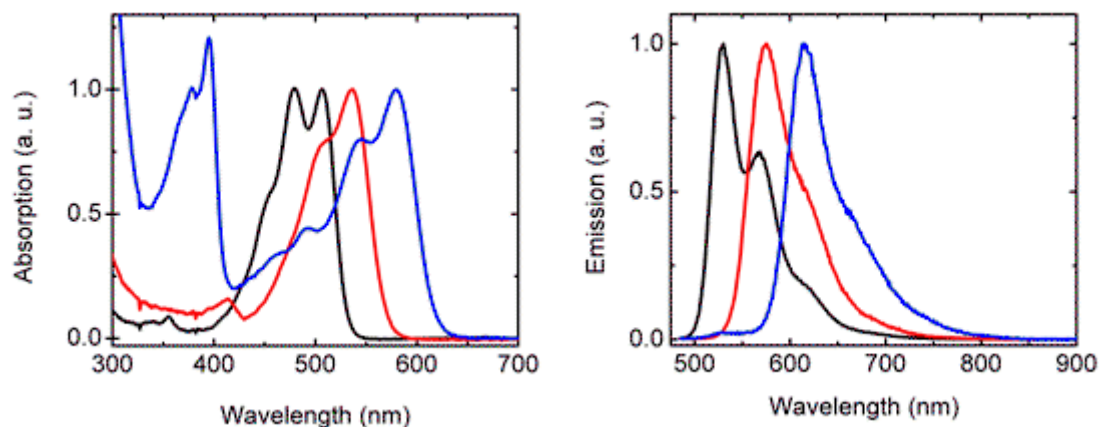


**Figure 5.1** Absorption (left) and emission (right) spectra of **3a** (black), **25a** (red), and **28** (blue). The spectra are normalized at their maximum for a good comparability. The excitation wavelength was 475 nm.

The blue line in figure 5.2 left is the absorption of compound **28** and shows two peaks; a shorter wavelength around 345 nm is due to the phenyleneethyne unit. The

peak at higher wavelength around 579 is due to the perylene core. The absorption maximum shows a bathochromic shift of 73 nm and 43 nm in comparison to the benchmark perylene dyes **3b** and **25a** respectively.

Similarly, the emission spectrum of compound **28** (blue line) shows a bathochromic shift of 85 nm and 40 nm in comparison to the dyes **3b** and **25a** (Figure 5.1, right).

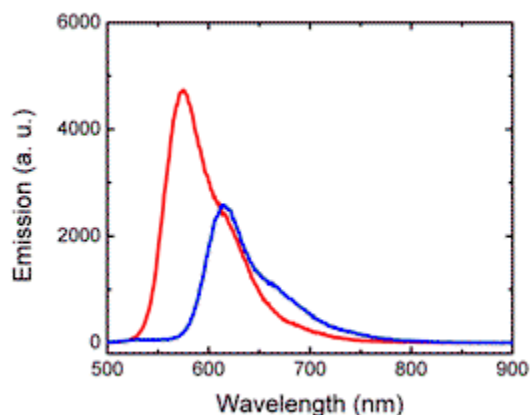


**Figure 5.2** The normalized emission spectra for **25a** (red) and **28** (blue).

The fluorescent quantum yield of the compound **28** was determined to be 0.49 by using Eq. 2.1 and the dye **25a** was taken as reference with a quantum yield of 0.86<sup>73</sup> (Figure 5.2).

In summary, alkynyl-substituted perylenemonoimide dye **28** was synthesized successfully. The photophysical studies show that the dye has absorption maximum at 585 nm, emission maximum at 615 nm with a fluorescence quantum yield of 0.49. This fluorophore has poor solubility and also poor yield (34%). In order to improve the solubility, synthetic modifications are necessary. By exchanging the methoxy group for isopropoxy group, the solubility might increase.

## Chapter 6

### Summary

Perylenemonoimide and aryloxy-substituted perylenemonoimide were synthesized successfully. Amino-substituted perylenemonoimide dyes **6c-6e** were synthesized successfully starting from tribrominated perylenemonoimide. These dyes have also been synthesized following a different route starting from monobrominated perylenemonoimide. The photophysical studies show that there is dual fluorescence for the amino-substituted PMI and it is structure specific. The dual fluorescence predominantly observed for the dyes **6d** and **6e** and this effect increases with increase in the solvent polarity. The dye **6e** was used as an acceptor for FRET study and this can be used as proton sensor.

Similarly, alkynyl-substituted dye **28** was synthesized and the photophysical studies show absorption maximum at 585 nm and emission maximum at 615 nm with a fluorescence quantum yield of 0.49.

A series of oligoPPEs with HOM and TIPS as the orthogonal protecting groups, were synthesized by the usual convergent-divergent process. Similarly, another series of oligoPPEs was synthesized by following same convergent-divergent approach where HOE and TIPS are the orthogonal protecting groups. The HOE group was successfully removed by the  $\gamma\text{MnO}_2$  /KOH. Freshly prepared  $\gamma\text{MnO}_2$  is necessary for the removal of HOM and HOE groups. The resulting free acetylenes were used as spacer for the construction of molecular ruler.

A PMI(OAr)<sub>3</sub>/PMI(Py) labeled oligoPPE or dyad **14<sub>2</sub>** was successfully synthesized. The photophysical studies show that the energy transfer process takes place from PMI(OAr)<sub>3</sub> to the PMI(Py). Interestingly, reverse FRET was observed for the protonated dyad **14<sub>2</sub>**. This dyad can be used as proton sensor.

A series of linear and kinked dyads were synthesized, where PMI **3b** and PMI(OAr)<sub>3</sub> **25a** were used as fluorescent probes. In both of these dyads, the energy transfer process takes place from PMI **3b** to the PMI(OAr)<sub>3</sub> **25a**. The FRET efficiencies for both of the linear and kinked dyads were calculated from the decrease in emission intensities and decrease in lifetime decays of the donor in presence of the acceptor and also from the increase in emission intensity of the acceptor. The correlation between  $E$  and the calculated inter-fluorophore distance  $R$  shows that the efficiency  $E$  decreases as the distance  $R$  increases. This result is in very good agreement with the dependency of FRET efficiency on the inverse sixth power of distance  $R$ . Secondly, the FRET efficiencies of the linear dyads were comparatively higher than the kinked dyads, which suggests that the FRET efficiency depends on the relative orientation of the transition dipole moments of the fluorophores. This is in good agreement with the Förster theory. Therefore, the PMI/PMI(OAr)<sub>3</sub> labeled oligoPPEs are the appropriate molecular ruler for FRET studies.

## Chapter 7

### Experimental

#### 7.1 General methods and instruments

Perylene-dianhydride, 2,6-diisopropylaniline, Imidazole,  $\text{Zn}(\text{OAc})_2 \cdot 2\text{H}_2\text{O}$ ,  ${}^n\text{Bu}_4\text{NF}$  (1M in THF), pyrrolidine, and DMF (anhydrous) were purchased from Acros Organics and  $\text{Pd}_2(\text{dba})_3$ ,  $p(o\text{-toly})_3$  were from Aldrich. Bromine,  $\text{Et}_3\text{N}$ , toluene and 4-*tert*-butylphenol were purchased from Merck. All chemicals were used as received.  $\text{CDCl}_3$  and  $\text{CD}_2\text{Cl}_2$  were obtained from Flora Chemicals. Previously synthesized compounds 1,4-dihexyl-2,6-diiodobenzene, iodomonomer **7a<sub>1</sub>**, iododimer **7b<sub>2</sub>** and tetramer **8a<sub>4</sub>** were available from our laboratory. PMI(pip) **6c**, PMI(EtHex) **6d**, PMI(Py) **6e**, and PMI(Me)<sub>2</sub> **6g**, used for the photophysical studies were synthesized by Ms. Miriam Schulte starting from monobromo perylenemonoimide PMI(Br) **4c** under my assistance.

The photophysical studies were carried out in cooperation with Prof. Dr. Markus Sauer's group at the Department of Physics, Bielefeld University. These experiments were carried out together with Dr. Ralf Brune.

Absorption spectra were taken on a UV/Vis spectrophotometer (Perkin Elmer). Fluorescence spectra were recorded with a spectrofluorimeter (Cary Eclipse) at concentrations of below  $10^{-6}$  M. Ensemble fluorescence lifetime measurements were performed on a 5000 MC spectrometer (IBH, Glasgow, UK) using time-correlated single-photon counting (TCSPC). As excitation source a pulsed light emitting diode (center 450 nm) with a repetition rate of 1 MHz and a pulse length of 1~ns (FWHM) was used. With

this setup an instrument response function (IRF) of 1 ns (FWHM) was measured. Typically, 3000 photon counts were collected in the maximum channel using 2048 channels. The decay parameters were determined by least-square deconvolution, and their quality was judged by the reduced  $\chi^2$  values and the randomness of the weighted residuals. All fluorescence decays measured could be described satisfactorily by a monoexponential model. Measurements were performed at room temperature (20 °C).

- Thin layer chromatography (TLC)

Silica gel coated on aluminium plate with fluorescent indicator from Merck, silica gel size 60, F<sub>254</sub>, layer thickness 0.25 mm

Detection: UV-Lamp, Beneda 366/254, heidelberg

- Column chromatography

Silica gel MN-60 (Mesh size 40-63  $\mu\text{m}$  and 63-200  $\mu\text{m}$ ) from Merck

- HPLC

Aligent 1200 series

Detector: UV-Vis, Emission

Reverse Phase Column: C<sub>18</sub> Spiex from Macherey & Nagel.

- Nuclear magnetic resonance spectroscopy (NMR)

<sup>1</sup>H NMR

Instruments: Bruker AM 250 (250.133 MHz), DRX 500 (500.132, MHz), DRX 600 (600.133, MHz), with internal standards: CDCl<sub>3</sub> (7.25 ppm), CD<sub>2</sub>Cl<sub>2</sub> (5.32 ppm).

Measurement Temperature: 300 K

The chemical shifts are given in ppm, coupling constants ( $J$ ) are given in Hz. The multiplicity of the signals are given as s = singlet, d = doublets, t = triplets, q = quartets, and m = multiplets.

### $^{13}\text{C}$ NMR

Instrument: Bruker AM 250 (62.896 MHz), DRX 500 (125.772, MHz), with internal standards:  $\text{CDCl}_3$  (77.0 ppm),  $\text{CD}_2\text{Cl}_2$  (53.5 ppm).

Measurement Temperature: 300 K

- MALDI TOF

MALDI TOF mass spectra were recorded with a Vozager<sup>®</sup> DE instrument mounted with 1.2 m flight tube. Isolation was achieved using LSI nitrogen laser (337 nm beam wavelength, 3 ns pulse width, 3 Hz repetition rate). Depending on the mass range the ions were accelerated with 15 to 20 kV. If not mentioned differently, 2-[(2E)-3-(4-*t*-butylphenyl)-2-methylpro-2-enylidene]malononitrile was used as the matrix and THF as the solvent to prepare the samples.

## 7.2 General procedures

### 7.2.1 General procedure A: Alkyny-Aryl coupling for oligoPPEs

In a Schlenk flask the coupling components were taken along with dry THF and dry piperidine. The reaction mixture was degassed through freeze-pump-thaw cycles for three times.<sup>69,70</sup> To the degassed reaction mixture  $\text{Pd}(\text{PPh}_3)_2\text{Cl}_2$  (1 mol % with respect to the aryl halide) and  $\text{CuI}$  (2 mol % with respect to the aryl halide) were added. The reaction mixture was stirred at room temperature for 18 h. After 18 h,  $\text{Et}_2\text{O}$  and 2 N  $\text{HCl}$

was added successively. The phases were separated and the aqueous phase was extracted with Et<sub>2</sub>O. The combined organic phases were washed with water and then dried over Na<sub>2</sub>SO<sub>4</sub>. The products were isolated by column chromatography. In case of oligomers, the first fractions were collected as the dimer of the respective non-polar acetylene used for the coupling.

### 7.2.2 General procedure B: Synthesis of acetylene

To a solution of **8a<sub>n</sub>**, **15<sub>n</sub>**, and **17<sub>n</sub>** in THF, 1 M <sup>n</sup>BuN<sub>4</sub>F in THF (2 equiv.) was added and stirred at room temperature. After 2 h, Et<sub>2</sub>O and water were added to the reaction mixture and stirred for 5 minutes. The aqueous phase was separated and extracted with Et<sub>2</sub>O. The combined organic phases were washed with water. The organic phase was dried over Na<sub>2</sub>SO<sub>4</sub> and the solvent was evaporated to get the required products.

### 7.2.3 General procedure C: Synthesis of non-polar acetylene 9a<sub>n</sub>

The solution of oligoPPEs **8a<sub>n</sub>** (n = 5), and **8b<sub>n</sub>** (n = 6, 7, 9) in Et<sub>2</sub>O were treated with activated γ-MnO<sub>2</sub>/KOH in four portions, each at the interval of every one hour.<sup>79,70</sup> After completion of reaction, the reaction mixture was filtered through a pad of silica gel and subsequent evaporation of the solvent gave compounds **9a<sub>n</sub>** (n= 5-9).

In case of **8b<sub>9</sub>** THF was used as solvent and excess MnO<sub>2</sub>/KOH was added till completion of reaction. The duration of reaction for **9b<sub>6</sub>-9b<sub>9</sub>** was about 5-6 h.

### 7.2.4 General Procedure D: Alkynyl-aryl coupling using Pd<sub>2</sub>(dba)<sub>3</sub> and P(o-tolyl)<sub>3</sub>

In a Schlenk flask the coupling components (aryl halide, free acetylene) were taken along with toluene and Et<sub>3</sub>N and degassed for three times through freeze-pump-



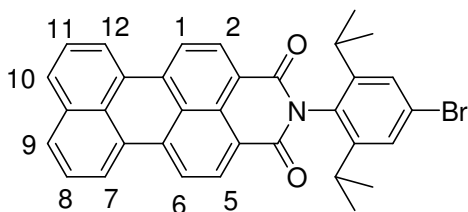
thaw cycles. To the degassed reaction mixture in frozen state  $\text{Pd}_2(\text{dba})_3$  (10 mol% with respect to the aryl halide) and  $\text{P}(o\text{-tolyl})_3$  (65 mol% with respect to the aryl halide) were added under argon.<sup>56</sup> The flask was evacuated and refilled with argon for three times. The reaction mixture was stirred at 65 °C. After 18 h, the reaction mixture was cooled to room temperature.  $\text{Et}_2\text{O}$  and 2 N HCl were added successively to it and the reaction mixture was stirred for 5 min. The aqueous phase was separated and extracted with  $\text{Et}_2\text{O}$ . The combined organic phases were washed with water and then dried over  $\text{Na}_2\text{SO}_4$ . The products were isolated by column chromatography.

### 7.2.5 General Procedure E: Synthesis of amino-substituted perylenemonoimide

A sample of **4**, and the corresponding amines (excess) were taken in a flask along with anhydrous DMF under argon. The reaction mixture was refluxed for 3 h. After cooling the reaction mixture to room temperature,  $\text{Et}_2\text{O}$ , 2N HCl were added successively and stirred for 5 min. The organic phase was separated out and the aqueous phase was extracted with  $\text{Et}_2\text{O}$  (3 x). The combined organic phases were washed with distilled water. The organic phase was dried over  $\text{Na}_2\text{SO}_4$  and the solvent was evaporated to get the crude materials. The products were isolated by column chromatography.

## 7.3 Synthesis of perylenemonoimide derivatives

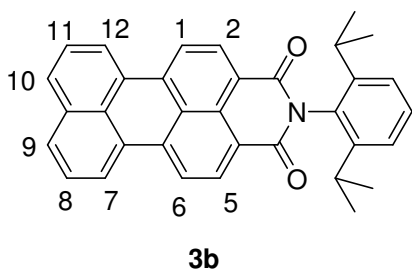
### 7.3.1 Synthesis of perylenemonoimide **3a**



**3a**

Following the procedure described by Lindsey *et al.*<sup>16</sup>, hydrobromide **1a** (600 mg, 2.05 mmol), perylene dianhydride **2** (1.58 g, 4.04 mmol), Zn(OAc)<sub>2</sub>·2H<sub>2</sub>O (540 mg, 2.46 mmol), imidazole (7.8 g), and distilled water (3.5 mL) were heated at 190 °C for 18 h in a thick walled pressure tube (35 mL, 17.8 cm x 25.4 mm). After cooling the reaction mixture to room temperature, the pressure was released. The crude material was suspended in distilled water and the suspension was filtered. The solid that had been filtered from the suspension was resuspended in (1:1) conc. HCl, MeOH and filtered. Finally the solid that had been filtered from the second suspension was suspended in MeOH and filtered. The solid was dried under vacuum. The solid obtained after drying was suspended in CHCl<sub>3</sub> (15 mL) and loaded on a column (silica gel, 4 × 30 cm<sup>2</sup>) and eluted with CHCl<sub>3</sub>. A slightly yellow byproduct (perylene) was eluted first, which was not collected. Subsequently, the required product **3a** was eluted in the 2<sup>nd</sup> fraction. The solvent was evaporated to afford **3a** as a red solid (303 mg, 30%). <sup>1</sup>H NMR data is identical to those reported by Lindsey.<sup>54</sup>

### 7.3.2 Synthesis of perylenemonoimide **3b**

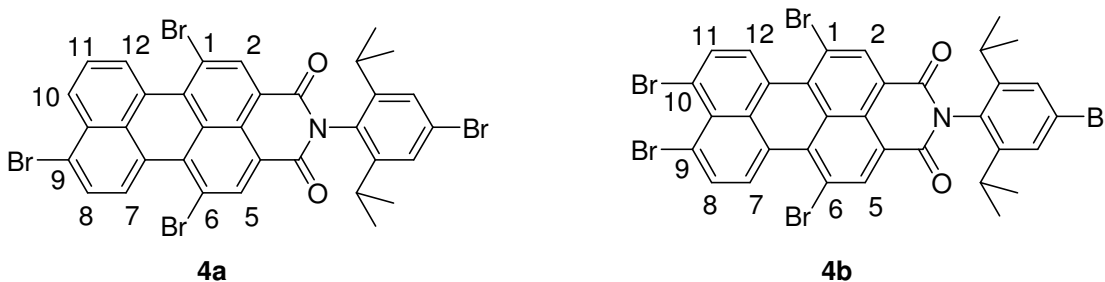


Following the procedure described by Lindsey *et al.*<sup>55</sup> for imidation and double decarboxylation in an autoclave but in a thick walled pressure tube (35 mL, 17.8 cm x 25.4 mm), a commercially available perylene dianhydride **2** (1.9 g, 4.04 mmol), 2,6-diisopropylaniline (470 mg, 2.65 mmol), Zn(OAc)<sub>2</sub>·2H<sub>2</sub>O (693 mg, 3.16 mmol), imidazole (9.9 g), and distilled water (4.0 mL) were heated at 190 °C for 18 h. After cooling the

reaction mixture to room temperature, the pressure was released. The crude material was suspended in distilled water and the suspension was filtered. The solid that had been filtered from the suspension was resuspended in (1:1) conc. HCl, MeOH and filtered. Finally the solid that had been filtered from the second suspension was suspended in MeOH and filtered. The solid was dried under vacuum. The solid obtained after drying was suspended in  $\text{CHCl}_3$  (15 mL) and loaded on a column (silica gel,  $4 \times 25 \text{ cm}^2$ ,  $\text{CHCl}_3$ ) and eluted with  $\text{CHCl}_3$ . A slightly yellow byproduct (perylene) was eluted first, which was not collected. Subsequently, the required product **3b** was eluted in the 2<sup>nd</sup> fraction. The solvent was evaporated to afford **3b** as red solid (600 mg, 47%,  $R_f = 0.13$ ).

$^1\text{H NMR}$  (500 MHz):  $\delta = 1.17$  (d,  $J = 6.9$  Hz, 12 H,  $\text{CH}(\text{CH}_3)_2$ ), 2.73-2.79 (m, 2 H,  $\text{CH}(\text{CH}_3)_2$ ), 7.33 (d,  $J = 7.8$  Hz, 2 H, Ar-H ortho to  $\text{CH}(\text{CH}_3)_2$ ), 7.47 (t,  $J = 7.8$  Hz, 1 H, Ar-H meta to  $\text{CH}(\text{CH}_3)_2$ ), 7.65 (t,  $J_1 = 7.8$  Hz, 2 H, H-8, H-11), 7.92 (d,  $J = 8.1$  Hz, 2 H, H-9, H-10/H-7, H-12). 8.47 and 8.48 (2 d,  $J_1 = 8.5$  Hz,  $J_2 = 8.0$  Hz, 4 H, H-1, H-2, H-5, and H-6), 8.66 (d,  $J = 8.0$  Hz, 2 H, H-7, H-12/H-9, H-10). - MALDI TOF:  $m/z = 482.6$ .

### 7.3.3 Synthesis of bromo-substituted perylenemonoimide **4**

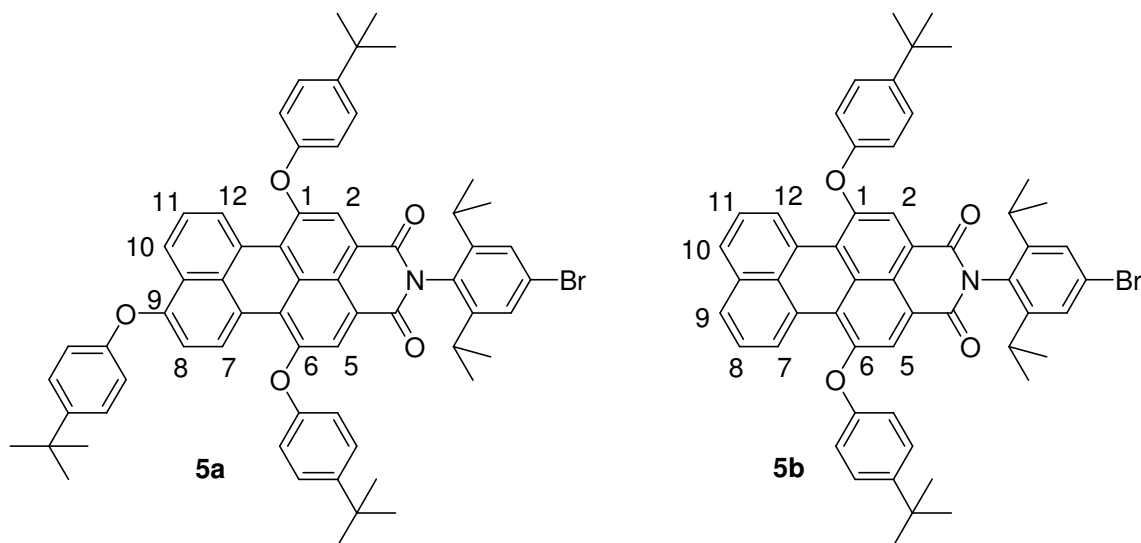


The procedure described by Lindsey *et al.*<sup>56</sup> was followed.  $\text{Br}_2$  (0.85 mL, 16.41 mmol) was added to a solution of **3a** (460 mg, 0.82 mmol) in  $\text{CHCl}_3$  (25 mL) and heated to reflux. After 3 h and 5 h, identical amounts of  $\text{Br}_2$  were added. After a total reaction

time of 8 h, the reaction mixture was cooled to room temperature with an ice bath. The cooled reaction mixture was treated with saturated aqueous  $\text{Na}_2\text{SO}_3$  solution (40 ml) and stirred for 3-4 min. suddenly; the reaction mixture came out from the flask due to exothermic reactions. The reaction mixture was collected and washed with  $\text{Na}_2\text{SO}_3$  solution. Finally, the organic phase was washed with water and then dried over  $\text{Na}_2\text{SO}_4$ . The solvent was evaporated to get the crude product. Column chromatography (4 x 30  $\text{cm}^2$  silica gel, (1:1)  $\text{CHCl}_3/n$ -hexane) afforded a 12.6:1.0 mixture (340 mg,  $R_f = 0.61$  in 3:1  $\text{CHCl}_3$  and  $n$ -hexane) of **4a** (313 mg, 48%) and **4b** (27 mg, 4%) as a red solid.

$^1\text{H}$  NMR (500 MHz) of **4a**:  $\delta = 1.15$  (d,  $J = 6.8$  Hz, 12 H,  $\text{CH}(\text{CH}_3)_2^*$ ), 2.63-2.68 (m, 2 H,  $\text{CH}(\text{CH}_3)_2^*$ ), 7.44 (s, 2 H, Ar- $H$  ortho to  $\text{CH}(\text{CH}_3)_2^*$ ), 7.81 (t,  $J = 8.1$  Hz, 1 H,  $H-11$ ), 7.99 (d,  $J = 8.3$  Hz, 1 H,  $H-7/8$ ), 8.46 (d,  $J = 8.4$  Hz, 1 H,  $H-12/10$ ), 8.90 and 8.92 (2 s, 1 H each,  $H-2$ ,  $H-5$ ), 9.11 (d,  $J = 8.3$  Hz, 1 H,  $H-8/7$ ), 9.33 (d,  $J = 7.5$  Hz, 1 H,  $H-10/12$ ). - MALDI TOF:  $m/z = 797.7$ .

\* These signals have higher intensity than expected and this higher intensity is due to the additional signal for the phenylene group at the imides moiety of **4b**. The remaining signals due to the compound **4b** are  $\delta = 8.11$  (d,  $J = 8.3$  Hz, 2 H,  $H-7$ ,  $H-12/H-8$ ,  $H-11$ ), 8.88 (s, 2 H,  $H-2$ ,  $H-5$ ), 8.94 (d,  $J = 8.3$  Hz, 2 H,  $H-8$ ,  $H-11/H-7$ ,  $H-12$ ).

7.3.4 Synthesis of aryloxy-substituted perylenemonoimide **5**

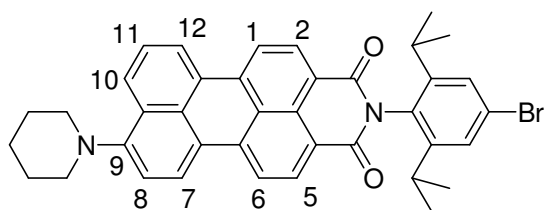
Following the procedure described by Lindsey *et al.*<sup>54</sup> a (12.6:1) mixture of **4a** and **4b** (340 mg, 0.43 mmol), 4-*tert*-butylphenol (767.8 mg, 5.11 mmol), and K<sub>2</sub>CO<sub>3</sub> (848 mg, 6.13 mmol) were dissolved in DMF (25 mL, anhydrous) under argon and refluxed at a bath temperature of 170 °C for 1 h. After cooling down the reaction mixture, the DMF was distilled off by vacuum distillation using the diaphragm pump and heating the reaction mixture to 60 °C. Water (100 mL) and CHCl<sub>3</sub> (100 mL) were added to the residue and stirred for 10 min. The organic phase was separated out and the aqueous phase was extracted with CHCl<sub>3</sub> (3 x 25 mL). The combined organic phases were dried over Na<sub>2</sub>SO<sub>4</sub>. The solvent was evaporated to get the crude product. Column chromatography (silica gel, 4 x 30 cm<sup>2</sup>, CHCl<sub>3</sub>/*n*-hexane (4:6)) afforded a 13.7:1.0 mixture (65 mg, *R*<sub>f</sub> = 0.33) of **5a** (61 mg, 16%) and **5b** (4 mg, 1%) as a magenta solid in the first fraction. In the second fraction a 32:1.0 mixture (180 mg) of **5a** (175 mg, 44%) and **5b** (5 mg, 1.5%) was isolated as a magenta solid. A 1.5:1.0 mixture (40 mg) of **5a**

(23 mg, 16%) and **5c** (17 mg, 44%) was isolated as third fraction, and subsequently **5c** was isolated (8 mg, 22%) with traces of unknown impurity in the 4<sup>th</sup> fraction.

<sup>1</sup>H NMR (500 MHz):  $\delta$  = 1.12 (d,  $J$  = 6.6 Hz, 12 H, CH(CH<sub>3</sub>)<sub>2</sub><sup>\*</sup>), 1.31, (3s, 9 H, *t*-butyl), 1.33, and 1.34 (s, 9 H each, *t*-butyl<sup>\*</sup>), 2.62-2.71 (m, 2 H, CH(CH<sub>3</sub>)<sub>2</sub><sup>\*</sup>), 6.89 (d,  $J$  = 8.8 Hz, 1 H, *H*-8/7), 7.00 (2 H, half of AA'XX' spinsystem, OAr-*H* meta to *t*-butyl<sup>\*</sup>), 7.06 and 7.09 (2 H each, half of AA'XX' spinsystem, OAr-*H* meta to *t*-butyl<sup>\*</sup>), <sup>\*</sup>7.36 (2 H, half of AA'XX' spinsystem, OAr-*H* ortho to *t*-butyl), <sup>\*</sup>7.38 (s, 2 H, Ar-*H* ortho to CH(CH<sub>3</sub>)<sub>2</sub>), <sup>\*</sup>7.41 (4 H, half of AA'XX' spinsystem, Ar-*H* ortho to *t*-butyl), 7.64 (t,  $J$  = 8.0 Hz, 1 H, *H*-11), 8.28 and 8.32 (2 s, 1 H each, *H*-2, *H*-5<sup>\*</sup>), 8.48 (d,  $J$  = 8.1 Hz, 1 H, *H*-10/12), 9.24 (d,  $J$  = 8.8 Hz, 1 H, *H*-7/8), 9.44 (d,  $J$  = 7.5 Hz, 1 H, *H*-12/10). MALDI TOF:  $m/z$  = 1005.22.

<sup>\*</sup>These signals have higher intensity than expected and this higher intensity is due to the additional signals for the phenylene group at the imide position and the aryloxy group present at the bay region (1 and 9 position) of **5b**. The remaining signals due to the compound **5b** are  $\delta$  = 7.59 (t,  $J$  = 7.9 Hz, 2 H, *H*-8, *H*-11), 7.91 (d,  $J$  = 8.1 Hz, 2 H, *H*-9, *H*-10/*H*-7, *H*-12), 9.36 (d,  $J$  = 7.9 Hz, 2 H, *H*-7, *H*-12/*H*-9, *H*-10).

### 7.3.5 Piperidinyl-substituted perylenemonoimide **6c**

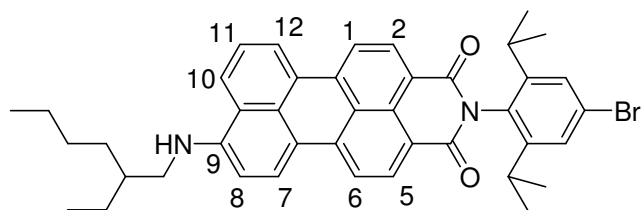


Following general procedure E, the mixture of **4a** and **4b** (25 mg, 0.03 mmol), piperidine (1.0 mL, 10.123 mmol) were refluxed with anhydrous DMF (3 mL) under argon for 3 h to obtain the required product **6c**. Column chromatography [4 x 15 cm,

silica gel,  $\text{CHCl}_3$ :*n*-Hexane (1:1) and then the solvent was changed to  $\text{CHCl}_3$  and later  $\text{MeOH}:\text{CHCl}_3$  (1:20)] afforded desired product **6c** as violet solid (9 mg, 45%).

$^1\text{H}$  NMR (250 MHz)  $\delta$  = 1.16 (d,  $J$  = 6.75 Hz, 12 H,  $\text{CH}(\text{CH}_3)_2$ ), 1.72 (m, 2 H,  $\text{CH}_2$   $\gamma$  to N), 1.89 (m, 4 H,  $\text{CH}_2$   $\beta$  to N), 2.75 (m, 2 H,  $\text{CH}(\text{CH}_3)_2$ ), 3.19 (m, 4 H,  $\text{CH}_2$   $\alpha$  to N), 7.19 (d,  $J$  = 8.3 Hz, 1 H, *H*-8), 7.43 (s, 1 H, Ar-*H* ortho to  $\text{CH}(\text{CH}_3)_2$ ), 7.61-7.67 (t,  $J$  = 7.75 Hz, 1 H, *H*-11), 8.25 (d,  $J$  = 8.5 Hz, 1 H, *H*-10), 8.31 (d,  $J$  = 8.3 Hz, 1 H, *H*-7). 8.38 and 8.42 (2d,  $J$  = 7.25 Hz, 1 H each, *H*-1, *H*-6), 8.47 (d,  $J$  = 6.8 Hz, 1 H, *H*-12), 8.56 and 8.62 (2d,  $J$  = 5.5 Hz, 1 H each, *H*-2, *H*-5).

### 7.3.6 2-Ethylhexylamine-substituted perylenemonoimide **6d**

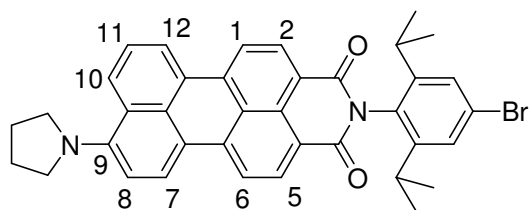


Following general procedure E, a sample of **4** (25 mg, 0.03 mmol), 2-ethylhexylamine (1.5 mL, 10.613 mmol) were refluxed with anhydrous DMF (3 mL) under argon for 3 h to obtain the required product **6d**. Column chromatography [4 x 15  $\text{cm}^2$  silica gel, 1:1 mixture of  $\text{CHCl}_3$  and *n*-Hexane. Later the solvent was changed to  $\text{CHCl}_3$  and finally a 1:20 mixture of MeOH and  $\text{CHCl}_3$ ] afforded desired product **6d** as a blue solid (12 mg, 57%).

$^1\text{H}$  NMR (600 MHz)  $\delta$  = 0.94 (m, 3 H,  $\text{CH}_2\text{CH}_3$ ), 1.01 (m, 3 H,  $\text{CH}_2\text{CH}_3$ ), 1.15 (d,  $J$  = 6.6 Hz, 12 H,  $\text{CH}(\text{CH}_3)_2$ ), 1.38 (m, 4 H,  $\text{CH}_2$ ), 1.52 (m, 4 H,  $\text{CH}_2$ ), 1.80 (m, 1 H,  $\text{CHCH}_2\text{NH}$ ), 2.72 (m, 2 H,  $\text{CH}(\text{CH}_3)_2$ ), 3.34 (t,  $J$  = 11.1 Hz, 2 H,  $\text{CH}_2\text{NH}$ ), 5.02 (t,  $J$  = 4.8

Hz, 1 H, *NH*), 6.77 (d,  $J = 8.4$  Hz, 1 H, *H-8*), 7.42 (s, 1 H, Ar-*H* ortho to  $\text{CH}(\text{CH}_3)_2$ ), 7.60 (t,  $J = 7.8$  Hz, 1 H, *H-11*), 7.86 (d,  $J = 8.4$  Hz, 1 H, *H-10*), 8.19 (d,  $J = 8.4$  Hz, 1 H, *H-7*), 8.37 and 8.39 (2d,  $J = 8.4$  Hz, 1 H each, *H-1*, *H-6*), 8.52 (d,  $J = 7.2$  Hz, 1 H, *H-2/5*), 8.54 (d,  $J = 7.8$  Hz, 1 H, *H-5/2*), 8.59 (d, 1H,  $J = 7.8$  Hz, *H-12*).

### 7.3.7 Pyrrolidnyl-substituted perylenemonoimide **6e**



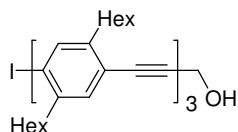
Following general procedure E, the mixture of **4a** and **4b** (202 mg, 0.25 mmol), pyrrolidine (4 mL, 48.7 mmol) and anhydrous DMF (10 mL) under argon were refluxed for 3 h to obtain **6e**. Column chromatography (4 x 22 cm<sup>2</sup> silica gel, Et<sub>2</sub>O) afforded **6e** as blue solid (132 mg, 82%).

<sup>1</sup>H NMR (250 MHz):  $\delta = 1.15$  (d,  $J = 7.5$  Hz, 12 H,  $\text{CH}(\text{CH}_3)_2$ ), 2.09 (t,  $J = 6.5$  Hz, 4 H,  $\text{CH}_2$ ), 2.73 (m, 2 H,  $\text{CH}(\text{CH}_3)_2$ ), 3.70 (t,  $J = 6.5$  Hz, 4 H,  $\text{CH}_2$ ), 6.95 (d,  $J = 8.7$  Hz, 1 H, *H-8*), 7.42 (s, 1 H, Ar-*H* ortho to  $\text{CH}(\text{CH}_3)_2$ ), 7.52-7.59 (t,  $J = 7.7$  Hz, 1 H, *H-11*), 8.21 (d,  $J = 8.5$  Hz, 1 H, *H-10*), 8.33-8.39 (3d,  $J_1 = 7.7$  Hz,  $J_2 = 8.8$  Hz,  $J_3 = 8.2$  Hz, 1 H each *H-1*, *H-6*, *H-7*), 8.50 (d,  $J = 7.2$  Hz, 1 H, *H-12*), 8.55 and 8.59 (2 d,  $J = 8.2$  Hz, 1 H each, *H-2*, *H-5*).



## 7.4 Synthesis of oligoPPEs

### 7.4.1 Iodotrimer **7a<sub>3</sub>**

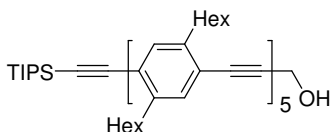


Following the general procedure A, a solution of free acetylene **9c<sub>2</sub>** (4.0 g, 6.75 mmol), 1,4-dihexyl-2,5-diiodobenzene (33.6 g, 67.46 mmol) in THF (95 mL) and piperidine (30 mL) was degassed for three times. Pd(PPh<sub>3</sub>)<sub>2</sub>Cl<sub>2</sub> (46.5 mg, 0.9 mol% with respect to **9c<sub>2</sub>**) and CuI (26.3 mg, 2.0 mol% with respect to **9c<sub>2</sub>**) were added to the degassed reaction mixture and stirred at room temperature for 18 h to afford the iodotrimer **7a<sub>3</sub>**. Flash chromatography (6 x 30 cm<sup>2</sup> silica gel, *n*-pentane) gave the 1,4-dihexyl-2,5-diiodobenzene (31.1 g, 92%, *R<sub>f</sub>* = 0.84) and **7a<sub>3</sub>** (3.42 g, 53%, *R<sub>f</sub>* = 0.4) as a yellow-brown solid by eluting with *n*-pentane/CH<sub>2</sub>Cl<sub>2</sub>, 3:1 v/v.

M.p.: 72-73 °C. - <sup>1</sup>H NMR (250 MHz, CD<sub>2</sub>Cl<sub>2</sub>): δ = 7.72 (s, 1 H, Ar-*H* ortho to iodo), 7.39 (s, 2 H, Ar-*H*), 7.36, 7.34, and 7.31 (3 s, 3 H, Ar-*H*), 4.53 (d, *J* = 6.1 Hz, 2 H, CH<sub>2</sub>OH), 2.87-2.65 (m, 12 H, Ar-CH<sub>2</sub>), 1.80-1.58 (m, 12 H, , ArCH<sub>2</sub>-CH<sub>2</sub>), 1.37-1.32 (m, 36 H, CH<sub>2</sub>), 1.06 (s), 1.05 (s, 1 H), 0.92-0.86 (m, 18 H, CH<sub>3</sub>). - <sup>13</sup>C NMR: δ = 144.3 (C, I-C-C-Hexyl), 143.4, 142.8, 142.5 and 142.4 (5 C, C-Hexyl), 139.9 (CH, arom.*CH* ortho to iodo), 132.9, 132.8 and 132.7 (4 CH, arom. *CH*), 123.4, 123.2, 123.1 and 122.4 (5 C, C- C≡C), 101.2 (C, C-I), 93.3, 92.9, 92.8 and 92.5 (4 C, C≡C), 84.5 (C, C≡CCH<sub>2</sub>OH), 52.0 (CH<sub>2</sub>, CH<sub>2</sub>OH), 40.6 (CH<sub>2</sub>, Ar-CH<sub>2</sub> ortho to iodo) 34.5, 34.3 and 34.2 (4 CH<sub>2</sub>, Ar-CH<sub>2</sub>), 32.2, 32.1, 31.1, 30.9, 30.6, 29.7, 29.6, 29.5, 29.4, 23.1 and 23.0 (14 CH<sub>2</sub>), 17.9

(CH<sub>3</sub>), 14.3 (CH<sub>3</sub>, CH<sub>2</sub>CH<sub>3</sub>), 12.8 (CH<sub>3</sub>). - MALDI TOF: *m/z* 962.40 [M<sup>+</sup>], 836.63 [M<sup>+</sup>-Iodo]. Anal. Calcd for C<sub>61</sub>H<sub>87</sub>IO (963.28): C, 76.06; H, 9.10. Found C, 75.96; H, 8.943.

#### 7.4.2 Pentamer **8a<sub>5</sub>**

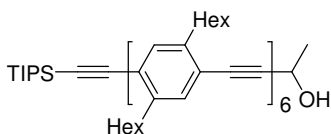


Following the general procedure A, a solution of iodotrimer **7a<sub>3</sub>** (1.64 g, 1.71 mmol) and the free acetylene **9a<sub>2</sub>** (1.33 g, 1.85 mmol) in THF (50 mL) and piperidine (15 mL) was degassed for three times. Pd(PPh<sub>3</sub>)<sub>2</sub>Cl<sub>2</sub> (12.2 mg, 1.0 mol%) and CuI (6.7 mg, 2.0 mol%) were added to the degassed reaction mixture and stirred at room temperature for 18.5 h to afford pentamer **8a<sub>5</sub>**. Column chromatography (5 x 25 cm<sup>2</sup> silica gel, *n*-pentane/CH<sub>2</sub>Cl<sub>2</sub>, 3:1 v/v) afforded **8a<sub>5</sub>** as a yellow solid with traces amount of impurity in 2<sup>nd</sup> fraction (1.19g) and 3<sup>rd</sup> fraction (1.23 g) respectively. The 3<sup>rd</sup> fraction was recolumned to afford **8a<sub>5</sub>** (985 mg) as a yellow solid with traces of impurity. However the 2<sup>nd</sup> fraction of the first column was dissolved in CH<sub>2</sub>Cl<sub>2</sub> (2-3 ml) and MeOH was slowly added to it. **8a<sub>5</sub>** was precipitated out and filtered to afford 971 mg with reasonable purity (*R<sub>f</sub>* = 0.47).

M.p. : 109-110 °C. <sup>1</sup>H NMR (250 MHz, CD<sub>2</sub>Cl<sub>2</sub>): δ = 7.42-7.36 (m, 8 H, Ar-*H*), 7.34 (s, 1 H, Ar-*H*), 7.32 (s, 1 H, Ar-*H*), 4.53 (s, 2 H, CH<sub>2</sub>OH), 2.90-2.72 (m, 20 H, Ar-CH<sub>2</sub>), 1.74-1.69 (m, 20 H, ArCH<sub>2</sub>-CH<sub>2</sub>), 1.37-1.25 (m, 60 H, CH<sub>2</sub>), 1.18 (s, 21 H, TIPS), 0.93-0.91 (m, 30 H, CH<sub>3</sub>). <sup>13</sup>C NMR: δ = 143.2, 142.8, 142.5 and 142.4 (4 C, C-Hexyl), 133.3, 132.9, and 132.8 (3 CH, arom. CH), 123.4, 123.3 and 122.4 (3 C, C-C≡C), 106.1 and 95.9 (2 C, C≡CTIPS), 93.5, 93.4, 92.5 (3 C, C≡C), 84.5 (C, C≡CCH<sub>2</sub>OH), 52.0

(CH<sub>2</sub>, CH<sub>2</sub>OH), 34.8, 34.6 and 34.3 (3 CH<sub>2</sub>, ArCH<sub>2</sub>), 32.3, 32.1, 31.4, 31.3, 31.2, 31.1, 31.0, 29.7, 29.5, 23.1 and 22.8 (12 CH<sub>2</sub>), 18.9 (CH<sub>3</sub>, CH<sub>2</sub>OHCH<sub>3</sub>), 14.3 (CH<sub>3</sub>, CH<sub>2</sub>CH<sub>3</sub>), 11.9 (CH, SiCH(CH<sub>3</sub>)<sub>3</sub>). – MALDI TOF: *m/z* 1553.98. Anal. Calcd for C<sub>112</sub>H<sub>164</sub>OSi (1554.64): C, 86.53; H, 10.63. Found C, 85.92; H, 11.09.

### 7.4.3 Hexamer **8b<sub>6</sub>**

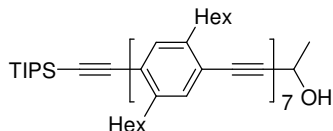


Following the general procedure A, a solution of iododimer **7b<sub>2</sub>** (160 mg, 0.23 mmol) and the free acetylene **9a<sub>4</sub>** (303 mg, 0.24 mmol) in THF (13 mL) and piperidine (4 mL) was degassed for three times. Pd(PPh<sub>3</sub>)<sub>2</sub>Cl<sub>2</sub> (1.6 mg, 1.0 mol%), CuI (1.3 mg, 3.0 mol%) were added to the degassed reaction mixture and stirred at room temperature for 18 h to afford hexamer **8b<sub>6</sub>**. The product was isolated as a yellow solid (334 mg, 80%, *R<sub>f</sub>* = 0.61) by flash chromatography (4 x 35 cm<sup>2</sup>, silica gel, *n*-pentane/CH<sub>2</sub>Cl<sub>2</sub> (1:1)).

M.p. : 119-121 °C. <sup>1</sup>H NMR (500 MHz, CD<sub>2</sub>Cl<sub>2</sub>): δ = 7.41-7.39 (m, 8 H, Ar-*H*), 7.35 (s, 2 H, Ar-*H*), 7.33 (s, 1 H, Ar-*H*), 7.29 (s, 1 H, Ar-*H*), 4.81-4.76 (m, 1 H, CHOH), 2.86-2.71 (m, 24 H, Ar-CH<sub>2</sub>), 1.98 (d, *J* = 5.0 Hz, 1 H, OH), 1.73-1.61 (m, 24 H, ArCH<sub>2</sub>-CH<sub>2</sub>), 1.56 (d, *J* = 6.2 Hz, 3 H, CH(OH)CH<sub>3</sub>), 1.44-1.35 (m, 72 H, CH<sub>2</sub>), 1.16 (s, 21 H, TIPS), 0.91-0.90 (m, 36 H, CH<sub>3</sub>). – <sup>13</sup>C NMR: δ = 143.1, 142.7, 142.4 and 142.3 (4 C, C-Hexyl), 133.2, 132.8 and 132.7 (3 CH, arom. CH), 123.1 and 122.4 (2 C, C-C≡C), 106.0 and 96.2 (2 C, C≡CTIPS), 95.8, 93.4, and 93.2 (3 C, C≡C), 82.8 (C, C≡CCHOH), 59.2 (CH, CHOH), 34.7, 34.5, 34.4 and 34.3 (4 CH<sub>2</sub>, ArCH<sub>2</sub>), 32.2, 32.1, 31.3, 31.2, 31.1,

31.0, 29.7, 29.6, and 23.1 (12 CH<sub>2</sub>), 24.7 (CH<sub>3</sub>, CHOHCH<sub>3</sub>), 18.9 (CH<sub>3</sub>, CH(CH<sub>3</sub>)<sub>2</sub>), 14.3 (CH<sub>3</sub>, CH<sub>2</sub>CH<sub>3</sub>), 11.8 (CH, SiCH(CH<sub>3</sub>)<sub>3</sub>). – MALDI TOF: *m/z* 1836.53. Anal. Calcd for C<sub>133</sub>H<sub>194</sub>OSi (1837.11): C, 86.96; H, 10.64. Found C, 86.93; H, 10.84

#### 7.4.4 Heptamer **8b<sub>7</sub>**

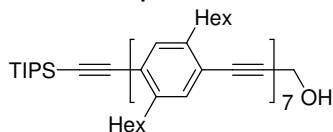


Following the general procedure A, a solution of iododimer **7b<sub>2</sub>** (195 mg, 0.28 mmol) and the free acetylene **9a<sub>5</sub>** (442 mg, 0.29 mmol) in THF (12 mL) and piperidine (4 mL) was degassed for three times. Pd(PPh<sub>3</sub>)<sub>2</sub>Cl<sub>2</sub> (3.0 mg, 1.5 mol%), CuI (1.5 mg, 2.8 mol%) were added to the degassed reaction mixture and stirred at room temperature for 19 h to afford heptamer **8b<sub>7</sub>**. The product was isolated as a yellow solid (565 mg, 97 %, *R<sub>f</sub>* = 0.57) by flash chromatography (4 x 25 cm<sup>2</sup> silica gel, *n*-pentane/Et<sub>2</sub>O, 4:1 v/v).

M.p. : 133-135 °C. <sup>1</sup>H NMR (500 MHz, CD<sub>2</sub>Cl<sub>2</sub>): δ = 7.41-7.39 (m, 10 H, Ar-*H*), 7.35 (s, 2 H, Ar-*H*), 7.33 (s, 1 H, Ar-*H*), 7.29 (s, 1 H, Ar-*H*), 4.79-4.77 (m, 1 H, CHOH), 2.87-2.71 (m, 28 H, Ar-CH<sub>2</sub>), 1.96 (d, *J* = 5.4 Hz, 1 H, OH), 1.76-1.61 (m, 28 H, ArCH<sub>2</sub>-CH<sub>2</sub>), 1.55 (d, *J* = 8.1 Hz, 3 H, CH(OH)CH<sub>3</sub>), 1.44-1.34 (m, 84 H, CH<sub>2</sub>), 1.16 (s, 21 H, TIPS), 0.91-0.89 (m, 42 H, CH<sub>3</sub>). – <sup>13</sup>C NMR: δ = 143.1, 142.7, 142.4 and 142.3 (4 C, C-Hexyl), 133.2, 132.8 and 132.7 (3 CH, arom. CH), 123.1 and 122.3 (2 C, C-C≡C), 106.0 and 96.2 (2 C, C≡CTIPS), 95.8, 93.4, and 93.2 (3 C, C≡C), 82.7 (C, C≡CCHOH), 59.2 (CH, CHOH), 34.7, 34.5, and 34.3 (3 CH<sub>2</sub>, ArCH<sub>2</sub>), 32.2, 32.1, 31.3, 31.2, 31.1, 30.9, 29.7, 29.5 and 23.1 (10 CH<sub>2</sub>), 24.7 (CH<sub>3</sub>, CHOHCH<sub>3</sub>), 18.8 (CH<sub>3</sub>, CH(CH<sub>3</sub>)<sub>2</sub>), 14.3 (CH<sub>3</sub>,

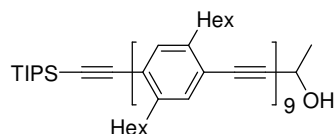
$\text{CH}_2\text{CH}_3$ ), 11.7 (CH,  $\text{SiCH}(\text{CH}_3)_3$ ). – MALDI TOF:  $m/z = 2103.44$ . Anal. Calcd for  $\text{C}_{153}\text{H}_{222}\text{OSi}$  (2105.56): C, 87.28; H, 10.63. Found C, 87.28; H, 10.45.

#### 7.4.5 Heptamer **8a<sub>7</sub>**



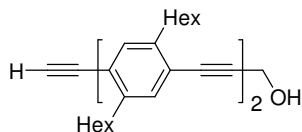
Following the general procedure A, a solution of iodotrimer **7a<sub>3</sub>** (110 mg, 0.11 mmol), and the free acetylene **9a<sub>4</sub>** (152 mg, 0.12 mmol) in THF (10 mL) and piperidine (4 mL) was degassed for three times.  $\text{Pd}(\text{PPh}_3)_2\text{Cl}_2$  (1.2 mg, 1.4 mol%) and CuI (1.0 mg, 4.0 mol%) were added to the degassed reaction mixture and stirred at room temperature for 19 h to afford the heptamer **8a<sub>7</sub>**. The product was isolated as a yellow solid (221 mg, 92 %,  $R_f = 0.63$ ) by flash chromatography (4 x 25 cm<sup>2</sup> silica gel, *n*-pentane/ $\text{CH}_2\text{Cl}_2$ , 1:1 v/v)

M.p. : 148-149°C. <sup>1</sup>H NMR (500 MHz,  $\text{CD}_2\text{Cl}_2$ ):  $\delta = 7.40$ -7.39 (m, 8 H, Ar-*H*), 7.35, 7.33, 7.30 (4 s, 1 H each, Ar-*H*), 7.32 (s, 2 H, Ar-*H*), 4.52 (d,  $J = 6.1$  Hz, 2 H,  $\text{CH}_2\text{OH}$ ), 2.87-2.72 (m, 28 H, Ar- $\text{CH}_2$ ), 1.75-1.63 (m, 28 H, , Ar $\text{CH}_2$ - $\text{CH}_2$ ), 1.50-1.26 (m, 84 H,  $\text{CH}_2$ ), 1.16 (s, 21 H, TIPS), 0.90-0.88 (m, 42 H,  $\text{CH}_3$ ). <sup>13</sup>C NMR (250 MHz,  $\text{CD}_2\text{Cl}_2$ ):  $\delta = 143.1$  , 142.8, 142.5 and 142.4 (4 C, C-Hexyl), 133. 3 and 132.8 (2 CH, arom. *CH*), 123.4, 123.2 and 122.4 (3 C, C- $\text{C}\equiv\text{C}$ ), 106.1 and 95.9 (2 C,  $\text{C}\equiv\text{CTIPS}$ ), 93.5, 93.3, 92.5 (3C,  $\text{C}\equiv\text{C}$ ), 84.5 (C,  $\text{C}\equiv\text{CCH}_2\text{OH}$ ), 77.9 (c), 52.0 ( $\text{CH}_2$ ,  $\text{CH}_2\text{OH}$ ), 34.8, 34.6 and 34.2 (3  $\text{CH}_2$ , Ar $\text{CH}_2$ ), 32.3, 32.1, 31.3, 31.2, 31.1, 30.9, 29.7, 29.5, 23.1 and 23.0 (10  $\text{CH}_2$ ), 18.9 ( $\text{CH}_3$ ,  $\text{CH}_2\text{OHCH}_3$ ), 14.3 ( $\text{CH}_3$ ,  $\text{CH}_2\text{CH}_3$ ), 11.8 (CH,  $\text{SiCH}(\text{CH}_3)_3$ ). – MALDI TOF:  $m/z = 2090.01$ . Anal. Calcd for  $\text{C}_{152}\text{H}_{220}\text{OSi}$  (2091.53): C, 87.29; H, 10.60. Found C, 86.51; H, 10.69.

7.4.5 Nonamer **8b<sub>9</sub>**

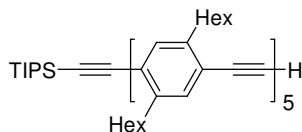
Following the general procedure A, a solution of iododimer **7b<sub>2</sub>** (45 mg, 0.06 mmol) and the free acetylene **9a<sub>7</sub>** (140 mg, 0.07 mmol) in THF (5 mL) and piperidine (2 mL) was degassed for three times. Pd(PPh<sub>3</sub>)<sub>2</sub>Cl<sub>2</sub> (1.1 mg, 2.5 mol%) and CuI (1.0 mg, 8.3 mol%) were added to the degassed reaction mixture and stirred at room temperature for 20 h to afford the iodotrimer **8b<sub>9</sub>**. The product **8b<sub>9</sub>** (133 mg, 79 %, *R<sub>f</sub>* = 0.20) was isolated as a yellow solid by flash chromatography (4 x 25 cm<sup>2</sup> silica gel, *n*-pentane/ CH<sub>2</sub>Cl<sub>2</sub>, 3:1 v/v).

M.p. : 162-165 °C. <sup>1</sup>H NMR (500 MHz, CD<sub>2</sub>Cl<sub>2</sub>): δ = 7.41-7.39 (m, 12 H, Ar-*H*), 7.35 (s, 2 H, Ar-*H*), 7.33 (s, 1 H, Ar-*H*), 7.32 (s, 2 H, Ar-*H*), 7.28 (s, 1 H, Ar-*H*), 4.79-4.77 (m, 1 H, *CHOH*), 2.87-2.45 (m, 36 H, Ar-*CH*<sub>2</sub>), 1.74-1.61 (m, 36 H, Ar-*CH*<sub>2</sub>-*CH*<sub>2</sub>), 1.55 (d, *J* = 6.5 Hz, 3 H, CH(OH)*CH*<sub>3</sub>), 1.44-1.26 (m, 108 H, *CH*<sub>2</sub>), 1.16 (s, 21 H, TIPS), 0.91-0.88 (m, 54 H, *CH*<sub>3</sub>). – <sup>13</sup>C NMR: δ = 143.1, 142.7, 142.4 and 142.3 (4 C, *C*-Hexyl), 133.2, 132.8 and 132.7 (3 CH, arom. *CH*), 123.1 and 122.3 (2 C, *C*-C≡C), 106.0 and 96.2 (2 C, C≡C-TIPS), 95.8, 95.6, 95.4, 93.4, and 93.2 (3 C, C≡C), 82.7 (C, C≡C-*CHOH*), 59.2 (CH, *CHOH*), 34.7, 34.5, and 34.3 (3 *CH*<sub>2</sub>, Ar-*CH*<sub>2</sub>), 32.2, 32.1, 31.3, 31.2, 31.1, 30.9, 30.1, 29.7, 29.5 and 23.1 (11 *CH*<sub>2</sub>), 24.7 (CH<sub>3</sub>, CH(OH)*CH*<sub>3</sub>), 18.8 (CH<sub>3</sub>, CH(*CH*<sub>3</sub>)<sub>2</sub>), 14.3 (CH<sub>3</sub>, *CH*<sub>2</sub>*CH*<sub>3</sub>), 11.7 (CH, Si-*CH*(CH<sub>3</sub>)<sub>3</sub>). – MALDI TOF: *m/z* = 2640.68. Anal. Calcd for C<sub>193</sub>H<sub>278</sub>OSi (2642.45): C, 87.73; H, 10.60. Found C, 87.10; H, 10.27.

7.4.10 Polar acetylene **9b<sub>1</sub>**

Following the general procedure B, a solution of **8a<sub>2</sub>** (5.16 g, 6.89 mmol) in THF (250 mL, PA grade), <sup>n</sup>BuN<sub>4</sub>F (13.8 mL, 13.78 mmol, 1 M in THF) was added and was stirred for 2 h at room temperature. After 2 h Et<sub>2</sub>O (200 mL) and water (100 mL) were added to the reaction mixture. The aqueous phase was separated and extracted with Et<sub>2</sub>O (50 mL x 3). The combined organic phases were washed with water. The organic phase was dried with Na<sub>2</sub>SO<sub>4</sub> and the solvent was evaporated to get a yellow oil. Column chromatography (5 x 20 cm<sup>2</sup> silica gel, *n*-pentane/CH<sub>2</sub>Cl<sub>2</sub>, 3:1 v/v) afforded the product **9c<sub>2</sub>** (4.38 g, 107 %, *R<sub>f</sub>* = 0.36) as a yellow oil.

<sup>1</sup>H NMR (250 MHz, CDCl<sub>3</sub>): δ = 7.32 and 7.31 (2 s, 3 H, Ar-*H*), 7.27 (s, 1 H, Ar-*H*), 4.53 (s, 2 H, CH<sub>2</sub>O), 3.29 (s, 1 H, C≡CH), 2.81-2.68 (m, 8 H, Ar-CH<sub>2</sub>), 1.72-1.53 (m, 12 H, ArCH<sub>2</sub>-CH<sub>2</sub>), 1.39-1.21 (m, 24 H, CH<sub>2</sub>), 1.05 (s, 15 H, ?), 0.91-0.83 (m, 12 H, CH<sub>3</sub>).

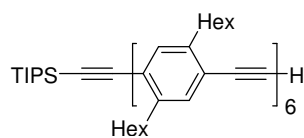
7.4.11 Non-polar acetylene **9a<sub>5</sub>**

Following the general procedure C, γ-MnO<sub>2</sub> (3.69 g, 42.48 mmol) and powdered KOH (1.21 g, 20.91 mmol) were added in four portion at a interval of 1 h to a solution of **8a<sub>5</sub>** (971 mg, 0.63 mmol) in Et<sub>2</sub>O (50 mL) to afford **9a<sub>5</sub>**. Column chromatography (4 x 20

cm<sup>2</sup>, silica gel, *n*-pentane/Et<sub>2</sub>O, 3:1 v/v) afforded **9a<sub>5</sub>** as a yellow solid (694 mg, 72%, *R<sub>f</sub>* = 0.96).

M.p. : 91-93 °C. <sup>1</sup>H NMR (500 MHz, CD<sub>2</sub>Cl<sub>2</sub>): δ = 7.40-7.39 (m, 6 H, Ar-*H*), 7.36 (s, 1 H, Ar-*H*), 7.35 (s, 2 H, Ar-*H*), 7.33 (s, 1 H, Ar-*H*), 3.37 (s, 1 H, C≡CH), 2.87-2.74 (m, 20 H, Ar-*CH*<sub>2</sub>), 1.72-1.61 (m, 20 H, ArCH<sub>2</sub>-*CH*<sub>2</sub>), 1.43-1.31 (m, 60 H, *CH*<sub>2</sub>), 1.16 (s, 21 H, TIPS), 0.90-0.86 (m, 30 H, *CH*<sub>3</sub>). <sup>13</sup>C NMR: δ = 143.3, 143.1, 142.4 and 142.3 (4 C, *C*-Hexyl), 133.3, 133.2, 132.8 and 132.7 (4 CH, arom. *CH*), 123.6, 123.1, 123.0 and 121.7 (5 C, *C*-C≡C), 106.0 and 95.8 (2 C, C≡CTIPS), 93.4, 93.2 and 93.1 (4 C, ArC≡CAr), 82.6 and 81.9 (2 C, C≡CH), 34.7, 34.5, 34.4 and 34.2 (4 CH<sub>2</sub>, ArCH<sub>2</sub>), 32.2, 32.0, 31.3, 31.2, 31.1, 31.0, 30.9, 29.7, 29.6, 29.5, and 23.0 (13 CH<sub>2</sub>), 18.8 (CH<sub>3</sub>, SiCH(CH<sub>3</sub>)<sub>3</sub>), 14.2 (CH<sub>3</sub>, CH<sub>2</sub>CH<sub>3</sub>), 11.7 (CH, SiCH(CH<sub>3</sub>)<sub>3</sub>). – MALDI TOF: *m/z* = 1523.77. Anal. Calcd for C<sub>111</sub>H<sub>162</sub>Si (1524.61): C, 87.45; H, 10.71. Found C, 87.59; H, 10.71

#### 7.4.12 Non-polar acetylene **9a<sub>6</sub>**

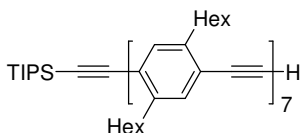


Following the general procedure C, γ-MnO<sub>2</sub> (312 mg, 3.59 mmol) and powdered KOH (105 mg, 1.84 mmol) were added in six portion at a interval of 1 h to a solution of **8b<sub>6</sub>** (50 mg, 0.03 mmol) in Et<sub>2</sub>O (5 mL) to afford **9a<sub>6</sub>**. **9a<sub>6</sub>** (48 mg, 98%, *R<sub>f</sub>* = 0.79) was isolated as a yellow solid.



M.p. : 113-114°C.  $^1\text{H}$  NMR (500 MHz,  $\text{CD}_2\text{Cl}_2$ ):  $\delta$  = 7.42-7.41 (m, 8 H, Ar-H), 7.40-7.34 (s, 4 H, Ar-H), 3.38 (s, 1 H,  $\text{C}\equiv\text{CH}$ ), 2.88-2.75 (m, 24 H, Ar- $\text{CH}_2$ ), 1.77-1.63 (m, 24 H, , Ar $\text{CH}_2$ - $\text{CH}_2$ ), 1.45-1.35 (m, 72 H,  $\text{CH}_2$ ), 1.17 (s, 21 H, TIPS), 0.92-0.90 (m, 36 H,  $\text{CH}_3$ ).  $^{13}\text{C}$  NMR:  $\delta$  = 143.3, 143.1, 142.5 and 142.3 (4 C, C-Hexyl), 133.4, 133.2, 132.8 and 132.7 (4 CH, arom. CH), 123.7, 123.2, 123.1 and 121.8 (4 C, C-C $\equiv$ C), 106.0 and 95.8 (2 C, C $\equiv$ CTIPS), 93.4, 93.3 and 93.1 (3 C, ArC $\equiv$ CAr), 82.6 and 81.9 (2 C, C $\equiv$ CH), 34.8, 34.6, 34.5, and 34.2 (4  $\text{CH}_2$ , Ar $\text{CH}_2$ ), 32.2, 32.0, 31.3, 31.2, 31.1, 30.9, 30.1, 29.8, 29.7, 29.6, 29.5, 23.1 and 23.0 (14  $\text{CH}_2$ ), 18.9 ( $\text{CH}_3$ , SiCH( $\text{CH}_3$ ) $_3$ ), 14.3 ( $\text{CH}_3$ ,  $\text{CH}_2\text{CH}_3$ ), 11.8 (CH, SiCH( $\text{CH}_3$ ) $_3$ ). – MALDI TOF:  $m/z$  = 1793.27. Anal. Calcd for  $\text{C}_{131}\text{H}_{190}\text{Si}$  (1793.06): C, 87.75; H, 10.68. Found C, 87.57; H, 10.53.

#### 7.4.13 Non-polar acetylene **9a<sub>7</sub>**

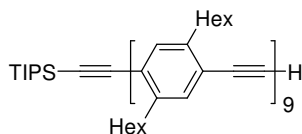


Following the general procedure C,  $\gamma\text{-MnO}_2$  (822 mg, 9.46 mmol) and powdered KOH (441mg, 7.72 mmol) were added in six portion at a interval of 1 h to a solution of **8b<sub>7</sub>** (400 mg, 0.19 mmol) in  $\text{Et}_2\text{O}$  (50 mL) to afford **9a<sub>7</sub>**. Column chromatography (4 x 20  $\text{cm}^2$ , silica gel,  $n$ -pentane/ $\text{Et}_2\text{O}$ , 20:1 v/v) afforded **9a<sub>7</sub>** (352 mg, 94%,  $R_f$  = 0.84 in  $n$ -pentane/ $\text{Et}_2\text{O}$ , 4:1 v/v) as a yellow solid.

M.p. : 131-133°C.  $^1\text{H}$  NMR (250 MHz,  $\text{CD}_2\text{Cl}_2$ ):  $\delta$  = 7.41 (s, 10 H, Ar-H), 7.37 (s, 1 H, Ar-H), 7.36 (s, 2 H, Ar-H), 7.34 (s, 1 H, Ar-H), 3.37 (s, 1 H,  $\text{C}\equiv\text{CH}$ ), 2.90-2.74 (m, 28 H, Ar- $\text{CH}_2$ ), 1.74-1.68 (m, 28 H, , Ar $\text{CH}_2$ - $\text{CH}_2$ ), 1.51-1.37 (m, 84 H,  $\text{CH}_2$ ), 1.17 (s, 21

H, TIPS), 0.93-0.90 (m, 42 H,  $CH_3$ ).  $^{13}C$  NMR:  $\delta$  = 143.3, 143.1, 142.5, and 142.4 (5 C, C-Hexyl), 133.4, 133.3, and 132.8 (4 CH, arom. CH), 125.8, 123.7, 123.3, and 121.9 (4 C, C-C $\equiv$ C), 106.1 and 95.9 (2 C, C $\equiv$ CTIPS), 93.5, 93.3 and 93.2 (3 C, ArC $\equiv$ CAr), 82.7 and 81.9 (2 C, C $\equiv$ CH), 34.8, 34.6 and 34.2 (4 CH<sub>2</sub>, ArCH<sub>2</sub>), 32.3, 32.1, 31.3, 31.2, 31.0, 30.5, 29.7, 29.5, 23.4, 23.1 and 23.0 (13 CH<sub>2</sub>), 18.9 (CH<sub>3</sub>, SiCH(CH<sub>3</sub>)<sub>3</sub>), 14.3 (CH<sub>3</sub>, CH<sub>2</sub>CH<sub>3</sub>), 11.9 (CH, SiCH(CH<sub>3</sub>)<sub>3</sub>). – MALDI TOF:  $m/z$  = 2060.38. Anal. Calcd for C<sub>151</sub>H<sub>218</sub>Si (2061.51): C, 87.98; H, 10.66. Found C, 87.49; H, 10.70.

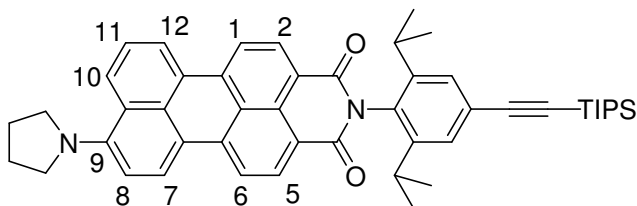
#### 7.4.14 Non-polar acetylene **9a<sub>9</sub>**



Following general procedure C, □-MnO<sub>2</sub> (849 mg, 9.77 mmol) and powdered KOH (412 mg, 7.21 mmol) were added in five porting, in a interval of 1 h, to a solution of **8b<sub>9</sub>** (130 mg, 0.05 mmol) in THF (15 mL) to afford **9a<sub>9</sub>**. Column chromatography (4 x 30 cm<sup>2</sup>, silica gel, *n*-pentane/CH<sub>2</sub>Cl<sub>2</sub>, 3:1 v/v) afforded **9a<sub>9</sub>** (85 mg, 67%,  $R_f$  = 0.96) as yellow solid in first fraction and **8b<sub>9</sub>** (17 mg, 13%,  $R_f$  = 0.50) as a yellow solid in third fraction.

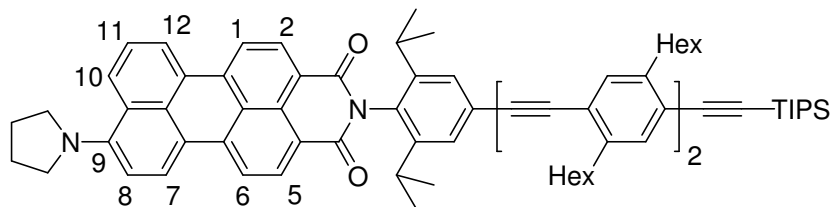
$^1H$  NMR (500 MHz, CD<sub>2</sub>Cl<sub>2</sub>):  $\delta$  = 7.37-7.36 (m, 14 H, Ar-H), 7.33 (s, 2 H, Ar-H), ), 7.31 (s, 1 H, Ar-H), 7.29 (s, 1 H, Ar-H), 3.29 (s, 1 H, C $\equiv$ CH), 2.85-2.82 (m, 36 H, Ar-CH<sub>2</sub>), 1.74-1.64 (m, 36 H, ArCH<sub>2</sub>-CH<sub>2</sub>), 1.42-1.25 (m, 108 H, CH<sub>2</sub>), 1.14 (s, 21 H, TIPS), 0.89-0.87 (m, 54 H, CH<sub>3</sub>).

## 7.5 Synthesis of PMI(Py) labeled oligoPPEs

7.5.1 PMI(Py) labeled oligoPPE **12<sub>0</sub>**

Following the general procedure D, a sample of **6e** (106 mg, 0.17 mmol) was coupled with TIPS acetylene (45  $\mu$ L, 0.20 mmol) in toluene (3.0 mL) and Et<sub>3</sub>N (0.5 mL) to afford **12<sub>0</sub>**. The crude material was dissolved in CH<sub>2</sub>Cl<sub>2</sub> (1-2 mL) and to it MeOH was added drop by drop. A blue solid was tops out, which was filtered and dried to afford **12<sub>0</sub>** as a blue solid (95mg, 77%, *R<sub>f</sub>* = 0.54 in Et<sub>2</sub>O).

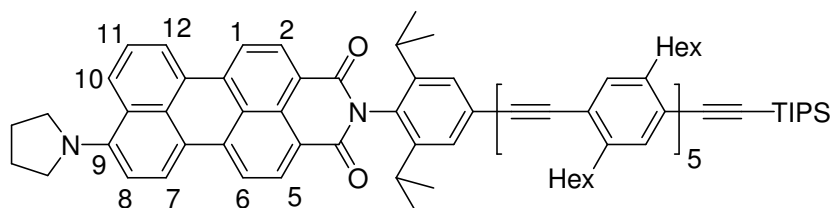
<sup>1</sup>H NMR (250 MHz):  $\delta$  = 0.88-0.92 (m, 12 H, CH(CH<sub>3</sub>)<sub>2</sub>), 1.15 (s, 21 H, TIPS), 2.09 (t, *J* = 6.3 Hz, 4 H, H  $\gamma$  to N), 2.73-2.87 (m, 2 H, CH(CH<sub>3</sub>)<sub>2</sub>), 3.70 (t, *J* = 6.3 Hz, 4 H, H  $\beta$  to N), 6.95 (d, *J* = 7.5 Hz, 1 H, H-8), 7. 29- 7.41 (4s, 1 H each , Ar-H), 7. 48 (s, 2 H, Ar-H ortho to CH(CH<sub>3</sub>)<sub>2</sub>), 7.56 (t, *J* = 8.2 Hz, 1 H, H-11), 8.22 (d, *J* = 8.5 Hz, 1 H, H-10), 8.33-8.39 (m, 3 H, H-1, H-6, H-7), 8.50 (d, *J* = 7.5 Hz, 1 H, H-12), 8.55 (d, *J* = 8.3 Hz, 1 H, H-5), 8. 61 (d, *J* = 8.0 Hz, 1 H, H-2).

7.5.2 PMI(Py) labeled oligoPPE **12<sub>2</sub>**

Following the general procedure D, a sample of **6e** (41 mg, 0.065 mmol) was coupled with **9a<sub>2</sub>** (52 mg, 0.072 mmol) in toluene (3.5 mL) and Et<sub>3</sub>N (0.7mL). Chromatography, (silica gel (4 x 25 cm), *n*-Pentane, Et<sub>2</sub>O (1:1)), afforded **12<sub>2</sub>** as a blue solid (66mg, 80%, *R<sub>f</sub>* = 0.59 in Et<sub>2</sub>O).

<sup>1</sup>H NMR (250 MHz):  $\delta$  = 0.88-0.92 (m, 12 H, CH(CH<sub>3</sub>)<sub>2</sub>), 1.15 (s, 21 H, TIPS), 1.31-1.43 (m, 24 H, CH<sub>2</sub>), 1.63-1.78 (m, 8 H, ArCH<sub>2</sub>-CH<sub>2</sub>), 2.09 (t, *J* = 6.3 Hz, 4 H, H  $\gamma$  to N), 2.73-2.87 (m, 10 H, Ar-CH<sub>2</sub>, CH(CH<sub>3</sub>)<sub>2</sub>), 3.70 (t, *J* = 6.3 Hz, 4 H, H  $\beta$  to N), 6.95 (d, *J* = 7.5 Hz, 1 H, H-8), 7.29-7.41 (4s, 1 H each, Ar-H), 7.48 (s, 2 H, Ar-H ortho to CH(CH<sub>3</sub>)<sub>2</sub>), 7.56 (t, *J* = 8.2 Hz, 1 H, H-11), 8.22 (d, *J* = 8.5 Hz, 1 H, H-10), 8.33-8.39 (m, 3 H, H-1, H-6, H-7), 8.50 (d, *J* = 7.5 Hz, 1 H, H-12), 8.55 (d, *J* = 8.3 Hz, 1 H, H-5), 8.61 (d, *J* = 8.0 Hz, 1 H, H-2).

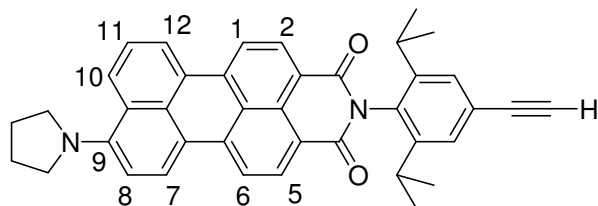
### 7.5.3 PMI(Py) labeled oligoPPE **12<sub>5</sub>**



Following the general procedure D, a sample of **6e** (45 mg, 0.07 mmol) was coupled with **9a<sub>5</sub>** (112 mg, 0.07 mmol) in toluene (7.5 mL) and Et<sub>3</sub>N (1.5mL). Chromatography, (4 x 25 cm<sup>2</sup> silica gel, 1:1 mixture of *n*-Pentane and Et<sub>2</sub>O) afforded **12<sub>5</sub>** as a blue solid (150 mg) in 3<sup>rd</sup> fraction, which was further dissolved in CH<sub>2</sub>Cl<sub>2</sub> (2 mL) and MeOH was added slowly drop by drop. A blue solid was tops out (115mg, 77%, *R<sub>f</sub>* = 0.70 in Et<sub>2</sub>O).

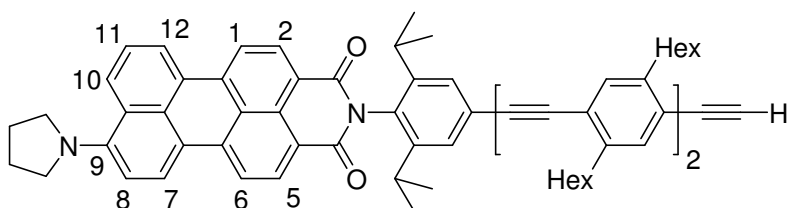
$^1\text{H}$  NMR (500 MHz,  $\text{CD}_2\text{Cl}_2$ ):  $\delta$  = 0.91-0.93 (m, 30 H,  $\text{CH}_2\text{CH}_3$ ), 1.16 (s, 21 H, TIPS), 1.19 (d,  $J$  = 6.8 Hz, 12 H,  $\text{CH}(\text{CH}_3)_2$ ), 1.31-1.52 (m, 60 H,  $\text{CH}_2$ ), 1.64-1.79 (m, 20 H,  $\text{ArCH}_2\text{CH}_2$ ), 2.08 (t,  $J$  = 6.2 Hz, 4 H, H  $\gamma$  to N), 2.76-2.91 (m, 22 H, Ar-H,  $\text{CH}(\text{CH}_3)_2$ ), 3.72 (t,  $J$  = 6.2 Hz, 4 H, H  $\beta$  to N), 6.92 (d,  $J$  = 8.7 Hz, 1 H, H-8), 7.40- 7.43 (m, 7 H, Ar-H), 7.47 (s, 1 H, Ar-H) 7.52 (s, 2 H, Ar-H ortho to  $\text{CH}(\text{CH}_3)_2$ ), 7.55 (t,  $J$  = 8.0 Hz, 1 H, H-11), 8.17 (d,  $J$  = 8.4 Hz, 1 H, H-6), 8.32 (d, 1 H,  $J$  = 9.0 Hz, H-7), 8.37 (d, 2 H,  $J$  = 8.7 Hz, H-1, H-10), 8.49 (d,  $J$  = 7.4 Hz, 1 H, H-12), 8.51 (d,  $J$  = 8.1 Hz, 1 H, H-5), 8.56 (d,  $J$  = 8.1 Hz, 1 H, H-2).

#### 7.5.4 Free acetylene **13<sub>0</sub>**



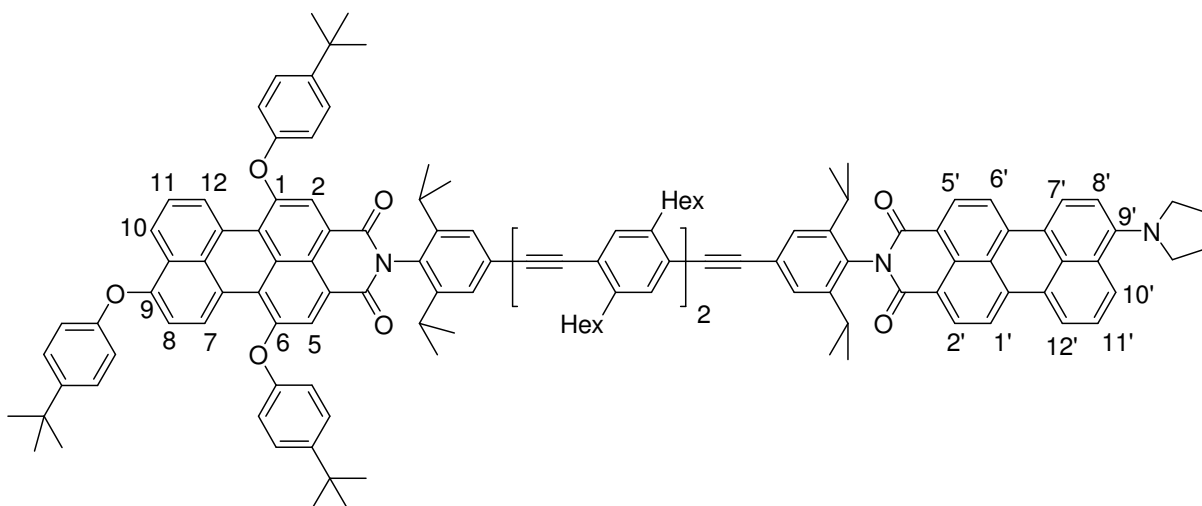
Following general procedure B, a sample of **12<sub>0</sub>** (95 mg, 0.13 mmol) was treated with  $^n\text{Bu}_4\text{NF}$  (260  $\mu\text{L}$ , 2 equiv., 1M in THF) in THF (5 mL). After 2 h distilled water (50 mL) was added to the reaction mixture and a blue solid was tops out. The solid was filtered and dried to afford **13<sub>0</sub>** (64 mg, 85%,  $R_f$  = 0.59 in  $\text{Et}_2\text{O}$ ).

$^1\text{H}$  NMR (250 MHz):  $\delta$  = 0.88-0.92 (m, 12 H,  $\text{CH}(\text{CH}_3)_2$ ), 2.09 (t,  $J$  = 6.3 Hz, 4 H, H  $\gamma$  to N), 2.73-2.87 (m, 2 H,  $\text{CH}(\text{CH}_3)_2$ ), 3.09 (s, 1 H,  $\text{C}\equiv\text{CH}$ ), 3.70 (t,  $J$  = 6.3 Hz, 4 H, H  $\beta$  to N), 6.95 (d,  $J$  = 7.5 Hz, 1 H, H-8), 7.29- 7.41 (4s, 1 H each, Ar-H), 7.48 (s, 2 H, Ar-H ortho to  $\text{CH}(\text{CH}_3)_2$ ), 7.56 (t,  $J$  = 8.2 Hz, 1 H, H-11), 8.22 (d,  $J$  = 8.5 Hz, 1 H, H-10), 8.33- 8.39 (m, 3 H, H-1, H-6, H-7), 8.50 (d,  $J$  = 7.5 Hz, 1 H, H-12), 8.55 (d,  $J$  = 8.3 Hz, 1 H, H-5), 8.61 (d,  $J$  = 8.0 Hz, 1 H, H-2). MS (MALDI TOP, 22 KV)  $m/z$  = 574.55.

7.5.5 Free acetylene **13**<sub>2</sub>

Following the general procedure B, a solution of **12**<sub>2</sub> (66 mg, 0.052 mmol) in THF (4 mL) was treated <sup>n</sup>Bu<sub>4</sub>NF (100 μL, 0.104 mmol, 1M in THF) to afford **13**<sub>2</sub> as a blue solid (52 mg, 89%, *R*<sub>f</sub> = 0.70 in Et<sub>2</sub>O). The product was used as such for next step.

<sup>1</sup>H NMR (250 MHz): δ = 1.18-1.21 (d, *J* = 7.0 Hz, 12 H, CH(CH<sub>3</sub>)<sub>2</sub>), 1.31-1.43 (m, 24 H, CH<sub>2</sub>), 1.63-1.74 (m, 8 H, ArCH<sub>2</sub>-CH<sub>2</sub>), 2.09 (t, *J* = 6.5 Hz, 4 H, H γ to N), 2.62-2.84 (m, 10 H, Ar-CH<sub>2</sub>, CH(CH<sub>3</sub>)<sub>2</sub>), 3.29 (s, 1 H, C≡CH), 3.71 (t, *J* = 6.5 Hz, 4 H, H β to N), 6.97 (d, *J* = 9.3 Hz, 1 H, H-8), 7.29- 7.41 (4s, 1 H each, Ar-H), 7.47 (s, 2 H, Ar-H ortho to CH(CH<sub>3</sub>)<sub>2</sub>), 7.56 (t, *J* = 8.2 Hz, 1 H, H-11), 8.23 (d, *J* = 8.5 Hz, 1 H, H-10), 8.33-8.41 (m, 3 H, H-1, H-6, H-7), 8.51 (d, *J* = 7.5 Hz, 1 H, H-12), 8.57 (d, *J* = 8.3 Hz, 1 H, H-5), 8.62 (d, *J* = 8.0 Hz, 1 H, H-2). MS (MALDI TOP, 22 KV) *m/z* = 1111.58.

7.5.6 PMI(OAr)<sub>3</sub>-(PPE)<sub>2</sub>-PMI(Py) dyad **14**<sub>2</sub>

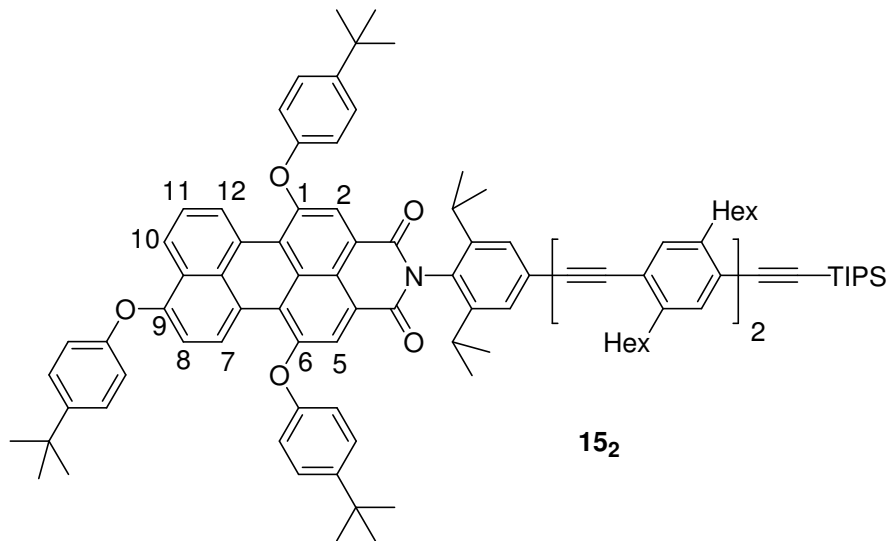
Following the general procedure D, a 93:7 mixture of compounds **5a** and **5b** (31 mg, 0.03 mmol) was coupled with free acetylene **13**<sub>2</sub> (37.7 mg, 0.03 mmol) in toluene (3.5 mL) and Et<sub>3</sub>N (0.7 mL). Chromatography (4 x 30 cm<sup>2</sup> silica gel, 1:1 mixture of *n*-pentane and Et<sub>2</sub>O) afforded **14**<sub>2</sub> as a blue solid (48 mg, 76%).

<sup>1</sup>H NMR (500 MHz):  $\delta$  = 0.86-0.91 (m, 12 H), 1.15-1.16 (d,  $J$  = 6.75 Hz, 12 H), 1.16-1.19 (d,  $J$  = 6.50 Hz, 12 H), 1.31, 1.33, and 1.34 (3s, 9 H each, *t*-butyl), 1.39-1.47 (m, CH<sub>2</sub>, 24 H), 1.69-1.76 (m, 8 H, ArCH<sub>2</sub>-CH<sub>2</sub>), 2.09 (broad singlet, 4 H, *H*- $\gamma$  to N), 2.69-2.84 (m, 12 H, ArCH<sub>2</sub>, CH(CH<sub>3</sub>)<sub>2</sub>), 3.71 (broad singlet, 4 H, *H*- $\alpha$  to N), 6.89 (d,  $J$  = 9.0 Hz, 1 H, *H*-8), 6.97 (d,  $J$  = 8.5 Hz, 1 H, *H*-8'), 7.01 (2 H, half of AA'XX' spinsystem, OAr-*H* meta to *t*-butyl), 7.08 (4 H, half of AA'XX' spinsystem, OAr-*H*-meta to *t*-butyl), 7.35-7.46 (m, 13 H, Ar-*H*, OAr-*H* ortho to *t*-butyl, Ar-*H* ortho to CH(CH<sub>3</sub>)<sub>2</sub>), 7.48 (s, 1 H, Ar-*H*), 7.57 (t,  $J$  = 8.0 Hz, 1 H, *H*-8'), 7.64 (t, 1 H,  $J$  = 8.0 Hz, *H*-8), 8.23 (d,  $J$  = 8.0 Hz, 1 H, *H*-10'), 8.30 (s, 1 H, *H*-5), 8.34-8.40 (m, 4 H, *H*-2, *H*-1', *H*-6', *H*-7'), 8.48 (d,  $J$  = 8.0

Hz, 1 H, *H*-10), 8.52 (d,  $J = 8.0$  Hz, 1 H, *H*-12'), 8.58 (d,  $J = 8.0$  Hz, 1 H, *H*-5'), 8.62 (d,  $J = 8.0$  Hz, 1 H, *H*-2'), 9.25 (d,  $J = 7.0$  Hz, 1 H, *H*-7), 9.45 (d,  $J = 7.0$  Hz, 1 H, *H*-12).

## 7.6 PMI(OAr)<sub>3</sub> labeled oligoPPEs **15<sub>n</sub>** (n = 2, 5, 7, and 9)

### 7.6.1 PMI(OAr)<sub>3</sub> labeled oligoPPEs **15<sub>2</sub>**



Following the general procedure D, a 93:7 mixture of **5a** and **5b** (63 mg, 0.06 mmol) was coupled with the free acetylene **9a<sub>2</sub>** (49.6 mg, 0.07 mmol) in toluene (4 mL) and Et<sub>3</sub>N (0.8 mL). Column chromatography (4 × 30 cm<sup>2</sup> silica gel, 1:1 CHCl<sub>3</sub> and *n*-hexane) afforded **15<sub>2</sub>** as a magenta solid (75 mg, 72%,  $R_f = 0.84$ ) in 3<sup>rd</sup> fraction. A mixture of the required product and traces amount of dba was isolated in the 4<sup>th</sup> fraction (42 mg, 41%).

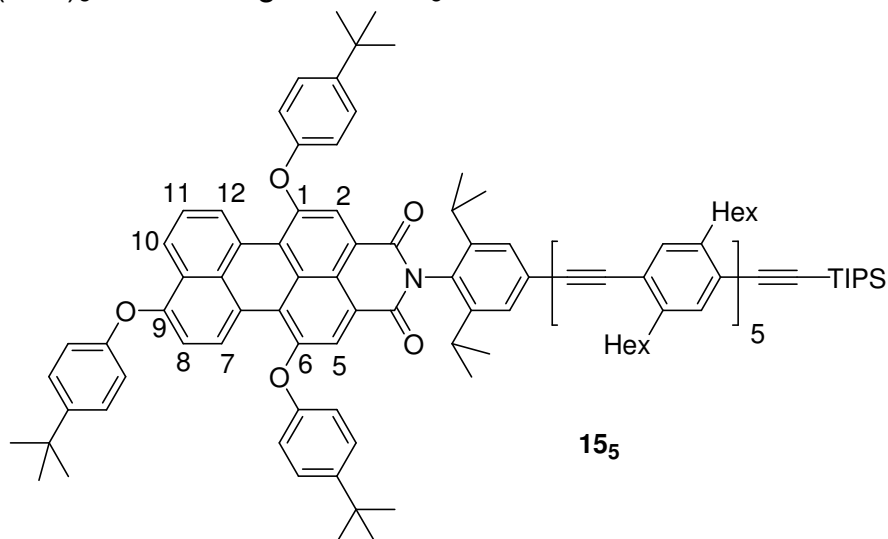
<sup>1</sup>H NMR (500 MHz): (CD<sub>2</sub>Cl<sub>2</sub>)  $\delta =$  \* 0.85-0.88 (m, 12 H, CH<sub>2</sub>CH<sub>3</sub>), \* 1.12 (d,  $J = 7.0$  Hz, 12 H, CH(CH<sub>3</sub>)<sub>2</sub>), \* 1.14 (s, 21 H, *tips*), \* 1.29-1.41 (m, 51 H, *t-butyl*, CH<sub>2</sub>), \* 1.68-1.72 (m, 8 H, ArCH<sub>2</sub>-CH<sub>2</sub>), \* 2.81-2.83 (m, 10 H, Ar-CH<sub>2</sub>, CH(CH<sub>3</sub>)<sub>2</sub>), 6.91 (d,  $J = 8.9$  Hz, 1 H, *H*-8/7), 7.05 (2 H, half of AA'XX' spinsystem, OAr-*H* meta to *t*-butyl), \* 7.09-7.13 (m, 4 H,



OAr-*H* meta to *t*-butyl), \*7.33, 7.35, 7.39 and 7.40 (4 s, 1 H each, Ar-*H*, *p*-polyphenylenes), \*7.37-7.45 (m, 8 H, Ar-*H*, OAr-*H* ortho to *t*-butyl, Ar-*H* ortho to CH(CH<sub>3</sub>)<sub>2</sub>), 7.67 (t, *J* = 8.1 Hz, 1 H, *H*-11), 8.25 and 8.28 (2 s, 1 H each, *H*-2, *H*-5), 8.50 (dd, *J*<sub>1</sub> = 8.2 Hz, *J*<sub>2</sub> = 1.2 Hz, 1 H, *H*-10/12), 9.28 (d, *J* = 8.8 Hz, 1 H, *H*-7/8), 9.48 (d, *J* = 8.2 Hz, 1 H, *H*-12/10); MS (MALDI TOP, 22 KV) *m/z* = 1644.6.

\* These signals have higher intensity than expected and this higher intensity is due to the additional signal for the PMI(OAr)<sub>2</sub> (**5b**) coupled product. The remaining additional signals are:  $\delta$  = 7.63 (t, *J* = 8.0 Hz, 2 H, *H*-8, *H*-11), 7.96 (d, *J* = 8.0 Hz, 2 H, *H*-7, *H*-12/*H*-9, *H*-10), 8.27 (s, 2 H, *H*-2, *H*-5), 9.40 (d, *J* = 7.7 Hz, 2 H, *H*-9, *H*-10/*H*-7, *H*-12).

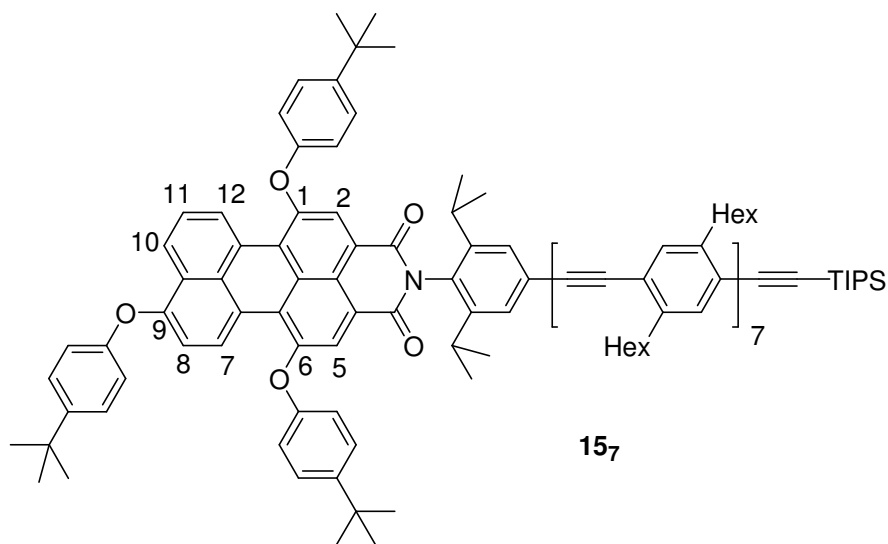
### 7.6.2 PMI(OAr)<sub>3</sub> labeled oligoPPEs **15<sub>5</sub>**



Following the general procedure D, a 97:3 mixture of **5a** and **5b** (47 mg, 0.05 mmol) was coupled with the free acetylene **9a<sub>5</sub>** (74 mg, 0.05 mmol) in toluene (5 mL) and Et<sub>3</sub>N (1 mL). Column chromatography (4 × 30 cm<sup>2</sup> silica gel, 1:1 CHCl<sub>3</sub> and *n*-hexane) afforded **15<sub>5</sub>** as a magenta solid (93 mg, 82%, *R<sub>f</sub>* = 0.74).

$^1\text{H}$  NMR (500 MHz): ( $\text{CD}_2\text{Cl}_2$ )  $\delta$  = 0.88-0.91 (m, 30 H,  $\text{CH}_2\text{CH}_3$ ), 1.14-1.16 (m, 33 H, *tips*,  $\text{CH}(\text{CH}_3)_2$ ), 1.31-1.46 (m, 87 H, *t-butyl*,  $\text{CH}_2$ ), 1.64-1.76 (m, 20 H,  $\text{ArCH}_2\text{-CH}_2$ ), 2.72-2.88 (m, 22 H,  $\text{Ar-CH}_2$ ,  $\text{CH}(\text{CH}_3)_2$ ), 6.91 (d,  $J$  = 8.8 Hz, 1 H,  $H-8/7$ ), 7.05 (2 H, half of AA'XX' spinsystem,  $\text{OAr-H}$  meta to *t-butyl*), 7.10-7.13 (m, 4 H,  $\text{OAr-H}$  meta to *t-butyl*), 7.33 and 7.35 (2 s, 1 H each,  $\text{Ar-H}$  of *p*-(polyphenylene)s), 7.39-7.48 (m, 16 H,  $\text{Ar-H}$  of *p*-(polyphenylene)s,  $\text{OAr-H}$  ortho to *t-butyl*,  $\text{Ar-H}$  ortho to  $\text{CH}(\text{CH}_3)_2$ ), 7.67 (t,  $J$  = 8.0 Hz, 1 H,  $H-11$ ), 8.25 and 8.28 (2 s, 1 H each,  $H-2$ ,  $H-5$ ), 8.50 (d,  $J$  = 9.0 Hz, 1 H,  $H-10/12$ ), 9.28 (d,  $J$  = 8.8 Hz, 1 H,  $H-7/8$ ), 9.49 (d,  $J$  = 7.4 Hz, 1 H,  $H-12/10$ ); MS (MALDI TOP, 22 KV)  $m/z$  = 2447.94.

### 7.6.3 PMI(OAr)<sub>3</sub> labeled oligoPPEs **15<sub>7</sub>**

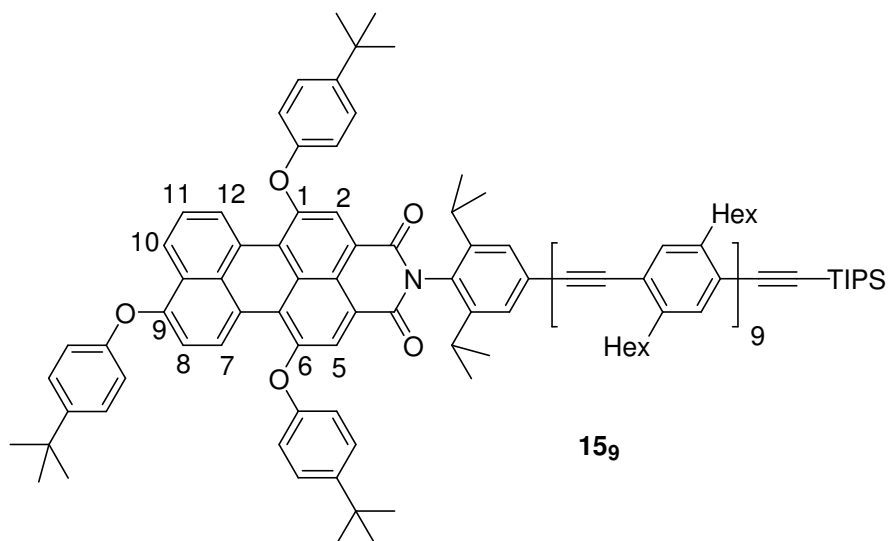


Following the general procedure D, a 97:3 mixture of **5a** and **5b** (21 mg, 0.02 mmol) was coupled with the free acetylene **9a<sub>7</sub>** (40 mg, 0.02 mmol) in toluene (5 mL) and  $\text{Et}_3\text{N}$  (1 mL). Column chromatography (4 × 20 cm<sup>2</sup> silica gel, 1:1 mixture of  $\text{CHCl}_3$  and *n*-hexane) afforded **15<sub>7</sub>** as a magenta solid (6 mg, 10%,  $R_f$  = 0.85) and (20 mg,

34%) in 2<sup>nd</sup> and 3<sup>rd</sup> fraction respectively. Around 22 mg of compound was isolated in 4<sup>th</sup> fraction which contains the product and traces amount of dba.

<sup>1</sup>H NMR (500 MHz): (CD<sub>2</sub>Cl<sub>2</sub>)  $\delta$  = 0.88-0.91 (m, 42 H, CH<sub>2</sub>CH<sub>3</sub>), 1.15 (d,  $J$  = 7.4 Hz, 12 H, CH(CH<sub>3</sub>)<sub>2</sub>), 1.16 (s, 21 H, *tips*), 1.31-1.46 (m, 111 H, *t-butyl*, CH<sub>2</sub>), 1.69-1.76 (m, 28 H, ArCH<sub>2</sub>-CH<sub>2</sub>), 2.71-2.88 (m, 30 H, Ar-CH<sub>2</sub>, CH(CH<sub>3</sub>)<sub>2</sub>), 6.91 (d,  $J$  = 8.8 Hz, 1 H, *H*-8/7), 7.05 (2 H, half of AA'XX' spinsystem, OAr-*H* meta to *t*-butyl), 7.10-7.13 (m, 4 H, OAr-*H* meta to *t*-butyl), 7.33 and 7.35 (2 s, 1 H each, Ar-*H* of *p*-(polyphenylene)s), 7.39-7.47 (m, 20 H, Ar-*H* of *p*-(polyphenylene)s, OAr-*H* ortho to *t*-butyl, Ar-*H* ortho to CH(CH<sub>3</sub>)<sub>2</sub>), 7.68 (t,  $J$  = 8.0 Hz, 1 H, *H*-11), 8.25 and 8.28 (2 s, 1 H each, *H*-2, *H*-5), 8.50 (d,  $J$  = 9.0 Hz, 1 H, *H*-10/12), 9.28 (d,  $J$  = 8.8 Hz, 1 H, *H*-7/8), 9.49 (d,  $J$  = 7.4 Hz, 1 H, *H*-12/10); MS (MALDI TOP, 22 KV)  $m/z$  = 2983.7.

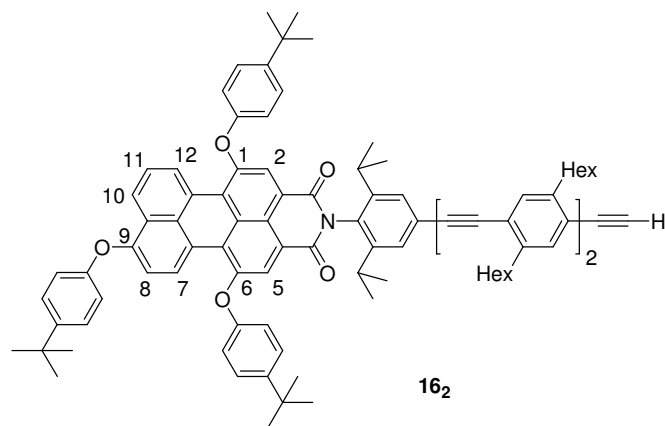
#### 7.6.4 PMI(OAr)<sub>3</sub> labeled oligoPPEs **15<sub>g</sub>**



Following the general procedure D, a 97:3 mixture of **5a** and **5b** (30 mg, 0.03 mmol) was coupled with the free acetylene **9a<sub>g</sub>** (81 mg, 0.03 mmol) in toluene (5 mL)

and Et<sub>3</sub>N (1 mL). The crude material was purified by column chromatography (4 × 20 cm<sup>2</sup> silica gel, a 1:1 mixture of CHCl<sub>3</sub> and *n*-hexane). and the 3<sup>rd</sup> fraction was recolumned (4 × 20 cm<sup>2</sup> silica gel, a 1:1 mixture of CHCl<sub>3</sub> and *n*-hexane). The 2<sup>nd</sup> and 3<sup>rd</sup> fractions of the 2<sup>nd</sup> column were isolated and solvent was evaporated to obtain red solids of 2 mg (2%) and 6 mg (6%) respectively, which contains a substantial amount of PMI(OAr)<sub>2</sub> related compound along with the required product. The 4<sup>th</sup> (62 mg, 59%, *R<sub>f</sub>* = 0.67) and 5<sup>th</sup> (2 mg, 2%, *R<sub>f</sub>* = 0.67) fraction gave **15<sub>9</sub>** as a red solid in reasonable pure.

<sup>1</sup>H NMR (500 MHz): (CD<sub>2</sub>Cl<sub>2</sub>) δ = 0.89-0.91 (m, 54 H, CH<sub>2</sub>CH<sub>3</sub>), 1.14-1.16 (m, 33 H, *tips*, CH(CH<sub>3</sub>)<sub>2</sub>), 1.31-1.46 (m, 135 H, *t-butyl*, CH<sub>2</sub>), 1.64-1.76 (m, 36 H, ArCH<sub>2</sub>-CH<sub>2</sub>), 2.72-2.88 (m, 38 H, Ar-CH<sub>2</sub>, CH(CH<sub>3</sub>)<sub>2</sub>), 6.91 (d, *J* = 8.8 Hz, 1 H, *H*-8/7), 7.05 (2 H, half of AA'XX' spinsystem, OAr-*H* meta to *t*-butyl), 7.10-7.12 (m, 4 H, OAr-*H* meta to *t*-butyl), 7.33 and 7.35 (2 s, 1 H each, Ar-*H* of *p*-(polyphenylene)s), 7.39-7.47 (m, 24 H, Ar-*H* of *p*-(polyphenylene)s, OAr-*H* ortho to *t*-butyl, Ar-*H* ortho to CH(CH<sub>3</sub>)<sub>2</sub>), 7.68 (t, *J* = 8.0 Hz, 1 H, *H*-11), 8.25 and 8.28 (2 s, 1 H each, *H*-2, *H*-5), 8.50 (d, *J* = 8.6 Hz, 1 H, *H*-10/12), 9.28 (d, *J* = 8.9 Hz, 1 H, *H*-7/8), 9.49 (d, *J* = 7.3 Hz, 1 H, *H*-12/10); MS (MALDI TOP, 22 KV) *m/z* = 3518.9.

7.7 Free acetylene **16<sub>n</sub>** (n = 2, 5, 7, and 9)7.7.1 Free acetylene **16<sub>2</sub>**

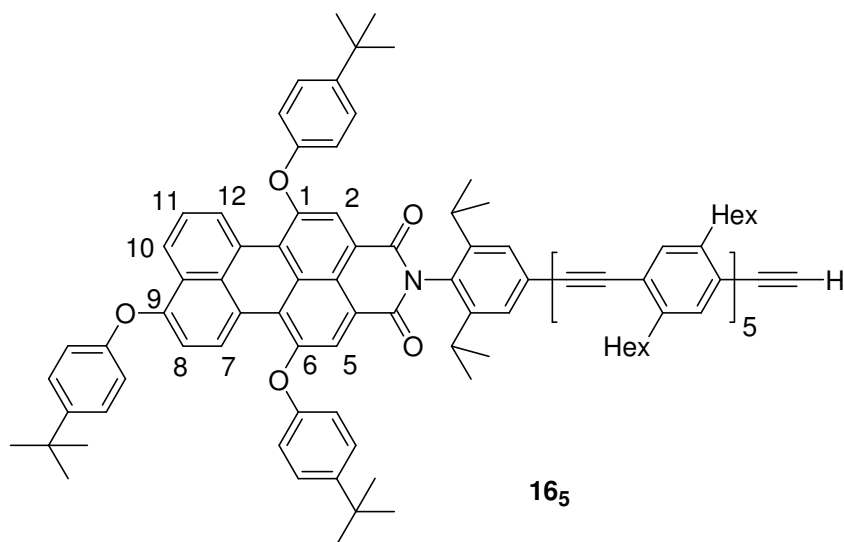
Following the general procedure B, 1 M <sup>n</sup>BuN<sub>4</sub>F in THF (50 μL, 2 equiv.) was added to a solution of **15<sub>2</sub>** (40 mg, 0.02 mmol) in THF (3.5 mL) and stirred for 2 h at room temperature to afford **16<sub>2</sub>** as a magenta solid (35 mg, 96%, *R<sub>f</sub>* = 0.62 in 3:7 CHCl<sub>3</sub>/*n*-hexane, v/v). The material was used as such for next reaction.

<sup>1</sup>H NMR (500 MHz): δ = \*0.85-0.99 (m, 12 H, CH<sub>2</sub>CH<sub>3</sub>), \*1.14-1.16 (12 H, CH(CH<sub>3</sub>)<sub>2</sub>), \*1.31-1.45 (m, 51 H, *t*-butyl, CH<sub>2</sub>), \*1.63-1.73 (m, 8 H, ArCH<sub>2</sub>-CH<sub>2</sub>), \*2.69-2.83 (m, 10 H, Ar-CH<sub>2</sub>, CH(CH<sub>3</sub>)<sub>2</sub>), \*3.29 (s, 1 H, C≡CH), 6.89 (d, *J* = 8.8 Hz, 1 H, *H*-8/7), 7.01, 7.07, and 7.09 (6 H, 3 halves of 3 AA'XX' spinsystems, OAr-*H* meta to *t*-butyl), \*7.32-7.46 (m, 12 H, Ar-*H* of *p*-(polyphenylene)s, OAr-*H* ortho to *t*-butyl, Ar-*H* ortho to CH(CH<sub>3</sub>)<sub>2</sub>), 7.64 (t, *J* = 8.1 Hz, 1 H, *H*-11), 8.30 and 8.33 (2 s, 1 H each, *H*-2, *H*-5), 8.48 (d, *J* = 8.2 Hz, 1 H, *H*-10/12), 9.24 (d, *J* = 8.8 Hz, 1 H, *H*-7/8), 9.45 (d, *J* = 7.7 Hz, 1 H, *H*-12/10).

\*These signals have higher intensity than expected and this higher intensity is due to the additional signal for the PMI(OAr)<sub>2</sub> (**5b**) coupled product. The remaining

signals are:  $\delta = 7.59$  (t,  $J = 8.0$  Hz, 2 H,  $H-8$  and  $H-11$ ),  $7.91$  (d,  $J = 7.8$  Hz, 2 H,  $H-7$ ,  $H-12$ /  $H-9$ ,  $H-10$ ),  $8.32$  (s, 2 H,  $H-2$ ,  $H-5$ ),  $9.36$  (d,  $J = 7.9$  Hz, 2 H,  $H-9$ ,  $H-10/H-7$ ,  $H-12$ ); MS (MALDI TOP, 22 KV)  $m/z = 1487.80$ .

### 7.7.2 Free acetylene **16<sub>5</sub>**

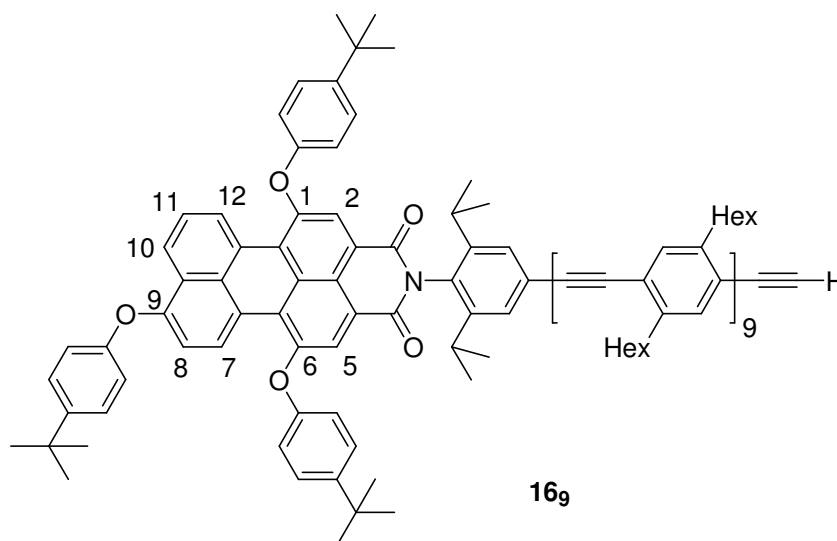


Following the general procedure B, 1 M TBAF in THF (42  $\mu$ L, 2 equiv.) was added to a solution of **15<sub>5</sub>** (58 mg, 0.02 mmol) in THF (5 mL) and stirred for 2 h at room temperature to afford **16<sub>5</sub>** as a magenta solid (53 mg, 97%,  $R_f = 0.67$  in 1:1  $\text{CHCl}_3$  and  $n$ -hexane). The material was used as such for next reaction.

$^1\text{H}$  NMR (500 MHz):  $\delta = 0.86$ - $0.99$  (m, 30 H,  $\text{CH}_2\text{CH}_3$ ),  $1.14$ - $1.16$  (12 H,  $\text{CH}(\text{CH}_3)_2$ ),  $1.31$ - $1.48$  (m, 87 H,  $t$ -butyl,  $\text{CH}_2$ ),  $1.64$ - $1.74$  (m, 20 H,  $\text{ArCH}_2\text{-CH}_2$ ),  $2.71$ - $2.84$  (m, 22 H,  $\text{Ar-CH}_2$ ,  $\text{CH}(\text{CH}_3)_2$ ),  $3.30$  (s, 1 H,  $\text{C}\equiv\text{CH}$ ),  $6.89$  (d,  $J = 8.8$  Hz, 1 H,  $H-8/7$ ),  $7.01$ ,  $7.07$ , and  $7.08$  (6 H, 3 halves of 3  $\text{AA}'\text{XX}'$  spinsystems,  $\text{OAr-H}$  meta to  $t$ -butyl),  $7.33$  (s, 2 H,  $\text{Ar-H}$  of  $p$ -(polyphenylene)s),  $7.35$ - $7.43$  (m, 16 H,  $\text{Ar-H}$  of  $p$ -(polyphenylene)s,  $\text{OAr-H}$  ortho to  $t$ -butyl,  $\text{Ar-H}$  ortho to  $\text{CH}(\text{CH}_3)_2$ ),  $7.64$  (t,  $J = 8.1$  Hz, 1

H, *H*-11), 8.30 and 8.34 (2 s, 1 H each, *H*-2, *H*-5), 8.49 (d,  $J = 8.9$  Hz, 1 H, *H*-10/12), 9.25 (d,  $J = 8.8$  Hz, 1 H, *H*-7/8), 9.45 (d,  $J = 7.4$  Hz, 1 H, *H*-12/10).

### 7.7.3 Free acetylene **16<sub>9</sub>**



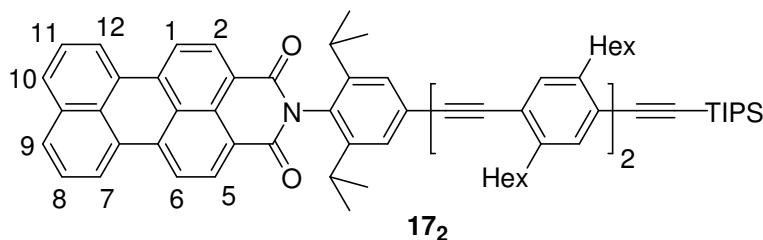
Following the general procedure B, 1 M TBAF in THF (30  $\mu$ L, 2 equiv.) was added to a solution of **15<sub>9</sub>** (53 mg, 0.02 mmol) in THF (3 mL) and stirred for 2 h at room temperature. Flash chromatography (4 x 30 cm<sup>2</sup> silica gel, 3:7 CHCl<sub>3</sub> and *n*-hexane) afforded **16<sub>9</sub>** as a magenta solid (46 mg, 91 %,  $R_f = 0.69$  in 1:1 CHCl<sub>3</sub> and *n*-hexane).

<sup>1</sup>H NMR (500 MHz):  $\delta = 0.87$ -0.88 (m, 54 H, CH<sub>2</sub>CH<sub>3</sub>), 1.15 (d,  $J = 6.4$  Hz, 12 H, CH(CH<sub>3</sub>)<sub>2</sub>), 1.31-1.41 (m, 135 H, *t*-butyl, CH<sub>2</sub>), 1.62-1.72 (m, 36 H, ArCH<sub>2</sub>-CH<sub>2</sub>), 2.62-2.83 (m, 38 H, Ar-CH<sub>2</sub>, CH(CH<sub>3</sub>)<sub>2</sub>), 3.30 (s, 1 H, C $\equiv$ CH), 6.89 (d,  $J = 8.6$  Hz, 1 H, *H*-8/7), 7.01, 7.07, and 7.09 (6 H, 3 halves of 3 AA'XX' spinsystems, OAr-*H* meta to *t*-butyl), 7.30-7.46 (m, 26 H, Ar-*H* of *p*-(polyphenylene)s, OAr-*H* ortho to *t*-butyl, Ar-*H* ortho to CH(CH<sub>3</sub>)<sub>2</sub>), 7.64 (t,  $J = 7.9$  Hz, 1 H, *H*-11), 8.30 and 8.33 (2 s, 1 H each, *H*-2, *H*-

5), 8.49 (d,  $J = 8.3$  Hz, 1 H,  $H-10/12$ ), 9.25 (d,  $J = 8.5$  Hz, 1 H,  $H-7/8$ ), 9.45 (d,  $J = 7.5$  Hz, 1 H,  $H-12/10$ ). MS (MALDI TOP, 22 KV)  $m/z = 3366.80$ .

## 7.8 PMI labeled oligoPPEs $17_n$ ( $n = 2, 5, 7,$ and $9$ )

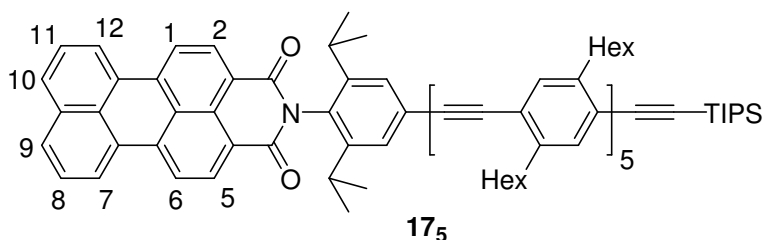
### 7.8.1 PMI labeled oligoPPE $17_2$



Following the general procedure D, PMI **3a** (14 mg, 0.03 mmol) was coupled with the free acetylene **9a<sub>2</sub>** (20 mg, 0.03 mmol) in toluene (5 mL) and Et<sub>3</sub>N (1 mL). Column chromatography (4 × 30 cm<sup>2</sup> silica gel, 3:1 mixture of CHCl<sub>3</sub> and *n*-hexane) afforded **17<sub>2</sub>** as a red solid (24 mg, 80%,  $R_f = 0.44$ ).

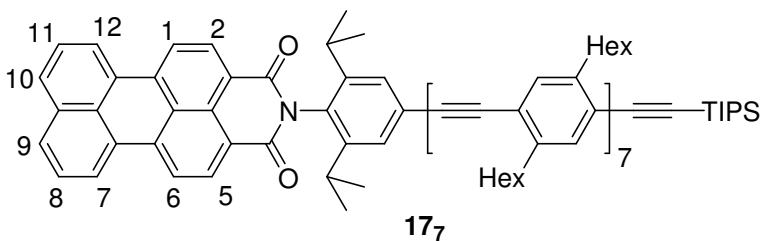
<sup>1</sup>H NMR (500 MHz):  $\delta = 0.86-0.90$  (m, 12 H, CH<sub>2</sub>CH<sub>3</sub>), 1.14 (s, 21 H, *tips*), 1.20 (d,  $J = 6.8$  Hz, 12 H, CH(CH<sub>3</sub>)<sub>2</sub>), 1.30-1.41 (m, 24 H, CH<sub>2</sub>), 1.68-1.73 (m, 8 H, ArCH<sub>2</sub>-CH<sub>2</sub>), 2.74-2.84 (m, 10 H, Ar-CH<sub>2</sub>, CH(CH<sub>3</sub>)<sub>2</sub>), 7.30, 7.32, 7.36 and 7.41 (4 s, 1 H each, Ar-*H* of *p*-(polyphenylene)s), 7.48 (s, 2 H, Ar-*H* ortho to CH(CH<sub>3</sub>)<sub>2</sub>), 7.67 (t,  $J = 7.9$  Hz, 2 H,  $H-8$ ,  $H-11$ ), 7.95 (d,  $J = 8.2$  Hz, 2 H,  $H-9$ ,  $H-10/H-7$ ,  $H-12$ ), 8.49 and 8.51 (2 d,  $J_1 = 8.4$  Hz,  $J_2 = 8.2$  Hz, 2 H each,  $H-1$ ,  $H-2$ ,  $H-5$ , and  $H-6$ ), 8.68 (d,  $J = 8.0$  Hz, 2 H,  $H-7$ ,  $H-12/H-9$ ,  $H-10$ ); MS (MALDI TOP, 22 KV)  $m/z = 1199.82$ .



7.8.2 PMI labeled oligoPPEs **17<sub>5</sub>**

Following the general procedure D, PMI **3a** (59 mg, 0.11 mmol) was coupled with the free acetylene **9a<sub>5</sub>** (169 mg, 0.11 mmol) in toluene (5 mL) and Et<sub>3</sub>N (1 mL). Column chromatography (4 × 30 cm<sup>2</sup> silica gel, a 3:1 mixture of CHCl<sub>3</sub> and *n*-hexane) afforded **15<sub>5</sub>** as a red solid (158 mg, 75%, *R<sub>f</sub>* = 0.73).

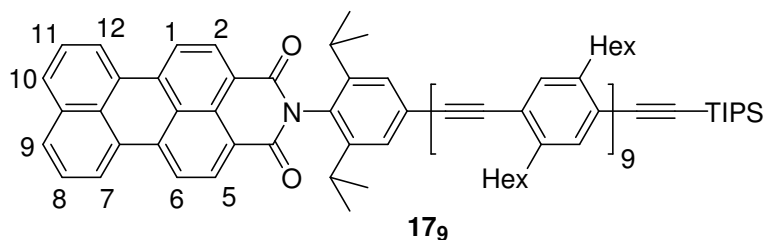
<sup>1</sup>H NMR (500 MHz): δ = 0.88-0.92 (m, 30 H, CH<sub>2</sub>CH<sub>3</sub>), 1.15 (s, 21 H, *tips*), 1.22 (d, *J* = 6.8 Hz, 12 H, CH(CH<sub>3</sub>)<sub>2</sub>), 1.30-1.42 (m, 60 H, CH<sub>2</sub>), 1.71-1.74 (m, 20 H, ArCH<sub>2</sub>-CH<sub>2</sub>), 2.77-2.84 (m, 22 H, Ar-CH<sub>2</sub>, CH(CH<sub>3</sub>)<sub>2</sub>), 7.30, 7.32, (2 s, 1 H each, Ar-*H* of *p*-(polyphenylene)s), 7.36-7.39 (m, 7 H, Ar-*H* of *p*-(polyphenylene)s), 7.43 (s, 1 H, Ar-*H* of *p*-(polyphenylene)s), 7.50 (s, 2 H, Ar-*H* ortho to CH(CH<sub>3</sub>)<sub>2</sub>), 7.65 (t, *J* = 7.8 Hz, 2 H, *H*-8, *H*-11), 7.93 (d, *J* = 8.2 Hz, 2 H, *H*-9, *H*-10/*H*-7, *H*-12), 8.47 and 8.48 (2 d, *J*<sub>1</sub> = 8.3 Hz, *J*<sub>2</sub> = 7.5 Hz, 2 H each, *H*-1, *H*-2, *H*-5, and *H*-6), 8.67 (d, *J* = 7.9 Hz, 2 H, *H*-7, *H*-12/*H*-9, *H*-10); MS (MALDI TOP, 22 KV) *m/z* = 2004.21.

7.8.3 PMI labeled oligoPPEs **17<sub>7</sub>**

Following the general procedure D, the PMI **3a** (58 mg, 0.10 mmol) was coupled with the free acetylene **9a<sub>7</sub>** (200 mg, 0.10 mmol) in toluene (6 mL) and Et<sub>3</sub>N (1.5 mL). Column chromatography (4 × 30 cm<sup>2</sup> silica gel, 3:1 mixture of CHCl<sub>3</sub> and *n*-hexane) afforded **17<sub>7</sub>** as a red solid (171 mg, 69%, *R<sub>f</sub>* = 0.56).

<sup>1</sup>H NMR (500 MHz): δ = 0.88-0.91 (m, 42 H, CH<sub>2</sub>CH<sub>3</sub>), 1.14 (s, 21 H, *tips*), 1.21 (d, *J* = 6.8 Hz, 12 H, CH(CH<sub>3</sub>)<sub>2</sub>), 1.28-1.42 (m, 84 H, CH<sub>2</sub>), 1.67-1.73 (m, 28 H, ArCH<sub>2</sub>-CH<sub>2</sub>), 2.76-2.84 (m, 30 H, Ar-CH<sub>2</sub>, CH(CH<sub>3</sub>)<sub>2</sub>), 7.30, 7.32 (2 s, 1 H each, Ar-*H* of *p*-(polyphenylene)s), 7.36-7.38 (m, 11 H, Ar-*H* of *p*-(polyphenylene)s), 7.43 (s, 1 H, Ar-*H* of *p*-(polyphenylene)s), 7.50 (s, 2 H, Ar-*H* ortho to CH(CH<sub>3</sub>)<sub>2</sub>), 7.67 (t, *J* = 7.8 Hz, 2 H, *H*-8, *H*-11), 7.94 (d, *J* = 8.2 Hz, 2 H, *H*-9, *H*-10/*H*-7, *H*-12), 8.49 and 8.50 (2 d, *J*<sub>1</sub> = 8.3 Hz, *J*<sub>2</sub> = 7.9 Hz, 2 H each, *H*-1, *H*-2, *H*-5, and *H*-6), 8.68 (d, *J* = 7.9 Hz, 2 H, *H*-7, *H*-12/*H*-9, *H*-10); MS (MALDI TOP, 22 KV) *m/z* = 2540.71.

#### 7.8.4 PMI labeled oligoPPEs **17<sub>9</sub>**

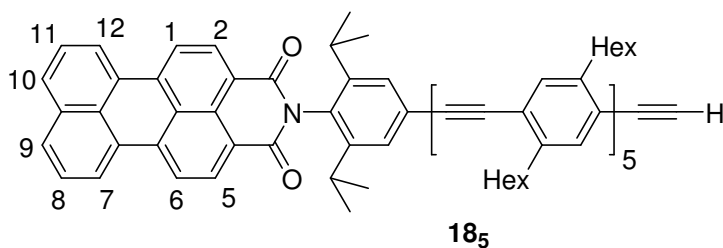


Following the general procedure D, the PMI **3a** (13 mg, 0.02 mmol) was coupled with the free acetylene **6a<sub>9</sub>** (60 mg, 0.02 mmol) in toluene (5 mL) and Et<sub>3</sub>N (1. mL). Column chromatography (4 × 20 cm<sup>2</sup> silica gel, 1:1 mixture of CHCl<sub>3</sub> and *n*-hexane) afforded **17<sub>9</sub>** as a red solid (57 mg, 80%, *R<sub>f</sub>* = 0.28).

$^1\text{H}$  NMR (500 MHz):  $\delta$  = 0.87-0.92 (m, 54 H,  $\text{CH}_2\text{CH}_3$ ), 1.14 (s, 21 H, *tips*), 1.20 (d,  $J$  = 6.8 Hz, 12 H,  $\text{CH}(\text{CH}_3)_2$ ), 1.29-1.47 (m, 108 H,  $\text{CH}_2$ ), 1.70-1.73 (m, 36 H,  $\text{ArCH}_2\text{-CH}_2$ ), 2.74-2.84 (m, 36 H,  $\text{Ar-CH}_2$ ,  $\text{CH}(\text{CH}_3)_2$ ), 7.30, 7.31 (2 s, 1 H each, *Ar-H* of *p*-(polyphenylene)s), 7.36-7.38 (m, 15 H, *Ar-H* of *p*-(polyphenylene)s), 7.43 (s, 1 H, *Ar-H* of *p*-(polyphenylene)s), 7.49 (s, 2 H, *Ar-H* ortho to  $\text{CH}(\text{CH}_3)_2$ ), 7.67 (t,  $J$  = 7.8 Hz, 2 H, *H-8*, *H-11*), 7.95 (d,  $J$  = 8.2 Hz, 2 H, *H-9*, *H-10/H-7*, *H-12*), 8.50 and 8.51 (2 d,  $J_1$  = 8.4 Hz,  $J_2$  = 8.1 Hz, 2 H each, *H-1*, *H-2*, *H-5*, and *H-6*), 8.68 (d,  $J$  = 7.8 Hz, 2 H, *H-7*, *H-12/H-9*, *H-10*); MS (MALDI TOP, 22 KV)  $m/z$  = 3077.84.

## 7.9 Free acetylene **18<sub>n</sub>** ( $n$ =5, 7, and 9)

### 7.9.1 Free acetylene **18<sub>5</sub>**

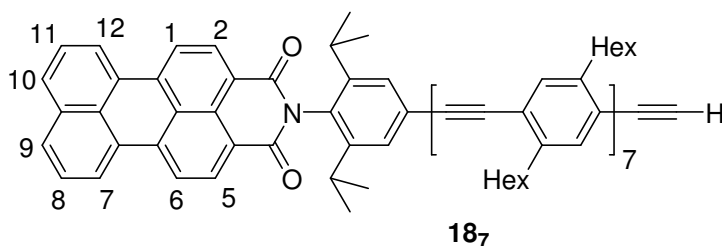


Following the general procedure B, 1 M TBAF in THF (120  $\mu\text{L}$ , 2 equiv.) was added to a solution of **17<sub>5</sub>** (120 mg, 0.06 mmol) in THF (4 mL) and stirred for 2 h at room temperature. Flash chromatography (4 x 20  $\text{cm}^2$  silica gel, 1:1  $\text{CHCl}_3$  and *n*-hexane) afforded **18<sub>5</sub>** as a red solid (89 mg, 80 %,  $R_f$  = 0.15).

$^1\text{H}$  NMR (500 MHz):  $\delta$  = 0.86-0.91 (m, 30 H,  $\text{CH}_2\text{CH}_3$ ), 1.20 (d,  $J$  = 6.8 Hz, 12 H,  $\text{CH}(\text{CH}_3)_2$ ), 1.30-1.41 (m, 60 H,  $\text{CH}_2$ ), 1.64-1.76 (m, 20 H,  $\text{ArCH}_2\text{-CH}_2$ ), 2.72-2.84 (m, 22 H,  $\text{Ar-CH}_2$ ,  $\text{CH}(\text{CH}_3)_2$ ), 3.30 (s, 1 H,  $\text{C}\equiv\text{CH}$ ), 7.33 (s, 2 H, *Ar-H* of *p*-(polyphenylene)s), 7.36-7.38 (m, 7 H, *Ar-H* of *p*-(polyphenylene)s), 7.42 (s, 1 H, *Ar-H* of *p*-(polyphenylene)s), 7.49 (s, 2 H, *Ar-H* ortho to  $\text{CH}(\text{CH}_3)_2$ ), 7.67 (t,  $J$  = 7.8 Hz, 2 H, *H-8*, *H-11*),

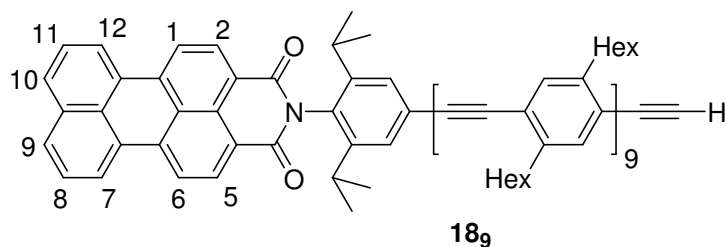
7.95 (d,  $J = 8.2$  Hz, 2 H,  $H-7$ ,  $H-12/ H-9$ ,  $H-10$ ), 8.50 and 8.51 (2 d,  $J_1 = 8.4$  Hz,  $J_2 = 8.2$  Hz, 2 H each,  $H-1$ ,  $H-2$ ,  $H-5$ , and  $H-6$ ), 8.68 (d,  $J = 8.0$  Hz, 2 H,  $H-9$ ,  $H-10/H-7$ ,  $H-12$ ). MS (MALDI TOP, 22 KV)  $m/z = 1847.9$ .

### 7.9.2 Free acetylene **18<sub>7</sub>**



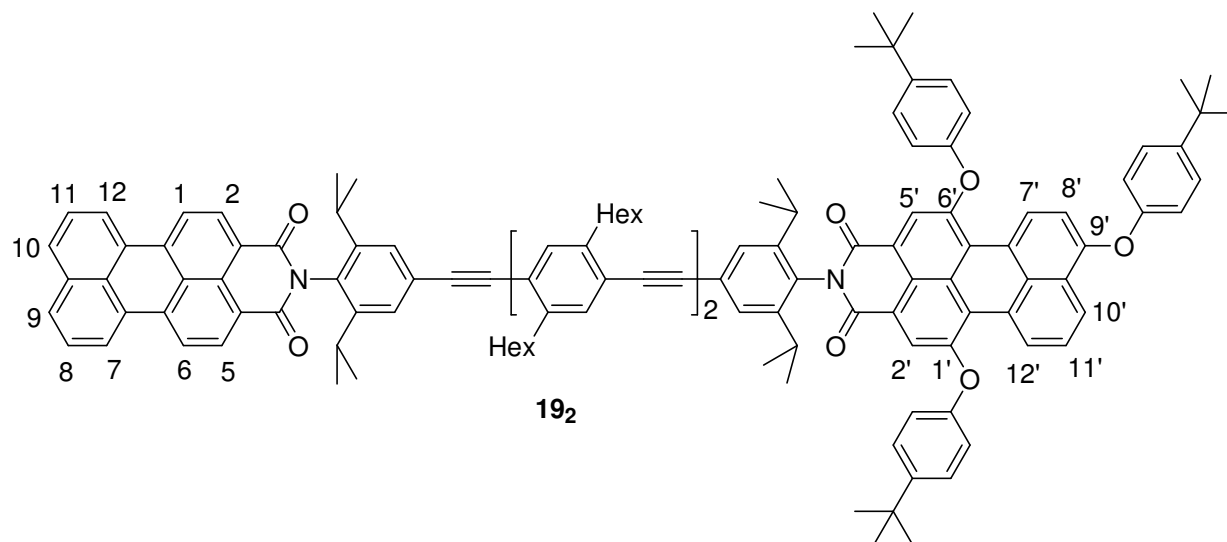
Following the general procedure B, 1 M TBAF in THF (87  $\mu$ L, 2 equiv.) was added to a solution of **17<sub>7</sub>** (110 mg, 0.04 mmol) in THF (5 mL) and stirred for 2 h at room temperature. Flash chromatography (4 x 20  $\text{cm}^2$  silica gel, 1:1  $\text{CHCl}_3$  and *n*-hexane) afforded **18<sub>7</sub>** as a red solid (69 mg, 80 %,  $R_f = 0.46$ ).

$^1\text{H}$  NMR (500 MHz):  $\delta = 0.86\text{-}0.92$  (m, 42 H,  $\text{CH}_2\text{CH}_3$ ), 1.22 (d,  $J = 6.8$  Hz, 12 H,  $\text{CH}(\text{CH}_3)_2$ ), 1.32-1.43 (m, 84 H,  $\text{CH}_2$ ), 1.68-1.76 (m, 28 H,  $\text{ArCH}_2\text{-CH}_2$ ), 2.72-2.84 (m, 30 H,  $\text{Ar-CH}_2$ ,  $\text{CH}(\text{CH}_3)_2$ ), 3.30 (s, 1 H,  $\text{C}\equiv\text{CH}$ ), 7.33 (s, 2 H,  $\text{Ar-H}$  of *p*-(polyphenylene)s), 7.36-7.38 (m, 11 H,  $\text{Ar-H}$  of *p*-(polyphenylene)s), 7.43 (s, 1 H,  $\text{Ar-H}$  of *p*-(polyphenylene)s), 7.50 (s, 2 H,  $\text{Ar-H}$  ortho to  $\text{CH}(\text{CH}_3)_2$ ), 7.65 (t,  $J = 7.8$  Hz, 2 H,  $H-8$ ,  $H-11$ ), 7.92 (d,  $J = 8.2$  Hz, 2 H,  $H-7$ ,  $H-12/ H-9$ ,  $H-10$ ), 8.47 and 8.48 (2 d,  $J_1 = 8.3$  Hz,  $J_2 = 7.5$  Hz, 2 H each,  $H-1$ ,  $H-2$ ,  $H-5$ , and  $H-6$ ), 8.67 (d,  $J = 7.9$  Hz, 2 H,  $H-9$ ,  $H-10/H-7$ ,  $H-12$ ) MS (MALDI TOP, 22 KV)  $m/z = 2385.0$ .

7.9.3 Free acetylene **18<sub>9</sub>**

Following the general procedure B, 1M TBAF in THF (20  $\mu$ L, 2 equiv.) was added to a solution of **17<sub>9</sub>** (21 mg, 0.01 mmol) in THF (3 mL) and stirred for 2 h at room temperature. Flash chromatography (4 x 20 cm<sup>2</sup> silica gel, 1:1 CHCl<sub>3</sub> and *n*-hexane) afforded **18<sub>9</sub>** as a red solid (22 mg, 74 %,  $R_f$  = 0.21).

<sup>1</sup>H NMR (500 MHz):  $\delta$  = 0.86-0.90 (m, 54 H, CH<sub>2</sub>CH<sub>3</sub>), 1.20 (d,  $J$  = 6.8 Hz, 12 H, CH(CH<sub>3</sub>)<sub>2</sub>), 1.33-1.47 (m, 108 H, CH<sub>2</sub>), 1.64-1.73 (m, 36 H, ArCH<sub>2</sub>-CH<sub>2</sub>), 2.72-2.83 (m, 38 H, Ar-CH<sub>2</sub>, CH(CH<sub>3</sub>)<sub>2</sub>), 3.30 (s, 1 H, C $\equiv$ CH), 7.33 (s, 2 H, Ar-*H* of *p*-(polyphenylene)s), 7.36-7.38 (m, 15 H, Ar-*H* of *p*-(polyphenylene)s), 7.43 (s, 1 H, Ar-*H* of *p*-(polyphenylene)s), 7.49 (s, 2 H, Ar-*H* ortho to CH(CH<sub>3</sub>)<sub>2</sub>), 7.67 (t,  $J$  = 7.8 Hz, 2 H, *H*-8, *H*-11), 7.95 (d,  $J$  = 8.2 Hz, 2 H, *H*-7, *H*-12/ *H*-9, *H*-10), 8.50 and 8.51 (2 d,  $J_1$  = 8.5 Hz,  $J_2$  = 8.1 Hz, 2 H each, *H*-1, *H*-2, *H*-5, and *H*-6), 8.68 (d,  $J$  = 7.8 Hz, 2 H, *H*-9, *H*-10/*H*-7, *H*-12); MS (MALDI TOP, 22 KV)  $m/z$  = 2919.84.

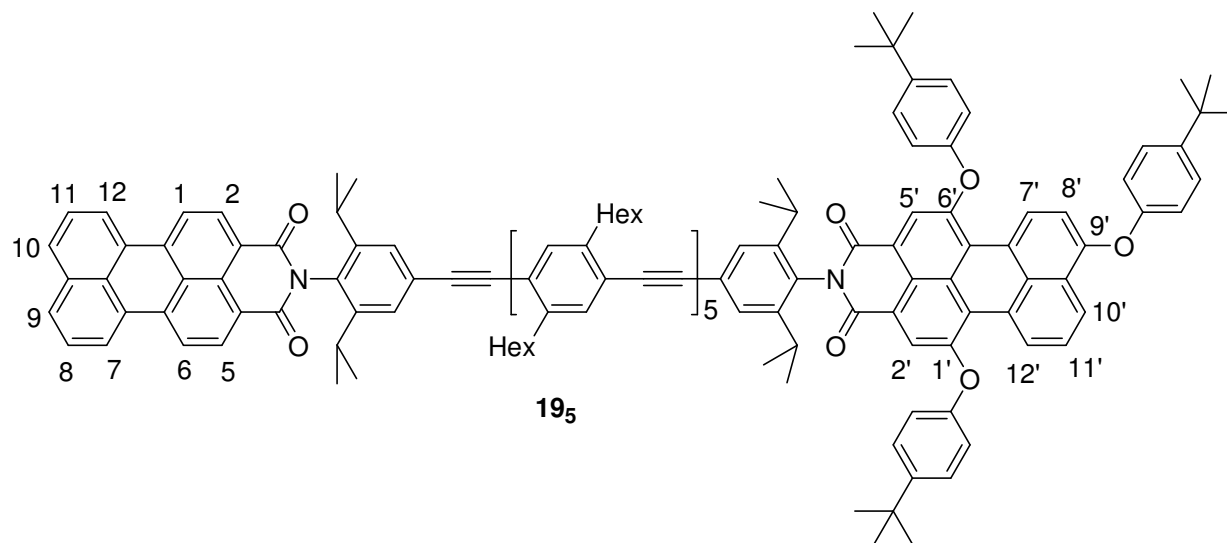
7.10 PMI-(PPE)<sub>n</sub>-PMI(OAr)<sub>3</sub> dyads **19<sub>n</sub>** (n = 2, 5, 7, and 9)7.10.1 Linear PMI-(PPE)<sub>2</sub>-PMI(OAr)<sub>3</sub> dyad **19<sub>2</sub>**

Following the general procedure D, PMI **3a** (12 mg, 0.02 mmol) was coupled with the free acetylene **16<sub>2</sub>** (35 mg, 0.02 mmol) in toluene (4 mL) and Et<sub>3</sub>N (0.8 mL). Column chromatography (4 × 15 cm<sup>2</sup> silica gel, 1:1 mixture of CHCl<sub>3</sub> and *n*-hexane) afforded **19<sub>2</sub>** as red solid (34 mg, 80%, *R<sub>f</sub>* = 0.36).

<sup>1</sup>H NMR (500 MHz): δ = 0.88-0.90 (m, CH<sub>2</sub>CH<sub>3</sub>, 12 H), 1.17 (d, *J* = 5.2 Hz, 12 H, CH(CH<sub>3</sub>)<sub>2</sub>), 1.20-1.22 (12 H, CH(CH<sub>3</sub>)<sub>2</sub>), 1.32-1.46 (m, 51 H, *t*-butyl, CH<sub>2</sub>), 1.74 (m, 8 H, ArCH<sub>2</sub>-CH<sub>2</sub>), 2.72-2.84 (m, 12 H, Ar-CH<sub>2</sub>, CH(CH<sub>3</sub>)<sub>2</sub>), 6.89 (d, *J* = 8.8 Hz, 1 H, *H*-8'/7'), 7.02, 7.08, and 7.10 (6 H, 3 halves of 3 AA'XX' spinsystems, OAr-*H* meta to *t*-butyl), 7.36-7.45 (m, 12 H, Ar-*H* of *p*-(polyphenylene)s, OAr-*H* ortho to *t*-butyl, Ar-*H* ortho to CH(CH<sub>3</sub>)<sub>2</sub>), 7.50 (s, 2 H, Ar-*H* ortho to CH(CH<sub>3</sub>)<sub>2</sub>), 7.59-7.65 (m, 3 H, *H*-8, *H*-11, and *H*-11'), 7.91 (d, *J* = 8.0 Hz, 2 H, *H*-9, *H*-10/*H*-7, *H*-12), 8.31 and 8.34 (2 s, 1 H each, *H*-2', *H*-5'), 8.43-8.49 (m, 5 H, *H*-1, 2, 5, and 6, *H*-10'), 8.65-8.66 (m, 2 H, *H*-7, *H*-12/*H*-9, *H*-

10), 9.24 (d,  $J = 8.8$  Hz, 1 H,  $H-7'/8'$ ), 9.44 (d,  $J = 7.9$  Hz, 1 H,  $H-12'/10'$ ); MS (MALDI TOP, 22 KV)  $m/z = 1967.98$ .

### 7.10.2 Linear PMI-(PPE)<sub>2</sub>-PMI(OAr)<sub>3</sub> dyad **19<sub>5</sub>**

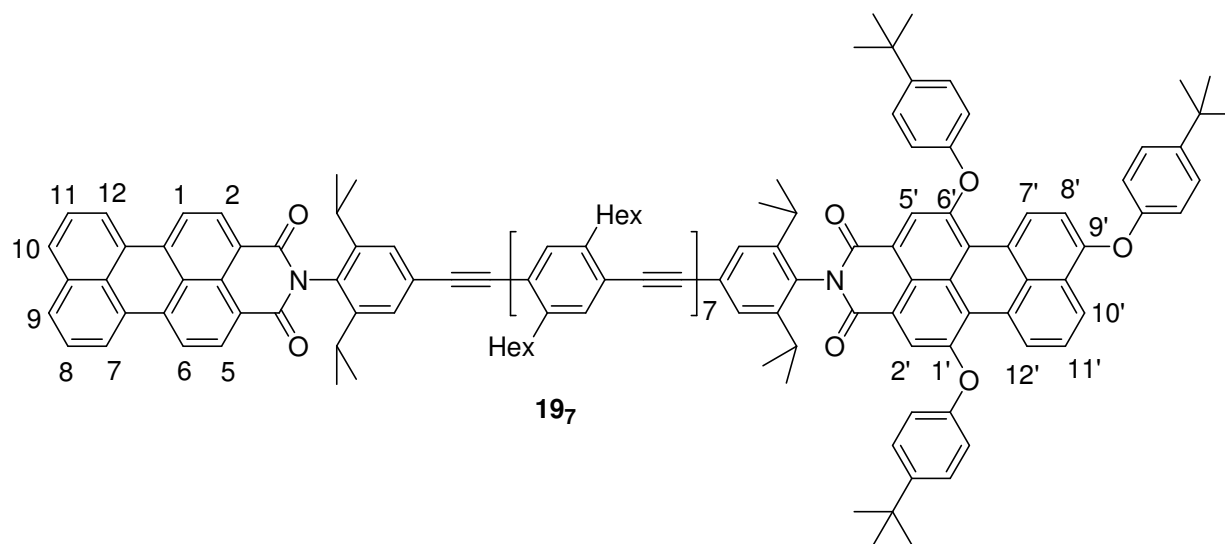


Following the general procedure D, PMI **3a** (11 mg, 0.02 mmol) was coupled with free acetylene **16<sub>5</sub>** (48 mg, 0.02 mmol) in toluene (5 mL) and Et<sub>3</sub>N (1 mL). Column chromatography (4 × 20 cm<sup>2</sup> silica gel, a 1:1 mixture of CHCl<sub>3</sub> and *n*-hexane) afforded **19<sub>5</sub>** as a red solid (28 mg, 51%,  $R_f = 0.08$ ).

<sup>1</sup>H NMR (500 MHz, CD<sub>2</sub>Cl<sub>2</sub>):  $\delta = 0.84$ - $0.91$  (m, CH<sub>2</sub>CH<sub>3</sub>, 30 H), 1.12-1.14 (12 H, CH(CH<sub>3</sub>)<sub>2</sub>), 1.17 (d,  $J = 6.8$  Hz, 12 H, CH(CH<sub>3</sub>)<sub>2</sub>), 1.30-1.44 (m, 87 H, *t*-butyl, CH<sub>2</sub>), 1.71-1.79 (m, 20 H, ArCH<sub>2</sub>-CH<sub>2</sub>), 2.69-2.85 (m, 24 H, Ar-CH<sub>2</sub>, CH(CH<sub>3</sub>)<sub>2</sub>), 6.88 (d,  $J = 8.8$  Hz, 1 H,  $H-8'/7'$ ), 7.03 (2 H, half of AA'XX' spinsystem, OAr-*H* meta to *t*-butyl), 7.08-7.11 (m, 4 H, OAr-*H* meta to *t*-butyl), 7.39-7.46 (m, 18 H, Ar-*H* of *p*-(polyphenylene)s, OAr-*H* ortho to *t*-butyl, Ar-*H* ortho to CH(CH<sub>3</sub>)<sub>2</sub>), 7.50 (s, 2 H, Ar-*H* ortho to CH(CH<sub>3</sub>)<sub>2</sub>), 7.63-7.67 (m, 3 H,  $H-8$ ,  $H-11$ , and  $H-11'$ ), 7.94 (d,  $J = 8.2$  Hz, 2 H,  $H-9$ ,  $H-10/H-7$ ,  $H-12$ ), 8.23

and 8.26 (2 s, 1 H each,  $H-2'$ ,  $H-5'$ ), 8.46-8.50 (m, 5 H,  $H-1$ , 2, 5, and 6,  $H-10'$ ), 8.63 (d,  $J = 7.9$  Hz, 2 H,  $H-7$ ,  $H-12/ H-9$ ,  $H-10$ ), 9.25 (d,  $J = 8.8$  Hz, 1 H,  $H-7'/8'$ ), 9.45 (d,  $J = 7.6$  Hz, 1 H,  $H-12'/10'$ ); MS (MALDI TOP, 22 KV)  $m/z = 2770.10$ .

### 7.10.3 Linear PMI-(PPE)<sub>2</sub>-PMI(OAr)<sub>3</sub> dyad **19<sub>7</sub>**



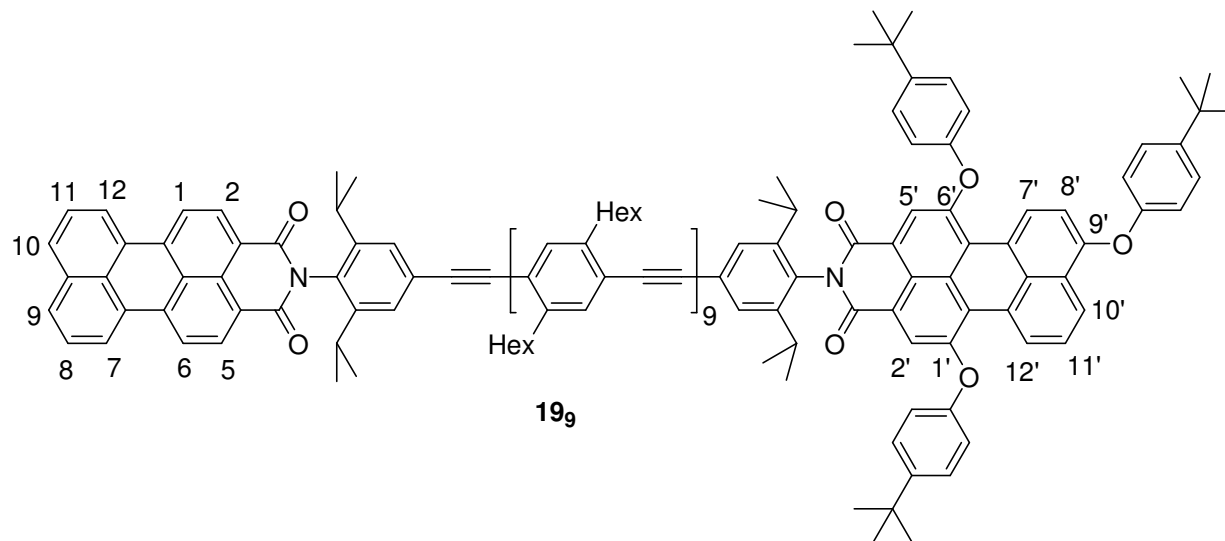
Following the general procedure D, a 97:3 the mixture of **5a** and **5b** (13 mg, 0.01 mmol) was coupled with free acetylene **18<sub>7</sub>** (32 mg, 0.01 mmol) in toluene (5 mL) and Et<sub>3</sub>N (1 mL). The crude material purified by chromatography silica gel, 4 × 20 cm<sup>2</sup>, (1:1) CHCl<sub>3</sub> and *n*-hexane) afforded **19<sub>7</sub>** as a red solid (24 mg, 56%,  $R_f = 0.13$ ).

<sup>1</sup>H NMR (500 MHz, CD<sub>2</sub>Cl<sub>2</sub>):  $\delta = 0.87$ - $0.90$  (m, CH<sub>2</sub>CH<sub>3</sub>, 42 H), 1.12-1.13 (12 H, CH(CH<sub>3</sub>)<sub>2</sub>), 1.17 (d,  $J = 6.8$  Hz, 12 H, CH(CH<sub>3</sub>)<sub>2</sub>), 1.31-1.44 (m, 111 H, *t*-butyl, CH<sub>2</sub>), 1.70-1.73 (m, 28 H, ArCH<sub>2</sub>-CH<sub>2</sub>), 2.69-2.85 (m, 32 H, Ar-CH<sub>2</sub>, CH(CH<sub>3</sub>)<sub>2</sub>), 6.89 (d,  $J = 8.8$  Hz, 1 H,  $H-8'/7'$ ), 7.03 (2 H, half of AA'XX' spinsystem, OAr-*H* meta to *t*-butyl), 7.08-7.10 (m, 4 H, OAr-*H* meta to *t*-butyl), 7.39-7.45 (m, 22 H, Ar-*H* of *p*-(polyphenylene)s, OAr-*H* ortho to *t*-butyl, Ar-*H* ortho to CH(CH<sub>3</sub>)<sub>2</sub>), 7.50 (s, 2 H, Ar-*H* ortho to CH(CH<sub>3</sub>)<sub>2</sub>), 7.64-7.68 (m, 3 H,  $H-8$ ,  $H-11$ , and  $H-11'$ ), 7.95 (d,  $J = 8.3$  Hz, 2 H,  $H-9$ ,  $H-10/H-7$ ,  $H-12$ ),



8.23 and 8.26 (2 s, 1 H each,  $H-2'$ ,  $H-5'$ ), 8.46-8.52 (m, 5 H,  $H-1$ , 2, 5, and 6,  $H-10'$ ), 8.64 (d,  $J = 7.9$  Hz, 2 H,  $H-7$ ,  $H-12/ H-9$ ,  $H-10$ ), 9.25 (d,  $J = 8.7$  Hz, 1 H,  $H-7'/8'$ ), 9.46 (d,  $J = 7.3$  Hz, 1 H,  $H-12'/10'$ ); MS (MALDI TOP, 22 KV)  $m/z = 3308.95$ .

#### 7.10.4 Linear PMI-(PPE)<sub>2</sub>-PMI(OAr)<sub>3</sub> dyad **19<sub>9</sub>**

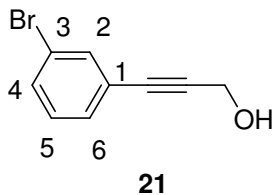


Following the general procedure D, PMI **3a** (7.4 mg, 0.01 mmol) was coupled with free acetylene **16<sub>9</sub>** (46 mg, 0.01 mmol) in toluene (5 mL) and Et<sub>3</sub>N (1 mL). Column chromatography (4 × 25 cm<sup>2</sup> silica gel, 3:7 mixture of CHCl<sub>3</sub> and *n*-hexane) afforded **19<sub>9</sub>** as a red solid (31 mg, 67%,  $R_f = 0.14$ ).

<sup>1</sup>H NMR (500 MHz, CD<sub>2</sub>Cl<sub>2</sub>):  $\delta = 0.84$ - $0.91$  (m, CH<sub>2</sub>CH<sub>3</sub>, 54 H), 1.12-1.14 (12 H, CH(CH<sub>3</sub>)<sub>2</sub>), 1.17 (d,  $J = 6.8$  Hz, 12 H, CH(CH<sub>3</sub>)<sub>2</sub>), 1.30-1.44 (m, 135 H, *t*-butyl, CH<sub>2</sub>), 1.69-1.73 (m, 36 H, ArCH<sub>2</sub>-CH<sub>2</sub>), 2.70-2.86 (m, 40 H, Ar-CH<sub>2</sub>, CH(CH<sub>3</sub>)<sub>2</sub>), 6.89 (d,  $J = 8.7$  Hz, 1 H,  $H-8'/7'$ ), 7.03 (2 H, half of AA'XX' spinsystem, OAr-*H* meta to *t*-butyl), 7.08-7.11 (m, 4 H, OAr-*H* meta to *t*-butyl), 7.40-7.46 (m, 26 H, Ar-*H* of *p*-(polyphenylene)s, OAr-*H* meta to *t*-butyl, Ar-*H* ortho to CH(CH<sub>3</sub>)<sub>2</sub>), 7.50 (s, 2 H, Ar-*H* ortho to CH(CH<sub>3</sub>)<sub>2</sub>), 7.65-7.68 (m, 3 H,  $H-8$ ,  $H-11$ , and  $H-11'$ ), 7.95 (d,  $J = 8.2$  Hz, 2 H,  $H-9$ ,  $H-10/H-7$ ,  $H-12$ ),

8.23 and 8.26 (2 s, 1 H each,  $H-2'$ ,  $H-5'$ ), 8.47-8.51 (m, 5 H,  $H-1$ , 2, 5, and 6,  $H-10'$ ), 8.64 (d,  $J = 7.8$  Hz, 2 H,  $H-7$ ,  $H-12'/H-9$ ,  $H-10$ ), 9.26 (d,  $J = 8.8$  Hz, 1 H,  $H-7'/8'$ ), 9.46 (d,  $J = 7.5$  Hz, 1 H,  $H-12'/10'$ ); MS (MALDI TOP, 22 KV)  $m/z = 3844.15$ .

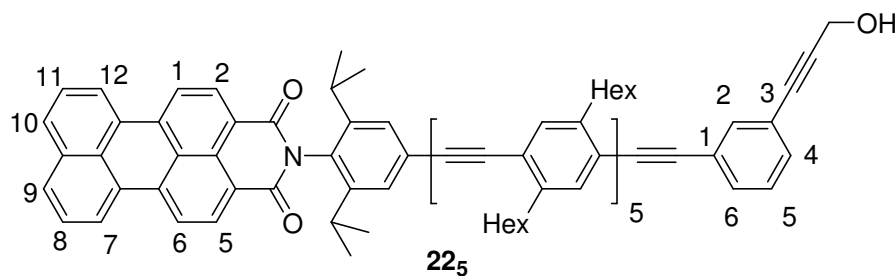
### 7.11 21



Following the general procedure A, a sample of 3-bromoiodobenzene (**20**) (1g, 3.54 mmol) was coupled with 2-propyn-1-ol (220  $\mu$ L, 1.05 equiv.) in THF (15 mL, dry), piperidine (5 mL, dry) under Ar. Column chromatography (4 x 20 cm<sup>2</sup> silica gel, 1:1 mixture of Et<sub>2</sub>O/*n*-pentane) afforded **21** as a light yellow solid (670 mg, 89% yield,  $R_f = 0.46$ ).

<sup>1</sup>H NMR (500 MHz):  $\delta$  (ppm) = 1.78 (broad singlet, 1 H, OH), 4.48 (d,  $J = 5.8$  Hz, 2 H,  $CH_2OH$ ), 7.17 (t,  $J = 7.9$  Hz, 1 H,  $H-5$ ), 7.35 (d,  $J = 7.7$  Hz, 1 H,  $H-6$ ), 7.45 (d,  $J = 8.0$  Hz, 1 H,  $H-4$ ), 7.57 (s, 1 H,  $H-2$ ).

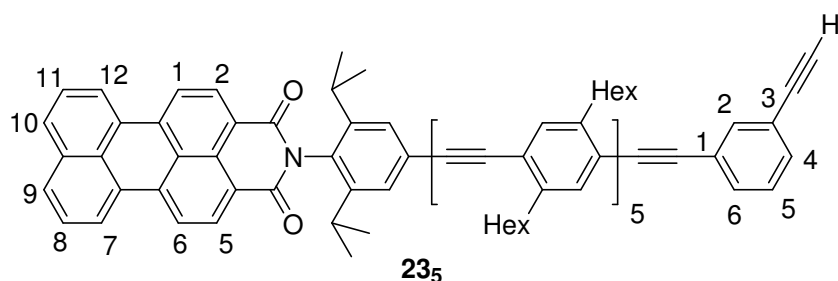
### 7.12 PMI labeled oligoPPE **22<sub>5</sub>**



Following the general procedure D, the bromo compound **21** (9.9 mg, 0.05 mmol) was coupled with the free acetylene **18<sub>5</sub>** (87 mg, 0.05 mmol) in toluene (6 mL) and Et<sub>3</sub>N (1.5 mL). Column chromatography (4 × 30 cm<sup>2</sup> silica gel, CHCl<sub>3</sub>) afforded **22<sub>5</sub>** as a red solid (32 mg, 34%, *R<sub>f</sub>* = 0.19).

<sup>1</sup>H NMR (500 MHz): δ = 0.88-0.91 (m, 30 H, CH<sub>2</sub>CH<sub>3</sub>), 1.20 (d, *J* = 6.8 Hz, 12 H, CH(CH<sub>3</sub>)<sub>2</sub>), 1.23-1.47 (m, 60 H, CH<sub>2</sub>), 1.70-1.75 (m, 20 H, ArCH<sub>2</sub>-CH<sub>2</sub>), 2.76-2.83 (m, 22 H, Ar-CH<sub>2</sub>, CH(CH<sub>3</sub>)<sub>2</sub>), 4.51 (d, *J* = 6.3 Hz, 2 H, CH<sub>2</sub>OH). 7.31 (t, *J* = 7.8 Hz, 1 H, *H*-5, *m*-phenylene), 7.36-7.42 (m, 11 H, Ar-*H* of *p*-(polyphenylene)s, *H*-6/4 of *m*-phenylene), 7.47 (d, *J* = 7.8 Hz, 1 H, *H*-4/6, *m*-phenylene), 7.49 (s, 2 H, Ar-*H* ortho to CH(CH<sub>3</sub>)<sub>2</sub>), 7.60 (s, 1 H, *H*-2, *m*-phenylene), 7.67 (t, *J* = 7.8 Hz, 2 H, *H*-8, *H*-11), 7.95 (d, *J* = 8.2 Hz, 2 H, *H*-9, *H*-10/*H*-7, *H*-12), 8.49 and 8.51 (2 d, *J*<sub>1</sub> = 8.5 Hz, *J*<sub>2</sub> = 8.1 Hz, 2 H each, *H*-1, *H*-2, *H*-5, and *H*-6), 8.68 (d, *J* = 7.9 Hz, 2 H, *H*-7, *H*-12/*H*-9, *H*-10); MS (MALDI TOP, 22 KV) *m/z* = 1976.1.

### 7.13 Free acetylene **23<sub>5</sub>**

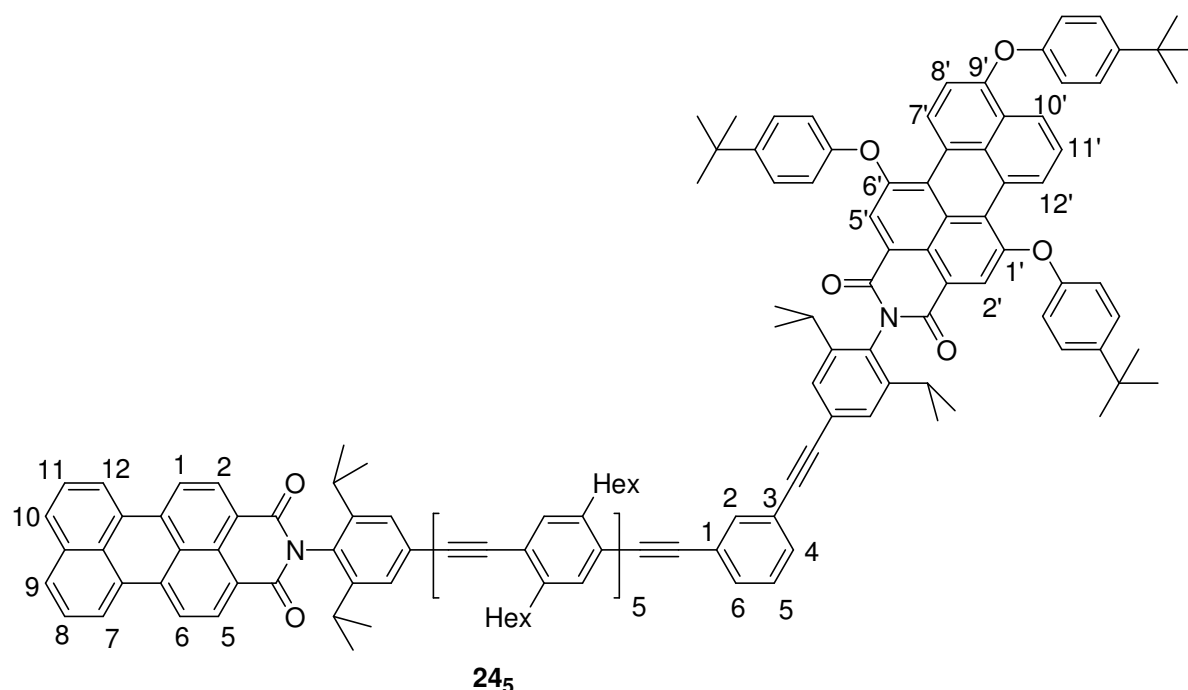


Following the general procedure C, to a solution of **22<sub>5</sub>** (32 mg, 0.02 mmol) in CH<sub>2</sub>Cl<sub>2</sub> (5 ml), γ-Mn<sub>2</sub>O (85 mg, 0.98 mmol) and powdered KOH (25 mg, 0.45 mmol) were added in two portion in an interval of 1 h to afford **23<sub>5</sub>** as a red solid (21 mg, 67 %, *R<sub>f</sub>* = 0.69 in CHCl<sub>3</sub>). The material was used as such for next reaction.

$^1\text{H}$  NMR (500 MHz):  $\delta$  = 0.88-0.91 (m, 30 H,  $\text{CH}_2\text{CH}_3$ ), 1.21 (d,  $J$  = 6.9 Hz, 12 H,  $\text{CH}(\text{CH}_3)_2$ ), 1.33-1.48 (m, 60 H,  $\text{CH}_2$ ), 1.67-1.76 (m, 20 H,  $\text{ArCH}_2\text{-CH}_2$ ), 2.75-2.84 (m, 22 H,  $\text{Ar-CH}_2$ ,  $\text{CH}(\text{CH}_3)_2$ ), 3.10 (s, 1 H,  $\text{C}\equiv\text{CH}$ ), 7.32 (t,  $J$  = 7.7 Hz, 1 H,  $H-5$ ,  $m$ -phenylene), 7.37-7.38 (m, 7 H,  $\text{Ar-H}$  of  $p$ -(polyphenylene)s), 7.43 (s, 1 H,  $\text{Ar-H}$  of  $p$ -(polyphenylene)s), 7.46 (d,  $J$  = 7.7 Hz, 1 H,  $H-6/4$  of  $m$ -phenylene), 7.49-7.50 (m, 3 H,  $H-4/6$  of  $m$ -phenylene,  $\text{Ar-H}$  ortho to  $\text{CH}(\text{CH}_3)_2$ ), 7.65 (m, 3 H,  $H-8$ ,  $H-11$  and  $H-2$  of  $m$ -phenylene), 7.93 (d,  $J$  = 8.2 Hz, 2 H,  $H-7$ ,  $H-12/H-9$ ,  $H-10$ ), 8.47 and 8.48 (2 d,  $J_1$  = 8.3 Hz,  $J_2$  = 7.7 Hz, 2 H each,  $H-1$ ,  $H-2$ ,  $H-5$ , and  $H-6$ ), 8.67 (d,  $J$  = 7.9 Hz, 2 H,  $H-9$ ,  $H-10/H-7$ ,  $H-12$ ).

## 7.14 Kinked PMI-(PPE) $_n$ -PMI(OAr) $_3$ dyads **24 $_n$** ( $n$ = 5, 7, and 9)

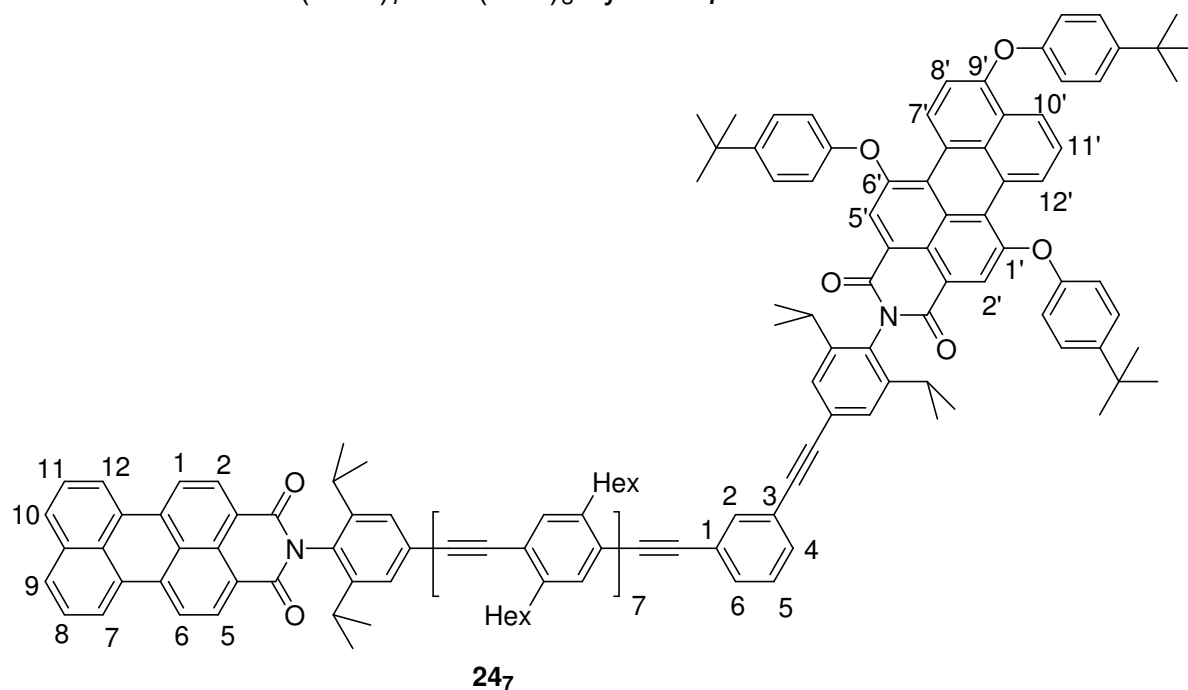
### 7.14.1 Kinked PMI-(PPE) $_5$ -PMI(OAr) $_3$ dyad **24 $_5$**



Following the general procedure D, a 97:3 mixture of **5a** and **5b** (9.9 mg, 0.01 mmol) was coupled with the compound **23 $_5$**  (20 mg, 0.01 mmol) in toluene (3.5 mL) and

Et<sub>3</sub>N (0.7 mL). Column chromatography (4 × 25 cm<sup>2</sup> silica gel, 1:1 mixture of CHCl<sub>3</sub> and *n*-hexane) afforded **24<sub>5</sub>** as a red solid (20 mg, 70%, *R<sub>f</sub>* = 0.27).

<sup>1</sup>H NMR (500 MHz): δ = 0.88-0.91 (m, CH<sub>2</sub>CH<sub>3</sub>, 30 H), 1.15-1.16 (12 H, CH(CH<sub>3</sub>)<sub>2</sub>), 1.20 (d, *J* = 6.8 Hz, 12 H, CH(CH<sub>3</sub>)<sub>2</sub>), 1.31-1.42 (m, 87 H, *t*-butyl, CH<sub>2</sub>), 1.71-1.73 (m, 20 H, ArCH<sub>2</sub>-CH<sub>2</sub>), 2.70-2.83 (m, 24 H, Ar-CH<sub>2</sub>, CH(CH<sub>3</sub>)<sub>2</sub>), 6.90 (d, *J* = 8.8 Hz, 1 H, *H*-8'/7'), 7.02, 7.07, and 7.09 (6 H, 3 halves of 3 AA'XX' spinsystems, OAr-*H* meta to *t*-butyl), 7.35-7.49 (m, 22 H, OAr-*H* ortho to *t*-butyl, Ar-*H* ortho to CH(CH<sub>3</sub>)<sub>2</sub>, Ar-*H* of *p*-(polyphenylene)s, *H*-5, *H*-6/4 of *m*-phenylene), 7.53 (d, *J* = 7.7 Hz, 1 H, *H*-4/6 of *m*-phenylene), 7.64-7.69 (m, 3 H, *H*-8, *H*-11, and *H*-11'), 7.73 (s, 1 H, *H*-2 of *m*-phenylene), 7.95 (d, *J* = 8.2 Hz, 2 H, *H*-9, *H*-10/ *H*-7, *H*-12), 8.30 and 8.33 (2 s, 1 H each, *H*-2', *H*-5'), 8.48-8.52 (m, 5 H, *H*-1, 2, 5, and 6, *H*-10'), 8.68 (d, *J* = 7.9 Hz, 2 H, *H*-7, *H*-12/*H*-9, *H*-10), 9.25 (d, *J* = 8.8 Hz, 1 H, *H*-7'/8'), 9.45 (d, *J* = 7.6 Hz, 1 H, *H*-12'/10'); MS (MALDI TOP, 22 KV) *m/z* = 2871.46.

7.14.2 Kinked PMI-(PPE)<sub>7</sub>-PMI(OAr)<sub>3</sub> dyad **24**<sub>7</sub>

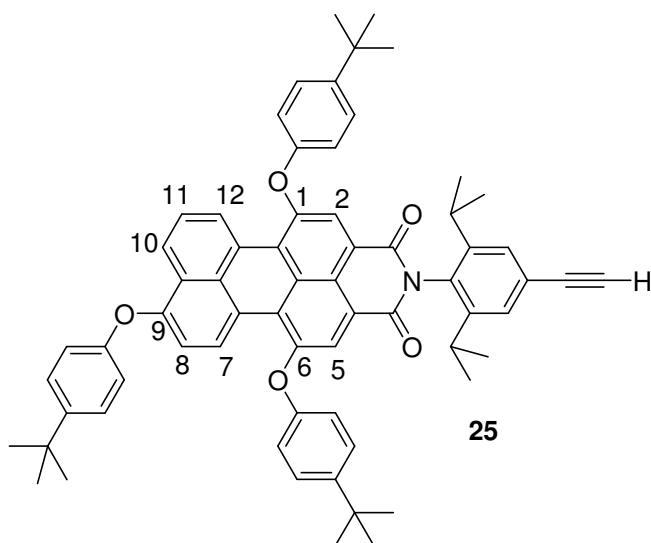
Following the general procedure D, the bromo compound **26** (12 mg, 0.01 mmol) was coupled with free acetylene **18**<sub>7</sub> (28 mg, 0.01 mmol) in toluene (3.5 mL) and Et<sub>3</sub>N (0.8 mL). Column chromatography (4 × 25 cm<sup>2</sup> silica gel, 1:1 mixture of CHCl<sub>3</sub> and *n*-hexane) afforded **24**<sub>7</sub> as a red solid (22 mg, 59%, *R*<sub>f</sub> = 0.27).

<sup>1</sup>H NMR (500 MHz): δ = 0.88-0.91 (m, 42 H, CH<sub>2</sub>CH<sub>3</sub>), 1.15-1.17 (12 H, CH(CH<sub>3</sub>)<sub>2</sub>), 1.21 (d, *J* = 6.8 Hz, 12 H, CH(CH<sub>3</sub>)<sub>2</sub>), 1.32-1.43 (m, 111 H, *t*-butyl, CH<sub>2</sub>), 1.72-1.73 (m, 28 H, ArCH<sub>2</sub>-CH<sub>2</sub>), 2.70-2.84 (m, 32 H, Ar-CH<sub>2</sub>, CH(CH<sub>3</sub>)<sub>2</sub>), 6.90 (d, *J* = 8.8 Hz, 1 H, *H*-8'/7'), 7.02, 7.08, and 7.09 (6 H, 3 halves of AA'XX' spinsystems, OAr-*H* meta to *t*-butyl), 7.36-7.50 (m, 26 H, OAr-*H* ortho to *t*-butyl, Ar-*H* ortho to CH(CH<sub>3</sub>)<sub>2</sub>, Ar-*H* of *p*-(polyphenylene)s, *H*-5, *H*-6/4 of *m*-phenylene), 7.53 (d, *J* = 7.6 Hz, 1 H, *H*-4/6 of *m*-phenylene), 7.63-7.68 (m, 3 H, *H*-8, *H*-11, and *H*-11'), 7.74 (s, 1 H, *H*-2 of *m*-phenylene), 7.94 (d, *J* = 8.3 Hz, 2 H, *H*-9, *H*-10/ *H*-7, *H*-12), 8.30 and 8.34 (2 s, 1 H each, *H*-2', *H*-5'), 8.47-8.51 (m, 5 H, *H*-1, 2, 5, and 6, *H*-10'), 8.68 (d, *J* = 7.8 Hz, 2 H, *H*-7, *H*-12/*H*-9, *H*-



*t*-butyl), 7.36-7.50 (m, 30 H, OAr-*H* ortho to *t*-butyl, Ar-*H* ortho to CH(CH<sub>3</sub>)<sub>2</sub>, Ar-*H* of *p*-phenylene)s, *H*-5, *H*-6/4 of *m*-phenylene), 7.53 (d, *J* = 7.6 Hz, 1 H, *H*-4/6 of *m*-phenylene), 7.64-7.68 (m, 3 H, *H*-8, *H*-11, and *H*-11'), 7.74 (s, 1 H, *H*-2 of *m*-phenylene), 7.93-7.95 (m, 2 H, *H*-9, *H*-10/ *H*-7, *H*-12), 8.30 and 8.34 (2 s, 1 H each, *H*-2', *H*-5'), 8.48-8.52 (m, 5 H, *H*-1, 2, 5, and 6, *H*-10'), 8.68 (d, *J* = 7.7 Hz, 2 H, *H*-7, *H*-12/*H*-9, *H*-10), 9.26 (d, *J* = 8.9 Hz, 1 H, *H*-7'/8'), 9.45 (d, *J* = 7.9 Hz, 1 H, *H*-12'/10'); MS (MALDI TOP, 22 KV) *m/z* = 3943.97.

### 7.15 Free acetylene **25**



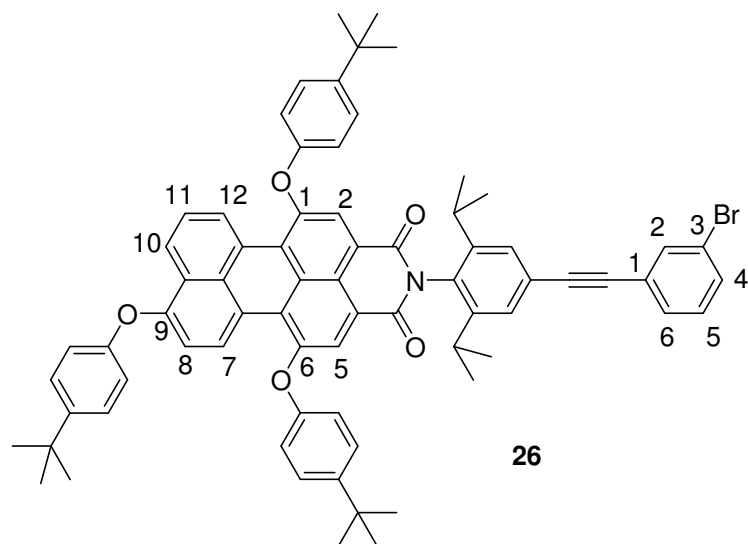
Following the general procedure D, Pd<sub>2</sub>(dba)<sub>3</sub> (13.7 mg, 0.01 mmol, 10 mol%), P(*o*-tolyl)<sub>3</sub> (29.4 mg, 0.09 mmol, 60 mol%) were added to the degassed reaction mixture of **5** (150 mg, 0.15 mmol), TMS acetylene (27 μL, 1.3 equiv.) and heated to 65 °C. After 18 h, Et<sub>2</sub>O (20 mL) was added to the reaction mixture followed by 2N HCl (10 mL) and stirred for five minute. The aqueous phase was separated and extracted with Et<sub>2</sub>O (3 x 20 mL). The combined organic phases were washed with distilled water 20 mL. The



organic phase was dried with  $\text{Na}_2\text{SO}_4$  and the solvent was evaporated to get crude product TMS protected product (185 mg). Subsequently, 5N NaOH solution (1 mL) was added to the TMS protected acetylene dissolved in a mixture of THF/MeOH (6 mL and 5 mL) at room temperature. After 2 h the reaction was stopped by adding distilled water (50 mL). Red solid tops out from the solution. The solid was filtered and washed with water and dried to get the crude product. The product was purified by chromatography (4 x 25 cm<sup>2</sup> silica-gel, 1:1  $\text{CHCl}_3$  and *n*-hexane) afforded **8a** as a magenta solid (100 mg, 70 % yield,  $R_f = 0.43$ ).

<sup>1</sup>H NMR (500 MHz):  $\delta$  (ppm) = 0.86-0.88 (m, 10 H, unknown), \* 1.12 (d-d,  $J_1 = 6.9$  Hz,  $J_2 = 1.2$  Hz, 12 H,  $\text{CH}(\text{CH}_3)_2$ ), 1.31, \* 1.33, and \* 1.34 (3 s, 9 H each, *t*-butyl), \* 2.63-2.72 (m, 2 H,  $\text{CH}(\text{CH}_3)_2$ ), 3.09 (s, 1 H,  $\text{C}\equiv\text{CH}$ ), 6.89 (d,  $J = 8.8$  Hz, 1 H, *H*-8/7), 7.01, 7.06, and 7.09 (6 H, 3 halves of 3 AA'XX' spinsystems, OAr-*H* meta to *t*-butyl), 7.36 (2 H, half of AA'XX' spinsystem, OAr-*H* ortho to *t*-butyl), \* 7.39-7.42 (m, 6 H, Ar-*H* ortho to  $\text{CH}(\text{CH}_3)_2$ , OAr-*H* ortho to *t*-butyl), 7.64 (t,  $J = 8.1$  Hz, 1 H, *H*-11), 8.28, 8.32 (2 s, 1 H each, *H*-2 and *H*-5), 8.48 (d,  $J = 8.1$  Hz, 1 H, *H*-10/12), 9.24 (d,  $J = 8.8$  Hz, 1 H, *H*-7/8), 9.44 (d,  $J = 7.5$  Hz, 1 H, *H*-12/10).

\*These signals have higher intensity than expected and this higher intensity is due to the additional signal for the  $\text{PMI}(\text{OAr})_2$  (**5b**) coupled product. The remaining signals are:  $\delta = 7.59$  (t,  $J = 8.1$  Hz, 2 H, *H*-8 and *H*-11), 7.91 (d,  $J = 7.8$  Hz, 2 H, *H*-7, *H*-12/ *H*-9, *H*-10), 9.36 (d,  $J = 8.0$  Hz, 2 H, *H*-9, *H*-10/*H*-7, *H*-12).

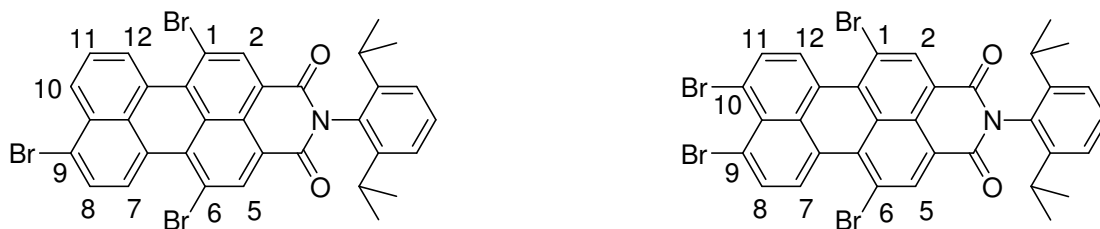
7.16 Synthesis of bromo compound **26**

Following general procedure A, Pd(PPh<sub>3</sub>)Cl<sub>2</sub> (1.4 mg, 2 mol%), CuI (1.1 mg, 5.8 mol%) were added to the degassed reaction mixture of 3-bromoiodobenzene (**20**) (28 mg, 0.10 mmol) and **25** (100 mg, 1.06 equiv.) and stirred at room temperature. After 18 h, Et<sub>2</sub>O (20 mL) and 2N HCl (20 mL) were added to the reaction mixture and stirred for 5 minute. The aqueous phase was separated and extracted with Et<sub>2</sub>O (3 x 20 mL). The combined organic phases were washed with water (2 x 20 mL). After drying from Na<sub>2</sub>SO<sub>4</sub>, the solvent was evaporated to obtain the crude material. Column chromatography (4 x 20 cm<sup>2</sup> silica gel, 1:1 mixture of CHCl<sub>3</sub> and *n*-hexane) afforded **26** as a red solid (80 mg, 73% yield, *R*<sub>f</sub> = 0.53).

<sup>1</sup>H NMR (500 MHz): δ (ppm) = 1.15 (dd, *J*<sub>1</sub> = 6.9 Hz, *J*<sub>2</sub> = 1.2 Hz, 12 H, CH(CH<sub>3</sub>)<sub>2</sub>), 1.31, 1.33, and 1.34 (3 s, 9 H each, *t*-butyl), 2.69-2.71 (m, 2 H, CH(CH<sub>3</sub>)<sub>2</sub>), 6.89 (d, *J* = 8.8 Hz, 1 H, *H*-8/7), 7.01, 7.07, and 7.09 (6 H, 3 halves of 3 AA'XX' spinsystems, OAr-*H* meta to *t*-butyl), 7.21 (t, *J* = 7.9 Hz, 1 H, *H*-5, bromo phenylene), 7.36, 7.40, and 7.42 (6

H, 3 halves of 3 AA'XX' spinsystems, OAr-*H* ortho to *t*-butyl), 7.41 (2 d,  $J_1 = 8.5$  Hz,  $J_2 = 8.4$  Hz, 4 H, OAr-*H* ortho to *t*-butyl) 7.43 (s, 2 H, Ar-*H* ortho to  $\text{CH}(\text{CH}_3)_2$ ), 7.46 (d, *H*-6 of bromo phenylene with fine structure due to coupling with *H*-2 and *H*-4), 7.48 (d, *H*-4 of bromo phenylene with fine structure due to coupling with *H*-2 and *H*-6) 7.64 (t,  $J = 8.1$  Hz, 1 H, *H*-11), 7.71 (t, 1 H, *H*-2 of bromo phenylene with insufficiently resolved fine structure due to coupling with *H*-4 and *H*-6 and a coupling constant of about 2 Hz), 8.29, and 8.33 (2 s, 1 H each, *H*-2, *H*-5), 8.48 (d,  $J = 8.2$  Hz, 1 H, *H*-10/12), 9.24 (d,  $J = 8.8$  Hz, 1 H, *H*-7/8), 9.45 (d,  $J = 7.8$  Hz, 1 H, *H*-12/10); MS (MALDI TOP, 22 KV)  $m/z = 1105.5$ .

### 7.17 Synthesis of tribromo perylenemonoimide **27**



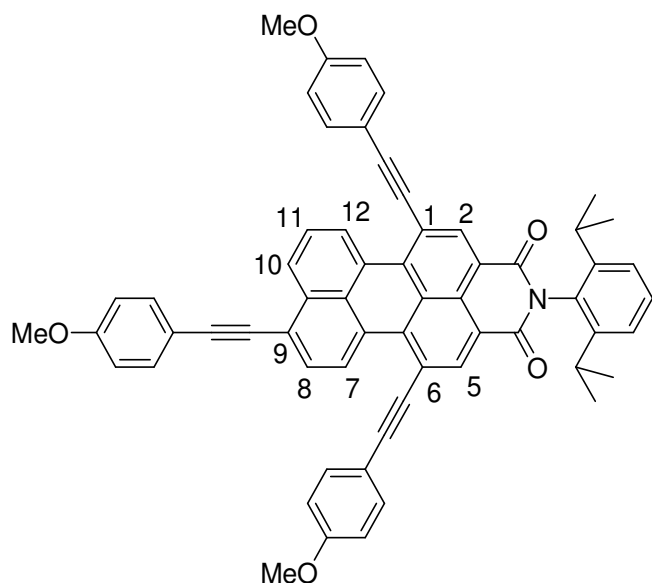
Following the procedure described by Lindsey *et al.*<sup>56,57</sup> a solution of **3b** (600 mg, 1.25 mmol) in  $\text{CHCl}_3$  (70 mL) was treated with  $\text{Br}_2$  (1.3 mL, 24.89 mmol) to afford bromoperylene monoimide **27**. Column chromatography (silica gel, 4 x 15 cm<sup>2</sup>,  $\text{CHCl}_3/n$ -hexane (3:1)), afforded a mixture of **27a** and **27b** as red solid (567 mg, 52%) in a ratio of 94:6.

<sup>1</sup>H NMR (500 MHz) of **27a**:  $\delta = 1.16$  (d,  $J = 6.9$  Hz, 12 H,  $\text{CH}(\text{CH}_3)_2^*$ ), 2.69 (m, 2 H,  $\text{CH}(\text{CH}_3)_2^*$ ), 7.33 (d,  $J = 7.8$  Hz, 2 H, Ar-*H* ortho to  $\text{CH}(\text{CH}_3)_2^*$ ), 7.47 (t,  $J = 7.8$  Hz, 1 H, Ar-*H* meta to  $\text{CH}(\text{CH}_3)_2^*$ ), 7.81 (t,  $J = 8.1$  Hz, 1 H, *H*-11), 7.99 (d,  $J = 8.2$  Hz, 1 H, *H*-

7). 8.45 (d,  $J = 8.2$  Hz, 1 H,  $H-12$ ), 8.90 and 8.92 (2s, 1 H each,  $H-2$ ,  $H-5$ ), 9.11 (d,  $J = 8.2$  Hz, 1 H,  $H-8$ ), 9.33 (d,  $J = 7.6$  Hz, 1 H,  $H-10$ ).

\*These signals have higher intensity than expected and this higher intensity is due to the additional signal for the phenyl group at the imides moiety of **27b**. The signals due to the compound **27b** are  $\delta = 8.12$  (d,  $J = 8.2$  Hz, 2 H,  $H-7$ ,  $H-12$ ), 8.89 (s, 2 H,  $H-2$ ,  $H-5$ ), 8.95 (d, 2 H,  $H-8$ ,  $H-11$ ).

### 7.18 Synthesis of alkynyl-substituted perylenemonoimide **28**



Following the general procedure D, the mixture of **4a** and **4b** (60 mg, 0.08 mmol) was treated with 3-(4-methoxyphenyl)ethyn-1-yl (35.4 mg, 3.15 mmol) in toluene (5 mL) and  $\text{Et}_3\text{N}$  (1 mL) to afford **28**. Column chromatography (silica gel,  $4 \times 25 \text{ cm}^2$ ,  $\text{CHCl}_3$ ) afforded **27** as pink solid (25 mg, 34 %).

$^1\text{H}$  NMR (500 MHz):  $\delta = 1.19$  (d,  $J = 6.9$  Hz, 12 H,  $\text{CH}(\text{CH}_3)_2$ ), 2.78 (m, 2 H,  $\text{CH}(\text{CH}_3)_2$ ), 3.86 (s, 6 H,  $\text{OMe}$  at 1 and 6), 3.88 (s, 3 H,  $\text{OMe}$  at 9), 6.93-6.97 (m, 6 H,  $\text{C}\equiv\text{CAr-H}$  meta to  $\text{OMe}$ ), 7.37 (d,  $J = 7.9$  Hz, 2 H,  $\text{Ar-H}$  ortho to  $\text{CH}(\text{CH}_3)_2$ ), 7.50 (t, 1 H,

Ar-*H* meta to CH(CH<sub>3</sub>)<sub>2</sub>, 7.55-7.58 (m, 4H, C≡CAr-*H* ortho to *OMe* at 1 and 6), 7.64 (d, *J* = 8.7 Hz, 2 H, C≡CAr-*H* ortho to *OMe* at 9), 7.84 (t, *J* = 8.0 Hz, 1 H, *H*-11), 7.94 (d, *J* = 8.1 Hz, 1 H, *H*-8), 8.66 (d, *J* = 8.1 Hz, 1 H, *H*-10), 8.78 and 8.89 (2s, 1 H each, *H*-2, *H*-5), 9.87 (d, *J* = 8.1 Hz, 1 H, *H*-7), 9.97 (d, *J* = 7.5 Hz, 1 H, *H*-12).

## Chapter 8

### References

1. Förster, T. *Ann. Physik.* **1948**, 437, 55-57.
2. Stryer, L.; Haugland, R. P. *Proc. Natl. Acad. Sci. USA* **1967**, 58, 719-726.
3. Lakowicz, J. R. *Principles of fluorescence spectroscopy*, 2nd ed.; Kluwer Academic/Plenum: New York, **1999**.
4. Valeur, B. *Molecular Fluorescence*; Willey-VCH Verlag GmbH, Germany, **2001**.
5. Steinberg, I. Z. *Annu. Rev. Biochem.* **1971**, 40, 83-114.
6. Stryer, L. *Annu. Rev. Biochem.* **1978**, 47, 819-846.
7. Fairclough, R. H.; Cantor, C. R. *Methods Enzymol.* **1978**, 48, 347-379.
8. Selvin, P. R. *Methods Enzymol.* **1995**, 246, 300-334.
9. Sapsford, K. E.; Berti, L.; Medintz, I. L. *Angew. Chem.Int. Ed.* **2006**, 45, 4562-4588.
10. Ha, T.; Enderle, T.; Ogletree, D. F.; Chemla, D. S.; Selvin, P. R.; Weiss, S. *Proc. Natl. Acad. Sci. U.S.A.* **1996**, 93, 6264-6268.
11. Deniz, A. A.; Dahan, M.; Grunwell, J. R.; Ha, T.; Faulhaber, A. E.; Chemla, D. S.; Weiss, S.; Schutz, P. G. *Proc. Natl. Acad. Sci. U.S.A.* **1999**, 96, 3670-3675.
12. Weiss, S. *Science*, **1999**, 283, 1676-1683.

13. Deniz, A. A.; Laurence, T. A.; Belligere, G. S.; Dahan, M.; Martin, A. B.; Chemla, D. S.; Dawson, P. G.; Schultz, P. G.; Weiss, S. *Proc. Natl. Acad. Sci. U.S.A.* **2000**, *97*, 5179-5184.
14. Weiss, S.; *Nat. Struct. Biol.* **2000**, *7*, 724-729.
15. Selvin, P. R. *Nat. Struct. Biol.* **2000**, *7*, 730-734.
16. Ha, T.; *Curr. Opin. Struct. Biol.* **2001**, *11*, 278-292.
17. Dietrich, A.; Buschmann, V.; Müller, C.; Sauer, M. *Rev. in Mol. Biotech.* **2002**, *82*, 211-231.
18. Kapanidis, A. N.; Laurence, T. A.; Lee, N. K.; Margeat, E.; Kong, X.; Weiss, S. *Acc. Chem. Res.* **2005**, *38*, 525-533.
19. Haas, E. *ChemPhysChem.* **2005**, *6*, 858-870.
20. Schuler, B.; Lipman, E. A.; Steinbach, P. J.; Kumke, M.; Eaton, W. A. *Proc. Natl. Acad. Sci. U.S.A.* **2005**, *102*, 2754-2759.
21. Lipman, E. A.; Schuler, B.; Bakajin, O.; Eaton, W. A. *Science*, **2003**, *301*, 1233-1235.
22. Lee, N. K.; Kapanidis, A. N.; Wang, Y.; Michalet, X.; Mukhopadhy, J.; Ebright, R. H.; Weiss, S. *Biophys. J.* **2005**, *88*, 2939-2953.
23. Muls, B.; Uji-i, H.; Melnikov, S.; Moussa, A.; Verheijen, W.; Soumillion, J.-P.; Josemon, J.; Müllen, K.; Hofkens, J. *ChemPhysChem* **2005**, *6*, 2286-2294.
24. Azov, V. A., Schlegel, A., Diederich, F., *Angew. Chem. Int. Ed.* **2005**, *44*, 4635-4638.

25. Matayoshi, E. D.; Wang, G. T.; Frafft, G. A.; Erickson, J. *Science* **1990**, *247*, 954.
26. Coskun, A.; Akkaya, E. U. *J. Am. Chem. Soc.* **2005**, *127*, 10464-10465.
27. Coskun, A.; Akkaya, E. U. *J. Am. Chem. Soc.* **2006**, *128*, 14474-14475.
28. Gulyev, R.; Coskun, A.; Akkaya, E. U. *J. Am. Chem. Soc.* **2009**, *131*, 9007-9013.
29. Stambuli, J. P.; Stauffer, S. R.; Shaughnessy, K. H.; Hartwig, J. F. *J. Am. Chem. Soc.* **2001**, *123*, 2677-2678.
30. Stauffer, S. R.; Beare, N. F.; Stambuli, J. P.; Hartwig, J. F. *J. Am. Chem. Soc.* **2001**, *123*, 4641-4642.
31. Stauffer, S. R.; Hartwig, J. F. *J. Am. Chem. Soc.* **2003**, *125*, 6977-6985.
32. Benson, S. C.; Singh, P.; Glazer, A. N. *Nucleic Acids Res.* **1993**, *21*, 5727.
33. Langhals, H.; Poxleitner, S.; Krotz, O.; Pust, T. Walter. A. *Eur. J. Org. Chem.* **2008**, 4559-4562.
34. Ozaki, H.; McLaughlin, L. W. *Nucleic Acids Res.* **1992**, *20*, 5205-5214.
35. Chiang, W.-Y.; Borbat, P. P.; Freed, J. H. *J. Magn. Reson.* **2005**, *172*, 279-295.
36. Jeschke, G.; Chechik, V.; Ionita, P.; Godt, A.; Zimmermann, H.; Banham, J.; Timmel, C. R.; Hilger, D., Jung, H. *Appl. Magn. Reson.* **2006**, *30*, 473-498.
37. Banham, J. E.; Timmel, C. R.; Abbott, R. J. M.; Lea, S. M.; Jeschke, G. *Angew. Chem.* **2006**, *118*, 1074-1077.
38. Godt, A.; Schulte, M.; Zimmermann, H.; Jeschke, G. *Angew. Chem. Int. Ed.* **2006**, *45*, 7560-7564.



39. Hugland, R. P.; Zguerabide, J. L.; Strzer, L. *Proc. Natl. Acad. Sci. U.S.A.* **1969**, *63*, 23-30.
40. Dale, R. E.; Eisinger, J. I.; Blumberg, W. E. *Biophys. J.* **1975**, *26*, 161-193.
41. Zollinger, H. *color Chemistry*; 2<sup>nd</sup> ed. VCH: Weinheim, 1991.
42. Langhals, H. *Heterocycles* **1995**, *40*, 477-500.
43. O'Neil, M. P.; Niemczyk, M. P.; Svec, W. A.; Gosztola, D.; Gaines, G. L. III; Wasielewski, M. R. *Science* **1992**, *257*, 63-65.
44. Hofkens, J.; Latterini, L.; De Belder, G.; Genesch, T.; Maus, M.; Vosch, T.; Karni, Y.; Schweitzer, G.; De Schryver, F. C.; Hermann, A.; Müllen, K. *Chem. Phys. Lett.* **1999**, *304*, 1-9.
45. Ebeid, E. M.; El-Daly, S. A.; Langhals, H. *J. Phys. Chem.* **1988**, *92*, 4565-4568.
46. Langhals, H. *Chem. Ber.* **1985**, *118*, 4641-4645.
47. Feiler, L.; Langhals, H.; Polborn, K. *Liebigs Ann.* **1995**, 1229-1244.
48. Miller, M. A.; Lammi, R. K.; Prathapan, S.; Holten, D.; Lindsey, J. S. *J. Org. Chem.* **2000**, *65*, 6634-6649.
49. Prathapan, S.; Yang, S. I.; Miller, M. A.; Bocian, D. F.; Holten, D.; Lindsey, J. S. *J. Phys. Chem. B* **2001**, *105*, 8237-8248.
50. Yang, S. I.; Prathapan, S.; Miller, M. A.; Seth, J.; Bocian, D. F.; Lindsey, J. S.; Holten, D. *J. Phys. Chem. B* **2001**, *105*, 8249-8258.
51. Yang, S. I.; Lammi, R. K.; Prathapan, S.; Miller, M. A.; Seth, J.; Diers, J. R.; Bocian, D. F.; Lindsey, J. S.; Holten, D. *J. Mater. Chem.* **2001**, *11*, 2420-2430.
52. Quante, H.; Müllen, K. *Angew. Chem. Int. Ed.* **1995**, *34*, 1323-1325.

53. Holtrup, F. O.; Müller, G. R. J.; Quante, H.; De Feyter, S.; De Schryver, F. C.; Müllen, K. *Chem. Eur. J.* **1997**, *3*, 219-225.
54. Schlichting, P.; Duchscherer, B.; Seisenberger, G.; Basche, T.; Braeuchle, C.; Müllen, K. *Chem. Eur. J.* **1999**, *5*, 2388-2395.
55. Rohr, U.; Kohl, C.; Müllen, K.; Craats, A. van de; Warman, J. *J. Mater. Chem.* **2001**, *11*, 1789-1799.
56. Loewe, R. S.; Tomizaki, K.-Y.; Chevalier, F.; Lindsey, J. S. *J. Porphyrins Phthalocyanines*, **2002**, *6*, 626-642.
57. Tomizaki, K.-y.; Thamyongkit, P.; Loewe, S. R.; Lindsey, J. S. *Tetrahedron*, **2003**, *59*, 1191-1207.
58. Gosztola, D.; Niemczyk, M. P.; Wasielewski, M. R. *J. Am. Chem. Soc.* **1998**, *120*, 5118-5119.
59. Fuller, M. J.; Wasielewski, M. R. *J. Phys. Chem. B* **2001**, *105*, 7216-7219.
60. Becker, S.; Böhm, A.; Müllen, K. *Chem. Eur. J.* **2000**, *6*, 3984-3990.
61. Leroy-Lhez, S.; Perrin, L.; Baffereau, J.; Hudhomme, P. *C. R. Chimie*, **2006**, *9*, 240-246.
62. Reichardt, C. *Solvents and solvent effects in organic chemistry*, 3<sup>rd</sup> ed.; WILEY-VCH Verlag GmbH & Co. KGaA, Weinheim, **2004**.
63. Grabowski, Z. R.; Rotkiewicz, K.; Rettig, W. *Chem. Rev.* **2003**, *103*, 3899-4031.
64. Rotkiewicz, K.; Rubaszewska, W. *Chem. Phys. Lett.* **1980**, *70*, 444-448.
65. Rettig, W. *Angew. Chem. Int. Ed. Eng.* **1986**, *25*, 971-988.
66. Paczkowski, J.; Neckers, D. C. *Macromolecules* **1991**, *24*, 3013-3016.
67. Moore, J. S. *Acc. Chem. Res.* **1997**, *30*, 402-413.

68. Tour, J. M. *Chem. Rev.* **1996**, *96*, 537-553.
69. Kukula, H.; Veit, S.; Godt, A. *Eur. J. Org. Chem.* **1999**, 277-286.
70. Godt, A. *J. Org. Chem.* **1997**, *62*, 7471-7474.
71. Sluch, M. I.; Godt, A.; Bunz, U. H. F.; Berg, M. H. *J. Am. Chem. Soc.* **2001**, *123*, 6447-6448.
72. Ziener, V.; Godt, A. *J. Org. Chem.* **1997**, *62*, 6137-6143.
73. Tomizaki, K.-y.; Loewe, R. S.; Kirmaier, C.; Schwartz, J. K.; Retsek, J. L.; Bocian, D. F.; Holten, D.; Lindsey, J. S. *J. Org. Chem.* **2002**, *67*, 6519-6534.
74. Stracke, F.; Bium, C.; Becker, S.; Müllen, K.; Meixner, A. *J. Chem. Phys. Lett.* **2000**, *325*, 196-202.
75. Fuller, M. J.; Guser, A. K.; Wasielewski, M. R. *Israel Journal of Chemistry* **2004**, *44*, 101-108.
76. Zoon, P. D.; Brouwer, A. M. *ChemPhysChem*, **2005**, *6*, 1574-1580.
77. Fox, M. A.; Whitesell, J. K. *Organische Chemie.* **1994**. Spektrum.
78. Edvinsson, T.; Li, C.; Pschirer, N.; Schöneboom, J.; Eickemeyer, F.; Sens, R.; Boschloo, G.; Herrmann, A.; Müllen, K.; Hagfeldt, A. *J. Phys. Chem. C* **2007**, *111*, 15137-15140.
79. Brune, R. *Inauguraldissertation*, **2009**.

## Curriculum Vitae

Mr. Dhananjaya Sahoo



### Personal Information

Date of birth: 23<sup>rd</sup> Jan. 1978

Gender: Male

Nationality: Indian

Occupation: Chemist

### Scientific Curriculum

- Apr. 05-expected  
time Oct.09      Ph.D. Chemistry  
Bielefeld University, Bielefeld, Germany  
Title of Thesis: "Synthesis of Molecular Rulers to Study Distance and Orientation Dependent Förster Resonance Energy Transfer"  
Advisor: Prof. Dr. Adelheid Godt
- Sept. 04-Mar. 05      Graduate Program in Nanomolecular Science (*Discontinued*)  
Jacobs University Bremen, Germany  
Advisor: Prof. Dr. Thomas Nugent
- Nov. 02-Mar. 03      Junior Research Fellow  
Indian Institute of Technology Madras (IITM), India  
Project: Synthesis of Newkome-type dendrimer (up to 2<sup>nd</sup> gen.)  
Advisor: Prof. Dr. Sundarbabu Bhaskaran
- Sept. 99-Oct. 01      M.Sc. Chemistry  
Berhampur University, Orissa, India  
Specialization: Applied Organic Chemistry

Aug. 96-Jul. 99    B.Sc. Chemistry (Honors)  
Salipur College Salipur, Utkal University, Orissa, India  
Other Subjects: Physics and Mathematics

---

### Work Experience

Apr. 03-Aug. 04    Senior Project Assistant  
Chembiotek Research International Pvt. Ltd. India  
Main activities and responsibilities: Research and development

---

### Distinctions and Awards

Sep. 04-Mar. 05    Graduate Student Fellowship, Jacobs University Bremen, Germany  
for Graduate Program in Nanomolecular Science

Jun. 04              Lectureship Qualification Examination, Successfully Passed the  
“Lectureship Qualification Examination (for all the Indian Universities  
in Chemical Sciences) Conducted by the Council of Scientific and  
Industrial Research (CSIR)”, Delhi, India

2002 & 2003        Qualified all India level Graduate Aptitude Test in Engineering  
(GATE), Category: Chemical Sciences.

---

### Publications (in preparation)

1. D.Sahoo, M. Schulte, A. Godt; “A Update on the Synthesis of Monodisperse oligo(*para*-phenyleneethynylene)s using Orthogonally Pro-TECTING Groups with Different Polarity”.
2. D. Sahoo, B. Ralf, M. Sauer, A. Godt; “Aryloxy and Pyrrolidine-substituted Perylenemonoimides Labeled oligoPPE: A New Donor-Acceptor Labeled Dyad Showing Reverse FRET after Protonation”.
3. D. Sahoo, B. Ralf, M. Sauer, A. Godt; “Synthesis of New Molecular Ruler for the Spectroscopic Ruler FRET”.

---

### Conferences and Workshops

#### Poster Presentation

1. B. Ralf, D. Sahoo, S. Doose, M. Sauer, A. Godt “A Molecular Ruler to Study Distance and Orientation Dependent Energy Transfer” at 21<sup>st</sup> Lecture Conference of the GDCh-division Photochemistry, Bielefeld, Germany, Oct. 2008.
2. D. Sahoo, B. Ralf, M. Sauer, G. Jeschke, A. Godt “Synthesis of

Donor-Acceptor Labeled oligoPPEs: A Comparative Study of Distance Measurement by FRET and EPR” at 2<sup>nd</sup> EuChem Chemistry Congress, Torino, Italy, Sept. 2008.

3. D. Sahoo, B. Ralf, M. Sauer, G. Jeschke, A. Godt “Donor-Acceptor Labeled Nanorods: Synthesis and Photophysical Properties” at ORCHEM 2008, Wiemar, Germany, Sept. 2008.
4. D. Sahoo, B. Ralf, M. Sauer, G. Jeschke, A. Godt “Synthesis of Fluorescent Labeled oligoPPES for a Comparative Study of Distance Measurement by EPR and FRET” at Science Fair (perspective 2007) Bielefeld University, Germany, Nov. 2007.
5. D. Sahoo, B. Ralf, M. Sauer, G. Jeschke, A. Godt “Synthesis of Donor-Acceptor Labeled oligoPPEs: A Comparative Study of Distance Measurement by EPR and FRET” at Wiissenschaftsforum Chemie 2007, Universität Ulm, Germany, Sept. 2007.
6. D. Sahoo, M. Sauer and A. Godt “Fluorescent Labeled oligoPPEs for the Investigation of Conformational Dynamics by FRET Measurement” at Science Fair (perspective 2006) Bielefeld University, Germany, Nov. 2006.

#### Oral Presentation

1. D. Sahoo, B. Ralf, M. Sauer, A. Godt “Molecular Rulers for the Spectroscopic Ruler FRET”, Workshop on Conjugated Oligomer and Polymer from Synthesis to Electronic Function, Heinrich-Fabri-Institut, Blaubeuren, Germany, Sept. 2009.

---

#### Membership

Gesellschaft Deutscher Chemiker (GDCh)